Evaluating adjuvant, formulation, and antigen in the development of a Powassan virus vaccine

Michael W. Crawford

A DISSERTATION

March 2026

Thesis submitted to the Department of Molecular Microbiology and Immunology at the Oregon Health and Science University School of Medicine in partial fulfillment of the requirements for the degree of Doctor of Philosophy.

Advisor: Alec J. Hirsch, Professor, Ph.D.

Committee Chair: Daniel N. Streblow, Professor, Ph.D.

Committee Member: Victor R. DeFilippis, Professor, Ph.D.

Committee Member: Julie Mitchell, Assistant Professor, Ph.D.

External Reviewer: William B. Messer, Professor, M.D., Ph.D.

I. TABLE OF CONTENTS

II. List of Figures

III. Common Abbreviations

ADE	antibody-dependent enhancement
AHFV	Alkhurma hemorrhagic fever virus
APC	antigen-presenting cell
BBB	blood-brain barrier
BCR	B cell receptor
cDC	conventional dendritic cell
CHIKV	chikungunya virus
CITEseq	cellular indexing of transcriptomes & epitopes by sequencing
CNS	central nervous system
CoP	correlate(s) of protection
DC	dendritic cell
DENV(-1-4)	dengue virus (serotype 1 through 4)
dLN	draining lymph node
dsRNA	double-stranded RNA
EBOV	Ebola virus
ED(I-III)	envelope protein domain (1 through 3)
EDE	envelope dimer epitope
ELISA	enzyme-linked immunosorbent assay
FL	fusion loop
FLE	fusion loop epitope
FRNT	focus reduction neutralization test
GC	germinal center
GCR	germinal center response
HA	hemagglutinin

HBV	hepatitis B virus
HEV	hepatitis E virus
HIV	human immunodeficiency virus
IFN (-I, -II, -III)	interferon (types 1, 2, and 3)
Ig (D, M, G, A)	immunoglobulin (isotypes D, M, G, A)
im	intramuscular(ly)
ip	intraperitoneally
JEV	Japanese encephalitis virus
KFDV	Kyasanur Forest disease virus
LBP	LPS-binding protein
LN	lymph node
LPS	lipopolysaccharide
MBC	memory B cell
MBFV	mosquito-borne flavivirus
MHC	major histocompatibility complex
NHP	non-human primate
NK cell	natural killer cell
NK T cell	natural killer T cell
OHFV	Omsk hemorrhagic fever virus
PAMP	pathogen-associated molecular pattern
pDC	plasmacytoid dendritic cell
POWV	Powassan virus
PRR	pattern recognition receptor
RSV	respiratory syncytial virus
sc	subcutaneous(ly)
ssRNA	single stranded RNA
TBEV	tick-borne encephalitis virus

TBFV	tick-borne flavivirus
TGN	trans-Golgi network
TLR	Toll-like receptor
USUV	Usutu virus
VLP	virus-like particle
WNV	West Nile virus
YFV	yellow fever virus
ZIKV	Zika virus

IV. Acknowledgments

I would like to thank everyone involved in these projects without whom this dissertation would not have been possible. The work presented here represents the collaborative effort of scientists across multiple institutions and is built on work from countless individuals dedicated to improving human health. Thank you to my mentors Alec Hirsch and Jessica Smith for supporting me and providing me with the foundation necessary to pursue a career in virology and vaccine research. Thank you to all the members of the Hirsch Lab, past and present, for the education and for making the lab feel like home: Chris Parkins, Henry Harrison, Beatrice Hirsch, Tong Kraivong, Oradee Khammaneejan, Jessica Smith, and Alec Hirsch. Thank you to everyone at HDT Bio for the opportunity to work with such great people at the cutting edge of vaccine research: Taylor Stone, Nikki Warner, Jesse Erasmus, Karen Gaffney, Kiara Hatzakis, Heather Kain, and everyone. Thank you to my dissertation advisory committee, Dan Streblow, Vic DeFilippis, and Julie Mitchell as well as Bill Messer for your guidance and insights. Thank you to the Messer and Streblow labs for your comradery and arbovirus expertise.

Thank you to my partner, Naman Mody, for providing the spark to pursue a PhD and the patience and support that made it possible. Thank you to Irini Topalidou for your friendship, mentorship, and encouragement. Thank you to my

mom, dad, brother, and the rest of my family for your support. Thank you to all my friends in Portland, Seattle, and elsewhere. And thank you to everyone in the 2021 PBMS cohort for making grad school an unforgettable experience: Brent Bever, Deja Brooks, Miffy Guo, Margaret Haerr, Leah Huey, Dylan Kain, Sam Medica, Marin Miner, Rachel Morrill, Kayla Nguyen, Sam Osman, Ravina Pandita, Caitlin Peaslee, Jackie Phipps, Holly Sandborg, Tori Schuster, Allison Tammen, and Kayla Williams.

V. Abstract

There are numerous pathogenic flaviviruses distributed across the globe that cause debilitating, often lethal diseases in humans. Yet there are a limited number of flavivirus vaccines available, and these are all based on vaccine platforms using live attenuated or inactivated viruses. These platforms have significant shortcomings including potential risk to vaccinees and, in the case of inactivated virus vaccines, suboptimal immunogenicity. Fortunately, there are new vaccine technologies which offer safer and more effective ways to elicit robust protective immune responses to these viruses.

Here, I demonstrate the effectiveness of virus-like particles (VLPs) adjuvanted with a novel synthetic Toll-like receptor (TLR) agonist in the development of a vaccine for Powassan virus (POWV), a lethal tick-borne flavivirus currently emerging in North America for which there is no vaccine. Much of this dissertation focuses on evaluating the immunogenicity of two TLR agonists as adjuvants for this vaccine. Additional work considers the use of lipid-based vaccine formulations, the maturity of the VLP antigen, and the correlates of protection for our POWV vaccine model. The studies reported here demonstrate the utility of novel vaccine strategies for improving our current flavivirus vaccine methodology while simultaneously presenting pre-clinical data on the efficacy of a novel vaccine candidate for a highly relevant pathogenic flavivirus.

Chapter 1: Introduction

Section 1.1: Preface

Pathogenic flaviviruses (genus *Orthoflavivirus*) constitute an emerging threat to human health around the globe. Vaccines continue to be our most effective defense against disease and death caused by flavivirus infections. The first part of this chapter provides background on flaviviruses, their transmission, distribution, the diseases they cause, and how our immune systems protect us against them, with emphasis placed on POWV as well as the more well-studied flavivirus pathogens dengue virus (DENV) and tick-borne encephalitis virus (TBEV). The second part of this chapter introduces vaccines, vaccine platforms, relevant immunology, adjuvants, and the current landscape of flavivirus vaccines.

Section 1.2: Flaviviruses

1.2.1 Classification and phylogeny

Flaviviruses are RNA viruses of the *Orthoflavivirus* genus [1, 2]. Most medically relevant flaviviruses are arthropod-borne viruses (arboviruses) maintained in nature by enzootic cycles between hematophagous arthropods and vertebrate hosts [3]. Flaviviruses cluster phylogenetically by their mode of

transmission as either mosquito-borne flaviviruses (MBFVs) or tick-borne flaviviruses (TBFVs) (Figure 1.2.1) [4, 5]. MBFVs further cluster by the genus of their most common vectors, *Culex* vs *Aedes* mosquitoes. Serocomplexes exist within these clusters as determined by cross-neutralization of polyclonal antibodies [6, 7]. Viruses within serocomplexes often cause similar diseases in humans and share substantial similarity in their protein sequences.

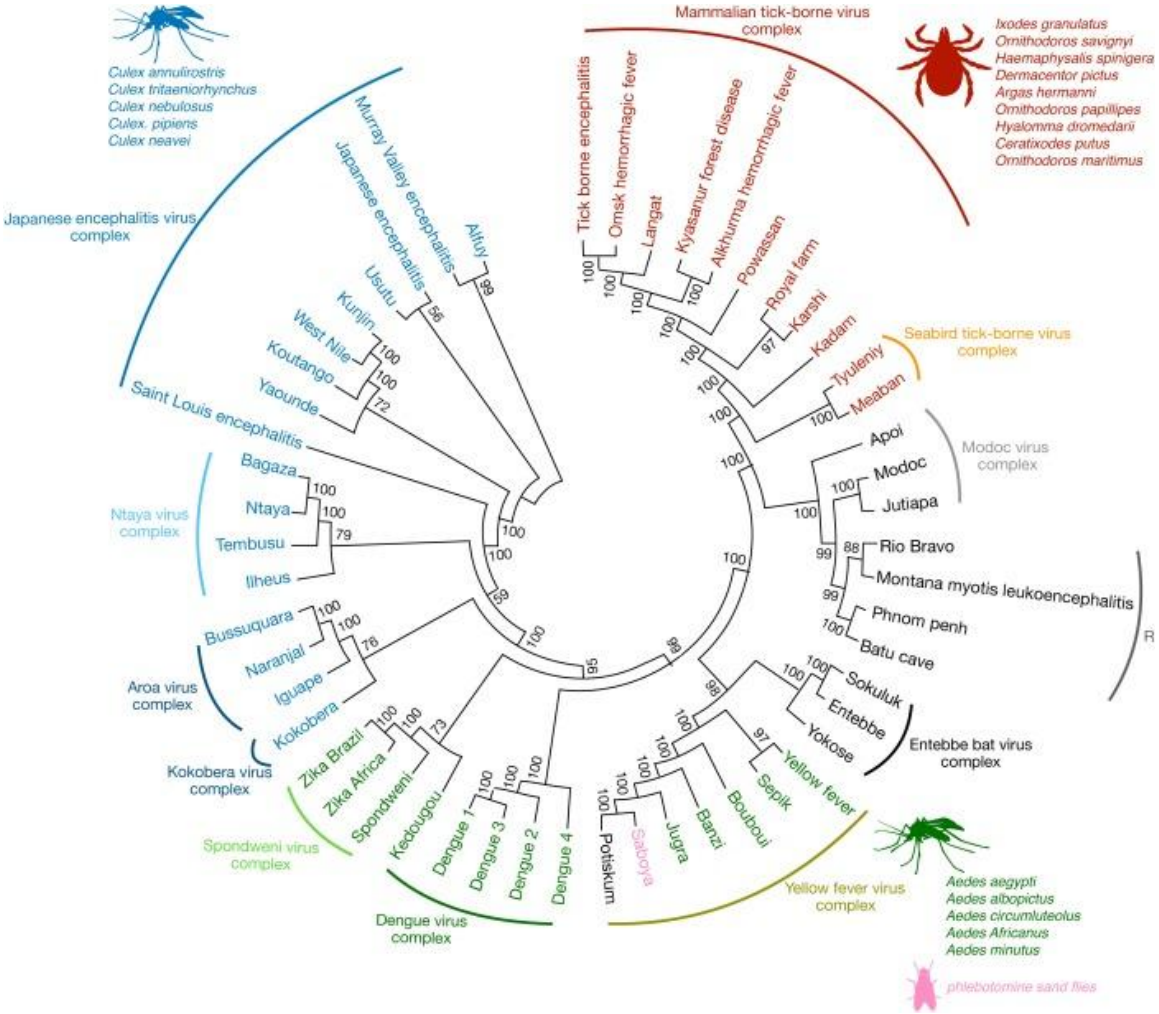

Figure 1.2.1: Phylogenetic map of flaviviruses.

Flaviviruses are colored according to their primary vectors with TBFVs in red, *Aedes*-vectored MBFVs in green, *Culex*-vectored in blue, and those with no known vector (vertebrate-specific) in black. Serocomplexes are indicated by arched lines. Figure unmodified from [5] published under Creative Commons license.

1.2.2 Genome

Flaviviruses are single-stranded, positive-sense RNA viruses [1, 2]. The viral genomes are 10-12.3kb with a type-I 5′ cap and no poly-A tail [1, 8]. The 5′ and 3′ UTRs are highly structured and essential for viral replication. The 5′ UTR contains structured promoters responsible for translation as well as association with the viral RNA-dependent RNA polymerase for viral replication [9, 10]. The 3′ UTR encodes subgenomic flaviviral RNA that suppresses host innate immunity [11]. Complementary regions between the 5′ and 3′ UTRs lead to cyclization of the genome necessary for replication [12]. The genome is translated as a single polyprotein which is cleaved by a combination of host and viral proteases into 10 individual proteins and a small 2kDa peptide. Three of these proteins, capsid (C), pre-membrane (prM), and envelope (E), are structural. The remaining seven are non-structural (NS) proteins: NS1, NS2a, NS2b, NS3, NS4a,

NS4b, and NS5. These proteins and their functions are discussed in the following sections.

1.2.3 Attachment and entry receptors

The viral replication cycle begins with weak attachment of a virion to a host cell membrane (Figure 1.2.2). These interactions are mediated by the viral lipid envelope, viral E glycoprotein, and host attachment factors including glycosaminoglycans such as heparan sulfate and the phosphatidylserine receptors TIM and TAM, which concentrate virions at the cell surface [13-15]. Subsequent interaction with cell surface entry receptors facilitates viral entry [16]. Putative entry receptors for flaviviruses in humans include lectins, integrins, and phospholipid receptors [17]. For DENV, these factors/receptors include the C-type lectins DC-SIGN, DC-SIGNR/L-SIGN, and CLEC5A; heat-shock proteins HSP90 and HSP70; the LPS receptor CD14; mannose receptor; laminin receptor; the phosphatidylserine receptors TIM and TAM; and the integrins Claudin-1 and $\alpha_v\beta_3$, just to name a few [15, 17, 18]. Many of these receptors are shared by other flaviviruses. There are also several putative receptors for DENV in insect cells, though these will not be discussed here. The diverse panel of molecules that facilitate virus binding and/or entry into host cells accounts for the ability of DENV to infect a diverse range of cell types in both arthropod and mammalian hosts. Specifically, expression of receptors such as DC-SIGN, L-SIGN, mannose receptor,

CD14, HSP70/90, and TIM-1 on macrophages, monocytes, dendritic cells, lymphocytes, and hepatocytes may explain the cellular tropism of DENV discussed in Section 1.2.8.

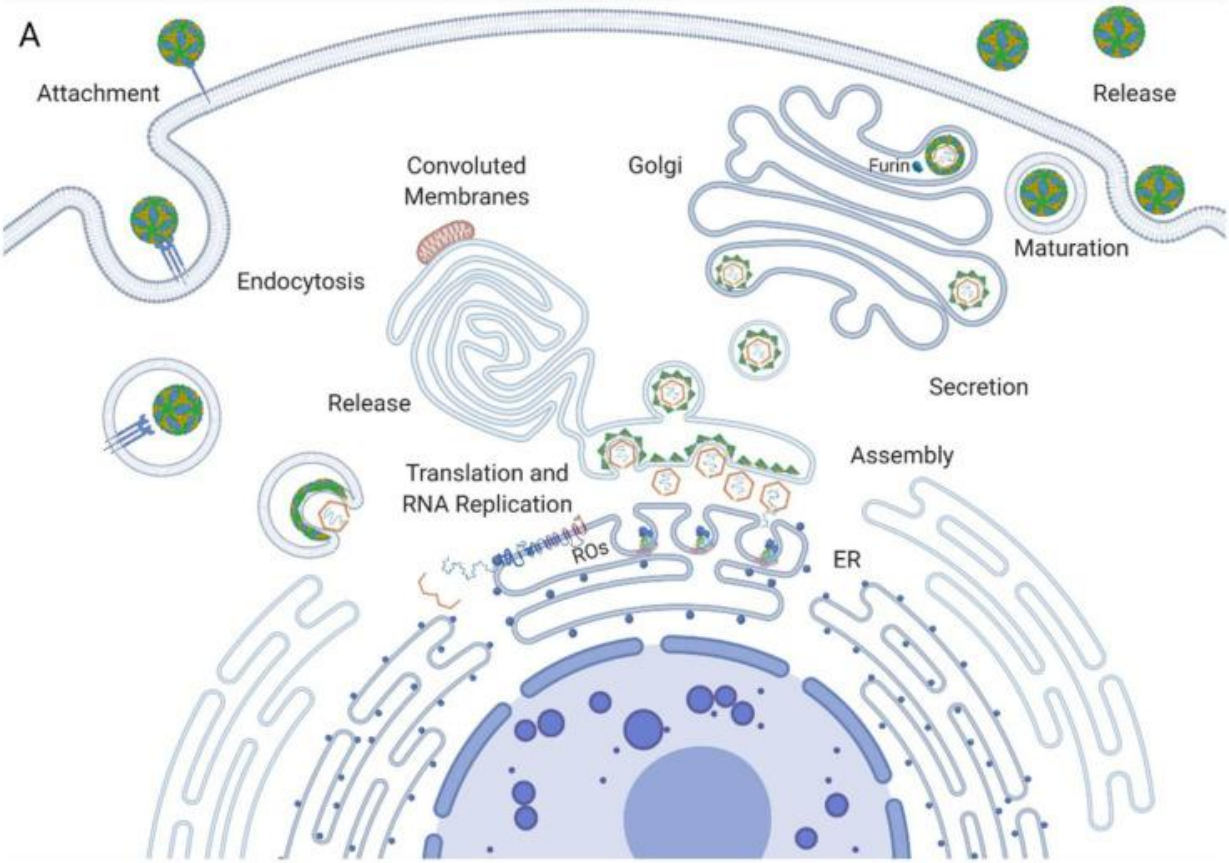

Figure 1.2.2: Flavivirus replication.

Schematic depicting viral replication cycle from 1) attachment, to 2) endocytosis, 3) release of the viral genome into the cytosol, 4) translation of viral proteins, 5) viral RNA replication within replication organelles (RO), 6) new virion assembly, 7) virion transit through the Golgi, 8) maturation of nascent particles by host furin, and 9) release of new virions into the extracellular environment. Figure unmodified from [19] published under Creative Commons license.

While no published studies have identified the attachment factors or entry receptors for POWV, inferences can be made from the closely related TBEV. Although much less is known about TBEV attachment and entry than for DENV, heparan sulphate appears to facilitate attachment for TBEV, though to a lesser degree than DENV and more so in lab-adapted strains than wild-type [20]. As for entry receptors, recent studies identified TIM-1 and the low-density lipoprotein receptor LRP8 as entry receptors for TBEV [21-23]. The expression of LRP8 in neurons and glial cells in the central nervous system (CNS) implicate this receptor in the neuropathologies associated with TBEV infection discussed in Section 1.2.8. This receptor does not appear to play a role in POWV infection, however [22, 23]. Alternatively, both DENV and TBEV enter cells via Fc-receptors discussed more in Section 1.2.10 [16, 24].

1.2.4 Entry

Receptor binding facilitates flavivirus entry into cells. This process normally involves clathrin-mediated endocytosis, though some studies have demonstrated clathrin-independent endocytosis for some flaviviruses in certain contexts [25, 26]. Clathrin-mediated endocytosis begins with the recruitment of adaptor and scaffold proteins including clathrin to clusters of entry receptors bound to virions on the cell surface (Figure 1.2.3). The assembly of these proteins

generates clathrin-coated pits via membrane invagination, surrounding the virion cargo. Vesicle scission mediated by dynamin produces clathrin-coated vesicles which are trafficked via Rab proteins to the endosomal compartment [27]. The low pH-environment of the endosome induces pH-dependent conformational changes on viral particles [28-31]. This results in the rearrangement of the smooth E dimers on mature virions into spiky trimers which exposes the fusion loop (FL) of E (Figure 1.2.4). Insertion of the hydrophobic FL into the endosomal membrane results in further conformational changes in E and the formation of a fusion pore between the viral envelope and endosomal membrane [32]. Viral RNA escapes through this pore into the cytosol to begin translation and replication.

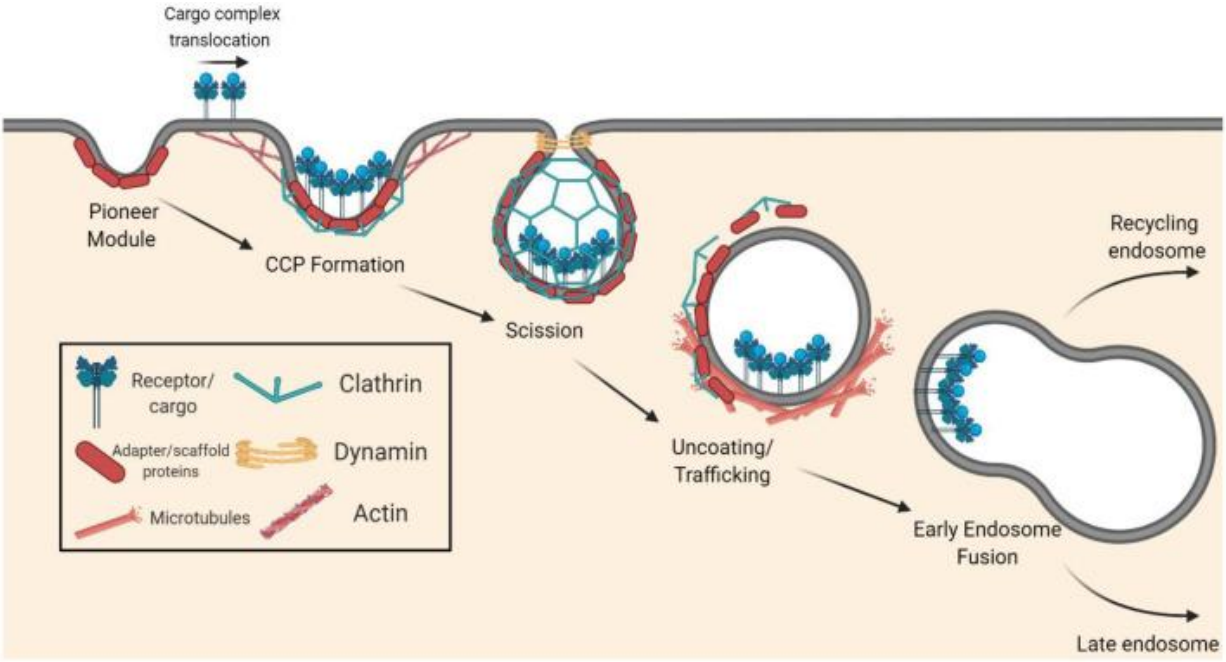

Figure 1.2.3: Clathrin-mediated endocytosis.

Schematic depicting clathrin-mediated endocytosis via the formation of clathrin-coated pits (CCP). After scission and uncoating, the vesicle is trafficked to the early endosome. Figure unmodified from [26] published under Creative Commons license.

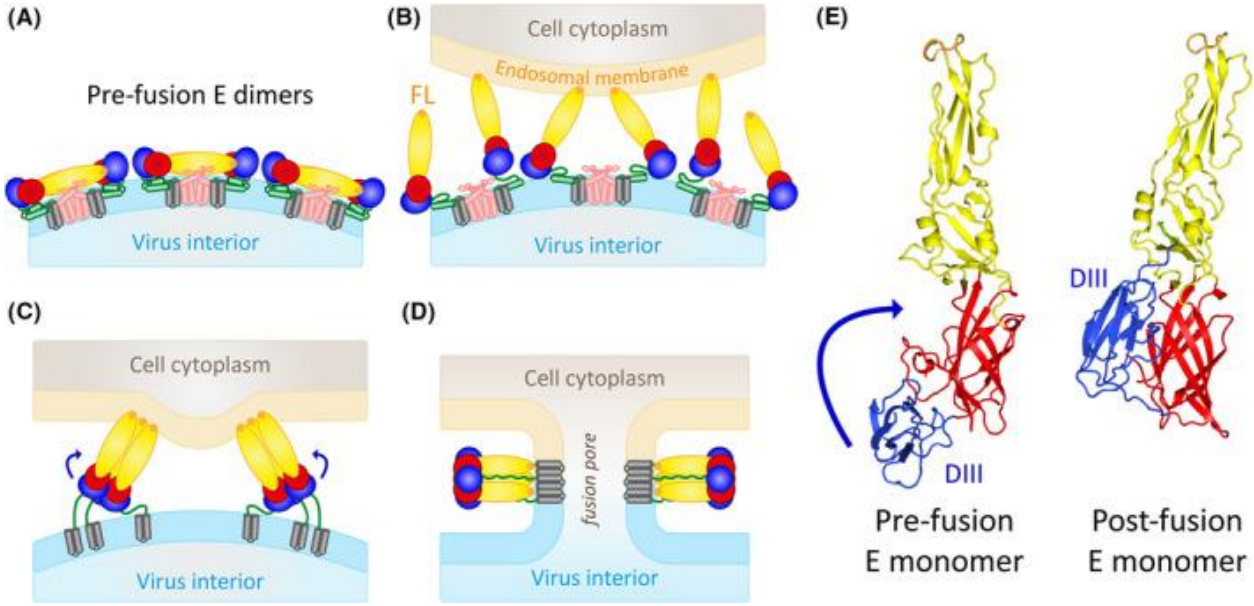

Figure 1.2.4: Fusion of flavivirus membrane with endosomal membrane.

Schematic depicting the conformational change in E from (A) to (B), to (C), and finally to (D) involving the exposure of the fusion loop (orange) which drives membrane-membrane fusion between the flavivirus envelope and endosome. Figure unmodified from [32] published under Creative Commons license.

1.2.5 Replication

Once inside the cytosol, host cell machinery treats the flavivirus positive-sense RNA as mRNA and translates the genome into a single polyprotein [1, 8]. During translation, the polyprotein is threaded back and forth across the membrane of the endoplasmic reticulum (ER) at sites of conserved signal sequences necessary for the generation of multiple soluble and membrane-anchored proteins in the cytosol and ER lumen (Figure 1.2.5) [33]. The polyprotein is cleaved into 3 structural (C, prM, E) and 7 non-structural (NS1, NS2a, NS2b, NS3, NS4a, NS4b, NS5) by both host factors and the viral protease NS3/NS2b [1, 34]. Once these discrete proteins are generated, replication of the viral genome begins. This replication is performed within replication organelles (ROs) which are pockets of invaginated ER membrane formed by the non-structural proteins NS1, NS2a, NS4a, NS4b (Figure 1.2.5) [35-42].

All seven non-structural proteins come together within these ROs to form the viral RNA replication complex [8, 36]. RNA replication and capping is performed by NS5, which acts as an RNA-dependent RNA polymerase and RNA methyltransferase, together with NS3, which acts as both helicase and 5′ RNA triphosphatase [8]. During this replication, the positive-sense RNA genome serves as template to produce negative-sense RNA, which in turn serves as a template to produce more positive-sense genomic RNA. Double-stranded RNA (dsRNA)

intermediates formed during this process are potent pathogen-associated molecular patterns (PAMPs) discussed in Section 1.2.9 [43]. The formation of ROs both concentrates the factors necessary for viral replication and sequesters PAMPs such as dsRNA to help evade the host immune response [36, 44-46]. A pore in the RO allows newly generated viral genomes to exit into the cytosol for packaging into new viral particles which bud into the ER often juxtaposing ROs (Figure 1.2.5) [47-50].

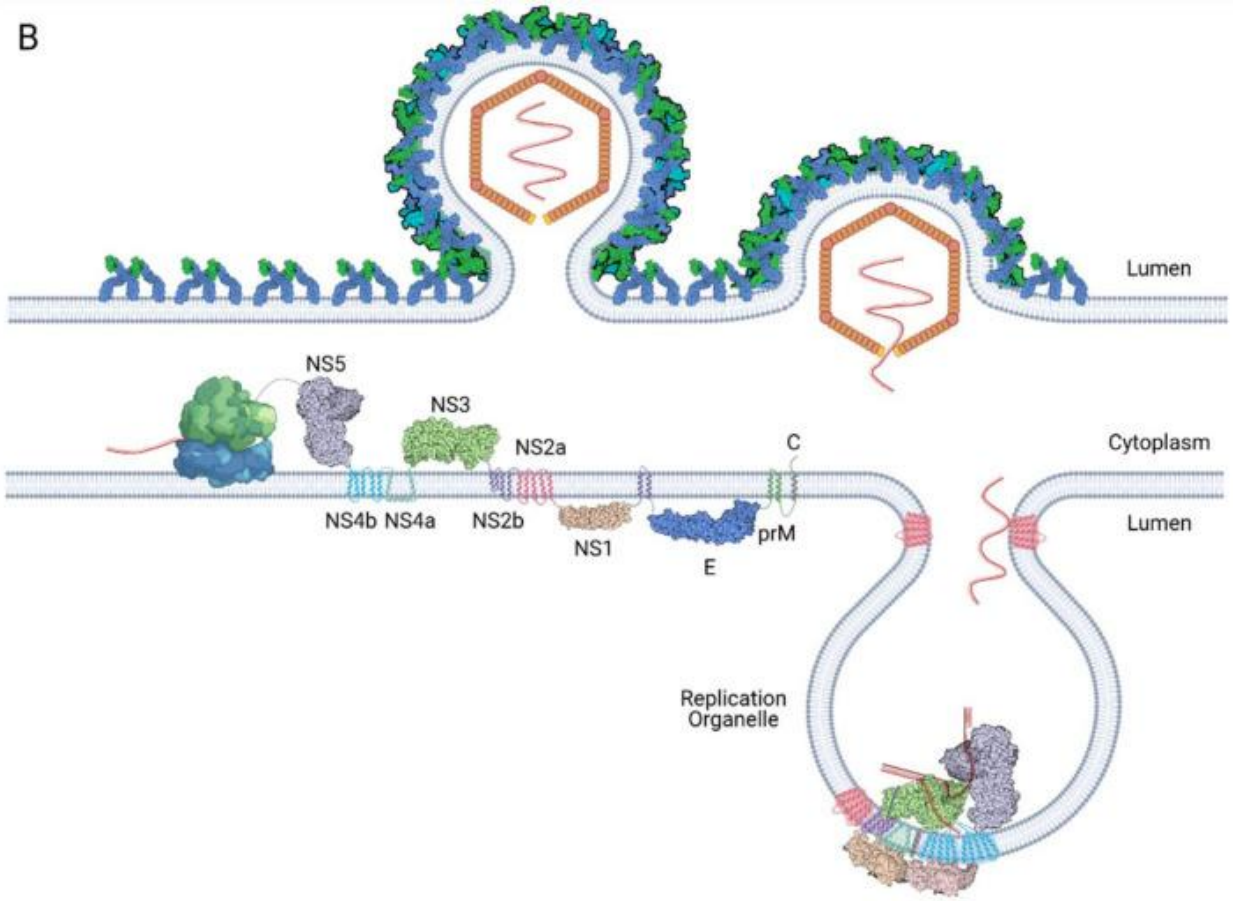

Figure 1.2.5: Flavivirus proteins, replication organelle, and assembly.

Schematic depicting 1) the translation of a flavivirus polyprotein at the ER membrane, 2) a replication complex generating new viral genomes inside a replication organelle generated by invagination of the ER membrane, and 3) the assembly of new viral particles on juxtaposing ER membrane. Figure unmodified from [19] published under Creative Commons license.

Genome packaging and particle assembly are coordinated by several viral proteins including the structural proteins C, prM, and E as well as NS2a, NS3, and NS5 [51-59]. Nascent viral particles in the ER are composed of a nucleocapsid core of ssRNA bound to C surrounded by an ER-derived lipid bilayer studded with 60 trimeric spikes of prM-E heterodimers [49, 60-62]. Particles then undergo a process of maturation as they transit through the trans-Golgi network (TGN) before exiting the cell as fully infectious virions to begin the entry and replication process anew in the next cell [8, 63].

1.2.6 Maturation

Flavivirus maturation is an important process that affects particle infectivity and the interaction between viral particles and the host immune response. The process begins with exposure of newly assembled viral particles to the mildly acidic lumen of the TGN as they traffic from the ER to be secreted at the

plasma membrane [1, 63, 64]. Under acidic conditions, the trimeric spikes of prM-E heterodimers undergo a conformational shift to become prM-E dimers that lie flat across the surface of the particle (Figure 1.2.6) [61-63, 65-68]. This shift exposes a site within prM that is cleaved into pr and M by the host protease furin in the TGN [63, 69, 70]. The pr peptide remains positioned over the FL of the E dimer until the particles are secreted and encounter the neutral pH of the extracellular environment at which point pr dissociates from the particle [68, 69]. A conserved histidine residue in E and aspartic acid in pr are likely responsible for post-cleavage association at low pH and dissociation at neutral pH [68, 71]. By capping the FL during maturation and remaining associated with the E dimers during egress, the pr peptide stabilizes the E dimer and prevents premature fusion with the cell of origin [29, 61, 68, 69, 72]. For MBFVs, prM cleavage stabilizes the E dimer which remains dimerized after secretion, while uncleaved prM-E dimers are only stable under acidic conditions and revert to trimers at neutral pH [62, 69]. For TBFVs, however, dimerization after exposure to low pH is irreversible regardless of prM cleavage [63, 73]. The maturation process for flaviviruses is variably efficient and can result in a spectrum of immature, partially mature, and fully mature virions [74-78].

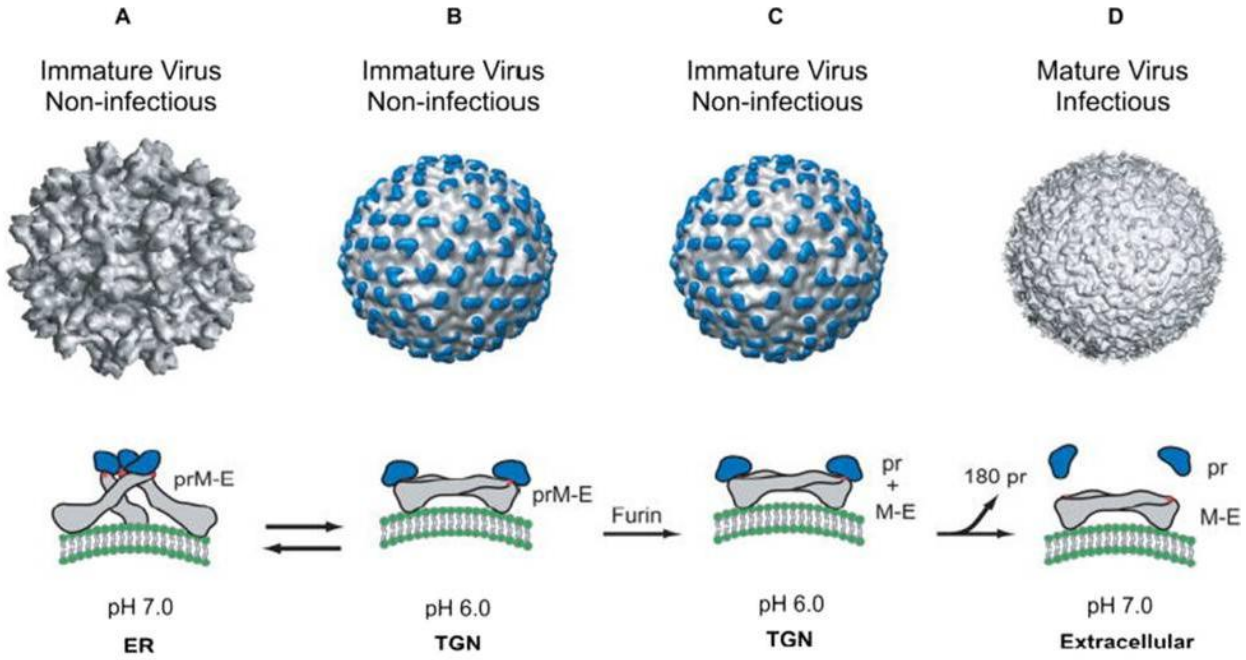

Figure 1.2.6: Flavivirus maturation.

Schematic depicting A) spiky immature virus with trimeric prM-E heterodimers at neutral pH in ER; B) the dimerization of prM-E after exposure to acidic conditions in the TGN generating 'smooth' particles; C) the cleavage of pr from M by furin in the TGN; and D) the dissociation of pr from the smooth mature particle as it exits into the neutral pH of the extracellular environment. Figure adapted from [79] published under Creative Commons license.

Particle maturity is largely considered necessary for infectivity, but there are notable exceptions [63, 69, 80]. Immature flaviviruses can still be infectious in the context of antibody-dependent enhancement (ADE) as discussed in Section 1.2.10, and both partially mature West Nile virus (WNV) and immature DENV appear to be capable of infecting DC-SIGN/DC-SIGNR+ cells via sugar groups on

prM and E [75, 81-83]. This infectivity may or may not require furin cleavage of prM during entry [81, 82, 84]. Additionally, new evidence suggests that TBFVs are uniquely infectious regardless of maturity due to the irreversible dimerization of E mentioned previously [73]. This permanent dimerization of E leaves the furin cleavage site of prM exposed and vulnerable to extracellular furin activity after secretion, rendering particles mature and infectious regardless of intracellular maturation.

Maturation plays a significant role in flavivirus immunity [75, 85, 86]. Particle maturity impacts the host immune response by altering the exposure of epitopes on the particle surface which sensitizes the antibody response to maturity [87, 88]. Indeed, antibodies derived from natural infection are often sensitive to maturity, with antibodies that target epitopes found only on immature or partially mature particles constituting a major component of the antibody response to natural DENV infection [88, 89]. This is highly relevant to immunity as antibodies targeting epitopes found on immature particles tend to be less neutralizing than those found on mature particles, though there is nuance to this and examples of neutralizing epitopes more accessible on less mature particles [75, 76, 87, 88, 90-100]. Furthermore, by varying the quantity and quality of neutralizing targets exposed on a particle's surface, maturation affects the susceptibility of viral particles to neutralization [75, 88, 90, 99, 101]. Finally, the infectious potential of a

particle can be enhanced by antibodies, especially those targeting epitopes that are hidden or absent on mature particles, which will be discussed more in Section 1.2.10 [76, 88, 90, 102-104]. In summary, by manipulating the host's antibody response and the susceptibility of individual particles to neutralization, maturation plays a critical role in the immune response to flaviviruses. It is surprising, therefore, that relatively few groups have directly investigated the effects of vaccine antigen maturity on flavivirus vaccine efficacy [87, 105-108]. Chapter 4 of this dissertation investigates the effect of particle maturity on POWV vaccination.

1.2.7 Transmission and distribution

Much of our knowledge concerning the viral etiology, arthropod transmission, and diseases caused by flaviviruses comes from the work of scientists including Carlos Finlay, Walter Reed, James Carroll, H. Graham, and Albert Sabin on yellow fever virus (YFV) and DENV in the late 1800s and early 1900s, many of whom used human subjects in their studies including prisoners, mental patients, medical students, and army personnel [109-114]. Most pathogenic flaviviruses are arboviruses maintained in nature by enzootic cycles of infection between arthropods and animals [3, 115]. Briefly, animal infections occur when an infected arthropod secretes virus-laden saliva into an animal's skin while taking a

bloodmeal [116-119]. The virus targets and replicates within the keratinocytes, Langerhans cells, and other skin-resident dendritic cells (DCs) at the site of inoculation [120-124]. Infected Langerhans cells and DCs then migrate to draining lymph nodes after which the virus disseminates to other tissues including the blood, resulting in viremia [124-127]. After a naïve arthropod takes a bloodmeal from a viremic animal, the virus spreads from the arthropod midgut to the salivary glands which prepares the insect to infect another animal, thus completing the enzootic cycle of transmission [128-132]. Alternatively, many flaviviruses have demonstrated capacity to transmit vertically within arthropods which may be specifically important for the maintenance of TBFVs in nature [133-137]. TBFVs also rely on transstadial persistence of infection through the multiple life stages of a tick and on co-feeding transmission in which ticks feeding from the same animal at the same time transmit virus to one another through a non-viremic host [119, 137-140].

Human infections are often incidental and occur when humans come in proximity to infected arthropods. For many flaviviruses such as WNV, Japanese encephalitis virus (JEV), TBEV, and POWV, humans are dead-end hosts that do not experience sufficient viremia to perpetuate the spread of these viruses. However, some pathogenic flaviviruses such as DENV, YFV, and Zika virus (ZIKV) are adapted sufficiently to humans to cause urban transmission cycles in

which virus from viremic humans spreads back into arthropods and perpetuates infections within a human population [141]. Other modes of transmission to humans include vertical transmission (observed for DENV and ZIKV), sexual transmission (ZIKV), alimentary transmission via breast milk from infected nursing mothers (ZIKV and TBEV), and alimentary transmission of TBEV from unpasteurized dairy products of infected livestock [142-149].

Productive infection of both animals and arthropods poses major challenges to flaviviruses which must evade two distinct immune systems and replicate in multiple tissues across evolutionarily distinct hosts. These hurdles create selective pressures that affect host and vector competence which determines the geographic distribution of flaviviruses [150, 151]. POWV, for example, is a rare TBFV primarily confined to regions in the United States and Canada corresponding to the distribution of its two principal *Ixodes* vector species [152, 153]. In contrast, DENV, is a MBFV maintained both within sylvatic cycles between non-human primates and *Aedes* mosquitoes as well as within urban cycles between humans and domestic *Aedes aegypti aegypti* and peridomestic *Aedes albopictus* [154]. The competency of humans as reservoir hosts coupled with the wide distribution and domestic nature of these mosquitoes places roughly 40% of the global population at risk for acquiring dengue fever with an estimated 390

million annual infections globally of which nearly 100 million are symptomatic [155, 156].

Factors such as climate change, deforestation, and changes in human travel are actively affecting the distribution of flavivirus vectors and contact between vectors and humans which has led to the emergence and re-emergence of many flaviviruses across the globe [157, 158]. Vaccine development for emerging flaviviruses is critical to prevent a future in which increasingly large numbers of people are subject to the death and disease caused by these pathogens.

1.2.8 Disease and pathogenesis

Comparison of flavivirus seroprevalence to case numbers suggests that most flavivirus infections are asymptomatic [157, 159, 160]. When illness does occur, it is often biphasic [161]. The initial phase of symptoms are general arthralgia, malaise, headache, and other flu-like symptoms which may resolve on their own but can progress to a more severe second phase of illness that reflects the tissue tropism of the viruses [157, 161]. For hemorrhagic fever flaviviruses like DENV, YFV, Omsk hemorrhagic fever virus (OHFV), Alkhurma hemorrhagic fever virus (AHFV), and Kyasanur Forest disease virus (KFDV) which target peripheral tissues and cause visceral disease, outcomes include renal failure, liver failure, vascular leakage, and hemorrhagic syndromes [157]. In contrast,

neurotropic flaviviruses such as JEV, WNV, ZIKV, TBEV, and POWV which target the CNS cause encephalitis, meningitis, seizures, and paralysis. ZIKV, which also replicates in the placenta, can cause congenital disease.

The tissue tropism of pathogenic flaviviruses as well as the mechanism by which neurotropic flaviviruses gain access to privileged tissues such as the CNS are a matter of intensive study. There are several proposed mechanisms by which neurotropic flaviviruses invade the CNS including 1) hematogenous invasion after disruption of the microvascular endothelial cells of the brain by cytokines and viral factors increasing blood-brain barrier (BBB) permeability; 2) transport of viral RNA into the brain via neurons and olfactory nerves; and 3) transcellular invasion after replication in the microvascular endothelial cells of the BBB [162-172].

Clinical manifestations of flavivirus infections are attributed to both the pathogenic effects of viral replication as well as injury incurred from the host immune response [157, 173]. Among the direct effects of viral infection are apoptosis induced by viral replication and vascular leakage attributed to the non-structural protein NS1, the secreted form of which has been shown to induce the production of pro-inflammatory cytokines and endothelial barrier dysfunction in a tissue-specific manner reflecting the disease tropism of the major pathogenic flaviviruses [162, 173-175]. Indirect pathologies associated with the immune response to flavivirus infection are also implicated and are associated with robust

cytokine responses, infiltration of the CNS by $CD8^+$ T cells, and inflammatory responses in the brain which have been shown to exacerbate illness and decrease survival after infection with neurotropic flaviviruses [176-181].

1.2.9 Host immune response to infection

There are numerous mechanisms the human body utilizes to control flavivirus replication and clear infection. These fall into two broad categories: innate and adaptive immunity [43]. These are discussed at length in Sections 1.3.4 and 1.3.7. Briefly, innate immunity is comprised of immediate, non-specific, often transient immune responses elicited early in infection that are the prerequisite for subsequent adaptive immune responses. Adaptive immunity involves delayed immune responses that are highly specific to the invading pathogen and establish long-lasting protection from future infections with the same pathogen.

The innate immune responses to flavivirus infection involve pattern recognition receptors (PRRs) that recognize pathogen-associated molecular patterns (PAMPs) associated with flaviviruses. The major PAMPs of flaviviruses include viral ssRNA and the dsRNA produced during viral replication [182-186]. These are recognized by the cytosolic PRRs RIG-I, which recognizes uncapped ssRNA and short dsRNA, and MDA5, which recognizes long dsRNA [187-189]. Recognition of viral RNA by RIG-I and MDA-5 initiates a signaling cascade that

drives the production of type I interferons (IFN-I) [190-192]. IFN-I signaling in turn drives the production of interferon-stimulated genes (ISGs) with antiviral functions [193-197]. Other host innate factors involved in stemming flavivirus infection include cGAS-STING, which senses the DNA released by mitochondria damaged during flavivirus replication, and the Toll-like receptors 3 and 7 (TLR3 and TLR7), which recognize viral dsRNA and ssRNA, respectively [198-201]. Flaviviruses have evolved multiple mechanisms to evade these innate immune responses [182, 201]. These include sequestration of dsRNA into replication organelles, capping viral RNA, and actively antagonizing PRRs and IFN signaling with viral proteins [45, 182, 196, 201].

Adaptive immune responses to flaviviruses involve both humoral and cellular immunity. Humoral immunity is the production of antibodies that neutralize, opsonize, and activate complement pathways to clear infectious particles, secreted viral proteins, and/or infected cells [43, 202-207]. Neutralizing antibodies have been identified as the primary correlate of protection for symptomatic flavivirus infections [206, 208-211]. These neutralizing responses tend to target the E protein and can prevent particle attachment and fusion [207, 211-214].

The antibody responses to flaviviruses tend to be cross-reactive to viruses with high E sequence homology which leads to complex immune interactions

between heterologous viruses [211]. For example, infection with one DENV serotype often results in antibody responses that can neutralize the other serotypes, though titers wane over time and are only cross-protective for a short period [215, 216]. Additional DENV infections may even elicit neutralizing antibody responses against the more distantly related ZIKV [217]. In another example, monoclonal antibodies developed from TBEV infected individuals can also cross-neutralize many other TBFVs [218].

Flavivirus infection also induces cellular immune responses characterized by long-lived T cell responses which can be cross-reactive to similar flaviviruses [219, 220]. These responses have been associated with protection from severe disease and can be protective in the absence of a neutralizing antibody response [221-223]. However, more work is required to determine whether T cell responses are reliable correlates of protection [206, 211, 224].

1.2.10 Antibody-dependent enhancement

As discussed previously, antibodies are a crucial component of adaptive immunity with neutralizing antibody responses considered the standard correlate of protection for flaviviruses. However, antibodies can also be detrimental and increase the severity of an infection. This paradoxical phenomenon was first noticed in 1964 when a virologist named Dr. Royle A. Hawkes at the Australian

National University found that diluted antisera from chickens inoculated with various flaviviruses and alphaviruses could increase plaque forming units of both homotypic and heterotypic viruses in cell culture [225]. This enhancement was later attributed to the antibodies in antisera, setting the foundation for the concept of antibodies enhancing viral infections [226]. Meanwhile, in 1967 while studying human DENV infections in Thailand, the epidemiologist Dr. Scott B. Halstead and colleagues found that previous infection with DENV was a major risk factor for developing dengue hemorrhagic fever and dengue shock syndrome during subsequent infection [227]. Halstead postulated that prior infection with one serotype of DENV increases the risk of severe disease during infection with a second serotype. Subsequent experiments by Halstead *et al.* confirmed that prior immunity to DENV could enhance subsequent DENV infections in vivo in non-human primates (NHPs) [228, 229]. In the first of these experiments in 1973, a large rhesus macaque study demonstrated that prior infection with one DENV serotype could increase the viremia and symptoms experienced during a secondary infection with a second serotype [228]. In a following experiment in 1979, the passive transfer of human DENV-2-immune cord blood into rhesus macaques enhanced DENV-2 viremia after infection, demonstrating *in vivo* that antibodies drive this increased susceptibility to secondary infections [229].

A truly striking example of the consequences of this secondary-infection enhancement of DENV occurred in Cuba around this same time [230]. In 1977, the country experienced an epidemic of DENV-1, its first DENV epidemic since 1945. Yet despite a staggering 4.5 million reported infections, there were no cases of severe disease. In contrast, a subsequent epidemic of DENV-2 in 1981 resulted in more than 10,000 cases of dengue hemorrhagic fever and 158 deaths despite a lower total number of infected individuals [231]. Nearly all of these severe cases were associated with secondary infections [230]. No cases were observed in 1- or 2-year-old children, consistent with the fact that this would be one of the only groups without antibodies to DENV-1. This phenomenon, now known as antibody-dependent enhancement (ADE), is a critical subject in the field of flavivirus vaccines and remains one of the biggest challenges facing DENV vaccine development today. Here, I will summarize what we know about how ADE works and how current practices in vaccine development are focused on minimizing risk of ADE.

To begin a discussion into the mechanism behind ADE, we need to review the distinct functions of antibodies in the context of viral infections. Antibodies generated against a viral pathogen fall into two broad categories, those that neutralize the pathogen directly and those that mediate their effects through the antibody Fc region [43]. Neutralization occurs when a sufficient number of

antibodies bind to domains required for virus replication, rendering the virus non-infectious. For example, an antibody may neutralize a virus by binding its receptor binding site or fusion domain, preventing cell attachment, entry, structural changes required for infection, and/or fusion [207, 212-214]. These neutralizing antibodies are the major focus of virus vaccine research and tend to correlate strongly with protection [211]. However, antibodies may also mediate protection through any of several Fc-effector mediated functions [207]. For example, antibodies bound to a virion can themselves act as binding sites for complement proteins whose deposition leads to clearance of the pathogen-complement complex via Fc receptor- and complement receptor 1-mediated phagocytosis by cells such as monocytes, macrophages, and dendritic cells [43, 232]. This antibody-dependent cellular phagocytosis (ADCP) acts to clear and destroy viruses in circulation during infection.

In 1977, Halstead and colleagues published two studies that laid the foundation for our current understanding of ADE. They first identified those cells that participate in ADCP, mononuclear phagocytes, as a key target of DENV [233]. Further, they demonstrated that DENV complexed with homotypic or heterotypic anti-DENV antibodies was more efficient at infecting these phagocytes in an Fc receptor-dependent manner, implicating ADCP as the cause of ADE [234]. This established the concept we now know as *extrinsic* ADE whereby antibody-coated

DENV is targeted to highly permissive Fc receptor-bearing cells, increasing the efficiency and magnitude of DENV infection [235]. This has since been demonstrated with other flaviviruses as well as viruses from other families such as alphaviruses, human immunodeficiency virus (HIV), influenza, and RSV [236-241]. In addition, ADE-mediated infection *in vitro* has been shown to dampen cellular antiviral immune responses, alter cytokine responses, and result in more robust infection independently of extrinsic ADE in a process termed *intrinsic* ADE [242-245]. Indeed, altered cytokine responses have been correlated with more severe disease outcomes in DENV infected patients [246].

ADE is mediated both by non-neutralizing antibodies as well as neutralizing antibodies that are not concentrated enough to fully neutralize a particle and prevent infection after ADCP, which explains why only dilute antisera enhanced viral plaque formation in Hawkes' original experiments. ADE also explains why prior DENV infection is a major risk factor for severe disease from secondary infection. After a given period of time, the antibodies generated to a primary serotype may still cross-bind to a secondary serotype but have waned enough to no longer effectively cross-neutralize, generating infectious antibody:virus complexes which are more efficiently taken up by Fcγ receptor-bearing cells and can lead to more robust, less controlled infection. In 2017,

Katzelnick *et al.* confirmed that ADE of DENV occurs in individuals with low antibody titers acquired from prior infection [247].

ADE is a critical topic in the field of flavivirus vaccinology, as acutely demonstrated by the failure of the first approved vaccine for DENV, Dengvaxia (Sanofi Pasteur). Dengvaxia is a combination vaccine of four chimeric live attenuated viruses composed of DENV1-4 prM-E structural proteins in an attenuated YFV (17D) backbone [248]. It was licensed in more than 20 countries between 2015-2017 before safety signals arose suggesting increased risk for hospitalization in children under the age of 9 [249, 250]. It was later shown that the vaccine protected DENV-seropositive individuals who had already experienced natural infection but sensitized seronegative individuals to more severe disease [251]. Many attribute this to ADE caused by an imbalanced immune response to the different serotype components of the vaccine, thereby mimicking primary DENV infection and priming seronegative individuals for a severe secondary infection [252-258]. Recommendations for Dengvaxia were subsequently limited to seropositive individuals before a lack of demand led Sanofi Pasteur to discontinue production of Dengvaxia in 2025 [259, 260]. Requirements for the evaluation of future DENV vaccines following this crisis are now more stringent to ensure higher safety standards including evaluation of ADE risk [248, 261].

Though DENV is the only flavivirus for which ADE has been confirmed in humans, ADE has been demonstrated under experimental conditions *in vitro* and *in vivo* for numerous others including both MBFVs and TBFVs [24, 235, 247, 262, 263]. Monoclonal antibody therapy for TBEV in Europe has been associated with ADE leading to the discontinuation of this form of therapy [264-266]. Experimental results have often demonstrated that monoclonal antibodies or polyclonal serum targeting one flavivirus induce ADE for other closely related flaviviruses similar to what is seen with the ADE observed after heterologous DENV serotype infection [24, 263, 267]. This interaction between the immune responses to related flaviviruses is attributed to the generation of cross-reactive antibodies that do not cross-neutralize. It is prudent, therefore, to evaluate both correlates of protection (such as neutralizing antibodies) and risk (such as cross-reactive, poorly neutralizing antibodies) for flavivirus vaccines and monoclonal antibody therapies. To this end, additional features of antibody responses to flavivirus infections and vaccination have been identified for their ability to contribute to ADE risk. Antibodies targeting immunodominant epitopes such as prM and the FLE of E have been identified as highly cross-reactive promoters of ADE with little to moderate neutralizing potential and the ability to rescue less infectious immature particles [84, 89-94, 268, 269]. In contrast, antibodies targeting other epitopes such as the third domain of E (EDIII) or quaternary E dimer epitopes

(EDE) at the interface between E dimers on mature particles have been identified as potently neutralizing (Figure 1.2.7) [91, 95-100, 270-274]. Finally, because neutralizing antibodies contribute to ADE at low enough concentrations, the durability of the neutralizing antibody response is an important metric to evaluate the long-term consequences of immunity.

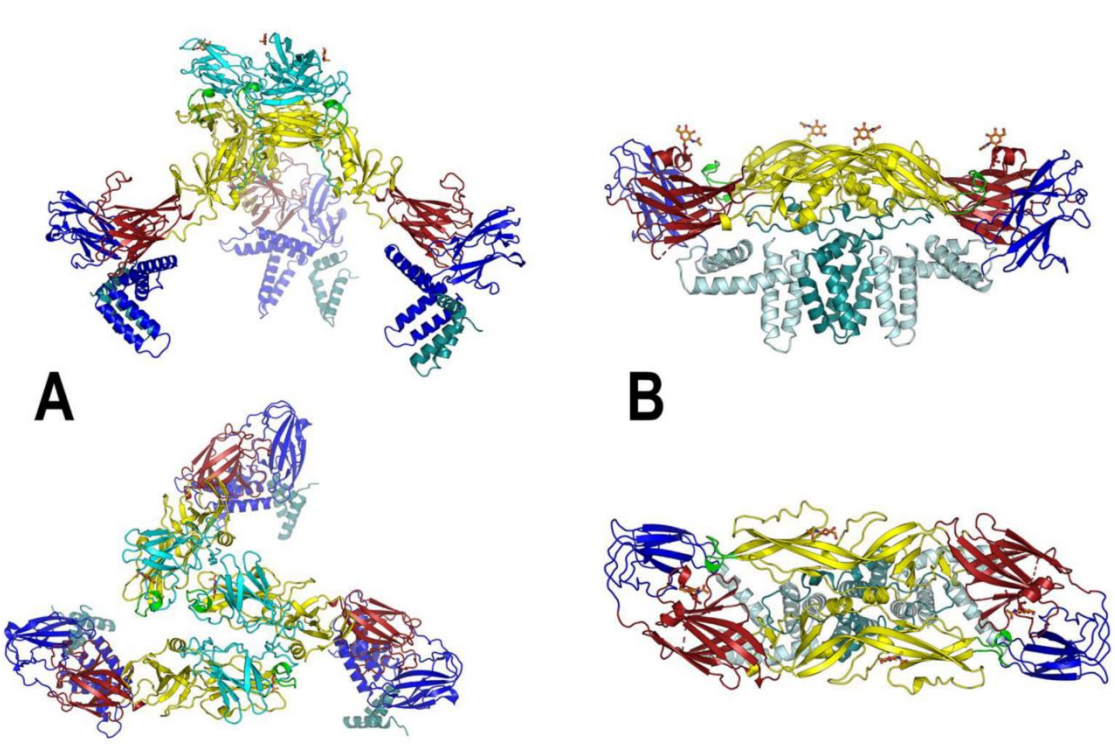

Figure 1.2.7: Immature and mature (pr)M-E complexes colored by domain/region.

Models of A) immature DENV-I trimer and B) mature USUV dimer depicted from the side (top images) or from above (bottom). EDI is in red, EDII yellow, EDIII blue, FL green, prM cyan, E stem light blue, M teal, and with glycosylation depicted by orange ball-and-stick models. Interaction between adjacent E monomers to form the EDE can be seen in the lower panel of B. Figure adapted from [275] published under Creative Commons license.

1.2.11 Powassan virus

POWV is a pathogenic TBFV found in North America and the Russian Far East [276-278]. Transmission to humans occurs through two ixodid tick vectors *Ixodes scapularis* (the black-legged tick or deer tick) and *Ix. cookei* (the groundhog tick), though the virus has been documented in mosquitoes and numerous other tick species [276, 279, 280]. *Ix. scapularis* is implicated as the main pathogenic vector of POWV due to its aggressive human-feeding behavior, while *Ix. cookei* may be less medically relevant due to its lack of questing behavior and preference for groundhogs and mustelids [276, 278]. However, *Ix. cookei* appears to be more aggressive towards humans in Maine and may be responsible for a greater share of transmission in that state [281]. It is believed that POWV is maintained in nature by enzootic cycles between multiple tick vectors and their hosts [278]. Several vertebrates have been implicated as possible reservoir hosts based on seroprevalence data, viremia, and/or tick-feeding behavior. These possible

reservoirs include groundhogs, opossum, raccoons, porcupines, weasels, birds, woodchucks, skunks, white-footed mice, voles, red squirrels, and chipmunks [276, 279, 280, 282-288]. Vertical and transstadial transmission have also been demonstrated for POWV in *Ix. scapularis* which may be important for maintenance of the virus in nature [289]. Milk-borne vertical transmission has also been experimentally demonstrated in goats, a route of transmission often associated with outbreaks of the closely related TBEV [290, 291].

POWV was originally discovered in the brain of a child who died of encephalitis in Powassan, Ontario in 1958 [292]. Twenty-seven cases of POWV disease were reported over the following four decades in Canada and the United States indicating that spillover into humans was rather rare [288]. However, the incidence of cases has been rising sharply over the past two decades with 60 reported cases in 2024 in the United States alone and a total of 397 cases in the United States since 2004 (Figure 1.2.8). Case distribution has also been expanding well beyond the northeastern United States, Great Lakes region, and eastern Canada where most cases were historically concentrated [158, 288]. POWV disease in humans has now been recorded as far west as North Dakota and as far south as North Carolina (Figure 1.2.9) [158, 293]. Similar trends in Lyme disease (also spread by *Ix. scapularis*) have been observed with roughly nine-fold more cases of Lyme disease in the United States in 2023 than in 1992 [294, 295]. The emergence

of POWV is likely due to multiple factors including increased diagnosis and case reporting [158]. However, a growing body of evidence indicates that it is most likely due to an increased burden of POWV in nature caused by ecological disturbances and climate change leading to increased density and distribution of POWV vectors such as *Ix. scapularis* [152, 158, 296-298].

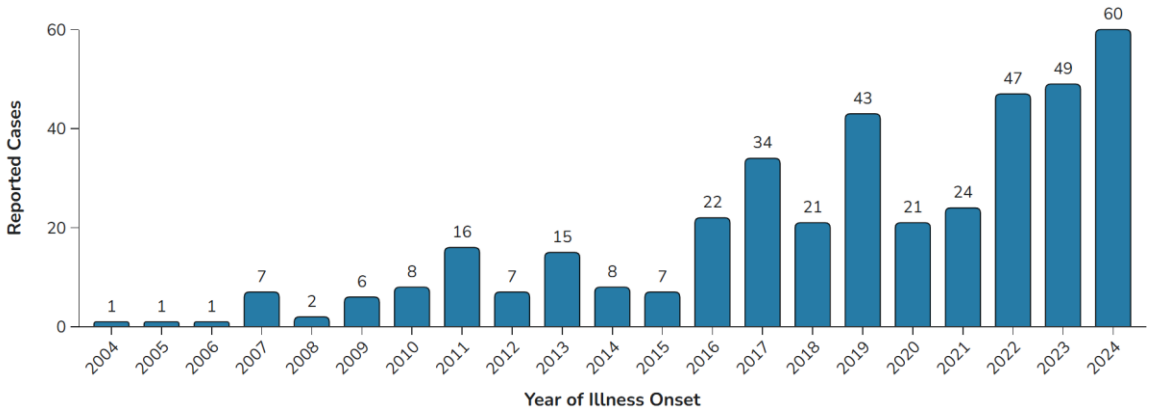

Figure 1.2.8: POWV cases in the United States by year, 2004-2024.

Reported cases of POWV disease in humans by year, beginning in 2004. Figure adapted from the CDC [299].

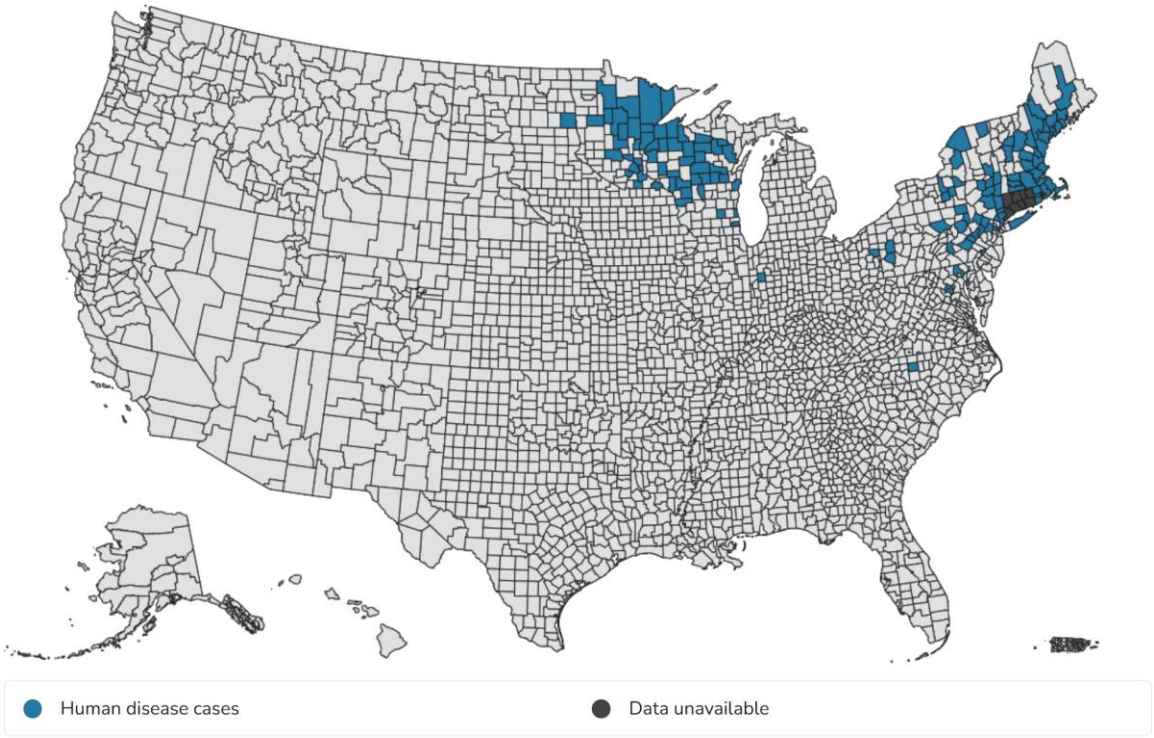

Figure 1.2.9: POWV cases in the United States by county, 2004-2024.

Reported cases of POWV disease in humans by county, beginning in 2004. Data unavailable for Connecticut by county due to recent changes in data collection. Figure adapted from the CDC [299].

There are two recognized lineages of North American POWV transmitted by distinct tick species: POWV lineage I (POWV-I) transmitted by *I. cookei* and lineage II (POWV-II) transmitted by *I. scapularis* [276, 300, 301]. POWV-II is often referred to as deer tick virus (DTV), though these lineages share 84% nucleotide sequence identity and 94% amino acid sequence identity, similar to the 83-86% nucleotide identity and 93-95% amino acid identity shared between subtypes of TBEV [302, 303]. These lineages appear to have diverged approximately 500 years

ago and share a common ancestor with isolates of POWV from the Russian Far East that existed during the last Ice Age [304, 305]. Both POWV-I and -II appear to cause similar neuroinvasive diseases in humans. However, there are notable differences in the pathology of infected mice, suggesting that there may be a difference in human cases of disease if the same level of scrutiny were applied [306]. Though the two lineages are serologically indistinguishable, POWV-II is believed to be more medically relevant due to the more aggressive human-feeding nature of *I. scapularis*, [158, 276, 307].

Infection with POWV occurs quickly after the bite of an infected tick [308]. As with other pathogenic flaviviruses, most infections appear to be largely asymptomatic. Seropositivity indicating prior POWV infection ranges from 0.4% in individuals bitten by *Ix. scapularis* or *Ix. cookei* in Maine, to 2-4% in individuals with no reported tick-borne disease in Wisconsin, to 9.4% in individuals with tick-borne disease in Wisconsin, and 22.9% in individuals with prior history of Lyme disease in the Northeast [309-313]. Based on high seropositivity and low case burden, it is estimated that only about 23% of POWV infections result in neuroinvasive disease [311].

POWV disease is most prevalent from May to July with a second peak in October and November corresponding to the seasonality of human exposures to *Ix. scapularis* and activity of *Ix. cookei* [293, 314, 315]. Symptoms begin 1-4 weeks

after a tick bite [159]. Illness is biphasic with fever, headache, and nausea that may resolve before progressing to a more serious second phase characterized by replication of the virus in the CNS [316]. Clinical features of severe disease include encephalitis, meningitis, and meningoencephalitis with symptoms ranging from headache to decreased mental status, seizures, cranial nerve palsies, ataxia, paresis, paralysis, cerebral edema, and coma [159, 316]. Clinical POWV disease is nationally notifiable and defined by the CDC as having signs of disease with no other likely explanation along with either 1) isolation of the virus from the patient, 2) a 4-fold increase in antibody titers, 3) anti-POWV IgM with virus neutralization, or 4) IgM specific for POWV and no other endemic arboviruses [317]. Epidemiological data suggests a case fatality rate of 12.5%, with disease in children often less fatal than in the elderly [316]. Long-term neurological deficits are reported in roughly 50-62.7% of POWV cases [316].

There are currently no therapies or vaccines for POWV. Development of a vaccine is critical as we continue to witness the emergence of this deadly virus in North America. This dissertation focuses on the development of an adjuvanted VLP-based vaccine for POWV capable of eliciting durable protection from viral neuroinvasion, disease, and death while maintaining high standards of safety. The sections that follow will elaborate on vaccine platforms, vaccine immunology, adjuvants, and current flavivirus vaccines.

Section 1.3: Vaccines

1.3.1 A brief history of vaccines

Edward Jenner is often credited as the father of vaccines after developing a method to safely immunize against smallpox. However, inoculating individuals against smallpox (not yet termed vaccination) had been widespread throughout Europe well before Jenner, and the invention of vaccines dates much further back in time [318]. The observation that smallpox survivors were immune from subsequent infections is noted as far back as 430BC, a foundational observation on which modern vaccinology is built. The first instances of inoculation against smallpox can be traced back to the 10th century in China with records describing the inoculation of naïve individuals with scabs, fluids, or pus of smallpox survivors. By the 17th century, inoculation was practiced in Africa and India, and the practice made its way into Europe via Turkey to gain traction in the west in the 18th century where it boasted a low mortality rate of 2% compared to the 14% of natural smallpox infection. Jenner is credited with introducing cowpox-based inoculation, a safer form of inoculation which he termed vaccination, though he was not the first to practice this method. In fact, the observation that cowpox exposure protected against smallpox had been well understood in India "since the

earliest recollection of man [319]." However, Jenner was certainly instrumental in the popularization of vaccination which grew into a global effort that saw the eradication of smallpox by 1979 and has saved countless lives.

Vaccination against other diseases grew from Robert Koch's germ theory in the 1870-80s [320]. The ability to isolate and study pathogens in a laboratory setting quickly led to the development of both inactivated and live attenuated vaccines. In 1886, Daniel Salmon and Theobald Smith demonstrated that heat-killed *Salmonella* (named after Daniel Salmon) generated protective immunity in pigeons [321]. (As a side note, Smith later went on to be the first to discover that some pathogens spread to mammals from insects while studying *Babesia bigemina* transmission to cattle from ticks [322, 323].) Meanwhile, the effectiveness of inactivated vaccines was independently discovered in the lab of Louis Pasteur while developing inactivated vaccines for typhoid, cholera, and plague [324].

Live attenuated vaccines for anthrax, rabies, and chicken cholera were developed in the 1880s in the labs of William Greenfield (UK) and Louis Pasteur (France) via continuous subculture, chemical, heat, and environmental attenuation [325-327]. (Some consider the first Pasteur rabies vaccine to be inactivated, and the vaccine was indeed later transitioned to a chemically inactivated version.) This was followed by Albert Calmette and Camille Guérin developing a tuberculosis vaccine by attenuating *Mycobacterium bovis* in the 1920s and Max Theiler

developing the 17D yellow fever virus (YFV) vaccine of the 1930s by attenuation [325]. The development of *in vitro* cell culturing brought another wave of live attenuated vaccines for polio, measles, mumps, and rubella in the 1960s.

1.3.2 Vaccine platforms: from live attenuated to virus-like particles

Vaccination methods, or 'platforms,' continued to evolve throughout the 1900s leading to more effective vaccines with less risk (Figure 1.3.1) [320]. The advent of tissue culture led to the ability to propagate virus for inactivated viral vaccines in large quantities [328, 329]. Inactivated vaccines offer a much safer alternative to live attenuated vaccines which are not recommended for pregnant or immunocompromised individuals due to risk of reversion, transmission, and disease. However, inactivated vaccines still carry risk. Vaccine injury caused by incomplete inactivation has occurred more than once [330]. For example, in 1955, the pharmaceutical company Cutter Laboratories distributed incompletely inactivated poliovirus vaccine resulting in 51 cases of permanent paralysis and 5 deaths [331]. Though federal requirements for vaccine manufacture have been revised, and no other major incident has occurred in the United States, the tragedy of 'The Cutter Incident' and other incidences outside the United States highlight the inherent risk of inactivated pathogen vaccines and the need for safer alternatives [331].

Subunit vaccines were another major advance in vaccinology. These were developed to reduce the risk of adverse events and the reactogenicity inherent in live attenuated and inactivated pathogen vaccines. Instead of targeting entire pathogens, subunit vaccines elicit protective immune responses to individual pathogenic antigens such as toxins or proteins found on the surface of a pathogen. In the 1920s, the first inactivated toxin subunit (toxoid) vaccines for diphtheria and tetanus were developed by inactivating toxins with formaldehyde [320, 332, 333]. Half a century later, the first non-toxoid subunit vaccine was developed in the 1970s by disrupting the viral lipid envelop of influenza to reduce the reactogenicity common to whole inactivated pathogen vaccines [334, 335]. Subunit vaccines with minimal reactogenicity were also developed for pneumococcus and pertussis using polysaccharides and surface proteins from the pathogens, respectively [336, 337]. The safety and versatility of subunit vaccines make them incredibly useful for designing highly specific vaccines. However, the reduced reactogenicity of this vaccine platform comes at the cost of immunogenicity, and adjuvants and protein carriers are added to these vaccines to boost the immune response as discussed later in Section 1.3.8 [320].

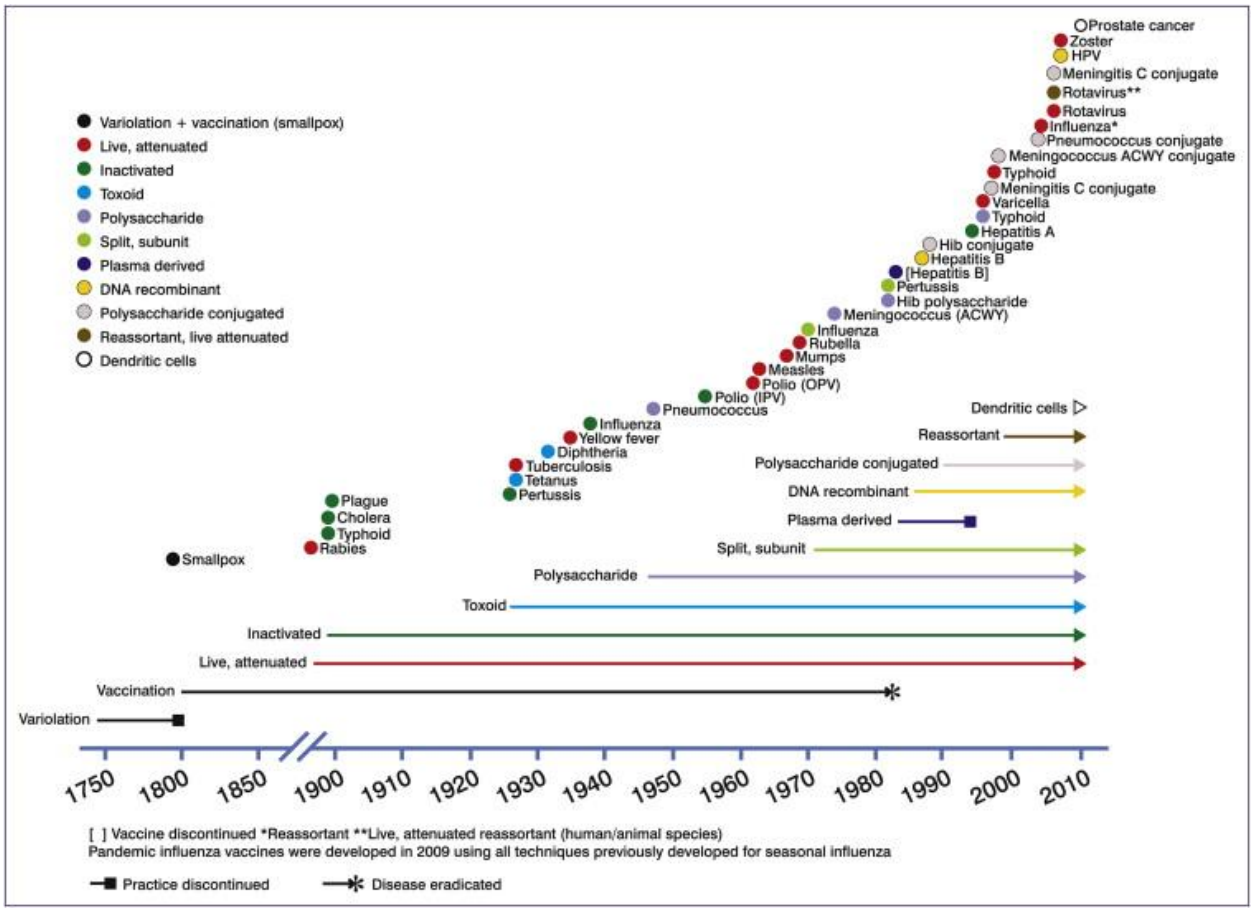

Figure 1.3.1: The evolution of vaccine platforms.

The timeline of vaccine development for various diseases depicted by colored dots corresponding to the color key of vaccine platforms in the top left and the colored arrows depicting when these platforms came about. Figure unmodified from [320] published under Creative Commons license. Please note, this figure was published in 2011 before mRNA vaccines made their debut.

Virus-like particle vaccines

The advancement of recombinant DNA technology in the 1960s and '70s led to the development of the first vaccine using proteins made from DNA recombination in the '80s for HBV (Recombivax-HB) [338-341]. This was a major milestone in vaccinology. Most vaccines in development today are composed of purified proteins made using recombinant DNA [338]. Recombivax-HB is also the first use of virus-like particles (VLP) as vaccine antigen.

The term VLP was first coined by the Nobel Laureate Macfarlane Burnet in 1933 to describe non-infectious particles that resemble infectious virus but without genetic material and, therefore, without the potential to replicate [342, 343]. VLPs are generated by expressing viral structural proteins in yeast, insect, mammalian, or plant tissue [344]. These proteins then self-assemble into VLPs that mimic the structure of the viruses from which they are derived. These particles can serve as vaccine antigen to elicit immune responses to the target pathogen. VLPs are inherently safer than whole pathogen vaccines, because they are nonpathogenic and lack the genetic material necessary for replication. Additionally, VLPs are quite immunogenic and can induce both humoral and cellular immunity which arises from multiple factors [345]. Firstly, VLPs display structural proteins that are often the target for neutralizing antibody responses in a highly-repetitive near-native conformation [346]. This makes them ideal targets for multimeric IgM and

complement C1q interactions which leads to more efficient follicular dendritic cell (FDC) deposition compared to that seen with soluble protein [347]. Antigen deposition on FDCs facilitates humoral immunity as discussed later in Section 1.3.7. Secondly, the repetitive display of antigen is excellent at activating B cell receptors (BCRs), especially when complexed with complement [346, 348]. Thirdly, due to their size and by interacting with complement, IgM, and BCRs, VLPs are efficiently trafficked to lymph nodes (LNs) for display during germinal center reactions (GCRs) [349, 350]. Fourthly, their size and antigenic features, which often include repetitive glycosylated proteins, promote phagocytosis by and stimulation of antigen-presenting cells (APCs) such as DCs to help promote cellular immune responses [345, 351-353]. Lastly, they are excellent antigens for producing high-quality antibody responses, because VLPs maintain native epitope structure without the need for formalin inactivation which may damage epitopes [354, 355].

After the licensure of Recombivax-HB for HBV, the first prophylactic cancer vaccine (Gardasil) was developed using bivalent human papilloma (HP)-VLP to protect against two types of cancer-causing HPV [356-358]. Today, there are several licensed VLP-based vaccines targeting HBV, HPV, hepatitis E virus (HEV), chikungunya virus (CHIKV), and even *Plasmodium* [343, 344, 353, 359, 360]. VLP-

based vaccines targeting HIV, rotavirus, influenza, and flaviviruses are also being explored.

Modern technological advances continue to generate new vaccine strategies. Our repertoire of vaccine strategies now includes viral-vector, DNA, and mRNA vaccines, with this last platform emerging just in time to prevent millions of deaths during the COVID-19 pandemic [361-364]. Though each of these strategies has its own unique strengths, the focus of this dissertation is on the use of VLP as vaccine antigen due to this platform's proven safety, scalability, and demonstrated potential for eliciting protection against multiple flaviviruses [106, 365-368].

1.3.3 Vaccine immunology

Vaccines are our greatest public health resource. Childhood vaccination programs against just 14 common pathogens have saved an estimated 154 million lives over the past 50 years alone [369]. Vaccines accomplish this by co-opting our natural immune responses to confer immunity to a given pathogen without the disease associated with natural infection. These immune responses can be divided into two categories: innate and adaptive. Innate immunity refers to immediate, often transient, non-specific defenses including molecular and cellular mechanisms that rapidly target a wide range of pathogens. Adaptive immunity

(also known as acquired immunity) refers to the durable immune response generated against a specific pathogen after vaccination or natural infection as an 'adaptation' to that pathogen [43]. In this section and those that follow, I will discuss the concepts of innate and adaptive immunity and how we co-opt these processes with vaccines to generate protection against infectious diseases.

Protection by adaptive immunity is the goal of vaccination and stems from the observation that natural infection often elicits immunity to future infections from the same pathogen. This phenomenon has been observed for millennia, with the first written record dating back to ~430BC when Thucydides of Ancient Greece noted that "the same person was never attacked twice—never at least fatally" during the Plague of Athens [370]. Seminal experiments in 1890 led by Emil von Behring demonstrated that adaptive immunity could be conferred to naïve animals via the humor (serum) of immune animals [371]. These experiments gave rise to the concept of humoral immunity and antitoxins which were later renamed 'antibodies' [372]. Paul Ehrlich was the first to propose a model for how antibody responses to *anti*body *gen*erating substances (antigens) were responsible for generating this humoral adaptive immunity [373]. However, it was Frank Macfarlane Burnet later in 1957 who proposed the clonal selection theory of immunology to provide our current model for how antibodies are generated against foreign antigens which set the stage for modern immunology [374].

According to this theory, individual cells exist in the body that each produce a distinct "reactive site" on their surface which may be liberated as soluble antibody. These cells (now known as B cells) allow the immune system to recognize virtually any foreign antigen that may be encountered. Upon antigen-recognition by its unique surface receptor, a given B cell proliferates to generate a "variety of descendants" which produce antibodies to react with the antigen and ensure that the re-introduction of this antigen can be met with swiftly by a large clonal population of antigen-specific B cells. This clonal selection theory is foundational to modern molecular immunology, adaptive immunity, and vaccinology.

It is now understood that the theory of clonal selection applies to both B cells and T cells [43]. The receptors on these cells are generated by a form of DNA rearrangement that results in unique B cell receptors (BCRs) and T cell receptors (TCRs) which each recognize distinct non-self antigenic epitopes. B and T cells circulate through blood and lymphoid tissues to survey for their cognate antigen. When these cells encounter their cognate antigen along with the appropriate co-stimulatory signals discussed in the following section, they proliferate and differentiate into effector cells that confer protective adaptive immunity.

The function of vaccines is to present foreign antigens to the immune system in such a way that stimulates these protective B and T cell responses outside the context of infection. To accomplish this, vaccines must provide the

proper antigenic target and co-stimulatory signals to drive an adaptive immune response. In sections 1.3.4 through 1.3.6, I will discuss how our innate immune system recognizes pathogens and provides the appropriate stimulatory factors to drive an adaptive immune response. In section 1.3.7, I will describe the adaptive immune response in greater depth and explain how it provides protection from future infections. In section 1.3.8, I will discuss how vaccine adjuvants co-opt these processes to enhance the protective efficacy of vaccines.

1.3.4 Innate immunity and pattern recognition receptors

While Burnet's theory of clonal selection revolutionized our understanding of the immune system, it had gaps that led to the fallacy that all foreign antigens are in and of themselves capable of generating an adaptive immune response [375, 376]. Multiple lines of evidence challenged this view, however, and led to a new model in which an adaptive immune response to foreign antigen requires two signals: 1) recognition of antigen by a BCR or TCR *and* 2) co-stimulatory signals associated with infection [375, 377]. Recognizing that there must be a system for distinguishing between harmless and harmful antigens for this two-signal model to function, Charles A. Janeway, Jr. famously predicted the existence of pattern recognition receptors (PRRs) that recognize pathogen-associated molecular patterns (PAMPs) in 1989. He proposed that the recognition of PAMPs by PRRs

generates the co-stimulatory signal required for an adaptive immune response to infectious antigens and that this checkpoint helps prevent harmful immune responses to self-antigen.

Janeway and others later confirmed the existence of PRRs with the discovery of a Toll-like receptor 4 (TLR4) whose activation leads to the expression of co-stimulatory molecules on APCs [378]. It was later discovered that TLR4 recognizes a component of bacterial cell membranes, solidifying Janeway's theory on the existence of PRRs [379]. The concept of PAMPs and PRRs revolutionized immunology. It is now well-established that stimulation of an innate immune response via PRRs is key to the initiation of an adaptive immune response, and that this can be achieved either through infection or the use of adjuvants to generate co-stimulatory signals outside the context of infection.

Pattern recognition receptors

There are six groups of PRRs in humans: AIM2-like receptors (ALRs), C-type lectin receptors (CLRs), cyclic AMP-GMP synthase and stimulator of interferon genes (cGAS), nucleotide-binding domain and leucine-rich repeat-containing receptors (NLRs), retinoic acid-inducible gene I (RIG-I)-like receptors (RLRs), and Toll-like receptors (TLRs) [380]. The transmembrane TLRs and CLRs are found on the cell surface and intracellular membranes while the other PRRs

are found in the cytosol. Each receptor recognizes its own specific PAMPs. For example, TLR4 recognizes bacterial lipopolysaccharide (LPS) while TLR7 recognizes viral ssRNA (Figure 1.3.2) [381]. Expression of these receptors varies by cell type, with some expressed relatively exclusively and others more broadly. TLR7, for example, is expressed most strongly in plasmacytoid dendritic cells (pDCs) while TLR5, which recognizes flagellated bacteria, is found in the intestinal epithelium, macrophages, and DCs [43, 382-385].

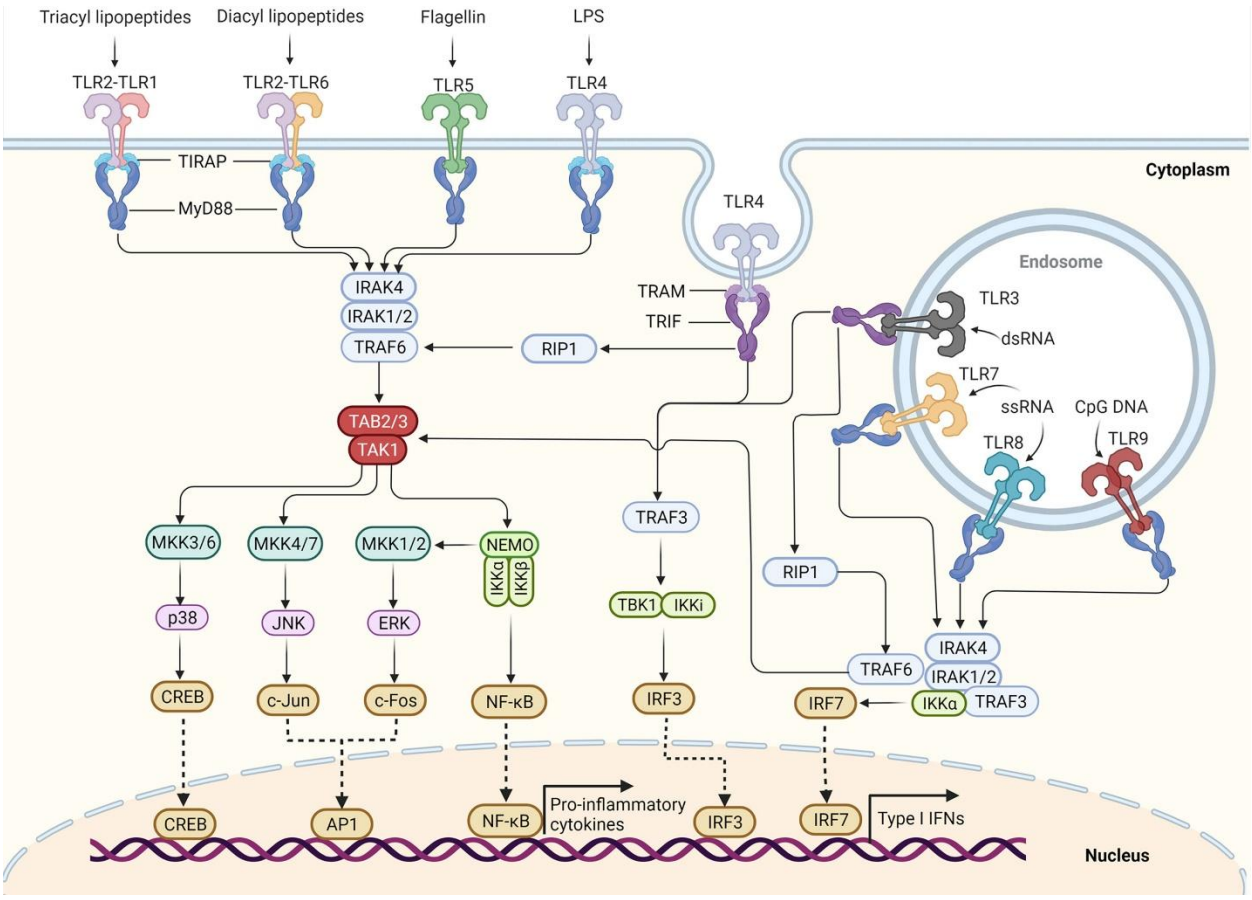

Figure 1.3.2: TLRs: their subcellular location, agonists, and signaling pathways.

A depiction of human TLRs, where they are located in the cell, the PAMPs they recognize, and their downstream signaling pathways. Figure unmodified from [381] published under Creative Commons license.

The stimulation of these receptors by PAMPs induces signaling cascades that can trigger interferon (IFN) responses, pro-inflammatory cytokine responses, and cell death, with the responses differing by receptor, cell type, and manner of stimulation [43]. These responses help to inhibit viral replication, recruit and activate innate immune effectors like APCs, and ultimately promote adaptive immunity. Much of vaccine development is focused on understanding how to trigger the proper innate immune response to achieve the desired adaptive immune response. As this dissertation focuses on the use of TLR agonists as vaccine adjuvants to improve adaptive immune responses, I will focus on this family of PRRs in the following section.

1.3.5 Toll-like receptors

TLRs are one of the best studied families of PRRs. There are ten functional TLRs in humans (TLR1-10) and 12 in mice (TLR1-9 and TLR11-13) [386]. These are membrane-bound receptors found either on the cell surface (TLR1, 2, 4, 5, 6, 10),

intracellular compartments (TLR3, 4, 7, 8, 9, 11, 12, 13), or both (TLR4) (Figure 1.3.2) [386-388]. The ectodomains of TLRs contain leucine-rich-repeats which are connected to a cytoplasmic Toll-interleukin-1 receptor (TIR) domain via a single pass transmembrane domain [43, 389]. The ectodomains of TLRs are responsible for PAMP recognition (Figure 1.3.2) [43]. For example, TLR7 recognizes the ssRNA genome of flaviviruses while TLR3 recognizes the dsRNA replicative intermediate of flavivirus genomes [43, 390]. Ligand recognition by some TLRs involves accessory factors such as MD-2 and CD14 for facilitating TLR4 binding LPS [43, 391].

Ligand binding induces TLR heterodimerization (for TLR1+2, TLR2+6) or homodimerization (all other TLRs) which brings the intracellular TIR domains into proximity for downstream signaling [43, 392]. Dimerized TIR domains interact with the adaptor proteins TRIF-related adaptor molecule (TRAM) and/or TIR-containing adaptor protein (TIRAP) which recruit the signaling factors TIR domain containing adaptor-inducing IFN-β (TRIF) and myeloid differentiation factor 88 (MyD88), respectively (Figure 1.3.2) [381, 389]. All TLRs interact with MyD88/TIRAP except for TLR3 which interacts exclusively with TRIF/TRAM. TLR4 interacts with both MyD88/TIRAP on the cell surface and TRIF/TRAM in the endosomal compartment [43, 393, 394].

The result of TLR activation depends both on the signaling factor (MyD88 vs TRIF) and on the cell type. MyD88 signaling downstream of TLR1, -2, -4, -5, and -6 culminates in the activation of the transcription factors nuclear factor kappa B (NF-κB) and activator protein 1 (AP-1) which drive transcription of inflammatory gene products [381, 389]. In pDCs, which selectively express endosomal TLR7 and TLR9 along with constitutively high levels of interferon regulatory factor (IRF)-7, MyD88 signaling from the endosome activates IRF-7 to drive an IFN-I response as well as IRF-5 to induce the production of inflammatory cytokines such as interleukin 6 (IL-6), IL-12, and tumor necrosis factor alpha (TNF-α) [381, 389, 395, 396]. TLR8, another MyD88-dependent endosomal TLR, appears to be most active in monocytes, granulocytes, macrophages, conventional dendritic cells (cDCs), and monocyte-derived DCs (moDCs) which express low levels of IRF-7 and where downstream MyD88 signaling drives more of an inflammatory response through NF-κB and IRF-5 rather than an IFN-I response [397-400]. The TRIF signaling downstream of TLR3 and intracellular TLR4 activates NF-κB, AP-1, and IRF-3 to drive both inflammatory and IFN-I responses [381, 401].

In addition to inducing pro-inflammatory and IFN responses, TLR signaling also promotes the maturation of APCs and their migration to the LN for antigen presentation and priming of T cells discussed in section 1.3.7 [402]. In this way, TLRs help bridge innate and adaptive immunity. The distinct ligands,

signaling pathways, and cellular distribution of these TLRs help to tune the adaptive immune response to the specific pathogen being encountered through differential activation of APCs, IFN, and pro-inflammatory cytokines. This makes TLR agonists excellent adjuvants for enhancing and shaping adaptive immune responses to vaccines.

TLR7 and TLR8

As TLR4, TLR7, and TLR8 are important for this dissertation, I will discuss these in more depth here, beginning with TLR7 and TLR8. These PRRs are generally described as both recognizing ssRNA, but there are subtleties to this and differences to the ligands each detects. Both TLR7 and TLR8 have two distinct ligand binding pockets which bind products of ssRNA generated by endogenous endo- and exonucleases [403, 404]. In TLR7, these pockets bind guanosine and/or guanosine 2′,3′-cyclic phosphate (2′,3′-cGMP) alongside pyrimidine-rich oligoribonucleotides, while in TLR8 they bind uridine and purine-cyclophosphate-terminated oligoribonucleotides [403-407]. The difference in the ligands recognized by TLR7 and TLR8 translates to a difference in the agonists that stimulate these receptors as discussed in section 1.3.8.

In humans, TLR7 is expressed most strongly in pDCs but also in B cells, monocytes, and cDCs [382, 397, 408-411]. TLR8 is expressed most strongly in

monocytes but also found in cDCs, moDCs, granulocytes, and to some extent in B cells. In mice, TLR8 is also expressed in pDCs but does not recognize the same ligands as human TLR8 [409, 412-415]. There are, however, discrepancies between studies on which cells express which TLRs, and expression of a TLR within a cell population does not guarantee it is functional within those cells. In one study investigating the functionality of TLR7 and TLR8 in different human cell populations, Bender *et al.* found that TLR7 stimulation of PBMCs induces expression of IL-1β from monocytes and moDCs, while TLR7-stimulated pDCs produce TNFα and IFNα [397]. Meanwhile, monocytes and moDCs were the major responders to a TLR8 adjuvant and induced expression of IL-6, IL-1β, and TNFα. Despite evidence of TLR7 expression, B cells did not respond to either TLR7 or TLR8 activation as measured by IFNα, IL-6, IL-1β, and TNFα.

TLR4

In both humans and mice, TLR4 is constitutively expressed in monocytes, macrophages, moDCs, cDCs, and granulocytes as well as various other non-hematopoietic tissues, whereas mice additionally express TLR4 in pDCs, lymphoid cells, and muscle cells which may or may not express TLR4 in humans [382, 397, 408-411, 416, 417]. TLR4 signals from two distinct compartments and sets of signaling factors. It first signals through MyD88 at the cell surface to activate

NF-κB and MAPK [389]. TLR4 is subsequently endocytosed, after which it signals through TRIF from the endosome to activate NF-κB, MAPK, and IRF-3.

The major ligand of TLR4 is LPS on Gram-negative bacterial cell walls, though it also recognizes several other PAMPs including lipoteichoic acid (LTA), fibrinogen, and β-glucans among others [418]. Furthermore, TLR4 also appears to play a role in flavivirus infections by recognizing flavivirus NS1 [419, 420]. Ligand binding requires adaptor molecules. These include MD-2 which is required for the recognition of LPS by TLR4, LPS-binding protein (LBP) which binds soluble LPS and brings it to the cell membrane, and membrane-bound CD14 which brings LBP:LPS to TLR4:MD-2 on the cell surface [418].

1.3.6 The interferon response

Chapter 6 begins to explore the role of the IFN response in vaccination, so I will describe this response in detail here. IFNs are cytokines released in response to infection that have direct antipathogenic effects and help regulate adaptive immunity [421]. There are three types of IFN responses, each with their own distinct IFNs. Type 1 IFN (IFN-I) responses involve IFN-β and IFN-α (the latter of which has multiple subtypes, but which I will refer to collectively as IFN- α); IFN-II involves IFN-γ; and IFN-III involves IFN-λ (Figure 1.3.3). Different cells produce different IFNs. During a viral infection, IFN-β can be produced by nearly any

infected cell while IFN-α is more restricted to pDCs which produce IFN-Is in excess [421]. For this reason, pDCs are sometimes called interferon-producing cells [422]. Natural killer (NK) cells, T cells, NK T cells, and innate lymphoid cells (ILCs) are the major sources of IFN-γ [423-425]. IFN-λ is mainly expressed at epithelial barriers where it helps control infection at surfaces like the intestine and lung [426]. I will discuss IFN-I and IFN-II here for their relevance to this dissertation. I will focus on their role in modulating adaptive immunity rather than orchestrating direct antiviral effects, as this is more relevant to the role IFNs play in vaccines.

IFN-Is are produced in response to both bacterial and viral infections, but they are most well known as antiviral cytokines [43]. Their production is mainly mediated by IRF-3 and IRF-7. Activation of these factors by relevant PRR signaling pathways leads to the expression of IFN-β and/or IFN-α [43]. These IFNs then work in both an autocrine and paracrine fashion through the interferon-α receptor (IFNAR) to activate the JAK/STAT signaling pathway (Figure 1.3.3). Briefly, binding of IFN-α or IFN-β activates STAT1 and STAT2 which dimerize and interact with IRF-9 to form a transcription complex that induces the expression of interferon-stimulated genes (ISGs) [43]. IFNAR signaling also activates various other STATs including STAT4 which together with IRF-5 induces the expression of IFN-γ [427, 428]. IFN-γ is initially produced by NK cells and ILCs in response to various cytokines including IFN-α and IFN-β [424, 425]. IFN-γ signals through

the IFN-γ receptor (IFNGR) which activates and dimerizes STAT1 leading to the expression of IFN-γ-regulated genes.

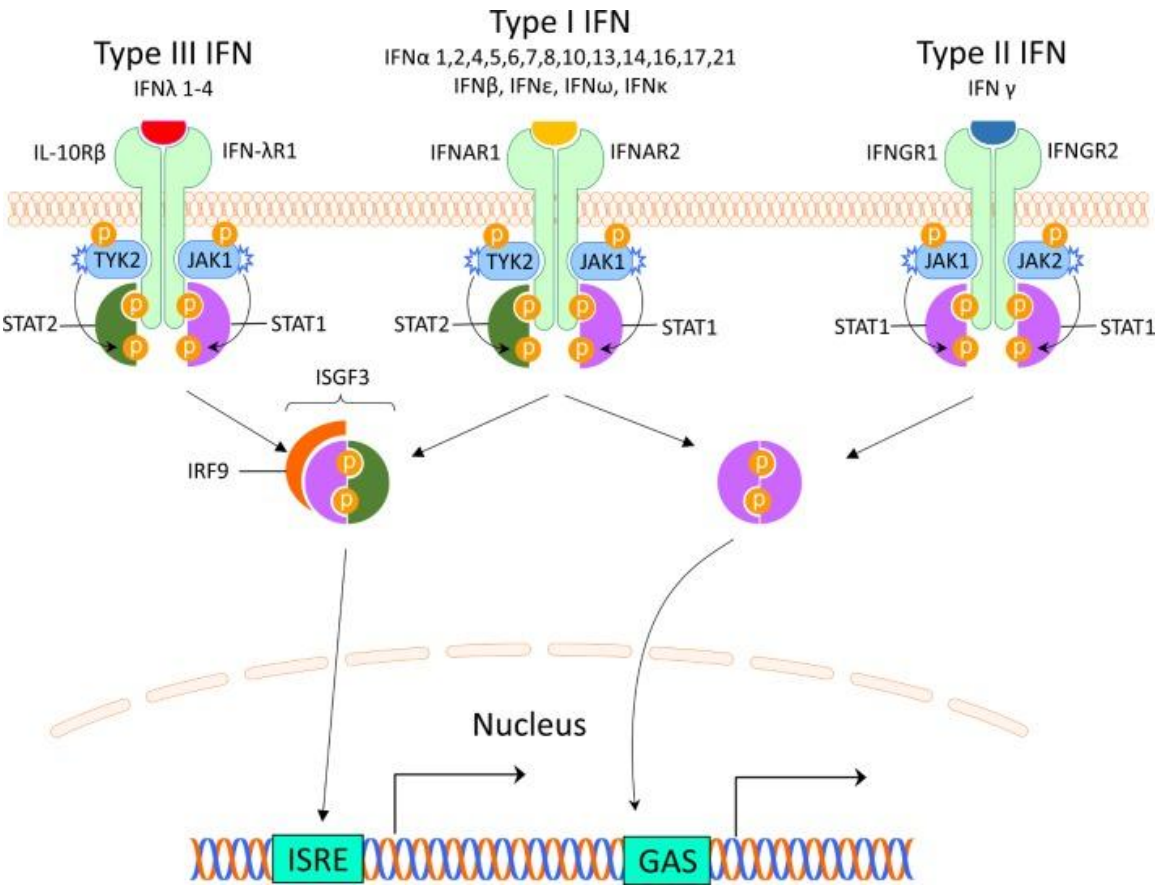

Figure 1.3.3: The IFN signaling pathways.

IFN-I, -II, and -III signaling pathways along with the individual IFNs that initiate them. IFN-Is (middle; IFN-α1, -α2, -α4, -α5, -α6, -α7, -α8, -α10, -α13, -α14, -α16, -α17 and -α21, IFN-β, IFN-ε, IFN-κ, and IFN-ω in humans) bind to the dimeric IFN α/β receptor (IFNAR) consisting of IFNAR1 and IFNAR2 subunits [429]. IFN-II (IFN-γ) binds to the IFN-γ receptor (IFNGR). IFN-IIIs (IFN-λ1, -λ2, -λ3, and -λ4) binds to the IFN-λ receptor (IFN-λR) consisting of IFNLR1 and IL-10Rβ. Ligand binding dimerizes the receptor subunits, resulting in the autophosphorylation and activation of Janus activated kinase (JAK) family receptors: JAK1 and TYK2 for IFN-I and -III; JAK1 and JAK2 for IFN-II. The classical signaling pathway that follows begins with the phosphorylation of STATs: STAT1 and STAT2 for IFN-I and -III; STAT1 only for IFN-II. These STATs then dimerize. For IFN-I and -III, STAT1-STAT2 then associate with IRF-9 to form the ISG factor 3 (ISGF3) which translocates to the nucleus and binds IFN-stimulated response elements (ISREs) to promote the expression of ISGs. For IFN-II, STAT1-STAT1 translocate to the nucleus and bind IFN-γ-activated site (GAS) elements which promotes expression of another set of ISGs. Figure unmodified from [430] published under Creative Commons license.

Together, both IFN-I and -II responses play an important role in generating adaptive immunity by activating APCs, B cells, and T cells [425, 431]. IFN-α and IFN-β enhance cellular immunity by directly stimulating DC maturation, monocyte differentiation into moDCs, and T cell activation to promote T cell priming and the cross-priming required for cytotoxic T lymphocyte (CTL) responses to subunit vaccines [432-440]. IFN-I signaling also promotes IFN-II

production from $CD4^+$ T cells which is important for T_H1 cell differentiation, promoting intracellular pathogen clearance by macrophages, and CTL responses [425, 437]. Furthermore, IFN-I promotes humoral immunity by directly and indirectly enhancing B cell activation, proliferation, and GCRs [431, 437, 441-443].

pDCs are a unique cell type that play an important role in the IFN-I response [444]. These rare cells are recruited to sites of inflammation and infection whereby they secrete large amounts of IFN-α and IFN-β upon stimulation of PRRs like TLR7 and TLR9 [445]. pDCs, therefore, play an important role in both cellular and humoral immune responses. Mice lacking pDCs have reduced IFN-I, IFN-II, and CTL responses [445, 446]. Additionally, the IFN produced by pDCs in response to TLR7 stimulation upregulates TLR7 expression in B cells which can then be stimulated themselves by TLR7 to proliferate and differentiate to secrete antibodies independently of T cells [447].

Given the immunogenic nature of IFN-I, it is not surprising that it has been shown to be a powerful vaccine adjuvant [448, 449]. Unfortunately, direct administration of IFN is known to cause significant side-effects [450]. Instead, adjuvants such as TLR7 agonists chosen to enhance the IFN-I response to vaccines are becoming more popular in preclinical vaccine studies and are demonstrating immense potential [451]. These adjuvants will be discussed more in section 1.3.8.

1.3.7 Adaptive immunity

Antigen Presentation

A protective adaptive immune response is the goal of vaccination. Adaptive immune responses fall into two categories: humoral immunity mediated by B cells and cellular immunity mediated by T cells [43]. Both begin with the presentation of antigen by specialized APCs. DCs, specifically cDCs, are potent APCs that take up antigens at the site of infection [43]. cDCs can be found both as residents of lymphoid tissue such as LNs and the spleen, as well as in non-lymphoid tissue like the lung and skin [452]. Other DCs that play a role in antigen presentation include Langerhans cells of the skin, moDCs, and pDCs, though these are variably efficient as APCs with pDCs playing a particularly minor role in antigen presentation [444, 453]. Macrophages and B cells also play a role in antigen presentation, though not as efficiently as DCs [454].

After antigen uptake, antigens inside APCs are processed by cellular proteases into peptides in the cytosol or endosome for presentation on MHC-I or MHC-II, respectively [455]. APCs like DCs express numerous PRRs and cytokine receptors [456]. PAMPs from invading pathogens and cytokines produced by other cells promote DC maturation, a process during which 1) the chemokine receptor CCR7 is expressed which facilitates migration of activated DCs toward the chemokine CCL21 produced by lymphoid tissue; 2) MHC-I and -II are

upregulated for more efficient antigen presentation to T cells; and 3) the co-stimulatory molecules B7.1 (CD80) and B7.2 (CD86) are expressed to prime T cells [43].

T cell priming

Naïve T cells migrating through secondary lymphoid tissues such as LNs, the spleen, and mucosa-associated lymphoid tissues will encounter activated DCs (diagram of a LN in Figure 1.3.4) [43]. Adhesion factors on T cells and DCs ensure both cells stay in contact for long enough for T cells to sample the peptide:MHC complexes present on the surface of DCs. Once a naïve T cell recognizes its cognate peptide:MHC antigen, changes in the adhesion proteins stabilize this association which can then last for several days. During this time, the APC activates the T cell which proliferates and differentiates into a clonal population of effector T cells. There are three signals that are canonically required for activating or *priming* a naïve T cell (Figure 1.3.5). The first is the stimulation of a T cell receptor (TCR) and co-receptor, either CD4 or CD8, by cognate peptide:MHC. The second set of signals comes from co-stimulatory molecules B7.1 and B7.2 which signal through CD28 on T cells to trigger entry into the G_1 phase of the cell cycle as well as enhanced production of IL-2 and expression of a high-affinity IL-2 receptor. IL-2 and other cytokines provide T cells with the final third signal critical for priming.

IL-2 works in an autocrine fashion to stimulate T cell activation, proliferation, and differentiation. In addition to IL-2, activated T cells express several additional receptors that potentiate co-stimulation. These include ICOS which is stimulated by ICOSL on activated DCs; CD27 which binds CD70 on DCs; OX40 which interacts with OX40L on DCs; CD40L which binds CD40 on DCs; and CD137 which interacts with 4-1BBL on DCs. In addition to stimulating T cells, CD40L:CD40 and CD137:4-1BBL signaling works bidirectionally to further potentiate APC activation [43]. All of these signals stimulate T cells to proliferate and differentiate into a clonal population of thousands of effector T cells bearing the same TCR.

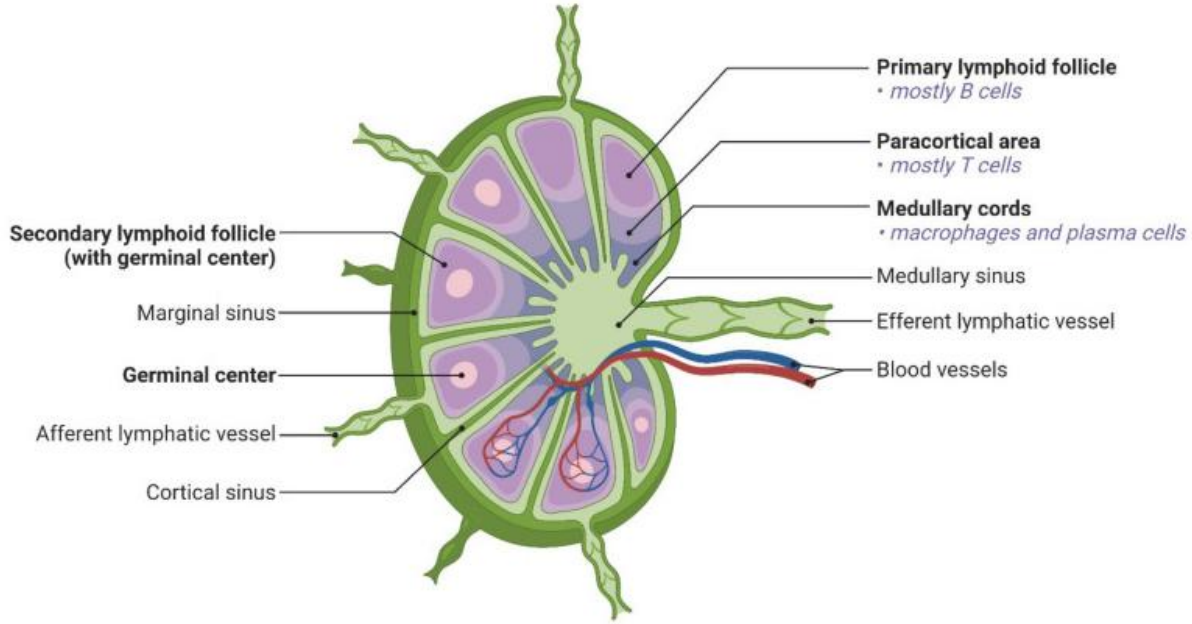

Figure 1.3.4: The compartments of a lymph node.

A diagram of a lymph node (LN) depicting the afferent lymphatic vessel by which antigens enter the LN; the marginal sinus (also called the subcapsular space) through which antigens pass to enter the LN; the B cell zone (primary and secondary lymphoid follicles) which houses B cells as well as follicular dendritic cells (FDCs); the T cell zone or paracortical area which houses T cells and dendritic cells (DCs); the medullary sinus and medullary cords which houses macrophages and plasma cells; the cortical sinus through which naïve T cells travel to leave the LN; and the efferent lymphatic vessel through which all cells exit. Germinal center reactions (GCRs) are depicted within the secondary lymphoid follicle. Figure adapted from [457] published under Creative Commons license.

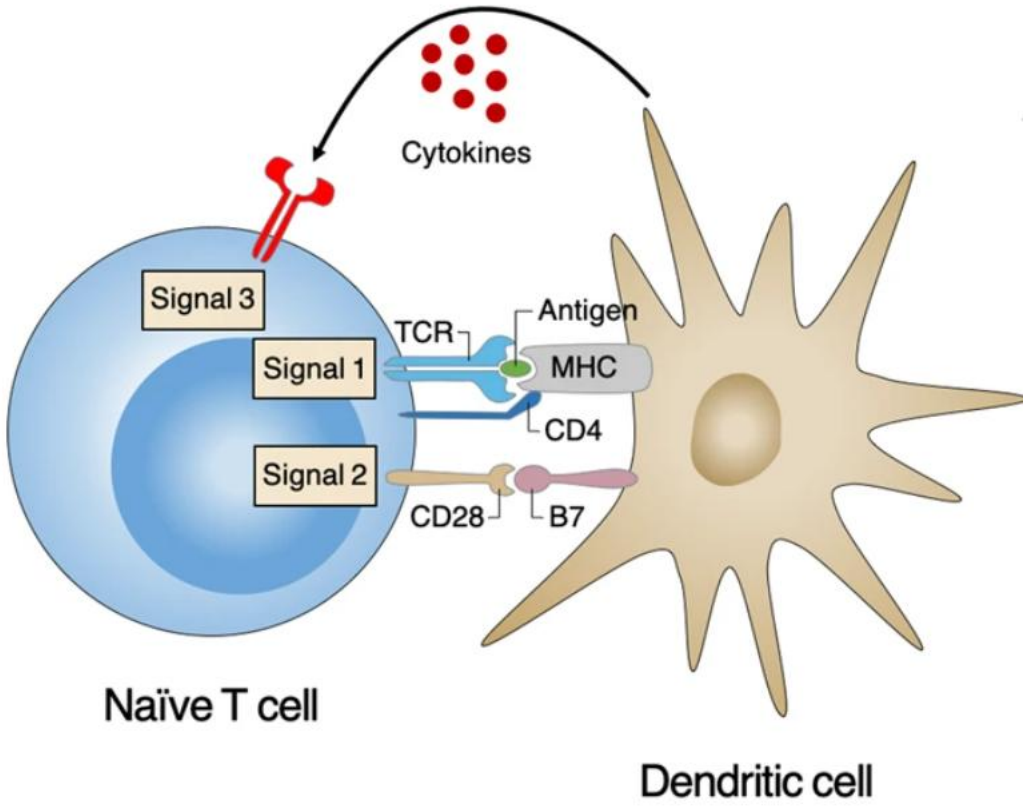

Figure 1.3.5: $CD4^+$ T cell priming.

Depiction of $CD4^+$ T cell priming depicting signals from the 1) TCR:CD4 and peptide:MHC-II interaction; 2) co-stimulation via APC B7 binding T cell CD28; and 3) receipt of additional cytokine signals. Figure adapted from [458] published under Creative Commons license.

$CD8^+$ T cells have greater activation requirements than $CD4^+$ T cells (discussed below) and often require help from activated $CD4^+$ effector cells [43]. This help comes from the CD40L and IL-2 expressed by activated $CD4^+$ T cells. CD40L binds to CD40 on DCs presenting cognate peptide:MHC-I to $CD8^+$ T cell which increases the expression of co-stimulatory factors B7 and 4-1BBL. This additional co-stimulation together with the IL-2 produced by the activated $CD4^+$ T cell helps to promote $CD8^+$ T effector cell differentiation [43].

Effector T cells

Effector T cells are licensed to act upon cells bearing their cognate peptide:MHC without further help from APCs [43]. These cells fall into two main categories: cytotoxic T cells bearing CD8 and helper T cells bearing CD4. Cytotoxic effector $CD8^+$ T cells are primed by APCs presenting cytosol-derived cognate antigen on MHC-I. These antigens originate from intracellular proteins of

invading microbes or, outside the context of infection, from endocytosed antigens that are cross-presented by DCs [43]. $CD8^+$ T cells act against infected cells bearing peptide-loaded MHC-I by releasing factors such as perforin and granzymes to kill the infected cell and by upregulating FAS-L to induce Fas-mediated apoptosis of the infected cell.

$CD4^+$ helper T cells are a more diverse group of T cells that recognize cognate peptide originating from the extracellular environment and presented by MHC-II. These fall into several subsets: T helper 1 (T_H1), T_H2, T_H9, T_H17, T_H22, regulatory T cells (T_{reg}), T regulatory cells 1 (T_r1), and T follicular helper cells (T_{FH}) [459-464]. Differentiation of a $CD4^+$ T cell into one of these helper cell subsets is determined by cytokine exposure during activation. PRRs like the TLR family play a critical role in tuning $CD4^+$ T cell differentiation by controlling the cytokine response to infection and vaccination. Exposure to IL-27 and IL-12 produced by APCs in response to PAMPs from intracellular pathogens such as foreign nucleic acid and LPS promotes differentiation into T_H1 cells [465-468]. These cells are specialized in aiding phagocytes like macrophages to kill intracellular pathogens by producing IFN_γ which stimulates microbicidal activities such as the production of nitric oxide, promoting pro-inflammatory M1 polarization, boosting autophagy, and enhancing phagocytosis [425]. IL-4 produced by natural killer T (NK T) cells and basophils responding to parasitic infections promotes T_H2 cell differentiation

[469-472]. T_H2 cells produce IL-4, IL-5, IL-9, and IL-13 to target extracellular parasites by promoting IgE class-switching and recruiting eosinophils to the sites infection. Differentiation into T_H17 cells is promoted by cytokines IL-6, TGF-β, and IL-23 produced in response to microbes such as bacteria and fungi [473]. These cells produce IL-17 and IL-22 and are important for extracellular bacterial and fungal infections by promoting neutrophil responses and inducing the production of antimicrobial peptides at epithelial barriers. IL-6 is important for the development of T_{FH} cells which are specialized in the activation, isotype switching, and affinity maturation of B cells discussed in the following section. T_H9, T_H22, T_{reg}, and T_r1 cells will not be relevant to this dissertation and so will not be discussed here.

The antibody response

Antibodies are the secreted form of the BCR. These immunoglobulin (Ig) proteins are composed of two pairs of proteins covalently linked by disulfide bonds: two identical heavy chains and two identical light chains (Figure 1.3.6) [43]. The constant domains in the crystallizable fragment (Fc) vary by antibody class and determine the Fc-mediated functions of the antibody. There are five main classes of antibody with distinct constant domains: IgM, IgD, IgG, IgA, and IgE.

The variable portions of an antibody come together to form two identical antigen binding regions in the antigen-binding fragment (Fab).

Antibody variable regions arise from rearrangement of the genes that code the BCR in a process called VDJ recombination. This results in a repertoire of B cells with receptors that can recognize virtually any foreign antigen and respond with pathogen-specific antibodies that bind to, opsonize, neutralize, and/or target the pathogens and their factors for complement deposition and clearance. Antibodies are a crucial component of the adaptive immune response to flaviviruses with neutralizing antibodies serving as the standard correlate of protection for flaviviruses as discussed in section 1.2.9 (page 21).

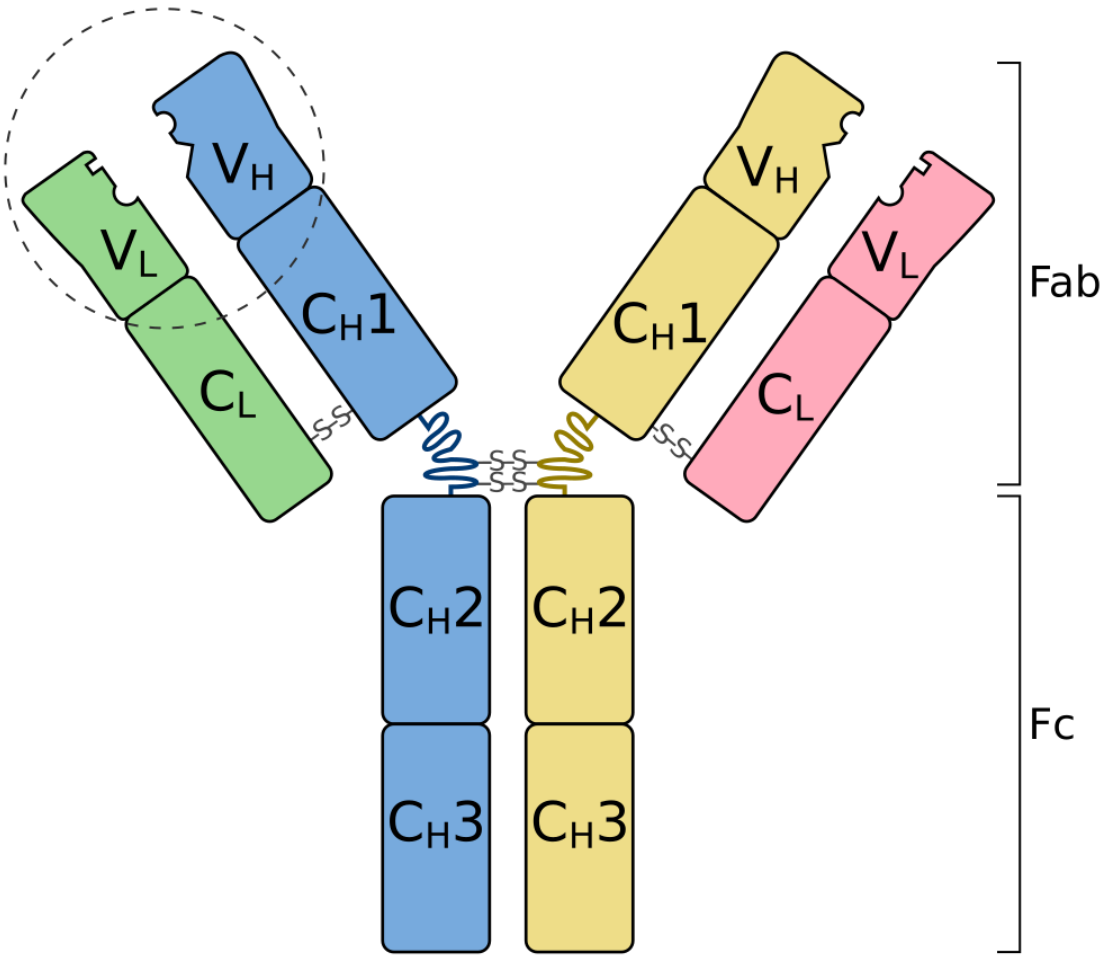

Figure 1.3.6: The antibody.

Diagram of an antibody consisting of two identical light chains (pink and green) and two identical heavy chains (blue and yellow) linked by disulfide bridges (-S-S-). Constant (C) and Variable (V) domains indicated by number and chain (L for Light, H for Heavy). One of two antigen binding regions circled. Fab and Fc fragments indicated to the right. Figure unmodified from [474] published under Creative Commons license.

Antibodies are the secreted form of BCRs. Therefore, a discussion of the antibody response is a discussion of B cell activation, differentiation, and

proliferation. Activation begins when B cells encounter cognate antigen displayed on subcapsular sinus macrophages, FDCs, and possibly cDCs in the LN [43, 475-478]. FDCs are a specialized residents of secondary lymphoid tissues that collect particulate antigens on their surface to present to scanning B cells. FDCs and marginal reticular cells produce CXCL13 to attract naïve B cells expressing CXCR5 to the LN follicle for BCR-antigen engagement [479, 480]. This engagement is the first signal required for B cell activation [43]. After antigen recognition, B cells internalize and process the antigen for display by MHC-II. B cell chemokine receptor expression then shifts towards EBI2 and CCR7 [43]. CCR7 is a chemokine receptor for CCL19 and CCL21 produced in the T cell zone, so this shift causes the B cells to migrate to the interface between the B cell follicle and T cell zone of the LN [481]. EBI2 is a chemokine receptor that drives migration towards EBI2L present in the interfollicular regions [482]. Activated pre-T_{FH} cells upregulate CXCR5 and EBI2 and downregulate CCR7 to traffic to the border between the B and T cell zones [481, 483]. Pre-T_{FH} cells at this interface recognize the peptide:MHC-II complexes presented by these B cells and provide the second set of signals necessary to drive B cell proliferation and differentiation [484]. These signals include the interaction between the co-stimulatory factor CD40L on the T_{FH} cell and CD40 on the B cell; IL-21 produced by T_{FH} cells signaling through the IL-21 receptor (IL21R) on B cells; and any number of additional cytokines that also

modulate the B cell response [481, 482, 485]. Activated B cells also express ICOSL which works in the other direction to promote further differentiation of pre-T_{FH} cells into T_{FH} cells via ICOS [482]. After activation, B cells decrease the expression of CCR7 and migrate to the outer follicle of the LN or the red pulp of the spleen to form a primary focus of differentiating and proliferating B cells. Primary foci in mice form and peak within the first week after infection or vaccination with a new pathogen/antigen [486]. During this time, activated B cells will become either plasmablasts, plasma cells, or memory B cells.

Plasmablasts are short-lived cells whose abundance peaks about one week post-infection or -vaccination [487]. After activation and proliferation, these cells leave the primary focus for the medullary cords in the LN or the red pulp of the spleen where they secrete large amounts of mostly IgM antibody before undergoing apoptosis as the primary infection or vaccine response subsides [487, 488]. This relatively quick transient burst of antibodies helps control active infections which makes plasmablasts a key feature of the adaptive immune response to infection. Their transient nature, however, makes them less desirable for generating durable vaccine immunity.

B cells destined to become plasma cells are led by CXCR5 back into the lymphoid follicle of the LN or the splenic bridging channels between the T cell area and the red pulp of the spleen [43, 482]. Here, they form germinal centers

(GCs) which may persist for several weeks to several months [486]. In the GC, B cells undergo germinal center reactions (GCRs). In these reactions, BCRs are mutated and selected for those that have the highest affinity for antigen. These processes, termed somatic hypermutation and affinity maturation, involve competition between newly mutated BCRs for antigen retained on FDCs in the GC. Only those BCRs that have the necessary affinity for their epitope can outcompete the BCRs of other cells for antigen and receive survival signals by presenting these as peptide:MHC-II to T_{FH} cells. In this way, GCRs produce B cells with BCRs of increasing affinity for the pathogen. Some of these B cells then leave the GC, stop proliferating, and become plasma cells. These cells migrate to the medullary cords of the LN or the red pulp of the spleen where they continue to secrete antibody for a short time, or to the bone marrow where they may persist indefinitely as long-lived plasma cells (LLPCs). The antibody secreted by LLPCs is the first line of defense to re-exposure to the same pathogen, which makes the induction of LLPCs a critical feature of durable vaccine responses.

Memory B cells (MBCs) are long-lived B cells that can arise both from GCRs or independently of them and constitute the second line of defense to re-exposure [43]. These cells do not secrete antibody but instead circulate or migrate to secondary lymphoid tissue where they are primed to respond to subsequent infections with the same pathogen. When MBCs re-encounter their cognate

antigen, they quickly differentiate into plasmablasts or form GCs, undergo somatic hypermutation and affinity maturation, and differentiate into higher affinity plasma cells and MBCs [489]. MBC responses result in a more rapid and protective antibody response than what is seen during primary infection.

After activation, many B cells class-switch from their initial IgM or IgD to IgG, IgA, or IgE depending on the cytokine signals they receive from T_{FH} cells during differentiation [43, 490]. The T_{FH} cells that provide these signals are influenced by the cytokine response to infection/vaccination and share characteristics with other T_H lineages such as T_H1, T_H2, or T_H17 cells [490]. T_{H1}-like T_{FH} cells (T_{FH1}) cells, for example, produce IFN_γ which promotes class switching to IgG2a/c in mice [481, 491, 492]. The IgG2 subclass in mice is efficient at complement fixation and Fc-receptor mediated functions which helps clear pathogens like flaviviruses. In contrast, T_{FH2} cells produce IL-4 which promotes the production of murine IgE as well as IgG1, a subclass with poor complement fixation and Fc-mediated activity [481, 491-493]. Lastly, IL-17 produced by T_{FH17} cells drives IgA production necessary for mucosal immunity [494]. This is another example of how the innate immune response to vaccination or infection influences the eventual characteristics of the adaptive immune response.

1.3.8 Vaccine adjuvants

Adjuvants are vaccine components that enhance the immune response to antigen [43]. They can be used to 1) boost the magnitude of the immune response to otherwise less-immunogenic or inert antigens; 2) enhance the durability of immunity; 3) tune the immune response to enhance features like cellular immunity; 4) decrease the number of doses required to reach protection; 5) achieve protection at lower antigen doses; and 6) enhance immunity in vaccinees with poor immune responses such as the elderly [495, 496]. The discovery of vaccine adjuvants is credited to two scientists in the early 20th century. The first was a veterinarian and biologist named Gaston Ramon who headed the production of diphtheria, tetanus, and gas-gangrene antitoxin at the Institut Pasteur during the early 20th century [497]. Between 1913 and 1925, Ramon observed that horses inoculated with diphtheria toxoid produced more antitoxin if they happened to develop inflammation and an abscess at the site of injection [498, 499]. He then found that mixing diphtheria toxoid with substances such as tapioca starch prior to immunization could artificially induce this inflammation and increase antitoxin yield [500]. These helpful substances, which he termed adjuvants, increased leukocyte infiltration and retention of the antigen at the site of immunization. He speculated that this allowed the immunized animal to utilize the inoculum to the fullest, resulting in more robust and durable immunity.

The following year in 1926, an immunologist named Alexander Glenny published work demonstrating that precipitating diphtheria toxoid with an aluminum salt (alum) before inoculation of guinea pigs elicited a more robust immune response [501]. This work led to the development of an alum-adjuvanted diphtheria toxoid vaccine for humans in the 1930s and later alum-adjuvanted vaccines for pertussis and tetanus [502-505]. Aluminum salts remained one of the only adjuvants approved for use in human vaccines until 1997 and remain the most widely used adjuvants today, contained in roughly 146 vaccines worldwide [506, 507]. See Table 1.3.1 (page 99) for a list of all vaccines currently licensed by the United States Food & Drug Administration (FDA) and note those that include alum (marked in orange). The only other approved adjuvant during this time was calcium phosphate which was used for a combined diphtheria-tetanus-pertussis-poliomyelitis vaccine produced by the Institut Pasteur for 20 years before being replaced by alum in the late '80s [508].

How adjuvants work

In 1989, the immunologist Charles Alderson Janeway, Jr. asked "Why do we need to use adjuvants? To be quite honest, the answer is not known" [375]. He postulated that adjuvants performed two functions: 1) increasing antigen uptake and presentation and 2) providing co-stimulatory signals. Though we've come a

long way since then in understanding the mechanism behind adjuvant-enhanced immunity, we are still learning.

Alum is a prime example. Despite its spotlight in vaccinology for several decades, the mechanism behind alum-adjuvantation is still not definitively understood. Since the discovery of alum's adjuvant properties by Glenny in the 1920s, its function has been attributed to a 'depot effect' in which antigens are rendered insoluble by alum-precipitation and are retained at the site of inoculation [501, 509]. This retention is thought to facilitate a slow release of antigen which triggers a sustained immune response. The depot effect was originally proposed by Ramon who speculated that the inflammation caused by delayed diphtheria toxoid absorption and elimination extended immune stimulation and improved the vaccine response [500]. In 1931, Glenny *et. al* and others did indeed find that diphtheria toxoid remained in tissue longer when adjuvanted with alum which remained the leading explanation for alum's effectiveness for several decades [509, 510]. However, in 2012, Hutchison *et. al* found that removal of the injection site 2 hours after alum-immunization did not alter subsequent antigen presentation in lymph node APCs, T cell responses, or antibody production [511]. Other groups have also demonstrated that alum rapidly releases adsorbed antigens, further contradicting the depot theory [512, 513].

Several competing theories for the mechanism by which alum functions as an effective vaccine adjuvant followed. One hypothesis is that alum enhances immunity by activating the NLRP3 inflammasome [514-516]. However, some studies found that this is not the case, and that alum's adjuvant activity is independent of the NLRP3-caspase-1 pathway [517, 518]. Another hypothesis formed around the observation that dsDNA accumulates at alum injection sites [519]. Indeed, DNase treatment of alum-immunized mice reduces antigen presentation, T cell responses, and antibody production [519, 520]. Subsequent findings indicated that alum increases the recruitment of neutrophils to the site of immunization and triggers NETosis, a form of cell death in which neutrophils release 'nets' of DNA to trap pathogens for phagocytosis [521]. Indeed, mice with a genetic deficiency for NETosis have reduced responses to alum. The current model is that the release of host DNA via NETosis triggers cGAS-STING IRF-3 signaling which enhances the immune response to alum-adsorbed antigen as demonstrated by reduced responses to alum in IRF-3- or STING-deficient mice [519, 520]. Alum induces the accumulation of IL-4-producing monocytes and eosinophils in the spleen after immunization which promotes a T_H2 response [516, 522]. Though there is still no consensus on alum's complete mechanism of action as an adjuvant, it is likely a combination of antigen depot, PRR activation,

increasing antigen uptake by macrophages, and promoting APC maturation [523-525].

The complexity of the immune system makes it difficult to fully elucidate the mechanism by which adjuvants help elicit the immune responses they do. This is true even for next-generation adjuvants with well-defined PRR targets discussed in the following section. Approaches such as systems vaccinology are gaining traction for better capturing the complexity behind adjuvant-induced immunity through multiomic approaches [526]. A better understanding of how adjuvants function is essential for the more rational selection of adjuvants for vaccines.

Next generation adjuvants

Despite its massive success, we now understand that alum has many shortcomings. First, alum-adjuvanted vaccines can cause local reactions at the injection site including erythema, allergic reactions, sensitivity, and the formation of subcutaneous nodules [495, 527]. Though these reactions are rare and usually minor, they are unpleasant and can lead to vaccine hesitancy [528]. Second, immune responses to alum are suboptimal and tend to lack cellular responses [495]. For this reason, alum-adjuvanted vaccines often require multiple primary doses and frequent booster doses to establish and maintain immunity (see dosing requirements of currently licensed alum-adjuvanted vaccines in Table 1.3.1, page

99). Third, alum-adjuvanted vaccines cannot be frozen which limits storage and complicates distribution [524]. Lastly, alum tends to stimulate the production of IL-4 to promote T_H2 cell responses, which are not ideal for vaccines targeting intracellular pathogens like flaviviruses [529]. These limitations underscore the need for new adjuvant technology in the development of vaccines for emerging pathogens like POWV.

Thankfully, research into alternative adjuvants continued during alum's 60-odd yearslong monopoly on vaccines. Today, there are multiple vaccines licensed for use in humans with more contemporary adjuvants including: the squalene-based oil-in-water adjuvant MF59 used in flu vaccines such as the FLUAD seasonal flu vaccine; the liposomal adjuvant AS01 that contains the TLR4 agonist monophosphoryl lipid A (MPL) and the saponin QS-21 used in the Shingrix varicella zoster virus (VZV) vaccine, Mosquirix malaria vaccine, and Arexvy respiratory syncytial virus (RSV) vaccine; the oil-in-water emulsion adjuvant AS03 which contains squalene, α-tocopherol, and polysorbate 80 surfactant and is used in several flu vaccines including Pandemrix and Arepanrix; the AS04 adjuvant which contains alum-adsorbed MPL and is used in the HBV vaccine Fendrix and the HPV vaccine Cervarix; the TLR9 agonist CpG 1018 used in the HBV vaccine Heplisav B; and the immune stimulating complex Matrix M composed of saponins, cholesterol, and phospholipids which is used in the SARS-CoV-2 vaccine

Nuvaxovid [530-533]. These adjuvants are highly effective and can help boost vaccine responses in populations like the elderly that tend to have weaker immune responses. There are two main types of next generation adjuvants which I will discuss in the following sections: lipid-based adjuvants and TLR agonists.

Lipid-based adjuvants

Lipid-based formulations have gained considerable traction in recent years as powerful vaccine adjuvants. There are multiple vaccines formulated with lipid-based adjuvants including MF59 and AS03 oil-in-water emulsions as well as the liposome-based AS01 [532]. I will discuss these here for their importance to Chapter 3.

Oil-in-water emulsions act both as antigen delivery systems as well as immunostimulants [534]. MF59 is an oil-in-water emulsion first licensed for use in an influenza vaccine in 1997 designed to improve the immune response to flu antigen in elderly individuals [535]. It is composed of squalene with the nonionic surfactants polysorbate 80 and Span 85 in citrate buffer. MF59 stimulates the release of ATP after intramuscular injection, an endogenous danger signal that can trigger purinergic PRRs to boost a T_H2-biased immune response in an NLRP3-independent ASC-dependent pathway and a TLR-independent MyD88-dependent pathway [534, 536]. MF59 promotes 1) the recruitment of APCs to the

site of injection, 2) retention of antigen in the lymph node for sustained antigen presentation, 3) the differentiation of monocytes into moDCs which act as the main APCs in MF59 vaccines, and 4) GCRs [532, 537-539]. AS03 is a similar oil-in-water emulsion adjuvant first licensed for use in an influenza vaccine in 2009 [534]. It is composed of squalene, α-tocopherol, and polysorbate 80 in phosphate-buffered saline and functions in much the same way as MF59 but with additional cytokine modulation mediated by α-tocopherol [534].

Liposomes are particulate vesicles composed of phospholipid bilayers surrounding an aqueous core. Liposomal adjuvants mainly function as antigen depots, helping to retain antigen at the site of injection [532]. They can also be utilized for the incorporation of immunostimulatory factors such as TLR agonists for more efficient delivery. Furthermore, their physical properties can be manipulated to modulate immune responses. Incorporating a positive charge on liposomes improves their ability to interact with negatively charged cell surfaces, retain antigen at the site of injection, and promote antigen uptake into DCs [540, 541]. AS01 is currently the only liposomal adjuvant in licensed vaccines. It is composed of phosphatidylcholine-cholesterol-based liposomes containing the TLR4 agonist MPL and the saponin QS-21. MPL and QS-21 work synergistically to promote strong T_H1-skewed cellular responses [542].

TLR agonists as adjuvants

A variety of synthetic PAMPs targeting a variety of PRRs have been developed for use as vaccine adjuvants. These include several TLR agonists such as TLR3 agonists derived from poly-I:C, TLR4 agonists derived from LPS, TLR5 agonists derived from flagellin, TLR7/TLR8 agonists derived from imidazoquinoline-like molecules, and TLR9 agonists derived from oligodeoxynucleotides [532]. These agonists have demonstrated great promise as adjuvants for vaccines targeting numerous viral pathogens [451].

In 2009, the FDA approved Cervarix, the first vaccine adjuvanted with a TLR agonist [543]. This VLP-based vaccine targets two types of oncogenic HPV (16 and 18) and is adjuvanted with AS04, a combination of the TLR4 agonist MPL (3-O-desacyl-4′-monophosphoryl lipid A) and aluminum salt [544]. The addition of MPL helps to boost humoral immunity and improves the efficacy of the vaccine in immunocompromised individuals [532, 545]. Today, there are multiple licensed vaccines adjuvanted with TLR agonists targeting viral pathogens such as HBV, HPV, RSV, and VZV (Table 1.3.1 page 99). The TLR agonist-adjuvanted vaccines for HBV and HPV variously demonstrate higher seroprotection, longer durability, and greater efficacy especially for those groups most vulnerable to disease compared to their alum-adjuvanted counterparts [546-548].

Much of this dissertation focuses on evaluating the use of two novel synthetic TLR agonists as vaccine adjuvants for POWV: the TLR4 agonist INI-2002 and the TLR7/8 agonist INI-4001. The following sections will discuss the use of synthetic TLR4 and TLR7/8 agonists as vaccine adjuvants in more depth.

Synthetic TLR4 agonists

Bacterial LPS found on the outer membrane of Gram-negative bacteria is the major ligand for TLR4 (see section 1.3.5). Although TLR4 activation by LPS generates excellent vaccine responses, use of LPS as an adjuvant is limited by its toxicity [549]. To circumvent this, Ribi *et al.* developed a process in the 1970s to generate a derivative of LPS, monophosphoryl lipid A (MPL or MPLA), which retains the immunostimulatory properties of LPS while greatly reducing its toxicity (Figure 1.3.7) [550, 551]. MPL was commercialized by Ribi Immunochemicals before ultimately being acquired by GlaxoSmithKline Biologicals which has incorporated the adjuvant into their next-generation adjuvant systems AS01 and AS04 [552]. Though MPL is valued for its safety and ability to promote a robust T_H1-skewed immune response, a variety of next-generation MPL-like TLR4 agonists have been developed that have improved tolerability and potency [553-559]. One of these, INI-2002, is evaluated in this

dissertation for its use as an adjuvant in a POWV vaccine and is discussed after the following section on TLR7/8 agonists.

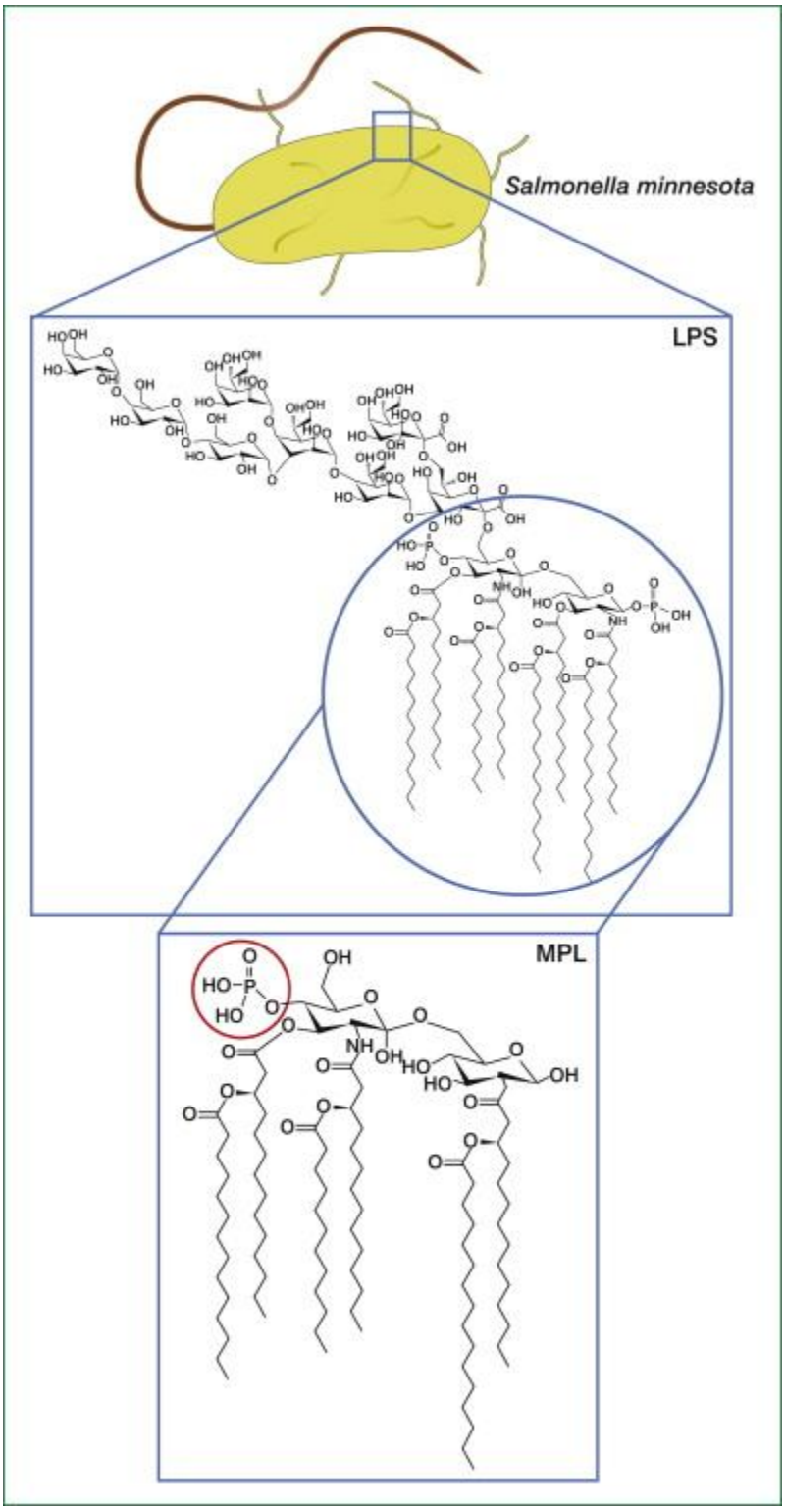

Figure 1.3.7: LPS and its derivative MPL.

Structure of LPS from *Salmonella minnesota* (top) composed of polysaccharide chains and Lipid A containing a bis-phosphorylated diglucosamine backbone bearing multiple acyl chains. MPL (bottom) is an acylated diglucosamine with fewer acyl groups, no polysaccharide side chains, and only one phosphate group. Figure unmodified from [560] published under Creative Commons license.

Synthetic TLR7, TLR8, and TLR7/8 agonists

There are a variety of synthetic ligands for TLR7 and TLR8. The TLR7 ligand imiquimod, an imidazoquinoline derivative, was one of the first TLR7 agonists developed and has been licensed since 1997 for use in topical creams to treat genital warts caused by HPV [561, 562]. It is now also recommended for the treatment of actinic keratosis and superficial basal cell carcinoma (FDA). Among the numerous other synthetic ligands for TLR7 and/or TLR8 are guanine-, pyrimidine-, and adenine-derivatives as well as heterocyclic organic compounds such as pteridinone-derivatives and the imidazoquinolines (Figure 1.3.8) [561, 563]. These compounds can be extensively modified to tune potency and specificity for activating TLR7, TLR8, or both TLR7/8. For example, the imiquimod-derivative resiquimod (R848) is a potent ligand that stimulates both TLR7 and TLR8 [561, 564-566].

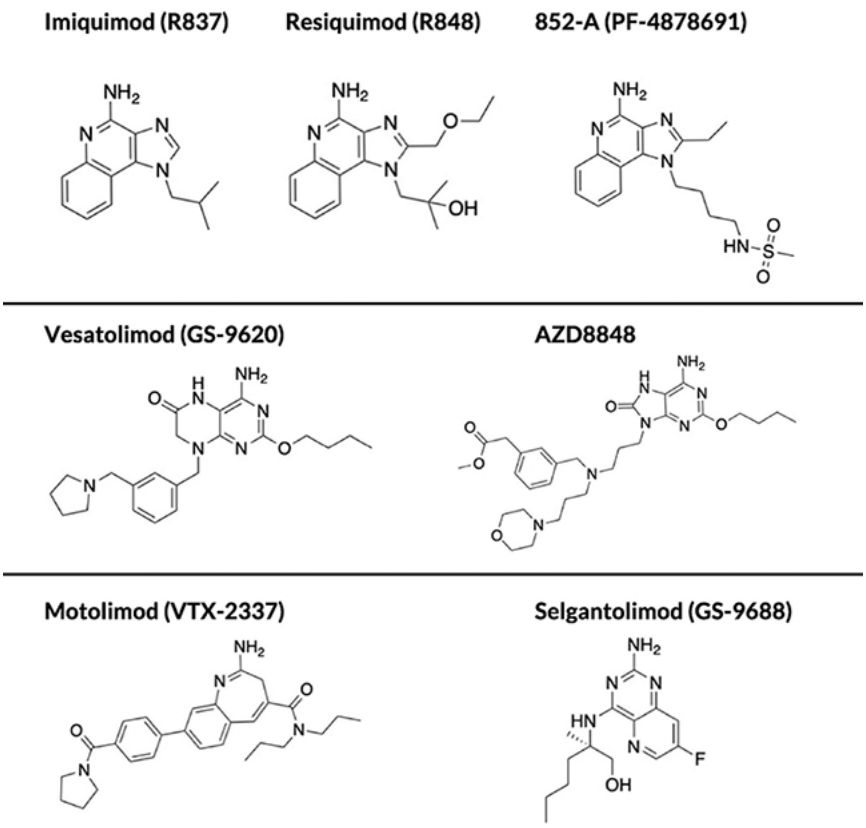

Figure 1.3.8: Various synthetic TLR7/TLR8 ligands.

Chemical structure of imidazoquinoline derivatives (top) including imiquimod, resiquimod, and 852-A; pteridinone-based vesatolimod (middle left); oxo-adenine AZD8848 (middle right); benzazepine analog motolimod (bottom left); and pyrimidine analog selgantolimod (bottom right). Figure adapted from [561] published under Creative Commons license.

Unfortunately, toxicity associated with systemic delivery of many of these compounds including imiquimod and resiquimod severely limits their use [561]. Methods for attenuating the systemic dissemination of these synthetic ligands include adsorption to alum, encapsulation in liposomes, and lipidation. Lipidation has proven to be particularly useful not only in reducing systemic toxicity but also

for tuning specificity of compounds to stimulate either TLR7, TLR8, or both TLR7/8 [567]. 3M-052 is a lipidated imidazoquinoline derivative recognized by both TLR7 and TLR8 that was designed to reduce systemic dissemination and enhance deliverability via liposomes and emulsions for vaccine adjuvantation [568-570]. Incorporation of 3M-052 in an oil-in-water emulsion or liposome allows for targeted co-delivery of antigen and agonist which has been shown to increase humoral and T_H1-skewed cellular immunity for a variety of vaccines [569, 571].

Synthetic TLR7 and TLR8 ligands have demonstrated great promise for the treatment of cancer, viral infections, and as vaccine adjuvants. These compounds stimulate signaling via MyD88 and often enhance IFN-I, IFNγ, TNFα, IL-12, IL-6, and IL-17 responses [398, 562, 572]. The specific responses depend on the compound and the relative stimulation of TLR7 and TLR8 [398]. Gorden *et al.* nicely demonstrated that TLR7 agonists potently induce an IFN-I response from pDCs in human PBMCs and to a lesser extent pro-inflammatory cytokines like TNFα and IL-12, while TLR8 agonists are more potent stimulators of pro-inflammatory TNFα and IL-12 responses from monocytes, cDCs, and moDCs than IFN-I [398]. TLR7/8 agonists are especially useful as they induce both IFN-I and pro-inflammatory responses. Through these cytokine responses, TLR7/8 agonists promote cross-presentation, T_H1 skewing, and $CD8^+$ T cell responses, which make them ideal adjuvants for vaccines targeting viruses [451, 561, 563, 567, 573]. One

such TLR7/8 adjuvant, imidazoquinoline gallamide (IMDG) adsorbed to alum, was used in an inactivated SARS-CoV-2 vaccine authorized for emergency use in India and other countries during the COVID-19 pandemic [574]. Another such adjuvant, INI-4001, is evaluated in this dissertation for its ability to improve a vaccine targeting POWV and is discussed in depth below.

INI-2002 and INI-4001

INI-2002 and INI-4001 are two novel synthetic TLR agonists developed by Inimmune Corporation that have shown great promise as vaccine adjuvants. INI-2002 is a pre-clinical TLR4 agonist derived from LPS that signals through both MyD88 and TRIF to induce the production of IL-6, TNFα, CXCL10, and IL-1β in human PBMCs (Figure 1.3.9B) [572, 575]. INI-4001 is a clinical stage TLR7/8 agonist composed of a lipidated-oxoadenine that is currently being evaluated in a phase 1 clinical trial for the treatment of cancer in patients with solid tumors (Figure 1.3.9A) [575, 576]. INI-4001 has a bias towards stimulating TLR7 over TLR8 and elicits a potent IFN-I response from human PBMCs [572]. Several studies have demonstrated the efficacy of both INI-2002 and INI-4001 as vaccine adjuvants. I will discuss some of these here.

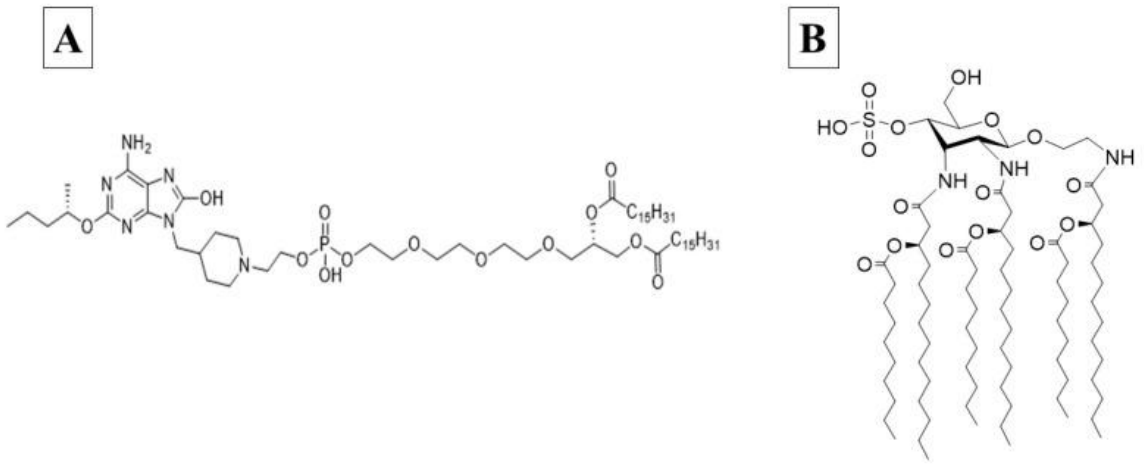

Figure 1.3.9: Chemical structure of INI-4001 and INI-2002.

Chemical structure of INI-4001 (A) and INI-2002 (B). Figure unmodified from [575] published under Creative Commons license.

Multiple studies have investigated the use of INI-2002 and INI-4001 in vaccines targeting SARS-CoV-2, the respiratory virus that caused the COVID-19 pandemic. In the first of these studies, Short *et al.* demonstrated that inclusion of INI-2002 in an AS03-like oil-in-water emulsion-adjuvanted vaccine targeting the RBD of SARS-CoV-2 enhanced the antibody response over emulsion alone [577]. They showed that INI-2002 skewed the cellular immune response towards T_H1 and T_H17. Meanwhile, incorporation of INI-4001 into AS03-like emulsion did not enhance the antibody response but did appear to skew the response towards T_H1. Combination of INI-2002, INI-4001, and emulsion did not improve the vaccine

response over either adjuvant-emulsion combination alone. Lathrop *et al.* validated these findings with a trimeric SARS-CoV-2 spike antigen and further demonstrated that emulsions with either INI-2002 or INI-4001 induced $CD8^+$ T cell responses to RBD and improved the functional breadth of the antibody response to divergent SARS-CoV-2 strains [578]. Interestingly, in this study INI-4001 not INI-2002 induced a T_H17 response which may be due to the particular dosing, antigen, and/or method of immunization. Siram *et al.* moved away from adjuvanted emulsions and demonstrated that both INI-2002 and INI-4001 efficiently adsorb to alum and that both INI-2002-alum and INI-4001-alum improved the antibody response to RBD over alum alone [575]. Furthermore, the induction of IFNγ by INI-4001 and IL17A by INI-2002 were both enhanced when these adjuvants were delivered in combination with alum.

Three studies have demonstrated the efficacy of INI-2002 and INI-4001 in combination with emulsions, liposomes, and nanoparticles in vaccines targeting influenza virus. Mehradnia *et al.* demonstrated that influenza hemagglutinin (HA) subunit vaccine adjuvanted with INI-4001-loaded cationic liposomes induced higher anti-HA IgG titers than HA alone [579]. Additionally, they showed that loading liposomes with INI-4001 improved the IFNγ and TNFα T cell responses. Abdelwahab *et al.* demonstrated that the antibody response to INI-4001 adjuvanted HA could be boosted by silica nanoparticles [580]. And lastly, Zhang

et al. demonstrated that a combination INI-2002- and INI-4001-emulsion-adjuvanted influenza HA peptide vaccine effectively boosted the total IgG response, neutralizing antibody response, and ability of the vaccine to improve survival and viral shedding post-challenge in pre-immune ferrets [581].

In addition to their efficacy as adjuvants for vaccines targeting viruses, INI-2002 and INI-4001 have demonstrated utility in vaccines designed to target substance use disorder and/or pathogenic bacteria. Miller *et al.* demonstrated that inclusion of INI-4001-alum in a vaccine against fentanyl-based hapten (F_1) conjugated to diphtheria cross-reactive material (CRM_{197}) enhanced the antibody response, T_H1 cell response, and the vaccine's ability to prevent fentanyl from entering the brains of mice [572]. Crouse *et al.* extended these results into rats and pigs, further demonstrating the effectiveness of INI-4001-alum-adjuvanted F_1-CRM_{197} at preventing fentanyl overdose [582]. Hamid *et al.* then demonstrated that INI-4001-loaded cationic liposomes did not improve the total IgG response to F_1-CRM_{197} over INI-4001-alum but did increase the IgG2a/IgG1 ratio [583]. Interestingly, they found that culturing macrophages with INI-4001-loaded liposomes improved activation over INI-4001-alum alone but that this was not the case for DCs. Lastly, Román-Cruz *et al.* demonstrated that INI-2002 improved the antibody and cytokine response to a CRM-conjugated prophage Pf which is a

virulence factor for the pathogen *Pseudomonas aeruginosa* (*Pa*) that plays a role in *Pa* biofilm formation and immune evasion [584].

Together, these studies demonstrate the utility of INI-2002 and INI-4001 as adjuvants for subunit vaccines targeting respiratory viruses, substance use disorder, and pathogenic bacteria. They also highlight the ability of these compounds to operate in combination with other adjuvant classes such as alum and cationic liposomes. More work is needed to assess 1) their effectiveness in vaccines targeting unique pathogens and pathologies, 2) the durability of the immune responses they elicit, 3) their dose-sparing properties, 4) their effectiveness as adjuvants for a broader set of vaccine platforms, and 5) the mechanisms by which they elicit their unique immune responses. The work in this dissertation addresses these points.

1.3.9 Flavivirus vaccines

The YFV 17D live attenuated vaccine developed by Max Theiler in the 1930s was one of the first virus vaccines ever made and is still in use today [585]. It is an extremely effective vaccine that generates both robust and durable humoral and cellular immunity [586, 587]. However, as a live attenuated virus, it comes with risks and is not recommended for certain at-risk groups including pregnant or immunocompromised individuals. Studies have found that roughly 1 in every

10,000-300,000 17D vaccinees experience vaccine-associated disease with the risk for severe adverse events highest in older individuals (≥70 years) [588, 589]. Despite this, it is still considered one of the most effective vaccines ever developed, and live attenuation of flaviviruses is still a popular method for the development of other flavivirus vaccines [590]. Live attenuated vaccines have been developed for DENV, JEV, and TBEV with varied success. SA14-14-2 is a very effective live attenuated vaccine for JEV developed by serial passage of wild-type virus [591]. IMOJEV (JEV) and Dengvaxia (DENV) are chimeric vaccines composed of pathogen-specific prM-E genes in a YFV 17D genomic backbone [590]. IMOJEV remains in use in several countries, whereas Dengvaxia will no longer be produced after this year due to safety concerns regarding ADE which restricted its use to DENV seropositive vaccinees as discussed in Section 1.2.10. There are fortunately now two additional live attenuated vaccines for DENV, Qdenga and Butantan-DV, which are both tetravalent vaccines like Dengvaxia (serotype-specific prM-E for all four DENV serotypes) but with attenuated DENV genomic backbones instead of YFV 17D [248, 592]. An attenuated strain of Langat virus (LGTV), a TBFV closely related to TBEV, was evaluated for use as a live attenuated vaccine for TBEV in Russia but was never licensed due to a high rate of severe adverse events [593].

Inactivated virus vaccines represent the other major vaccine platform used for flaviviruses. There are currently seven inactivated vaccines targeting TBEV,

one for KFDV, and two for JEV [206, 594-596]. All but the KFDV vaccine are adjuvanted with alum [597]. These vaccines generate mostly humoral immunity with poor cellular responses and most require multiple doses to establish and maintain immunity [206, 590, 595]. However, inactivated virus vaccines are still being pursued as a platform for other flaviviruses [590].

The limitations of live attenuated and inactivated virus vaccines for flaviviruses highlight the need to update flavivirus vaccine methodology by leveraging more current and effective technologies. To this end, there are numerous studies evaluating flavivirus vaccines using platforms including viral vectors, DNA, mRNA, subunit, peptide epitopes, and VLPs [590]. Adjuvants like TLR agonists are also currently being evaluated for multiple flavivirus vaccines including some for WNV, DENV, ZIKV, TBEV, and KFDV [451, 595, 598-600]. Despite the promise demonstrated by these next-generation platforms and adjuvants, they are severely underrepresented in flavivirus vaccines currently being evaluated in clinical trials [590]. There are no flavivirus VLP vaccines in clinical trials and very few using non-alum adjuvants.

Powassan virus vaccine candidates

There are currently no vaccines for POWV. Currently, all vaccines targeting other TBFVs are inactivated virus either without adjuvant (KFDV vaccine) or

adjuvanted with alum (TBEV vaccines) [206, 601]. Though highly effective at preventing disease and hospitalization, these vaccines have notable shortcomings [206, 602]. These include the risk of incomplete inactivation, the requirement of several initial doses to establish protection, and frequent booster doses to maintain protection. For example, the formalin inactivated KFDV vaccine requires 2 initial doses one month apart followed by a booster dose 6-9 months later and every year thereafter due to short lived immunity [603-605]. Meanwhile, the alum-adjuvanted inactivated TBEV vaccines require 2 initial doses 1-7 months apart followed by a booster dose 5-12 months later and subsequent booster doses every 1-5 years thereafter [206]. These shortcomings highlight the need to evaluate new platforms for the development of a POWV vaccine.

Mice are an excellent experimental model for evaluating vaccines for TBFVs, as they tend to mimic many of the pathologies seen in humans during infection [606-608]. Indeed, laboratory mouse strains such as C57BL/6 and BALB/c challenged with peripheral POWV infection replicate many features of human disease such as encephalitis, meningitis, meningoencephalitis, and mortality with visible neurological symptoms including weak grip, tremors, seizures, and hind limb paralysis [292, 306, 609-612]. These lab strains are also well suited for assessing additional metrics of POWV disease including viremia, neuroinvasion, and viral burden in peripheral organs [306, 613]. This makes mice an optimal

model system to evaluate novel vaccine candidates for POWV. This contrasts with flaviviruses such as DENV which require ablation of innate immune responses to mimic the mortality and features of disease seen in humans [614].

Evaluating candidate vaccines in non-human primates (NHPs) is a critical step in advancing vaccines towards clinical evaluation. Unfortunately, there are currently no good NHP models for POWV infection and only two published studies evaluating POWV infection in macaques. In the first of these studies published in 1980, Frolova *et al.* found that suspensions of POWV-infected mouse brain injected directly into the thalamus of rhesus macaques (*Macaca mulatta*) could lead to viral replication and infiltration of leukocytes into the CNS, neurological disorders, and viremia [615]. However, this route of delivery is not relevant for the evaluation of vaccines intended to protect from disease caused by neuroinvasion after peripheral infection. In the second study published in 2023, Illarionova *et al.* found that subcutaneous infection of crab-eating macaques (*Macaca fascicularis*) resulted in mild transient viremia and viral titers in the spleen with no overt symptoms of disease [616]. The authors argue that this demonstrates a more human-relevant model of infection to evaluate vaccine candidates given that human infections are generally asymptomatic, but this model lacks the severe outcomes of disease for which a POWV vaccine must be developed. Further work

is required to develop a relevant NHP model of POWV infection to evaluate vaccine candidates and antiviral therapies.

Several groups have recently developed pre-clinical vaccine candidates for POWV in mice using various platforms including mRNA, DNA, subunit, live attenuated virus, and VLPs [609, 613, 617-622]. In 2018, VanBlargan *et al.* developed a LNP-delivered POWV-II prM-E mRNA vaccine [613]. They demonstrated that 10μg prime-boost intramuscular (im) immunization induced impressive neutralizing antibody responses to multiple strains of POWV-II, the prototypical POWV-I LB strain, TBEV, LGTV, and the more distantly related Gadgets Gully virus (GGYV). Furthermore, the vaccine protected against lethal POWV-II and POWV-I challenge and viremia. Using passive transfer, they demonstrated that the humoral immune response was sufficient to mediate this protection. Lastly, they demonstrated full protection from lethal POWV-II challenge after a single 10μg dose. These findings clearly demonstrate the utility of an mRNA vaccine for POWV.

In 2020, Choi *et al.* developed a DNA vaccine targeting both POWV-I and -II prM-E [617]. They demonstrated that two 25μg doses delivered im elicit anti-POWV IgG and T cell responses. They used a truncated timeframe however, with prime-boost vaccinations two weeks apart and responses measured just one week post-boost. They showed that vaccinated mice were protected from lethal POWV-

I infection but only monitored their health for 14 days before sacrifice, which may exclude mice that would have succumbed to infection after this timepoint. Lastly, they demonstrated reduced burden of viral RNA in various tissues, but they compared mock vaccinated mice at days 7, 8, and 11 to vaccinated mice at day 14, which is not an ideal comparison. This study demonstrates the potential of DNA vaccination for POWV, but the efficacy and durability of the vaccine response require further evaluation.

In 2022, Malonis *et al.* were the first to consider a vaccine using POWV EDIII. The omission of prM and EDI-II was intended to avoid antibody responses to non-neutralizing epitopes that may contribute to ADE [618]. They demonstrated that three 15μg doses of self-assembling nanoparticle displaying POWV-II EDIII adjuvanted with MF59 delivered intraperitoneally (ip) elicited neutralizing antibodies against both POWV-I and -II reporter virus particles. They did not demonstrate protection in vaccinated mice but did show partial protection could be conferred through passive transfer of the sera from vaccinated mice.

In 2023, Cheung *et al.* generated a live attenuated chimeric vaccine with POWV-II prM-E in a YFV 17D backbone [619]. However, they found that this chimera rescued the virulence of 17D in mice. After further attenuating the chimera by removing a glycosylation motif in the NS1 protein, they found that subcutaneous (sc) vaccination with 10^4 PFU still caused disease and death in 10%

of vaccinated mice. Furthermore, they showed that two doses of 10^3 PFU only conferred 70% protection from lethal POWV-II infection and did not reduce viral burden in any tissue. Full protection was only achieved after a heterologous POWV-II 25ng EDIII boost. This study again highlights the potential risks involved in live attenuated vaccines.

In 2025, Himmler *et al.* generated another live attenuated vaccine candidate for POWV by passaging POWV isolated from ticks in Vero cells [621]. The passaged virus, LI9P, appeared to be completely attenuated in mice with no lethality after a $2X10^3$ FFU dose delivered sc. They demonstrated that multiple residues, including a key residue in the E protein, were responsible for this attenuation. Mice immunized with LI9P generated neutralizing antibodies and were fully protected from lethal challenge with the parent strain.

In 2021, Cimica *et al.* were the first to develop POWV-I VLP and demonstrate its utility as a vaccine antigen when adjuvanted with AddaVax and administered as a 10μg prime-boost im vaccine [620]. This platform elicited neutralizing and anti-EDIII antibodies. Our group later developed our own POWV-I VLP and demonstrated that prime-boost vaccination with 2μg alum-adjuvanted VLP im elicited full protection from lethal POWV-I challenge [609]. This dissertation represents a continuation of that work.

Section 1.4: Conclusion

There is an urgent need to develop vaccines for emerging pathogenic flaviviruses like POWV. Contemporary vaccine technologies including advanced vaccine platforms and novel adjuvants provide new opportunities to develop a highly effective and safe vaccine for POWV. The work in this dissertation is on the development of just such a vaccine. Chapter 2 focuses on evaluating the efficacy of two novel synthetic TLR agonists, INI-2002 and INI-4001, as adjuvants for a VLP-based vaccine targeting POWV. Chapter 3 explores the utility of formulating an INI-4001-adjuvanted POW-VLP with cationic liposomes or oil-in-water emulsion to improve the vaccine response. Chapter 4 explores the effects of VLP maturity on vaccine efficacy. Chapter 5 explores the correlates of protection in our POWV vaccine-challenge mouse model. Chapter 6 summarizes the results of this dissertation and introduces the future directions concerning evaluating the vaccine developed herein. Together, the studies in this dissertation lay groundwork for improving our current flavivirus vaccine methodology while demonstrating the efficacy of a novel vaccine for POWV.

Table 1.3.1: Current FDA-licensed vaccines in the United States.

A list of all vaccines licensed by the United States Food & Drug Administration (FDA) as of October 30, 2025. Entries include target pathogen, product trade name, vaccine type (platform), adjuvant used (if any), route of administration, and a general, simplified dosing schedule. Vaccines for flaviviruses are in blue. Alum adjuvanted vaccines are marked by orange. Vaccines discontinued or obsolete (i.e. plague vaccine) are not included. Conjugation is omitted. List compiled from information provided by the FDA [623].

Product Name	Trade Name	Platform	Adjuvant	Route	Number of doses
Adenovirus Type 4 and Type 7 Vaccine	No Trade Name	live attenuated		oral	1
Anthrax Vaccine Adsorbed, Adjuvanted	CYFENDUS	toxoid subunit	aluminum hydroxide + CpG 7909	intramuscular	2 doses 2 weeks apart
Anthrax Vaccine Adsorbed	Biothrax	toxoid subunit	aluminum hydroxide	intramuscular	3 primary doses at 0, 1, and 6 months; 2 booster doses 6 and 12 months after primary followed by booster every year
BCG Live	BCG Vaccine	live attenuated		percutaneous	1
BCG Live	TICE BCG	live attenuated		intravesical	6 doses weekly then monthly for 6-12 months
Chikungunya Vaccine, Recombinant	VIMKUNYA	VLP	aluminum hydroxide	intramuscular	1
Cholera Vaccine Live Oral	Vaxchora	live attenuated		oral	1
COVID-19 Vaccine, mRNA	MNEXSPIKE	mRNA		intramuscular	1 boost after initial COVID vaccination
COVID-19 Vaccine, Adjuvanted	NUVAXOVID	subunit	Matrix-M	intramuscular	1 boost after initial COVID vaccination
COVID-19 Vaccine, mRNA	Comirnaty	mRNA		intramuscular	1 boost after initial COVID vaccination
COVID-19 Vaccine, mRNA	SPIKEVAX	mRNA		intramuscular	2 to vaccine naïve individuals
Dengue Tetravalent Vaccine, Live	DENGVAXIA	live attenuated		subcutaneous	3 doses 6 months apart in DENV seropositive individuals
Diphtheria & Tetanus Toxoids & Acellular Pertussis Vaccine Adsorbed	Infanrix	subunit and toxoid subunit	aluminum hydroxide	intramuscular	5 doses at 2, 4, 6, 15-20 months and 4-6 years
Diphtheria & Tetanus Toxoids & Acellular Pertussis Vaccine Adsorbed	DAPTACEL	subunit and toxoid subunit	aluminum phosphate	intramuscular	5 doses at 2, 4, 6, 15-20 months and 4-6 years
Diphtheria & Tetanus Toxoids & Acellular Pertussis Vaccine Adsorbed, Hepatitis B (recombinant) and Inactivated Poliovirus Vaccine Combined	Pediarix	subunit, toxoid subunit, VLP, and	aluminum hydroxide + aluminum phosphate	intramuscular	3 doses at 2, 4, and 6 months

		inactivated virus			
Diphtheria and Tetanus Toxoids and Acellular Pertussis Adsorbed and Inactivated Poliovirus Vaccine	KINRIX	subunit, toxoid subunit, and inactivated virus	aluminum hydroxide	intramuscular	1 dose as the last boost of a polio or DTaP series
Diphtheria and Tetanus Toxoids and Acellular Pertussis Adsorbed and Inactivated Poliovirus Vaccine	Quadracel	subunit, toxoid subunit, and inactivated virus	aluminum phosphate	intramuscular	1 dose as the last boost of a polio or DTaP series
Diphtheria and Tetanus Toxoids and Acellular Pertussis Adsorbed, Inactivated Poliovirus, Haemophilus b Conjugate [Meningococcal Protein Conjugate] and Hepatitis B [Recombinant] Vaccine	VAXELIS	subunit, toxoid subunit, VLP, and inactivated virus	aluminum hydroxide + aluminum phosphate	intramuscular	3 doses at 2, 4, and 6 months
Diphtheria and Tetanus Toxoids and Acellular Pertussis Adsorbed, Inactivated Poliovirus and Haemophilus b Conjugate (Tetanus Toxoid Conjugate) Vaccine	Pentacel	subunit, toxoid subunit, and inactivated virus	aluminum phosphate	intramuscular	4 doses at 2, 4, 6, and 15-20 months
Ebola Zaire Vaccine, Live	ERVEBO	live attenuated		intramuscular	1
Haemophilus b Conjugate Vaccine (Meningococcal Protein Conjugate)	PedvaxHIB	subunit	aluminum hydroxide	intramuscular	2 doses 2 months apart and a booster after 15 months of age
Haemophilus b Conjugate Vaccine (Tetanus Toxoid Conjugate)	ActHIB	subunit		intramuscular	4 doses at 2, 4, 6, and 15-18 months
Haemophilus b Conjugate Vaccine (Tetanus Toxoid Conjugate)	Hiberix	subunit		intramuscular	4 doses at 2, 4, 6, and 15-18 months
Hepatitis A Vaccine, Inactivated	Havrix	inactivated virus	aluminum hydroxide	intramuscular	2 doses 6-12 months apart
Hepatitis A Vaccine, Inactivated	VAQTA	inactivated virus	aluminum hydroxide	intramuscular	2 doses 6-18 months apart
Hepatitis A Inactivated and Hepatitis B (Recombinant) Vaccine	Twinrix	inactivated virus	aluminum hydroxide + aluminum phosphate	intramuscular	3 doses at 0, 1, and 6 months
Hepatitis B Vaccine (Recombinant)	Recombivax HB	VLP	aluminum hydroxide	intramuscular	3 doses at 0, 1, and 6 months
Hepatitis B Vaccine (Recombinant)	Engerix-B	VLP	aluminum hydroxide	intramuscular	3 doses at 0, 1, and 6 months
Hepatitis B Vaccine (Recombinant), Adjuvanted	HEPLISAV-B	VLP	CPG 1018	intramuscular	2 doses at 0 and 1 month
Human Papillomavirus Quadrivalent (Types 6, 11, 16, 18) Vaccine, Recombinant	Gardasil	VLP	aluminum hydroxide	intramuscular	3 doses at 0, 2, and 6 months
Human Papillomavirus 9-valent Vaccine, Recombinant	Gardasil 9	VLP	aluminum hydroxide	intramuscular	3 doses at 0, 2, and 6 months
Human Papillomavirus Bivalent (Types 16, 18) Vaccine, Recombinant	Cervarix	VLP	AS04	intramuscular	3 doses at 0, 1, and 6 months
Influenza A (H1N1) 2009 Monovalent Vaccine	No Trade Name	inactivated virus		intramuscular	1 to 2 doses 1 month apart
Influenza A (H5N1) Virus Monovalent Vaccine, Adjuvanted	AREPANRIX	inactivated virus	AS03	intramuscular	2 doses 21 days apart
Influenza Virus Vaccine, H5N1 (for National Stockpile)	No Trade Name	inactivated virus		intramuscular	1
Influenza A (H5N1) Monovalent Vaccine, Adjuvanted	AUDENZ	inactivated virus	MF59	intramuscular	2 doses 21 days apart
Influenza Vaccine, Adjuvanted	Fluad Quadrivalent	inactivated virus	MF59	intramuscular	1
Influenza Vaccine, Adjuvanted	Fluad	inactivated virus	MF59	intramuscular	1
Influenza Vaccine	Afluria Quadrivalent	inactivated virus		intramuscular	1 to 2 doses 1 month apart

Influenza Vaccine	Flucelvax Quadrivalent	inactivated virus		intramuscular	1 to 2 doses 1 month apart
Influenza Vaccine	Flulaval Quadrivalent	inactivated virus		intramuscular	1 to 2 doses 1 month apart
Influenza Virus Vaccine	Afluria, Afluria Southern Hemisphere	inactivated virus		intramuscular	1 to 2 doses 1 month apart
Influenza Virus Vaccine	FluLaval	inactivated virus		intramuscular	1 to 2 doses 1 month apart
Influenza Vaccine, Live, Intranasal	FluMist	live attenuated		intranasal	2 doses 1 month apart
Influenza Virus Vaccine	Fluarix	inactivated virus		intramuscular	1 to 2 doses 1 month apart
Influenza Virus Vaccine	Fluvirin	inactivated virus		intramuscular	1 to 2 doses 1 month apart
Influenza Virus Vaccine	Agriflu	inactivated virus		intramuscular	1
Influenza Virus Vaccine	Fluzone, Fluzone High-Dose and Fluzone Intradermal	inactivated virus		intramuscular	1 to 2 doses 1 month apart
Influenza Virus Vaccine	Flucelvax	inactivated virus		intramuscular	1 to 2 doses 1 month apart
Influenza Vaccine (Trivalent)	Flublok	subunit		intramuscular	1
Influenza Vaccine (Quadrivalent)	Flublok Quadrivalent	subunit		intramuscular	1
Influenza Vaccine,Live, Intranasal	FluMist Quadrivalent	live attenuated		intranasal	2 doses 1 month apart
Influenza Virus Vaccine	Fluarix Quadrivalent	inactivated virus		intramuscular	1 to 2 doses 1 month apart
Influenza Virus Vaccine	Fluzone Quadrivalent	inactivated virus		intramuscular	1 to 2 doses 1 month apart
Japanese Encephalitis Virus Vaccine, Inactivated, Adsorbed	Ixiaro	inactivated virus	aluminum hydroxide	intramuscular	2 doses 1 month apart
Measles, Mumps and Rubella Vaccine, Live	PRIORIX	live attenuated		subcutaneous	2 doses at 12-15 months and 4-6 years
Measles, Mumps, and Rubella Virus Vaccine, Live	M-M-R II	live attenuated		intramuscular or subcutaneous	2 doses at 12-15 months and 4-6 years
Measles, Mumps, Rubella and Varicella Virus Vaccine Live	ProQuad	live attenuated		intramuscular or subcutaneous	2 doses at 12-15 months and 4-6 years
Meningococcal Groups A, B, C, W, and Y Vaccine	PENBRAYA	subunit	aluminum phosphate	intramuscular	2 doses 6 months apart
Meningococcal Groups A, B, C, W, and Y Vaccine	PENMENVY	subunit	aluminum hydroxide	intramuscular	2 doses 6 months apart
Meningococcal (Groups A, C, Y, and W-135) Oligosaccharide Diphtheria CRM197 Conjugate Vaccine	MENVEO	subunit		intramuscular	2 to 4 doses depending on age
Meningococcal (Groups A, C, Y and W-135) Polysaccharide Diphtheria Toxoid Conjugate Vaccine	Menactra	subunit		intramuscular	3 doses 15 months and 4 years apart
Meningococcal Group B Vaccine	BEXSERO	subunit	aluminum hydroxide	intramuscular	2 to 3 doses at 0, 1-2, and 6 months
Meningococcal Group B Vaccine	TRUMENBA	subunit	aluminum phosphate	intramuscular	2 to 3 doses at 0, 1-2, and 6 months
Meningococcal (Groups A, C, Y, W) Conjugate Vaccine	MenQuadfi	subunit		intramuscular	3 to 4 doses at 2, 4, 6, 12-18 months and 13+ years
Pneumococcal Vaccine, Polyvalent	Pneumovax 23	subunit		intramuscular or subcutaneous	1
Pneumococcal 13-valent Conjugate Vaccine	Prevnar 13	subunit	aluminum phosphate	intramuscular	4 doses at 2, 4, 6, and 12-15 months
Pneumococcal 15-valent Conjugate Vaccine	VAXNEUVANCE	subunit	aluminum phosphate	intramuscular	4 doses at 2, 4, 6, and 12-15 months

Pneumococcal 20-valent Conjugate Vaccine	Prevnar 20	subunit	aluminum phosphate	intramuscular	1 to 4 doses at 2, 4, 6, and 12-15 months
Pneumococcal 21-valent Conjugate Vaccine	CAPVAXIVE	subunit		intramuscular	1
Poliovirus Vaccine Inactivated (Monkey Kidney Cell)	IPOL	inactivated virus		intramuscular or subcutaneous	4 doses at 2, 4, 6-18 months, and 4-6 years
Rabies Vaccine	IMOVAX RABIES	inactivated virus		intramuscular	2, 3, or 5 doses depending on pre- or post-exposure
Rabies Vaccine	RabAvert	inactivated virus		intramuscular	3 to 6 doses depending on pre- or post-exposure
Rotavirus Vaccine, Live, Oral	ROTARIX	live attenuated		oral	2 doses 4 weeks apart
Rotavirus Vaccine, Live, Oral, Pentavalent	RotaTeq	live attenuated		oral	3 doses 4-10 weeks apart
Respiratory Syncytial Virus Vaccine	MRESVIA	mRNA		intramuscular	1
Respiratory Syncytial Virus Vaccine	ABRYSVO	subunit		intramuscular	1
Respiratory Syncytial Virus Vaccine, Adjuvanted	AREXVY	subunit	AS01E	intramuscular	1
Smallpox and Monkeypox Vaccine, Live, Non-Replicating	JYNNEOS	live attenuated		subcutaneous	2 doses 4 weeks apart
Smallpox and Mpox (Vaccinia) Vaccine, Live	ACAM2000	live attenuated		percutaneous	1
Tetanus & Diphtheria Toxoids, Adsorbed	TDVAX	toxoid subunit	aluminum phosphate	intramuscular	3 doses 4-8 weeks and 6-12 months apart with 10 year boosters
Tetanus & Diphtheria Toxoids Adsorbed for Adult Use	TENIVAC	toxoid subunit	aluminum phosphate	intramuscular	3 doses 2 and 6-8 months apart
Tetanus Toxoid, Reduced Diphtheria Toxoid and Acellular Pertussis Vaccine, Adsorbed	Adacel	subunit and toxoid subunit	aluminum phosphate	intramuscular	1 to 2 doses 5 and 8 years after TDaP
Tetanus Toxoid, Reduced Diphtheria Toxoid and Acellular Pertussis Vaccine, Adsorbed	Boostrix	subunit and toxoid subunit	aluminum hydroxide	intramuscular	1 to 2 doses 5 and 9 years after TDaP
Tick-Borne Encephalitis Vaccine	TICOVAC	inactivated virus	aluminum hydroxide	intramuscular	3 doses at 0, 1-3, and 5-12 months with boosters every 3 years
Typhoid Vaccine Live Oral Ty21a	Vivotif	live attenuated		oral	4 doses every other day
Typhoid Vi Polysaccharide Vaccine	TYPHIM Vi	subunit		intramuscular	1
Varicella Virus Vaccine Live	Varivax	live attenuated		intramuscular or subcutaneous	2 doses at 12-15 months and 4-6 years
Yellow Fever Vaccine	YF-Vax	live attenuated		subcutaneous	1
Zoster Vaccine, Live, (Oka/Merck)	Zostavax	live attenuated		subcutaneous	1
Zoster Vaccine Recombinant, Adjuvanted	SHINGRIX	subunit	AS01B	intramuscular	2 doses 1-6 months apart

Chapter 2: The TLR7/8 agonist INI-4001 enhances the immunogenicity of a Powassan virus-like particle vaccine

Michael W. Crawford[1,2], Walid M. Abdelwahab[3,4], Karthik Siram[3,4], Christopher J. Parkins[1], Henry F. Harrison[1], E. Taylor Stone[5], Samantha R. Osman[2], Dillon Schweitzer[3,4], David J. Burkhart[6], Amelia K. Pinto[7], James D. Brien[7], Jessica L. Smith[1,8], Alec J. Hirsch[1,8]

Affiliations

[1]Vaccine and Gene Therapy Institute, Oregon Health & Science University, Beaverton, OR, USA.

[2]Department of Molecular Microbiology and Immunology, Oregon Health & Science University, Portland, OR, USA.

[3]Department of Biomedical and Pharmaceutical Sciences, University of Montana, Missoula, MT, USA.

[4]Center for Translational Medicine – Adjuvant Research Team, University of Montana, Missoula, MT, USA.

[5]HDT Bio, Seattle, WA, USA.

[6]Inimmune Corporation, Missoula, MT, USA.

[7]Department of Microbiology, Immunology and Molecular Genetics, University of Kentucky College of Medicine, Lexington, KY, USA.

[8]Division of Pathobiology & Immunology, Oregon National Primate Research Center, Oregon Health & Science University, Beaverton, OR, USA

Author contributions

M.W.C., J.L.S., W.M.A., D.J.B., and A.J.H.: designed experiments. M.W.C., C.J.P., H.F.H., S.R.O., and J.L.S.: performed experiments. W.M.A., K.S., D.S., and D.J.B.: adjuvant synthesis and QCETS. A.K.P. and J.D.B.: T cell assays. M.W.C., J.L.S., and A.J.H.: prepared figures, wrote the paper. All authors reviewed the manuscript.

Published in NPJ Vaccines July 16th, 2025

DOI: 10.1038/s41541-025-01215-9

Abstract

Powassan virus (POWV) is a pathogenic tick-borne flavivirus that causes fatal neuroinvasive disease in humans. There are currently no approved therapies or

vaccines for POWV infection. Here, we develop a POW virus-like particle (POW-VLP) based vaccine adjuvanted with the novel synthetic Toll-like receptor 7/8 agonist INI-4001. We demonstrate that INI-4001 outperforms both alum and the Toll-like receptor 4 agonist INI-2002 in enhancing the immunogenicity of a dose-sparing POW-VLP vaccine in mice. INI-4001 increases the magnitude and breadth of the antibody response as measured by wholevirus ELISA, induces neutralizing antibodies measured by FRNT, reduces viral burden in the brain of infected mice measured by RT-qPCR, and confers 100% protection from lethal challenge with both lineages of POWV. We show that the antibody response induced by INI-4001 is more durable than standard alum, and 80% of mice remain protected from lethal challenge 9-months post-vaccination. Lastly, we show that the protection elicited by INI-4001 adjuvanted POW-VLP vaccine is unaffected by either CD4+ or CD8+ T cell depletion and can be passively transferred to unvaccinated mice indicating that protection is mediated through humoral immunity. This study highlights the utility of novel synthetic adjuvants in VLP-based vaccines.

Introduction

Powassan virus (POWV) is a tick-borne flavivirus comprising two lineages of pathogenic virus found in North America and Far Eastern Russia maintained in nature by enzootic cycles between various mammalian hosts and a few key species

of ixodid ticks [276-280, 283, 300, 624-626]. Human infection from tick bites can result in life-threatening neuroinvasive disease with a case fatality rate of ~12% and long-term neurological sequelae in 50% of survivors [293, 316]. Though cases of human infection have been historically rare, the incidence of POWV cases has been increasing and there is evidence that the virus is emerging in North America [276, 278, 627]. Most cases occur in the northeast and Great Lakes regions of the United States where the two main ixodid tick vectors *Ix. cookei* and *Ix. scapularis* are most abundant [158, 276, 628, 629]. However, the geographical distribution of POWV cases may expand as the climate continues to warm and POWV vectors continue to spread [153, 628-630]. There are currently no approved vaccines or therapies for POWV infections. These factors make POWV a growing public health concern for which the development of a vaccine should be prioritized.

Several groups have stepped forward in recent years to develop a vaccine for POWV using platforms including virus-like particles (VLPs), mRNA, DNA, subunit nanoparticles, and an attenuated viral chimera of POWV with the yellow fever 17D vaccine strain [613, 617-620, 631]. VLP-based vaccination stands out as a safe and effective platform for the development of a POWV vaccine as demonstrated by previous work from our group as well as Cimica *et. al* [609, 620]. VLPs are recombinant antigens of viral structural proteins that self-assemble into particles that resemble the virus itself, including critical quaternary epitopes ([620,

631-633] and reviewed in [100, 634-636]). Because they are not capable of replication, VLP-based vaccines are safer than inactivated or attenuated viruses which can pose a health risk to vaccinees if not completely inactivated or attenuated. Flavi-VLPs can be generated through the expression of the viral structural proteins pre-membrane (prM) and envelope (E), the latter being the main target of neutralizing antibody responses to flaviviruses. The resulting presentation of E in a near-native geometry and conformation can surpass formaldehyde-inactivated virus in its ability to induce neutralizing antibodies to structural epitopes [354, 355]. VLPs have been shown to induce not only robust, high-quality humoral responses for flaviviruses but also cellular immunity characterized by a Th1 and cytotoxic T lymphocyte (CTL) response making them ideal antigens for future tick-borne flavivirus-vaccines ([354, 368, 634, 637-640] and reviewed in [345, 641]).

Adjuvants are important in generating an effective and durable response to VLPs by enhancing processes that lead to an improved adaptive immune response [534, 642]. Adjuvants accomplish this by altering the uptake of antigens and/or triggering an innate immune response in the absence of infection. Alum is the most common vaccine adjuvant and has a number of proposed methods of action including activating the pattern recognition receptors (PRRs) cGAS-STING and NLRP3 as well as forming a gel-like structure that retains the antigen at the

injection site to promote a sustained immune response, though these methods of action are debated (reviewed in [643]). While alum has dominated the field for decades, there are many other PRR-targeting adjuvants that have shown great potential in preclinical and clinical vaccines for their ability to elicit robust, durable antibody responses as well as T-helper type 1 (Th1) responses. Among these are Toll-like receptor (TLR) agonists which mimic the pathogen-associated molecular patterns recognized by TLRs, a key class of PRR that mediates the initial innate immune and subsequent adaptive immune response to infection. TLR agonists have emerged as particularly effective in the development of virus vaccines. The TLR7/8 agonist INI-4001 (TLR7 agonist in mice and TLR7/8 agonist in humans [572, 644]) and the TLR4 agonist INI-2002 are two novel synthetic adjuvants that have proven effective at improving the humoral and cellular immune response in multiple candidate vaccines making them great candidates for the development of a POWV vaccine [572, 575, 577, 580, 582].

In this study, we describe the immunogenicity of a VLP-based vaccine for POWV adjuvanted with either alum, INI-2002, or INI-4001. We demonstrate that the addition of the TLR7/8 agonist INI-4001 significantly improves the neutralizing antibody response and protection against lethal infection from both lineages I and II of POWV. Vaccine adjuvanted with INI-4001 also significantly reduces the viral burden in the brain of infected mice and increases the durability of humoral

immunity which appears to mediate protection against challenge as demonstrated by passive transfer. We conclude that POW-VLP adjuvanted with INI-4001 is a highly promising vaccine candidate against POWV.

Results

A POW-VLP vaccine adjuvanted with a TLR7/8 agonist protects mice from lethal POWV challenge

Previously, we produced a cell line that expresses lineage 1 POWV LB strain (POWV-I) prM-E when induced with doxycycline [609]. Expression of POWV-prM-E leads to the self-assembly and secretion of Powassan virus-like particles (POW-VLP) into tissue culture supernatant, which can be collected and purified. We confirmed the secretion of particles with an average diameter of 25nm by electron microscopy (Figure 2.1A) and quantified these particles relative to infectious POWV by western blot and ELISA of E protein (Figure 2.1B). We confirmed the purity of our POW-VLP by Coomassie stain (Figure 2.1C). The two prominent protein bands seen near 55kDa and 17kDa correspond to E and prM, respectively (Figure 2.1C) [620]. These match well with those bands seen with an equivalent amount of E from POWV with an additional larger band that may be uncleaved M-E [620]. We previously demonstrated that prime-boost vaccination

of mice with 2X10^7 E-protein focus-forming-unit equivalents (FFUe) of POW-VLP adjuvanted with alum induced neutralizing antibodies in mice and conferred 100% protection from lethal challenge with POWV-I [609].

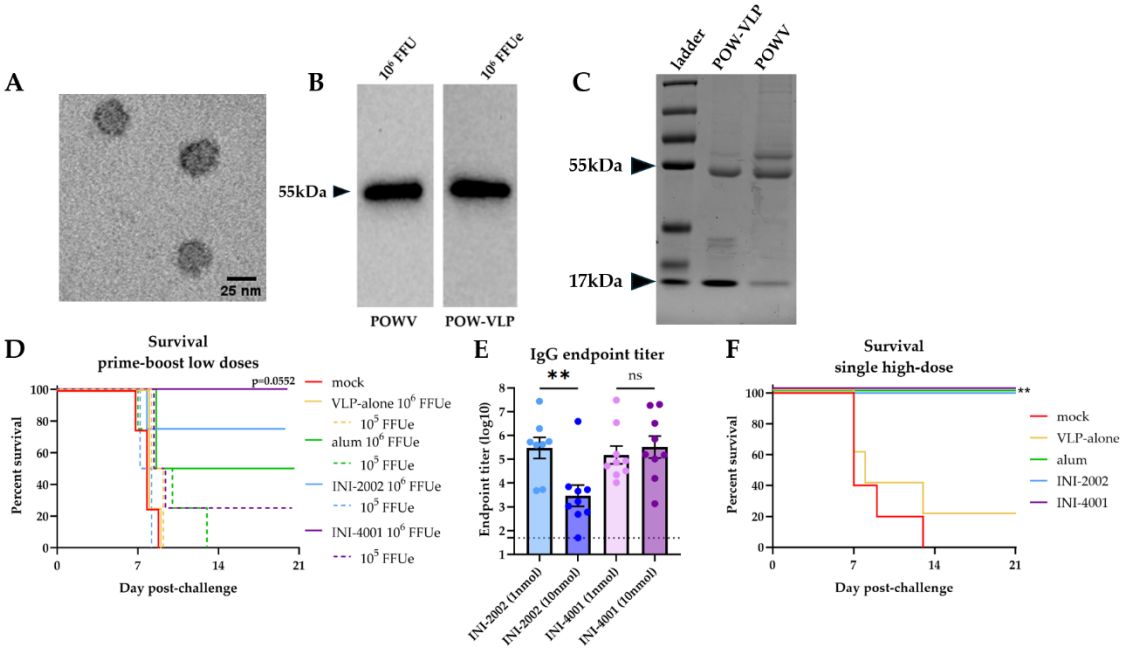

Figure 2.1: Quantifying VLPs and optimizing dosing.

(A) Purified POW-VLP visualized by transmission electron microscopy. (B) SDS-PAGE and western blot of POWV (left) and POW-VLP (right) stained with T077 anti-TBEV-E antibody. Expected migration at 54 kDa. (C) Coomassie Blue stained SDS-PAGE gel with ladder (left lane), 5 μl POW-VLP (middle lane), and $3x10^8$ FFU POWV (right lane). Uncropped images of (A) and (B) are shown in supplementary figures 3 and 4, respectively. **(**D) Mice prime-boost vaccinated 2 weeks apart *sc* with either 10^5 or 10^6 FFUe of VLP either alone or adjuvanted with 11μmol alum, 10nmol INI-2002, or 10nmol INI-4001. Mock group injected with PBS vehicle alone. Vaccinated mice were then challenged with a lethal 10^3 FFU dose of POWV-LB 2 weeks post-boost. Survival of mice assessed to day 20 post-challenge. n=4/group. Statistical significance determined by log rank test with Bonferroni correction to compare adjuvant groups to mock. (E) Mice prime-boost vaccinated 2 weeks apart *sc* with 10^6 FFUe of VLP adjuvanted with either varying concentrations of INI-2002 or INI-4001, n=8-9/group. Serum collected 2 weeks post-vaccination and analyzed by whole-virus ELISA with anti-mouse IgG. Endpoint titers are log-transformed and reported as means ± SEM. Dotted line represents the least dilute serum tested (1:50). Statistical significance determined by one-way ANOVA and Šídák's multiple comparisons test to compare doses within adjuvant treatment groups. Data represent two independent experiments. (F) Mice prime vaccinated *sc* with either $1.5X10^7$ FFUe of VLP alone or adjuvanted with either 11μmol (300 μg) alum, 1nmol INI-2002, or 10nmol INI-4001. Mock group injected with PBS vehicle alone. Vaccinated mice

were then challenged with a lethal 10^3 FFU dose of POWV-LB 3 weeks post-vaccination. Survival of mice assessed to day 21 post-challenge. n=5/group. Statistical significance determined by log rank test with Bonferroni correction to compare adjuvant groups to mock. ns = not-significant, ** = $p < 0.01$.

We sought to test whether the TLR4 agonist INI-2002 or the TLR7/8 agonist INI-4001 could improve our POW-VLP vaccine and allow us to reduce the antigen dose while maintaining immunogenicity and protection. Reduction of antigen also provides greater sensitivity to evaluating adjuvant efficacy. To determine what antigen dose was required for protection from lethal POWV challenge, we vaccinated C57BL/6 (B6) mice twice subcutaneously (*sc*) two weeks apart with either 10^5 or 10^6 FFUe of VLP (200- and 20-fold less antigen than we had previously used with alum, respectively) adjuvanted with 10nmol of either INI-2002 or INI-4001 in their aqueous formulations. We then challenged the mice 2 weeks post-boost with a lethal dose (10^3 FFU) of POWV-I [609]. We monitored mice for weight loss and other signs of disease for three weeks. Mice that exhibited clinical signs of morbidity including paralysis and/or substantial weight loss (≥ 20% original body weight) were humanely euthanized. All mock vaccinated mice died by day 9 post-challenge (Figure 2.1D). Of the low-dose vaccinated mice, only one mouse which had received INI-4001 survived (25% survival rate). The survival rate

increased to 100% for INI-4001-vaccinated mice with the higher antigen dose ($p = 0.055$ compared to the survival of mice in the mock group). Likewise, the survival for alum-vaccinated mice rose to 50% and 75% for INI-2002-vaccinated mice (not significantly different than mock after adjusting for multiple comparisons). Given the 100% protection for INI-4001-vaccinated mice and the stratification in efficacy between the other adjuvants, we moved forward with 10^6 FFUe for low-dose prime-boost vaccination.

Next, to determine the appropriate amount of adjuvant for vaccination, we vaccinated mice twice subcutaneously (*sc*) two weeks apart with 10^6 FFUe of VLP adjuvanted with either 1 or 10nmol of either INI-2002 or INI-4001 in their aqueous formulations. We then collected sera 2 weeks post-boost and measured endpoint IgG titer. INI-2002 generated a higher anti-POWV IgG antibody titer at the lower dose of 1nmol while INI-4001 induced equal IgG responses at both doses (Figure 2.1E). Previous studies with INI-4001 have shown that formulations with higher doses improve the immune response [572, 577]. Given this information, we chose 1nmol INI-2002 and 10nmol INI-4001 as the working doses for subsequent POWV vaccine studies.

We next sought to replicate our previous findings that a higher dose of VLP could protect mice with alum and whether this was also the case with INI-2002 and INI-4001. Additionally, we wanted to determine if a higher dose might induce

protection with a single immunization. For this, we vaccinated mice with a single dose of 1.5 X 10^7 FFUe VLP either alone or adjuvanted with alum, INI-2002, or INI-4001 and challenged mice 3 weeks post-vaccination with a lethal dose of POWV. All three adjuvanted formulations elicited full protection from POWV challenge (Figure 2.1F). This suggests that INI-4001 is specifically unique in its ability to generate a protective vaccine with low doses of antigen while all adjuvants are effective with higher dose vaccines.

Finally, to test the efficacy of each adjuvant at optimal adjuvant doses in a low-antigen prime-boost vaccine model, we vaccinated mice in the same manner as above with either VLP alone or VLP adjuvanted with alum, INI-2002, or INI-4001. Control mice were vaccinated with PBS vehicle alone. Sera collected 2 weeks post-boost vaccination were analyzed for whole-virus binding by ELISA. The mean log IgG endpoint titer in alum-vaccinated mice (3.1) was not significantly different than the background titer observed in mock-vaccinated animals (2.3) or in mice vaccinated with VLP alone (2.5) (Figure 2.2A). Between the two novel TLR agonists, only INI-4001 produced significantly higher IgG titers (4.9, $p = 0.014$) than alum. We then measured the neutralizing antibody titers of vaccinated mice and found that only 2/18 of the mice vaccinated with INI-2002 produced focus reduction neutralization test 50 (FRNT50) above the limit of dilution compared to 11/18 of the INI-4001-vaccinated mice (Figure 2.2B). Together these data

demonstrate that INI-4001, but not INI-2002, outperforms alum in inducing IgG and neutralizing antibodies targeting POWV in a low-dose prime-boost POW-VLP vaccine.

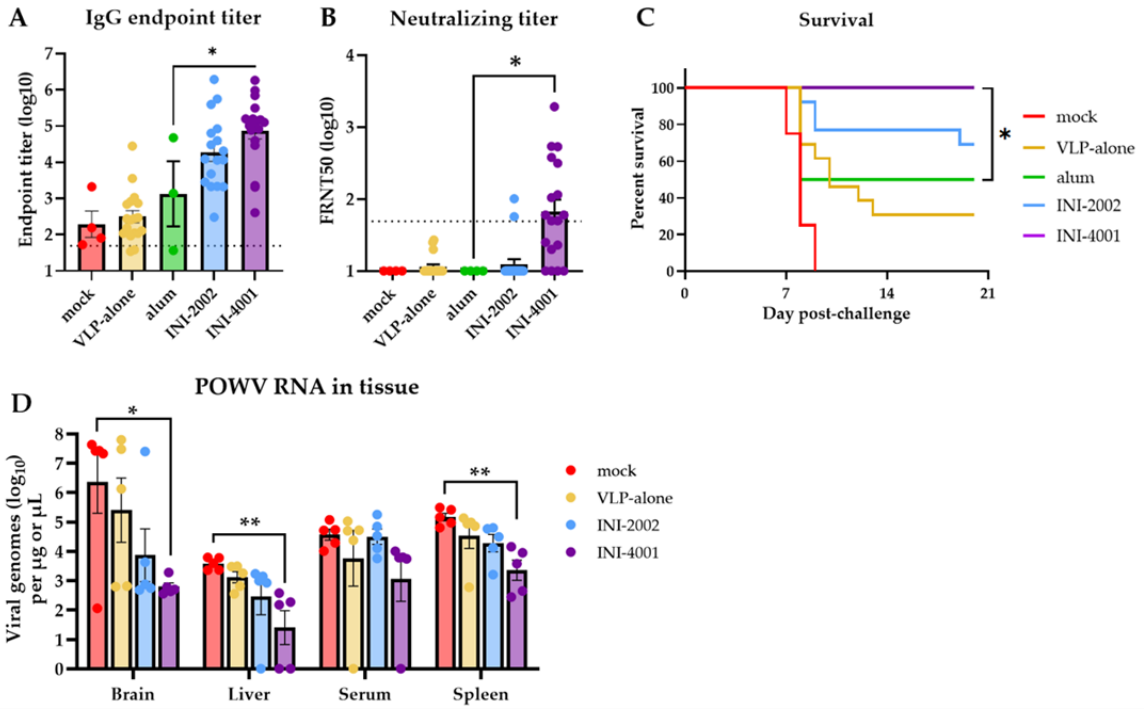

Figure 2.2: INI-4001-adjuvanted VLP elicits superior antibody response, protection from lethal POWV challenge, and decreases viral RNA burden in multiple tissues post-challenge.

(A-B) Mice prime-boost vaccinated 2 weeks apart *sc* with 10^6 FFUe of VLP alone or adjuvanted with 11 μmol (300 μg) alum, 1nmol INI-2002, or 10nmol INI-4001. Mock group injected with PBS vehicle alone. mock n=4; VLP-alone n=18-19; alum n=3-4; INI-2002 n=14; INI-4001 n=18. Serum collected 2 weeks post-boost and analyzed by whole-virus ELISA (A) or FRNT (B). Data are reported as log-transformed mean endpoint titer ± SEM for IgG titer and reciprocal FRNT50 for neutralizing titer. Dotted line represents least dilute sera tested (1:50). Data represent three independent experiments including data from 1E. (A) Statistical significance determined by one-way ANOVA and Šídák's multiple comparisons test to compare treatments to alum group after log transformation. * = $p < 0.05$. (B) Statistical significance determined by one-way ANOVA and Šídák's multiple comparisons test to compare alum group to INI-2002 and INI-4001. (C) Vaccinated mice challenged with a lethal 10^3 FFU dose of POWV-LB 2 weeks post-boost. Survival of mice assessed to day 20 post-challenge. mock n=4; VLP-alone n=13; alum n=4; INI-2002 n=13; INI-4001 n=13. Data represent three independent experiments including data from 1D. Statistical significance determined by log rank test with Bonferroni correction to compare adjuvant groups to VLP-alone. * = $p < 0.05$, ** = $p < 0.01$. (D) Mice prime-boost vaccinated 3 weeks apart with PBS, VLP alone, or adjuvanted VLP. n=5/group. Vaccinated mice infected *ip* with 10^4 FFU POWV-LB 4

weeks post-boost. Viral load was measured in tissues harvested 6 days post-infection by RT-qPCR. Data are reported as log-transformed mean ± SEM. Statistical significance was determined on log-transformed data using one-way ANOVA with Šídák's multiple comparisons to mock-vaccinated mice within each compartment. * = $p < 0.05$, ** = $p < 0.01$.

Stronger adaptive immune responses to numerous vaccines have been observed in both female mice and humans with evidence that this is due to higher TLR7 expression in B cells in females [645, 646]. TLR4 is also differentially expressed between the sexes with higher levels of TLR4 found on the surface of macrophages from male mice which respond more strongly to the TLR4 agonist lipopolysaccharide (LPS) [647]. To determine how sex affects the antibody response to INI-2002 and INI-4001, we evaluated the anti-POWV IgG and neutralizing antibody titers in both male and female mice (Supplemental Figure S2.1). Interestingly, we saw that female mice had significantly higher total IgG and neutralizing antibody responses to INI-2002 than males, while there were no differences in the response to INI-4001. These results seem to contradict the hypothesis that more TLR7 in females would lead to a stronger INI-4001 response while more TLR4 in males would increase the response to INI-2002. More experiments are needed to explain this phenomenon. For our current study, we

continued to evaluate our vaccines in male mice to provide more rigorous results and ensure our conclusions were not augmented by sex differences.

To determine whether these formulations could elicit protection from POWV, we challenged mice intraperitoneally (*ip*) at the time of serum collection with a lethal dose (10^3 FFU) of POWV-I. We monitored mice for weight loss and other signs of disease for three weeks. All mock-vaccinated mice died or were euthanized 7-9 days post-infection consistent with previous studies (Figure 2.2C) [306, 606, 609, 613, 648]. Survival of mice that received VLP alone with no adjuvant was 31%, whereas mice that received alum adjuvanted vaccine had a survival rate of 50%. Survival of INI-2002 vaccine mice was higher at 69% but this was not significantly different than the survival of alum-vaccinated mice. Mice vaccinated with INI-4001-adjuvanted POW-VLP were completely protected over the course of the study (100% survival, $p = 0.025$ compared to alum). Taken together, these data demonstrate that POW-VLP adjuvanted with the TLR7/8 agonist INI-4001 induces both higher IgG and neutralizing antibody titers than a standard alum formulation and confers significant improvement in protection from lethal challenge at this early timepoint.

INI-4001 decreases viral burden in brain, liver, and spleen of infected mice

POWV is neurotropic and can be detected in the brain of infected humans and mice [292, 306, 606, 648-650]. Similar to infection with the closely related tick-borne encephalitis viruses (TBEV), the neuropathologies associated with POWV are thought to be mediated both by viral neuroinvasion and cytotoxic CD8+ T cell infiltration into the central nervous system [176, 609]. It is therefore important for a vaccine to reduce POWV neuroinvasion. To determine whether POW-VLP adjuvanted with either INI-2002 or INI-4001 reduces dissemination of virus to the brain and other tissues, we infected vaccinated mice with a lethal dose of POWV-I and harvested the brain, liver, spleen, and blood at 6 days post-infection. We then measured viral RNA titer by RT-qPCR in homogenized tissues. Four of the five mock-vaccinated mice had substantial levels of POWV viral RNA in the brain at the time of harvest while INI-4001-vaccinated mice appeared to be largely protected from neuroinvasion with a significantly lower mean titer (Figure 2.2D). Although INI-2002-vaccinated mice trended towards lower POWV burden in the brain, this was not statistically significant. Similarly, INI-4001-vaccinated mice had significantly reduced viral loads in the liver and spleen compared to mock-vaccinated mice with no significant differences detected in the INI-2002-vaccinated mice. These results demonstrate that adjuvantation with INI-4001

reduces viral loads in multiple tissues post-infection, most prominently in brain tissue, consistent with the observed protection against POWV-induced mortality elicited by this formulation.

Passive transfer of sera from vaccinated mice protects naïve mice from challenge

Given the superior vaccine response and protection elicited by the adjuvant INI-4001 compared to INI-2002, we chose to continue to evaluate our POW-VLP vaccine formulated with INI-4001. We next sought to evaluate how the humoral and cellular arms of the adaptive immune response are contributing to the protection elicited by our vaccine. We first assessed the role of antibody-mediated protection by passively transferring the pooled sera of vaccinated mice into unvaccinated mice one day prior to lethal challenge. IgG and neutralizing antibody titers were measured in pooled sera and in recipient mice the day after transfer (Figs 3A and B). Mice that received sera from vaccinated mice had FRNT50 values very close to the mean measured in INI-4001-vaccinated mice in previous experiments (Figure 2B). Mice that received pooled sera from mock-vaccinated mice died 6-7 days post-challenge while four of the five mice that received vaccinated-mouse sera survived (Figure 2.3C). Interestingly, the one mouse that

succumbed to infection that received vaccinated-mouse serum didn't begin to decline until day 13 post-challenge (Figure 2.3D). Given that the half-life of mouse antibodies is on the order of one week, these data suggest that the transferred sera antibodies did not fully clear infection and the mouse succumbed after antibody titers declined below the protective threshold [651]. This experiment demonstrates that the antibody response elicited by our INI-4001-adjuvanted POW-VLP vaccine contributes to protection from lethal challenge.

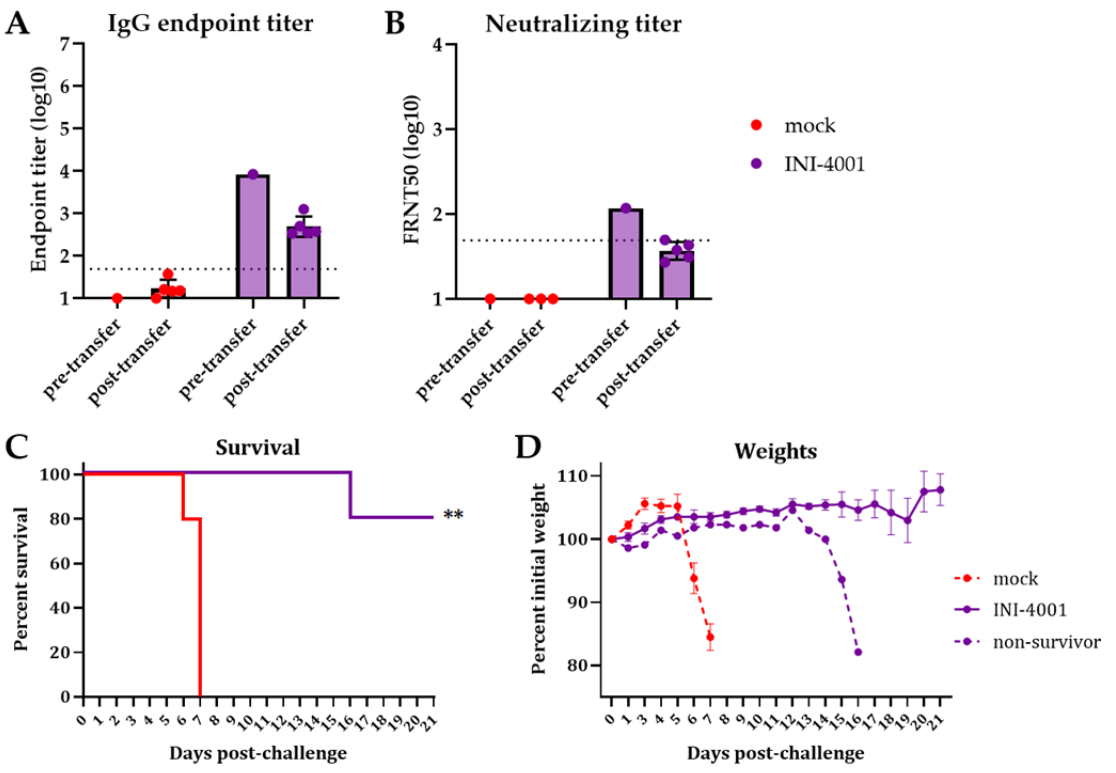

Figure 2.3: Passive transfer of vaccinated mouse sera protects naïve mice from lethal challenge.

Mice vaccinated twice 3 weeks apart. Sera collected 3 weeks post-boost and pooled. n=5/group for both vaccinated donors and unvaccinated recipients. Unvaccinated mice received 200uL of pooled sera *ip* one day before *ip* infection with 10^4 FFU POWV-LB. Serum collected one day post-transfer from recipient mice and analyzed alongside pre-transfer pooled sera by whole-virus ELISA (A) and FRNT (B). Data are reported as log-transformed mean endpoint titer ± SEM for IgG titer and reciprocal FRNT50 for neutralizing titer. Dotted line represents least dilute sera tested (1:50). Survival (C) and weights (D) monitored for 21 days post-challenge. (C) Statistical significance determined by log rank Mantel-Cox test to compare vaccinated animals to mock. ** = $p < 0.01$. (D) Weights represented as mean percent of initial weights ± SEM. All data represent single experiment.

Depletion of CD4+ or CD8+ T cells does not affect protection

The lack of measurable neutralizing titers in several mice that are protected from lethal POWV challenge (Figure 2B & C) raised the question of whether a portion of the vaccine-induced protection is mediated by non-humoral adaptive immunity. Although we were unable to detect POWV-specific T cell responses in vaccinated mice (Supplemental Figure S2.2), we assessed whether T cells are

required for mediating protection by performing T cell depletion in vaccinated animals prior to challenge and observing differences in survival. We depleted $CD4^+$ or $CD8^+$ T cells by administering CD4- or CD8-depleting antibodies in prime-boost vaccinated mice 3 days prior to and the day of challenge (Figure 2.4A). We confirmed T cell depletion by flow cytometry of blood 3 days post-challenge (Figs 4B-D). Survival of the infected mock-vaccinated animals was not impacted by either $CD4^+$ or $CD8^+$ T cell depletion compared to the isotype control group (Figure 2.4E), nor were there differences in weight loss for these animals (Figure 2.4F). Similarly, neither CD4- nor CD8-depletion affected the survival of INI-4001-vaccinated mice, with 100% of all mice surviving lethal challenge and maintaining weights regardless of depleting antibody. These data suggest that the protection from POWV challenge elicited by POW-VLP adjuvanted with the TLR7/8 agonist INI-4001 at this early timepoint does not rely on T cells.

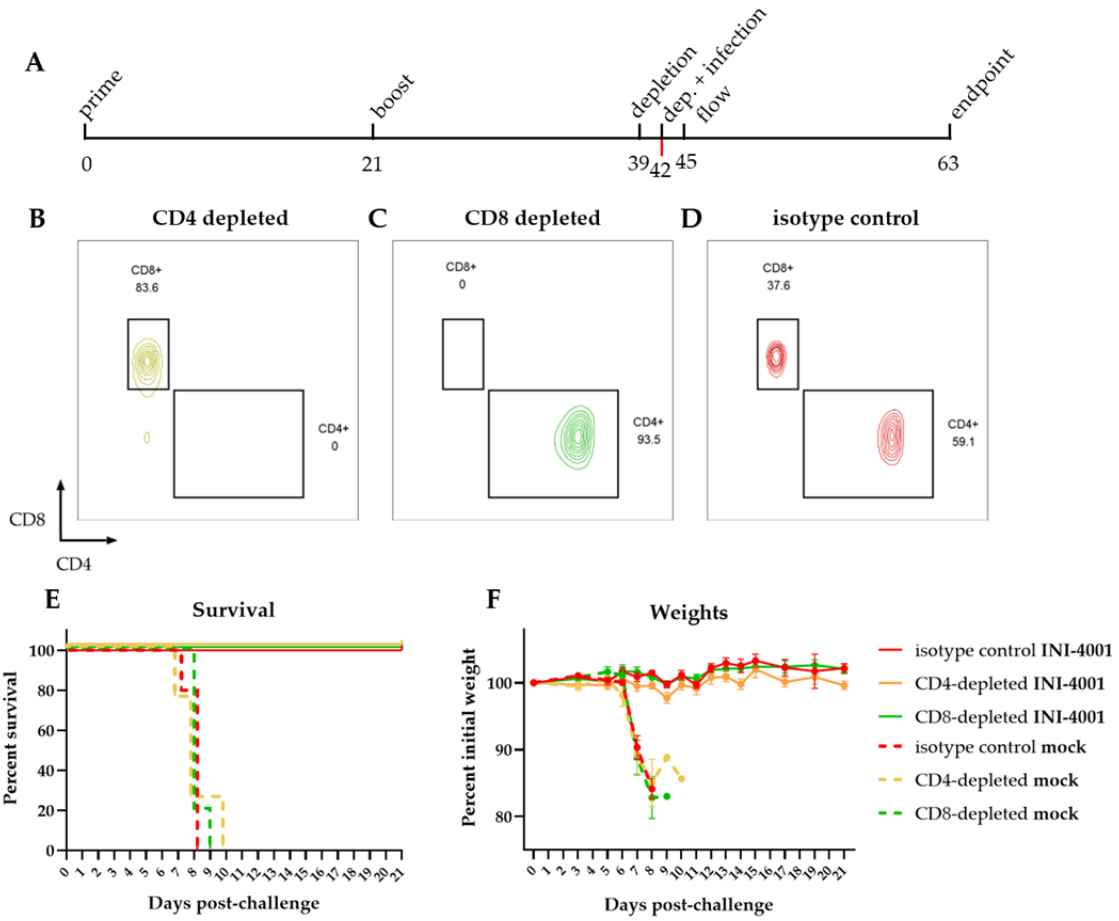
A
prime
boost
depletion
dep. + infection
flow
endpoint
0
21
39
42
45
63
B
CD4 depleted
CD8+
83.6
CD4+
0
C
CD8 depleted
CD8+
0
CD4+
93.5
D
isotype control
CD8+
37.6
CD4+
59.1
CD8
CD4
E
Survival
Percent survival
Days post-challenge
F
Weights
Percent initial weight
Days post-challenge
isotype control INI-4001
CD4-depleted INI-4001
CD8-depleted INI-4001
isotype control mock
CD4-depleted mock
CD8-depleted mock

Figure 2.4: T cell depletion does not affect survival of vaccinated mice.

(A) Timeline of experiment in days. Mice were prime-boost vaccinated 3 weeks apart (days 0 and 21) *sc* with 10^6 FFUe of POW-VLP adjuvanted with 10nmol INI-4001. The mock group was injected with PBS vehicle alone. Mice were then treated *ip* with 100 μg of either CD4-depleting, CD8-depleting, or non-depleting isotype control (n=5/group) 3 weeks post-boost (day 39) and again three days later (day 42). Mice were challenged with a lethal 10^4 FFU dose of POWV-LB *ip* at time of second depletion (day 42). Blood was collected by tail vein 3 days after second administration of depleting antibodies to confirm T cell depletion (day 45). Survival and weights of mice monitored to day 21 endpoint post-challenge (day 63). (B-D) Representative flow plots of T cells from (B) CD4, (C) CD8-, or (D) control-depleted mice 3 days post-depletion (gating strategy is shown in supplementary figure 5). Cells gated on $CD45^+$ $CD3^+$ $CD19^-$ $CD4^+/CD8^+$. (E-F) Survival (E) and weights (F) of mock (dashed lines) or INI-4001 (solid lines) vaccinated mice after depletion of either $CD4^+$ (yellow) or $CD8^+$ (green) T cells compared to isotype control (red). (E) Statistical significance determined by log rank test with Bonferroni correction to compare depleted groups to isotype control. No significant differences were found. (F) Weights represented as mean percent of initial weights ± SEM. Data represent one experiment.

Vaccine against POWV-I adjuvanted with INI-4001 agonist generates cross-reactive antibodies to other tick-borne flaviviruses and protects against lethal challenge from POWV-II

There are two lineages of POWV, both of which infect and cause disease in humans. POWV-LB is the prototype of the lineage I (POWV-I) whose genome we used to generate our POW-VLP and the virus used for challenge studies thus far. However, protection against both lineages is important to protect individuals against POWV disease. We therefore sought to evaluate the cross-reactivity of antibodies from vaccinated mice to the prototypical POWV-II Spooner strain as well as another more distantly related tick-borne flavivirus, Langat virus (LGTV), and an even more distantly related mosquito-borne flavivirus, West Nile virus (WNV). Vaccination with INI-4001 induced antibodies that could bind to both POWV-II and LGTV by ELISA, while alum did not generate any measurable cross-reactive binding activity (Figure 2.5A). Neither alum- nor INI-4001-vaccinated mice produced antibodies that could cross-react to WNV. INI-4001-vaccinated mice had minimal but measurable cross-neutralizing activity to POWV-II with estimated FRNT50s all falling below the line representing the least dilute serum tested (Figure 2.5B).

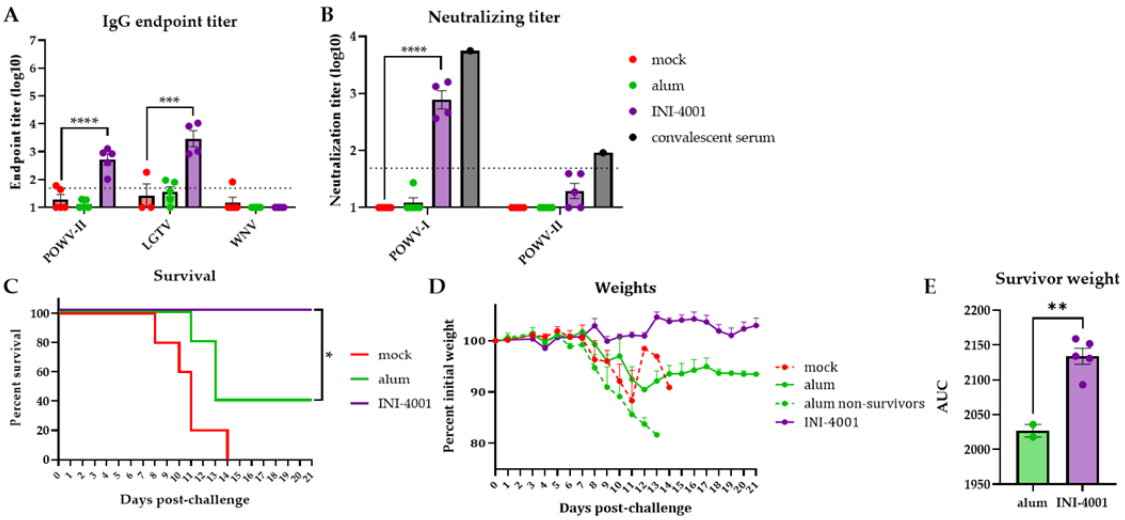
A
IgG endpoint titer
Endpoint titer (log10)
****
***
POWV-II
LGTV
WNV
B
Neutralizing titer
Neutralization titer (log10)
****
POWV-I
POWV-II
mock
alum
INI-4001
convalescent serum
C
Survival
Percent survival
Days post-challenge
*
mock
alum
INI-4001
D
Weights
Percent initial weight
Days post-challenge
mock
alum
alum non-survivors
INI-4001
E
Survivor weight
AUC
**
alum
INI-4001

Figure 2.5: Vaccination with INI-4001-adjuvanted POWV-I-VLP generates antibodies that bind POWV-II and LGTV and protects mice from lethal POWV-II challenge.

Mice prime-boost vaccinated 3-4 weeks apart *sc* with 10^6 FFUe of VLP alone or adjuvanted with 11μmol alum or 10nmol INI-4001. n=5/group. Mock group injected with PBS vehicle alone. Serum collected 3 weeks post-boost and analyzed by whole-virus ELISA (A) and FRNT (B). Data are reported as log-transformed mean endpoint titer ± SEM. Convalescent mouse serum from mouse that survived two POWV infections. (A-B) Statistical significance determined by one-way ANOVA with Šídák's multiple comparisons test to compare vaccinated mice to mock-vaccinated mice. (A) n=5/group except for LGTV n=3 for mock and n=4 for INI-4001. (B) n=5/group except for POWV-II mock n=4 and POWV-I INI-4001 n=4. (C-D) Mice challenged *ip* 3 weeks post-boost with 10^5 FFU dose of POWV-II. Survival (C) and weights (D) monitored for 21 days post-challenge. (C) Statistical significance determined by Mantel-Cox log rank test to compare alum and INI-4001 groups. * = $p = 0.05$. (D) Weights represented as mean percent of initial weights ± SEM. (E) Area under the curve (AUC) of individual alum and INI-4001 survivors. Statistical significance determined by Student's unpaired t-test. ** = $p < 0.01$. Data for POWV-II and LGTV ELISA, FRNT, survival, weights, and AUC represent one experiment; data for WNV represents independent experiment.

We next sought to evaluate whether POW-VLP adjuvanted with INI-4001 could protect from POWV-II challenge. Mock-vaccinated mice infected with a

lethal dose (10^5 FFU) of POWV-II all succumbed to infection by day 14 post-challenge with a median survival of 11 days (Figure 2.5C), as observed previously [609]. All five mice that received the INI-4001-adjuvanted vaccine survived POWV-II challenge while only two of five alum-vaccinated mice survived this challenge, which was a statistically significant difference. Both alum-vaccinated survivors lost 10% of their body weight before partially recovering back to ~93% of their initial weight (Figure 2.5D). Comparatively, the largest weight drop within the INI-4001-vaccinated group was ~3%, and the mean ranged from 99-105% and finished at 103%. Area under the curve analysis was performed on the surviving mice that received either alum- or INI-4001-adjuvanted VLP which revealed a statistically significant difference in weights between these groups over the course of the challenge ($p = 0.03$; Figure 2.5E). In conclusion, INI-4001 further outperforms alum as a vaccine adjuvant by inducing the production of cross-reactive antibodies to both POWV-II and LGTV and protects mice from lethal POWV-II challenge.

INI-4001 elicits a durable immune response

We lastly sought to evaluate the durability of the immune response elicited by alum, INI-2002, or INI-4001. To do this, we measured the IgG and neutralizing antibody titers in the sera from vaccinated mice every month for 8 months (36 weeks) post-boost vaccination. Anti-POWV-I IgG antibody titers induced by all

three adjuvanted vaccines peaked 8 weeks post-boost (Figure 2.6A) with peak log endpoint titers that were nearly 1,000-fold higher in mice that received INI-4001- compared to alum-adjuvanted VLP. By 20 weeks post-boost, the IgG titers in all adjuvant groups dropped to a lower plateau that was maintained to the last timepoint. While INI-2002-vaccinated mice had significantly higher titers than alum-vaccinated mice at only one timepoint, INI-4001-vaccinated mice maintained IgG titers that were significantly higher than alum-vaccinated mice throughout the experiment.

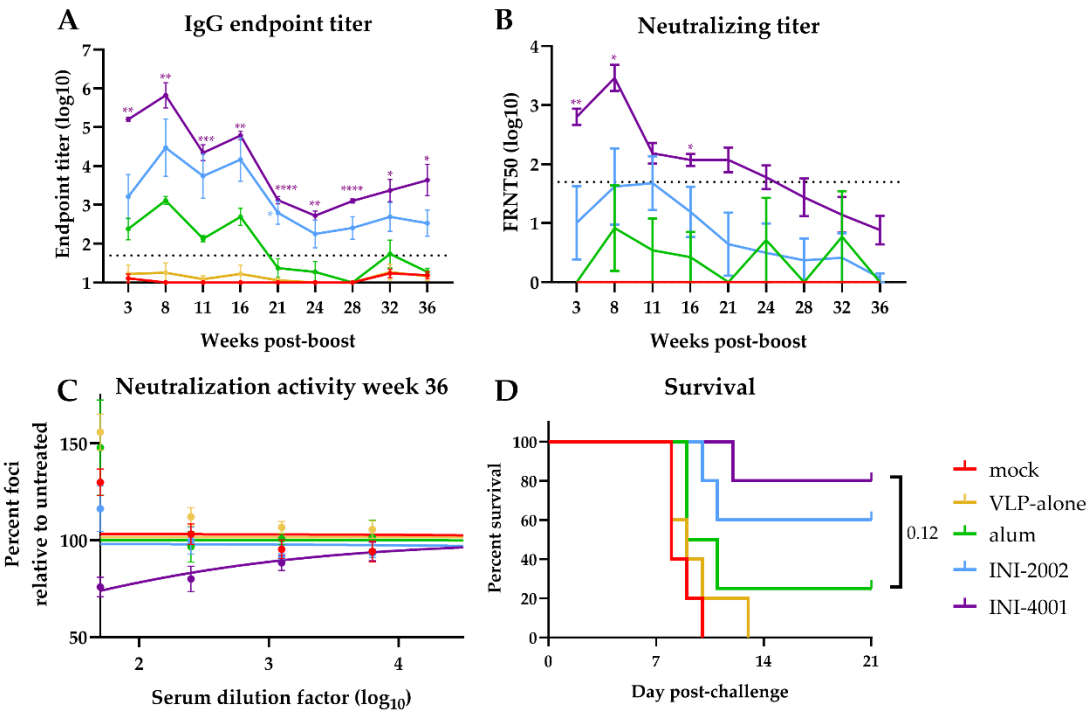

Figure 2.6: INI-4001-adjuvanted vaccine elicits durable antibody response with long-lasting protection.

(A-B) Mice vaccinated twice 4 weeks apart. Serum collected monthly for ~9 months post-boost and analyzed by whole-virus ELISA for IgG titer or reciprocal FRNT50 assay for neutralizing titers. (A,B) Data are log transformed and reported as means ± SEM. Statistical significance was calculated by repeated measure two-way ANOVA and Šídák's multiple comparisons test to compare TLR agonist treatments to alum-treated group after log transformation: * = $p < 0.05$; ** = $p < 0.01$; *** = $p < 0.001$; **** = $p < 0.0001$. Dotted line represents least dilute sera tested (1:50). (C) Neutralization activity of sera 36 weeks post-boost as measured by percent of foci per well of serum-treated virus relative to untreated control. Data represent treatment-group mean percentages ± SEM. Lines represent non-linear regression curves. (D) Mice infected *ip* at 9 months post-boost with 10^4 FFU POWV-LB. Survival monitored for 21 days. Statistical significance determined by log rank test with Bonferroni correction to compare adjuvant groups to alum treatment. All data represent single experiment. n=4 for alum; n=5/group for all other groups.

The neutralizing antibody responses in adjuvant-vaccinated animals also peaked by 8 weeks post-boost before slowly declining in all groups (Figure 2.6B). FRNT50 values peaked at dilutions of 1:8 for alum-vaccinated mice, 1:48 for INI-

2002, and 1:2,890 for INI-4001. By the end of the experiment, none of the alum-vaccinated mice had measurable neutralizing antibodies, and only one of the five INI-2002-vaccinated mice had a measurable titer. In contrast, four of the five INI-4001 mice had measurable titers. Though these final FRNT50 values fell below the limit of dilution and are therefore estimates, neutralization was readily observable in the sera of the INI-4001 group (Figure 2.6C). Throughout the experiment, INI-4001-adjuvanted VLP was the only vaccine that elicited mean neutralizing titers significantly higher than alum at any timepoint.

To test if these vaccine formulations induced durable protection, mice were challenged with POWV at 36 weeks post-boost. Only one of the four alum-vaccinated mice survived challenge compared to three of the five INI-2002-vaccinated mice and four of the five INI-4001-vaccinated mice (Figure 2.6D). Although the probability of survival in the INI-4001 vaccine group was not significantly different than in the alum group ($p=0.095$), this may be due to the small number of mice used in this study ($n=4$-5). Taken together, these results suggest that although the diminishing kinetics of the antibody responses were similar between vaccines, the higher initial response elicited by INI-4001-adjuvanted VLP creates a more durable antibody response and this translates to long-lasting protection from challenge nearly 9 months post-vaccination.

Discussion

POWV is a significant growing public health concern in North America for which there are currently no medical interventions. With an infection case fatality rate of 12% and a dramatic increase in the number of cases over the past two decades, the development of an effective and durable vaccine against POWV is critical [293, 316, 652]. There are several effective vaccines for other closely related tick-borne flaviviruses (TBFVs) including six approved vaccines for the tick-borne encephalitis viruses (TBEVs) and one for Kyasanur Forest disease virus [19-21]. These vaccines are all formalin-inactivated viruses, and those for TBEV are adjuvanted with alum. Though these vaccines are well-tolerated, immunogenic, and efficacious (reviewed in [19, 22, 23]), they have shortcomings including the risk posed by incomplete inactivation of virus used in vaccines, the possibility that important epitopes might be modified during inactivation, and the requirement for boosting every 1-5 years to maintain protective neutralizing titers [19-21, 24-26]. These points highlight the need to improve our current methodology for TBFV vaccines.

VLP-based vaccines have emerged as safe alternative vaccine candidates that maintain neutralizing epitopes and are thus expected to induce potent immune responses. Additionally, novel adjuvants such as TLR agonists have emerged as useful tools for improving vaccine responses and durability (reviewed

in [451]). Here, we demonstrate the potent combination of POW-VLP and the novel TLR7/8 agonist INI-4001 in the design of a POWV vaccine in mice. Prime-boost vaccination using a low-dose of 10^6 FFUe of POW-VLP adjuvanted with INI-4001 rapidly induced a significantly higher anti-POWV IgG and neutralizing antibody titer in mice compared to VLP adjuvanted with a standard alum formulation (Figs 2A-B) and conferred 100% protection from lethal POWV challenge (Figure 2.2C) validating the utility of this novel adjuvant.

The neuropathology associated with encephalitic TBFVs such as POWV is believed to arise from central nervous system (CNS) inflammation and leukocyte invasion following viral replication in the brain and CNS [306]. Mice that received INI-4001-adjuvanted vaccine had significantly reduced viral RNA loads in the brain, consistent with the protection from lethal challenge and absence of neurological symptoms in these mice (Figure 2.2D). INI-4001-vaccinated mice also had reduced viral RNA loads in the liver and spleen. Interestingly though, there was no difference in serum viremia between vaccinated and unvaccinated animals suggesting that tissue burden and viremia are independent at this timepoint. It is possible that earlier differences in viremia may have influenced the subsequent viral burden in these tissues, but that these differences were no longer apparent 6 days post-challenge. Santos *et. al* and Reynolds *et. al* have shown that POWV

viremia in mice peaks much earlier at about 1-2 days post-infection which supports this possibility [306, 648].

The need to develop TBFV vaccines that require less frequent boosting to maintain protection led us to test whether the vaccine response elicited by INI-4001-adjuvanted VLP was more durable than that of VLP adjuvanted with alum. Indeed, we found that POW-VLP adjuvanted with INI-4001 induced a more durable IgG and neutralizing antibody response (Figure 2.6A-B). Furthermore, vaccination with INI-4001-adjuvanted VLP protected 80% of mice from lethal infection 36 weeks post-boost compared to only 25% with alum-adjuvanted VLP (Figure 2.6C). The enhanced durability of the vaccine response induced by INI-4001 demonstrates the potential to improve our approach for both current and future TBFV vaccines.

The presence of two similar but genotypically distinct lineages of POWV, lineages I and II (POWV-I and POWV-II or deer tick virus) led us to investigate how broad the response to our POWV-I-based VLP vaccine is. We found that mice that received INI-4001-adjuvanted vaccine generated antibodies that bound not only POWV-II which shares 96% amino acid identity in the E protein to POWV-I, but also to LGTV which shares ~77% identity (Figure 2.5A). Mice that received alum-adjuvanted vaccines did not generate cross-binding antibodies to either of POWV-II or LGTV demonstrating that INI-4001 uniquely improves the breadth of

the antibody response. This improved breadth of the vaccine response translated to 100% protection from lethal POWV-II challenge in mice that received INI-4001-adjuvanted VLP compared to only 40% in those that received alum-adjuvanted VLP (Figure 2.5C).

Cell-mediated immunity characterized by antigen-specific cytotoxic CD8+ T cells and a Th1 response is ideal for the clearance of intracellular pathogens such as viruses (reviewed in [56]). Enhancing the T cell response to virus vaccines would likely improve efficacy and durability [206, 653]. Previous studies have shown that INI-4001 skews vaccine responses towards Th1 as do other TLR7/8 agonists [567, 569, 572, 577, 654]. We therefore sought to determine whether the protection conferred by our vaccine was mediated by humoral or cellular immunity. We found that while passive transfer of the pooled sera of vaccinated mice protected naïve mice from lethal challenge (Figure 2.3C), neither depletion of $CD8^+$ nor $CD4^+$ T cells affected vaccine-mediated protection (Figure 2.4E). We conclude that the protection elicited by our vaccine is therefore antibody mediated at this early timepoint 3-weeks post-boost. Whether the durability of our vaccine is cell mediated is worth future investigation.

Though neutralizing antibodies are considered the correlate of protection for several flaviviruses including the closely related TBEVs [655, 656], it is notable that a measurable neutralizing antibody titer at the time of challenge was not a

prerequisite for survival in our study (Figs 2 and 6). There were consistently higher percentages of survivors within each vaccine group than there were animals with measurable neutralizing titers at the time of infection: 31% survival vs 16% measurable FRNT50 for VLP-alone, 50% vs 0% for alum, 69% vs 11% for INI-2002, and 100% vs 78% for INI-4001. There are several possible explanations for this which are not mutually exclusive. First, the neutralizing titer necessary for protection may be lower than the level of detection for our assay. Second, a memory response to infection may raise neutralizing antibody titers to a protective level not seen at the time of serum collection. Work by Uhrlaub *et. al* supports this explanation by demonstrating that the protection elicited by a vaccine against WNV in older mice with minimal neutralizing antibody responses relies on a memory B-cell response to infection [657]. Third, there may be other non-neutralizing mechanisms to the observed protection, either humoral or cellular. Though we did not see a difference in protection after T cell depletion, which would suggest that cell-mediated mechanisms are not responsible for this, all of the INI-4001-vaccinated mice in the T cell depletion experiment had measurable neutralizing titers at the time of infection, so we cannot rule out the possibility that mice with no measurable neutralizing antibodies in previous experiments were protected through cell-mediated immunity. Lastly, non-neutralizing antibody-mediated protection such as antibody-dependent cellular cytotoxicity may be

responsible for protection in mice with no measurable neutralizing titer. Further investigation into the correlates of protection for POWV are needed.

In conclusion, our study highlights the utility of novel vaccine adjuvants in improving the protective immunogenicity of a VLP-based vaccine targeting POWV. We demonstrate that the TLR7/8 agonist INI-4001 outperforms alum as an adjuvant in multiple facets of the vaccine response elicited by a dose-sparing POWV-VLP vaccine. Further studies investigating whether combinations of INI-4001 alongside other adjuvants including alum and TLR4 agonists can improve upon this design are warranted. Further characterization of INI-4001 as well as other nanoparticle-based vaccine formulations is underway to better understand how this novel adjuvant induces such a potent protective immune response. Additional future experiments will focus on using this infection model and vaccine platform to interrogate the correlates of protection for POWV disease and how best to induce these responses for the development of a vaccine.

Materials & Methods

Mouse experiments

5-week old male or female C57BL/6 mice were purchased from Jackson Laboratory and housed in an ABSL-3 facility at Oregon Health & Science

University's (OHSU) Vaccine and Gene Therapy Institute accredited by the Association for Accreditation and Assessment of Laboratory Animal Care (AALAC) in compliance with protocols approved by the OHSU's Institutional Animal Care and Use Committee (IACUC) #1432. All experiments were performed with male mice unless otherwise stated.

Primary vaccinations were administered at 7-weeks of age subcutaneously (*sc*) in the dorsal region using 10^6 FFU equivalents of POW-VLP and either 11μmol of Alhydrogel 2% adjuvant, 1-10nmol of INI-2002, or 1-10nmol of INI-4001 diluted to a final volume of 100uL in sterile injection-grade PBS. INI-2002 and INI-4001 were synthesized as described by Miller *et. al* [572]. An aqueous formulation of INI-4001 was prepared using high-shear homogenization. INI-4001 was weighed into a glass vial, and an adequate volume of an aqueous buffered vehicle containing 50 mM TRIS buffer and 0.1% Tween 80 was added. The mixture was homogenized with a high-shear homogenizer (Silverson L5MA) at 10,000 rpm for 20 minutes. Meanwhile, the aqueous formulation of INI-2002 was prepared by solubilizing it in 2% glycerol using a bath sonicator (FB11201, Fisherbrand, Thermo Fisher Scientific) for 3 hours at a temperature below 35°C. Both INI-4001 and INI-2002 formulations were sterile-filtered using a 13 mm Millex GV PVDF filter with a pore size of 0.22 μm (MilliporeSigma). The formulations were characterized using a Zetasizer Nano-ZS (Malvern Panalytical, Malvern, UK) and

exhibited a hydrodynamic particle size of less than 120 nm. The concentrations of INI-4001 and INI-2002 were determined by RP-HPLC according to a previously published method [575]. Mock-vaccinated mice received 100uL of PBS alone. Boost-vaccinations were administered 2- to 4-weeks post-primary vaccination in the same manner. Blood was collected by tail-vein at specified timepoints post-vaccination and left to clot at room-temperature for 30 minutes before centrifugation twice at 10,600 x *g* to collect the serum. Serum was then stored at -20°C until use.

For lethal challenge infections, 10^4 FFU of POWV LB or 10^5 FFU POWV Spooner was diluted into 100uL sterile PBS and injected intraperitoneally (*ip*). Mice were monitored for up to three weeks for signs of morbidity including piloerection, hunched posture, ataxia, malaise, paralysis, and weight loss. Moribund mice were defined as those that experienced substantial weight loss ≥ 20% original body weight, paralysis, and/or other signs of morbidity. Moribund mice were euthanized by isoflurane followed by cervical dislocation to limit suffering.

Reverse transcription-quantitative polymerase chain reaction (RT-qPCR)

For tissue harvest, mice were euthanized with isoflurane and tissues were collected in TRIzol. Tissues were homogenized by bead-beating with SiLiBeads using a Precellys 24 bead beater homogenizer (Bertin Technologies). Samples were clarified by centrifugation at ~21,000 x *g* and supernatant RNA was isolated by Quick-RNA Viral Kit (Zymo Research #R1034). RNA was quantified by NanoDrop 2000c (ThermoFisher). For blood, serum was collected as described in "Mouse experiments" and combined with DNA/RNA Shield (Zymo Research #R1100) and processed for RNA using the Quick-RNA Viral Kit. RT-qPCR was performed on 200ng of total RNA from tissue per reaction or 4uL of serum RNA samples using POWV specific primers (Invitrogen: forward TGTTCTGCTGTTCCCGTGAGT; reverse GATGCGCAGCATGTCTTCTG), probe (Applied Biosystems: AGCATCCACGCGAGTG), and TaqMan RNA-to-CT 1-Step Kit (Catalog #4392656) on an AB StepOne Real-Time PCR System (ThermoFisher). Dilutions of known quantities of POWV cDNA were used to produce a standard curve for absolute genome quantitation.

Passive transfer

Mice were vaccinated as described in "Mouse experiments" with either INI-4001 adjuvanted vaccine or PBS alone. Sera were collected 3 weeks post-boost, pooled within each group, and heat-treated at 55°C for 30 minutes to inactivate complement. 200μL of pooled serum was passively transferred *ip* to unvaccinated mice. Mice were then challenged with 10^4 FFU of POWV LB *ip* the day after passive transfer and monitored for three weeks for signs of morbidity and survival.

T cell depletion and flow cytometry

Mice were vaccinated as described in "Mouse experiments". At both days 19- and 21-post boost-vaccination, 100 μg of either CD4-depleting antibody (Clone GK1.5 IgG2b Fisher), CD8-depleting antibody (Clone 2.43 IgG2b Fisher), or non-depleting isotype control (Clone LTF-2 Fisher) was administered *ip*. Mice were then challenged with 10^4 FFU of POWV LB as described in "Mouse experiments". To confirm depletion, 100μL of blood was collected by tail vein 3 days post-infection into 500uL of 100mmol EDTA (Invitrogen), washed with FACS buffer (PBS with 5% FBS and 1mM EDTA), and stained with CD45 AlexaFluor 700 (BioLegend rat anti-mouse clone 30-F11 Cat#103218), CD3 BUV395 (BD Horizon rat anti-mouse Clone 17A2 (RUO) Cat#: 569614), CD19 PE (BioLegend rat anti-mouse clone 1D3/CD19 Cat#: 152408), CD4 V450 (BD Horizon rat anti-mouse

clone: RM-4-5 Cat#: 560468), and CD8b PerCP/Cy5.5 (BioLegend rat anti-mouse clone YTS156.7.7 Cat#: 126609) for 30 minutes at room temperature. Cells were then washed and fixed using RBC lysis/fixation solution (BioLegend #422401) for 10 minutes, washed, and resuspend in FACS buffer. Cells were then analyzed by flow cytometry using a BD FACSymphony Spectral Cell Analyzer. T cells were gated as CD45+ CD3+ CD19-.

Peptide restimulation of T cells

7-week-old mice were vaccinated twice 4 weeks apart and then euthanized 4 weeks post-boost. Spleens were processed to a single-cell suspension over a 40μm cell strainer and suspended in RPMI supplemented with 5% FBS and 1% HEPES. 1×10^6 cells were plated per well in a round-bottom 96-well plate and stimulated for 6 hours at 37°C, 5% CO2 in the presence of 10μg/mL brefeldin A and either α-CD3 (clone 2C11) as a positive control, PBS, or 10μg/mL of peptide. Previously defined antigen specific epitopes were used to quantify antigen specific T cells with POWV-$E_{525\text{-}535}$ to stimulate $CD4^+$ T cells and POWV-$E_{282\text{-}291}$ to stimulate $CD8^+$ T cells [609]. Following peptide restimulation, cells were washed twice with 1X PBS and stained overnight in 1X PBS at 4°C for the following surface antigens: CD4 (clone RM-4-5), CD8α (clone 53-6.7), and CD19 (clone 1D3). Cells were then washed twice with 1X PBS and fixed in 2% paraformaldehyde at 4°C for 10

minutes. Following fixation, cells were permeabilized with 0.5% saponin and stained in this solution for 1 hour at 4°C for intracellular IFN-γ (clone B27). Following intracellular staining, cells were washed with 0.5% saponin twice, followed by one wash with 1X PBS. Cells were resuspended in 200μl 1X PBS and analyzed by flow cytometry using an Attune NxT focusing flow cytometer. For analysis, T cells were gated on lymphocytes, CD19-, and either CD4-/CD8+ or CD4+/CD8- cells. Antigen specific cells were identified as those producing IFN-γ in the presence of the POWV envelope epitope.

Cells

HEK293T and Vero E6 cells were maintained in Dulbecco's Modified Eagle Medium (DMEM) (Corning) supplemented with 5% fetal bovine serum (FBS; HyClone #3039603), 100U/mL penicillin, 100 μg/mL streptomycin, and 292 μg/mL L-glutamine (Gibco #10378016). HEK293T cells were passaged using citrate buffer. Vero cells were passaged using trypsin 0.05% EDTA (Gibco #25-300-120).

VLP production

The generation of HEK293 cells expressing POWV prM-E was described previously [609]. In short, HEK293 cells were transfected with pLVX-Tet-On Advanced (Takara) to express the tetracycline-controlled transactivator. Tet-

transactivator expressing HEK293 cells were then transduced with pseudotyped lentivirus containing pLVX-POWVprME packaged using the packaging vector pSPAX2 and vesicular stomatitis virus G protein expression vector pMD2.G. Transduced cells were selected for by using 1 μg/mL puromycin to generate a HEK293 cell line that expresses POWV-prME when induced with doxycycline.

To produce POW-VLP, HEK293-POWV-prME cells were cultured with 1μg/mL doxycycline in DMEM supplemented with 2% FBS, 100U/mL penicillin, 100 μg/mL streptomycin, and 292 μg/mL L-glutamine. Supernatant was collected 4 days post-induction, centrifuged at 1,000 x *g* for 10min, and filtered through a 0.45μm to remove cellular debris. VLPs were then concentrated and purified by ultra-centrifugation through a 20% sorbitol 50mM Tris 1mM $MgCl_2$ pH 8.0 buffer at 150,000 x *g* for 2 hours at 4°C. Pellets were then resuspended in 1/100th of the original volume with 10mM Tris 150mM NaCl buffer supplemented with 5% trehalose for protein stability and stored at -80°C until use. For quantification, virus and VLP preparations were boiled at 95°C for 5 minutes in reducing sample buffer. Samples were then run on 10% SDS-PAGE gel. For Coomassie staining, the gel was transferred to Coomassie Brilliant Blue R-250 Staining Solution (Bio-Rad #1610435) for 5 hours at room-temperature, then destained in a solution of 50% water, 40% methanol, and 10% glacial acetic acid for several hours. For western blot, gels were transferred to Immobilon-P PVDF 0.45μm Membrane

(MilliporeSigma #IPVH00010), and immunoblotted with T077 (described in ELISA methods) to visualize E using monkey IgG gamma peroxidase-conjugated antibody (Rockland #617-103-012) and Pierce ECL Western Blotting Substrate (ThermoFisher #32106). Pictures were taken using G:Box imager (Syngene) or ChemiDoc Touch Imaging System (Bio-Rad).

Viruses

POWV LB and Spooner strains were generously provided by Michael S. Diamond (Washington University School of Medicine, St. Louis, MO). LGTV TP21 (NR-51658) was obtained from the Biodefense and Emerging Infections Research Resources Repository (BEI Resources). All viruses were propagated on Vero E6 cells (5 days for LGTV; 7 days for POWV and WNV 385-99 [658]). Supernatant was collected, centrifuged at 1,000 x *g* for 10min, and filtered through a 0.45µm to remove cellular debris. Virus was then concentrated and purified by ultra-centrifugation through a 20% sorbitol 50mM Tris 1mM $MgCl_2$ pH 8.0 buffer at 150,000 x *g* for 2 hours at 4°C. Pellets were then resuspended in 1/100th of the original volume in DMEM with 0.1% FBS and stored at -80°C until use. Viruses were titered using limited dilution focus forming assay on Vero cell monolayers. Briefly, cells were infected by rocking for 1 hour at 37°C in 5% CO_2. Cells were then overlaid with a formula consisting of 2 parts DMEM with 5% FBS, 100U/mL

penicillin, 100 μg/mL streptomycin, and 292μg/mL L-glutamine and 1 part 1% high / 1% low viscosity carboxymethylcellulose (CMC) diluted in a 60% PBS aqueous solution. Cultures were then aspirated and fixed at 48 hours post-infection with 4% paraformaldehyde for 30 minutes. Staining protocol to visualize foci was then performed as described in "Focus reduction neutralization test (FRNT)" section of methods. Foci were counted using AID Elispot 7.0 (Autoimmun Diagnostika GMBH) and titers were determined from these numbers.

Enzyme-linked immunosorbent assay (ELISA)

To titer whole virus binding antibodies, Corning Costar Brand 96-Well EIA/RIA plates (ThermoFisher) were coated with 10^5 FFU of POWV-I, LGTV, or WNV or $3.2X10^4$ FFU of POWV-II in purified through a sorbitol cushion as described in "Viruses" methods above and resuspended in PBS containing 0.1% FBS for stabilizing particles. Viruses were plated in 100μL PBS per well overnight at 4°C. Titers used for plating were chosen to be consistent with our validated 10^5 FFU/well for POWV-I (Figure S2.6, page 157). $3.2X10^4$ FFU of POWV-II was chosen as this was the highest titer without significant background binding. Plates were then washed with PBS 0.05% Tween 20 (ThermoFisher) and blocked in wash buffer with 5% milk (Safeway). Serum complement was heat inactivated at 55°C for 30

minutes and serially diluted in blocking buffer with the least dilution of 1:50. Sera dilutions were then incubated on ELISA plates for 1.5 hours at room temperature. These were then washed and stained with anti-mouse IgG (γ-chain specific)−peroxidase antibody (MilliporeSigma #A3673) diluted 1:10,000 in wash buffer for 1 hour at room temperature. Secondary antibody was then washed and replaced with 100μL of 4μg/mL o-Phenylene diamine in a buffer of 50mM citric acid 100mM dibasic sodium phosphate 0.01% hydrogen peroxide pH 5.0 for 10 minutes before color change reaction was stopped with equal amount of 1M HCl. Absorbance at 490nm was measured using BioTek Synergy HTX Multimode Reader and Gen5 Microplate Reader and Imager Software v3.11 (Agilent). Background absorbance was defined as the lowest absorbance value on a plate and subtracted from each well. Linear regression curves were fit using Microsoft Excel INTERCEPT and SLOPE functions to determine endpoint titer defined as when absorbance was 0.1, a baseline absorbance not exceeded by negative controls (Figure S2.6, page 157). Values < 1 were adjusted to an endpoint titer = 1 for figures. Values below the least dilute serum tested (log(1/50)= 1.7) were set to 1.7 for all statistical analyses.

To titer VLPs, plates were coated similarly to assay described above, but with serially diluted VLP alongside POWV of known titer. Plates were blocked and washed as described and stained for 1 hour at room temperature with T077

anti-E antibody (described in the next section) followed by 1 hour with monkey IgG gamma peroxidase-conjugated antibody (Rockland). Endpoint titers were calculated in the same manner as described previously, and these were used to determine the FFUe of VLP using the known FFU of POWV as standard.

Focus reduction neutralization test (FRNT)

Serial dilutions of sera were prepared in DMEM with 2% FBS and incubated with POWV-I for 1 hour at 37°C to allow for antibody binding. Serum treated virus was then used to infect monolayers of Vero cells and overlaid with CMC as described previously in "Viruses". The least dilute serum used to neutralize virus was 1:50. Cells were then fixed with 4% paraformaldehyde at 48 hours post-infection for 30 minutes, blocked and permeabilized in PBS with 2% goat serum (ThermoFisher) and 0.4% Triton X-100 (ThermoFisher). Cells were then stained with T077, a monoclonal antibody from a TBEV-infected individual sequenced and characterized by Agudelo *et. al* that binds both POWV-I and -II [218]. We cloned the T077 heavy and light variable chain sequences into pcDNA-3-RhIgG1 and -RhIgK, respectively, for antibody production in Expi293 cells. POWV foci were then visualized by secondary staining with monkey IgG gamma peroxidase-conjugated antibody (Rockland) diluted 1:1,000 in blocking buffer followed by Vector VIP Substrate Peroxidase (HRP) Kit (Vector Laboratories SK-4600) after

washing. Foci were counted using AID Elispot 7.0 (Autoimmun Diagnostika GMBH) and reciprocal FRNT50s determined by non-linear regression analysis with a variable slope on GraphPad Prism v10.2.2. Values < 1 were adjusted to FRNT50 = 1 for figures. Values extrapolated by GraphPad below the least dilute serum tested (log(1/50)= 1.7) were set to 1.7 for all statistical analyses.

Area under the curve (AUC) analysis

Areas under the curve of individual mouse weights were measured for curves of percent initial weight from day 0 through 21 using GraphPad Prism v10.2.2.

Statistical analyses

All appropriate statistical analyses were performed using GraphPad Prism v10.2.2.

Examination of VLPs by TEM negative stain

Glow discharged, carbon-coated Formvar copper grids, 400 mesh, were floated onto a 5 μl aliquot suspension for 2 min. Excess solution was wicked off with filter paper and stained with 1% aqueous uranyl acetate. Stain was removed

with filter paper, air dried, and examined on an FEI Tecnai T12 TEM, operated at 80 kV, and digital images were acquired with an AMT Nanosprint12 4k × 3k camera.

Data availability

The raw data analyzed and presented in this study are available upon request from the corresponding author hirschal@ohsu.edu.

Acknowledgements

Electron microscopy was performed at the Multiscale Microscopy Core, a member of the OHSU University Shared Resource Cores, RRID: SCR_022652.

Competing interests

D.J.B. is an employee of and/or shareholder of Inimmune Corp., which holds an exclusive license for the INI-4001 and INI-2002 used in this study. The funders had no role in the design of the study; in the collection, analyses, or interpretation of data; in the writing of the manuscript; or in the decision to publish the results. All other authors declare no competing interests.

Supplemental figures

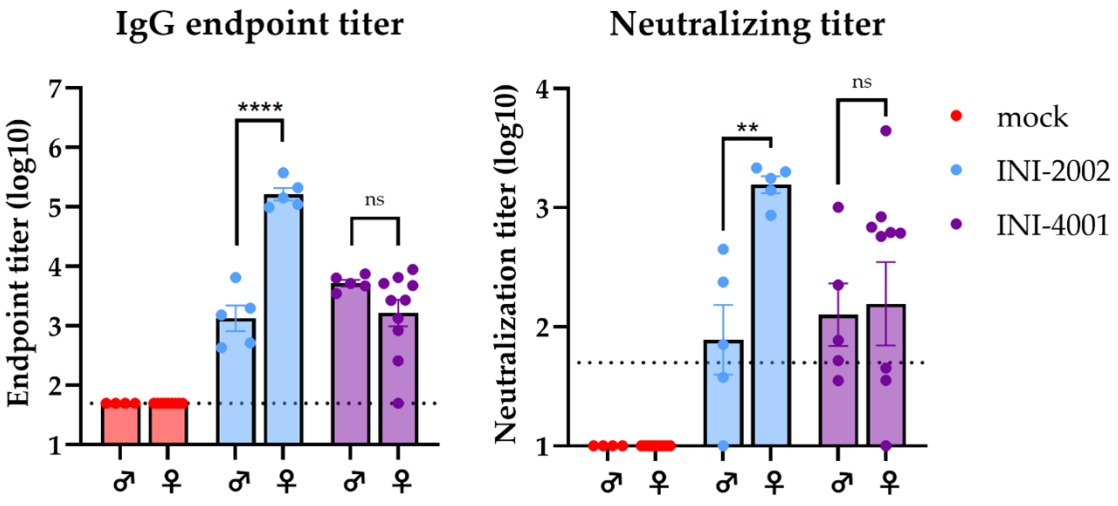

Figure S2.1: The antibody response to INI-2002 is higher in female mice than males. (A-B) Male and female mice prime-boost vaccinated 3 weeks apart sc with 10^6 FFUe of VLP adjuvanted with 1nmol INI-2002 or 10nmol INI-4001. Mock group injected with PBS vehicle alone. n=4-10. Serum collected 3 weeks post-boost and analyzed by whole-virus ELISA (A) or FRNT (B). Data are reported as log-transformed mean endpoint titer ± SEM for IgG titer and reciprocal FRNT50 for neutralizing titer. Dotted line represents least dilute sera tested (1:50). Data represent three independent experiments. (A-B) Statistical significance determined by one-way ANOVA and Šídák's multiple comparisons to compare male to female within treatment groups after log transformation. ns = not-significant, ** = $p < 0.01$, **** = $p < 0.0001$.

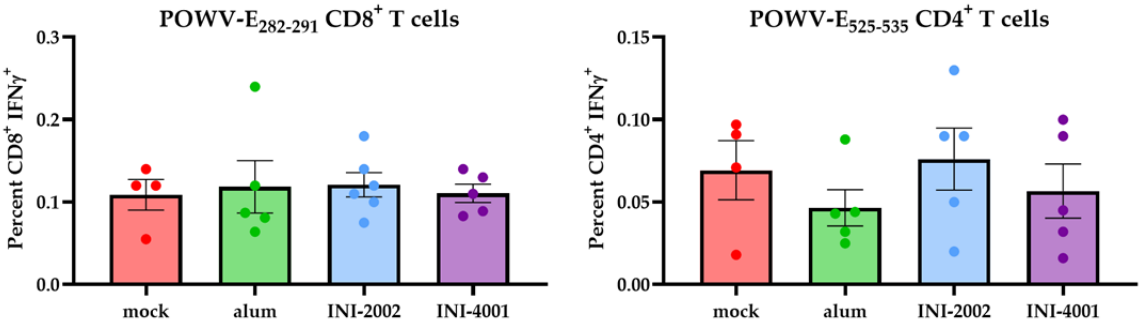

Figure S2.2: Vaccination does not induce measurable CD8+ or CD4+ T cell responses. Mice prime-boost vaccinated 4 weeks apart sc with 106 FFUe of VLP alone or adjuvanted with 11µmol alum, 1nmol INI-2002, or 10nmol INI-4001. Mock group injected with PBS vehicle alone. n=4-5. Spleens collected 4 weeks post-boost, and splenocytes incubated with POWV-E282-291 (A) or POWV-E525-535 (B) for CD8+ and CD4+ T cells, respectively. Cells were then stained and gated on CD19- CD4+/CD8+ and intracellularly stained for IFNγ. Data are reported as percentage of IFNγ+ T cells either within the CD8+ (A) or CD4+ (B) compartments ± SEM. Data represent one experiment. Statistical significance determined by one-way ANOVA and Šídák's multiple comparisons test to compare treatments to mock; no statistically significant differences were found.

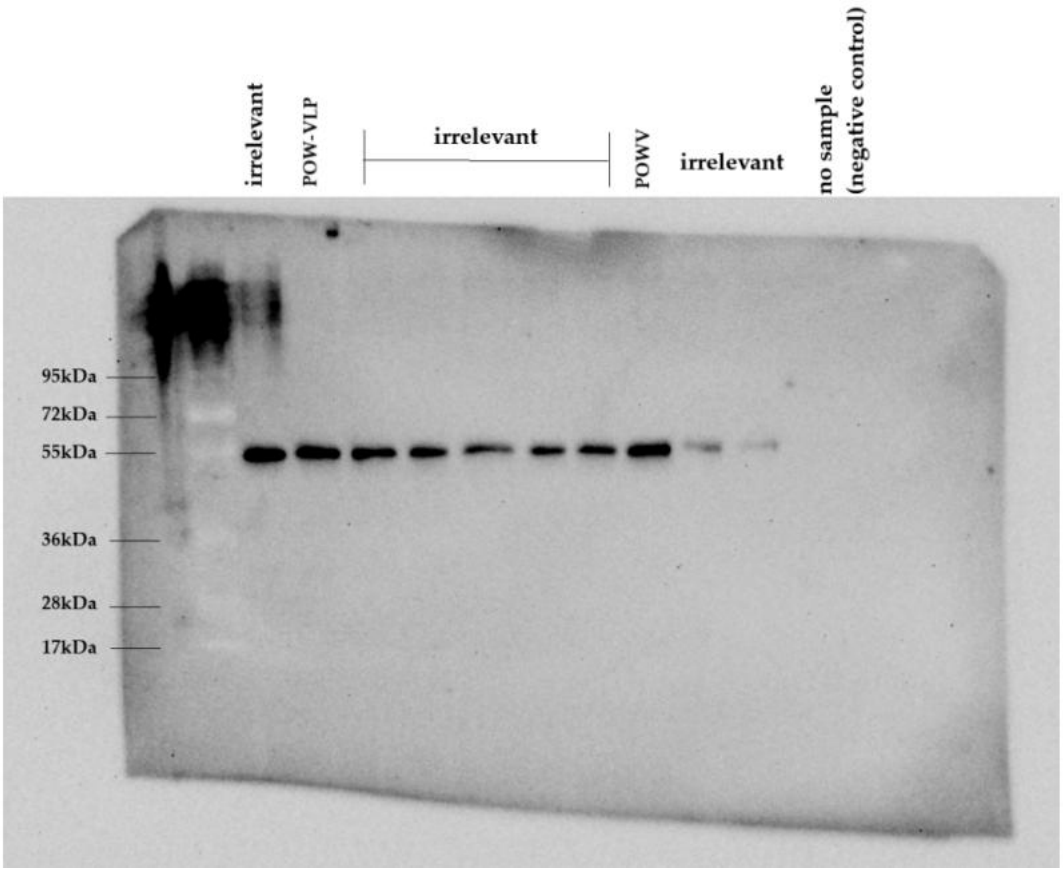
irrelevant
POW-VLP
irrelevant
POWV
irrelevant
no sample
(negative control)
95kDa
72kDa
55kDa
36kDa
28kDa
17kDa

Figure S2.3: Uncropped western blot from Figure 1B.

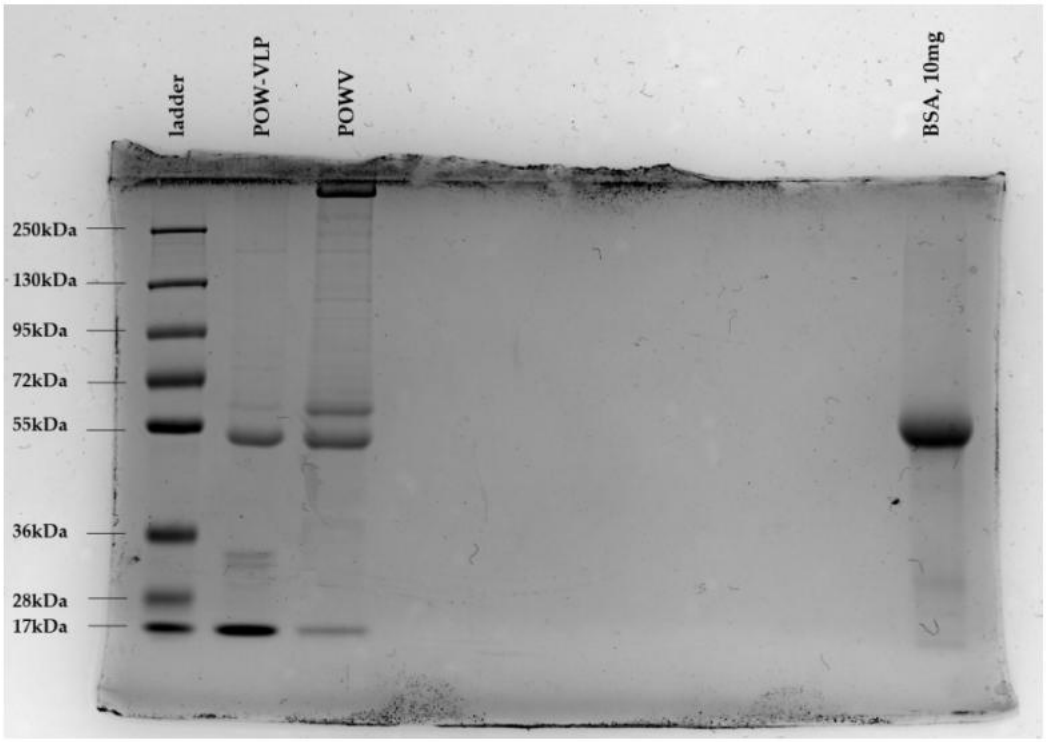

Figure S2.4: Uncropped Coomassie Blue stained SDS-PAGE gel from Figure 1C.

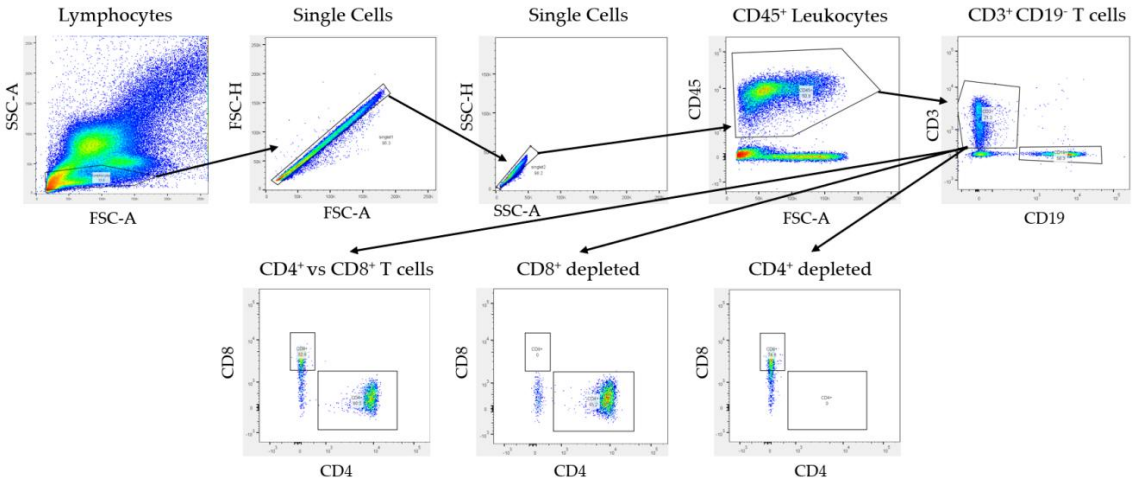

Figure S2.5: Flow gating strategy.

Gating strategy to determine CD4+ and CD8+ T cell depletion began with initial gates for lymphocytes and two gates for isolating single cells using forward- and side-scatter. T cells were then isolated by sequentially gating for CD45+ cells followed by CD3+ CD19-. CD45+ CD3+ CD19- cells were then gated as either CD4+ or CD8+ T cells.

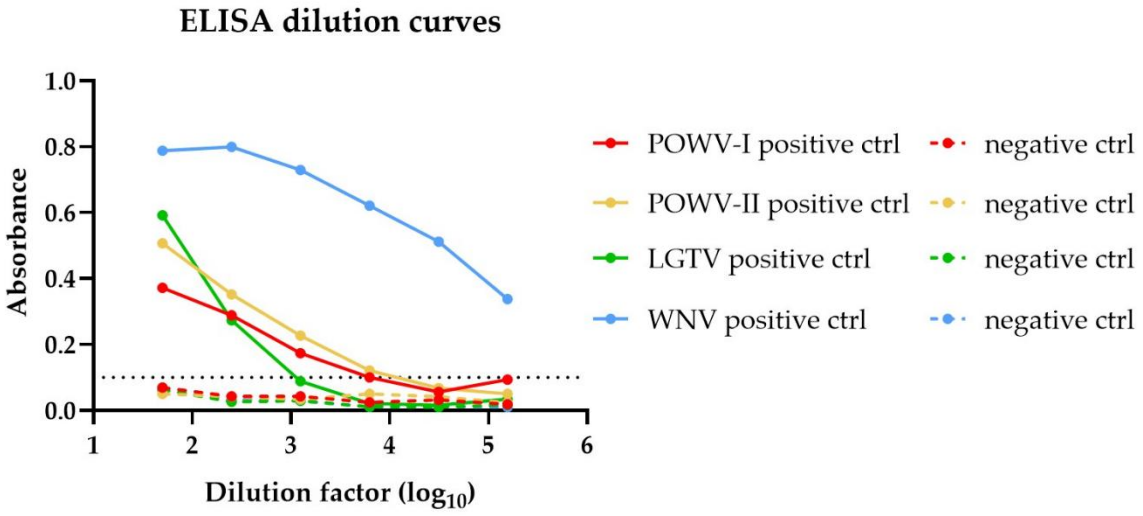

Figure S2.6: ELISA dilution curves for assay validation.

High-binding Costar 96-well plates were coated with 105 FFU of POWV-I, LGTV, or WNV or 3.2X104 FFU of POWV-II in final volumes of 100uL PBS per well. Representative positive (unbroken lines) and negative (dotted lines) serum controls tested for anti-flavivirus binding are shown. Dotted line at y = 0.1 represents baseline for determining endpoint titers. Positive control for: POWV-I and -II is convalescent serum from a mouse that twice-survived infection with POWV-I without vaccination; LGTV is serum from mouse prime-boost vaccinated 3 weeks apart with low-dose POW-VLP adjuvanted with INI-4001 and bled 3 weeks post-boost; WNV is convalescent serum from a WNVimmune mouse. Negative controls are all PBS-vaccinated mice.

Chapter 3: Lipid formulations to improve the efficacy of a TLR7/8 agonist-adjuvanted Powassan virus-like particle vaccine

Michael W. Crawford[1,2], Christopher J. Parkins[1], Henry F. Harrison[1], Fatemeh Mehradnia[3,4], Walid M. Abdelwahab[3,4], Karthik Siram[3,4], David J. Burkhart[5], Jessica L. Smith[2,6], Alec J. Hirsch[2,6]

Affiliations

[1]Vaccine and Gene Therapy Institute, Oregon Health & Science University, Beaverton, OR, USA

[2]Department of Molecular Microbiology and Immunology, Oregon Health & Science University, Portland, OR, USA

[3]Department of Biomedical and Pharmaceutical Sciences, University of Montana, Missoula, MT, USA.

[4]Center for Translational Medicine – Adjuvant Research Team, University of Montana, Missoula, MT, USA.

[5]Inimmune Corporation, Missoula, MT, USA.

[6]Division of Pathobiology & Immunology, Oregon National Primate Research Center, Oregon Health & Science University, Beaverton, OR, USA

Author contributions

Conceptualization and methodology MWC, CJP, WMA, JLS, AJH; investigation MWC, CJP, HFH, JLS; project administration MWC, CJP, JLS; resources MWC, JLS, AJH, FM, WMA, KS, DJB; data curation, formal analysis, validation, visualization, and writing of original draft MWC; funding acquisition, supervision, and review & editing AJH.

Unpublished

Abstract

Powassan virus (POWV) is a tick-borne flavivirus emerging in North America for which there is no vaccine. We previously developed a low-dose lineage 1 Powassan virus-like particle- (POW-VLP)-based vaccine adjuvanted with INI-4001 that protects mice from both lineages of POWV. Here, we investigate the effectiveness of re-formulating our vaccine with either cationic liposomes or an AS03-like emulsion. We find that both liposome and emulsion formulations improve the neutralization capacity and breadth of the antibody response. We also

find that incorporating liposome or emulsion into our vaccine significantly reduces the burden of POWV RNA in infected mice and dissemination of cytotoxic effector cells into the brain. We conclude that formulating our POW-VLP vaccine with either INI-4001-adjuvanted cationic liposome or AS03-like emulsion improves vaccine efficacy.

Introduction

Lipid-based formulations are increasingly prominent components of modern vaccines. There are multiple lipid-based technologies employed in licensed vaccines including the oil-in-water emulsion AS03 used in multiple influenza vaccines and the liposome-based AS01 used in vaccines against varicella zoster virus, respiratory syncytial virus, and malaria. The lipid components of these systems can act as delivery vehicles for adjuvants, influence antigen deposition and uptake, and directly modulate the immune response to vaccination [532].

Liposomes are best known for their function as antigen depots to retain antigen at the site of injection. However, liposomes can also have direct immunomodulatory effects that enhance antigen-presenting cell maturation and recruit immune effectors to the site of injection [659-662]. Liposomes are also utilized for the incorporation of other immunostimulatory factors such as MPL

and QS-21 in AS01 [532]. Furthermore, their physical properties can be manipulated to modulate immune responses. Incorporating a positive charge to the lipid components improves their ability to interact with negatively charged cell surfaces, retain antigen at the site of injection, and increase antigen uptake into dendritic cells [540, 541].

Oil-in-water emulsions are also utilized for their ability to enhance antigen delivery and promote favorable immune responses [534]. The AS03 emulsion-based adjuvant system contains the immunostimulatory components squalene and α-tocopherol and improves the magnitude and breadth of antibody responses to vaccination [534, 663, 664]. Like liposomes, emulsions such as AS03 can also be utilized to deliver additional adjuvants such as TLR agonists to further improve and tune vaccine responses [577, 578, 581].

We previously developed a low-dose virus-like particle- (VLP)-based vaccine adjuvanted with the novel synthetic TLR7/8 agonist INI-4001 to target Powassan virus (POWV), a rare tick-borne flavivirus currently emerging in North America [665]. We demonstrated that this vaccine elicits a robust, durable neutralizing antibody response and fully protects mice from lethal challenge with either lineage of POWV. Here, we investigate whether formulating our vaccine with cationic liposomes or an AS03-like emulsion improves the vaccine response. We find that liposomes with or without INI-4001 as well as INI-4001-adjuvanted

emulsion enhance the neutralizing antibody response beyond that of aqueous INI-4001 alone. Furthermore, unadjuvanted cationic liposome and adjuvanted emulsion improve the breadth of the antibody response to the second lineage of POWV (POWV-II) as well as the closely related Langat virus (LGTV). Lastly, we demonstrate that INI-4001-adjuvanted liposome and emulsion are particularly effective at reducing the tissue burden of POWV RNA in infected mice while also reducing dissemination of cytotoxic effector cells into the brain. We conclude that formulation with either INI-4001-adjuvanted cationic liposome or AS03-like emulsion improves the efficacy of our POWV vaccine.

Results

Improving the vaccine response to POW-VLP with liposome and emulsion formulations

We first sought to test whether formulating our POW-VLP vaccine with cationic liposomes or an AS03-like emulsion affects the antibody response. Mice were prime-boost vaccinated subcutaneously (sc) 3 weeks apart with 10^6 FFUe of POW-VLP adjuvanted either with aqueous INI-4001 or one of four formulations: liposomes or emulsion each formulated either with or without INI-4001. Sera were collected 3 weeks post-boost and analyzed by whole-virus binding ELISA to quantify anti-POWV-I IgG titers. All vaccine groups had comparable anti-POWV

IgG responses (Figure 3.1A). Statistical significance was assessed using multiple comparisons to determine 1) whether the new formulations improved the antibody response compared to aqueous INI-4001 alone, and 2) whether the addition of INI-4001 to liposomes or emulsion improved the antibody response within these respective groups. There was no significant difference between the titers of mice that received aqueous INI-4001 and those that received reformulated vaccines. However, there was a significant improvement to the binding antibody response elicited by INI-4001-adjuvanted emulsion compared to emulsion alone.

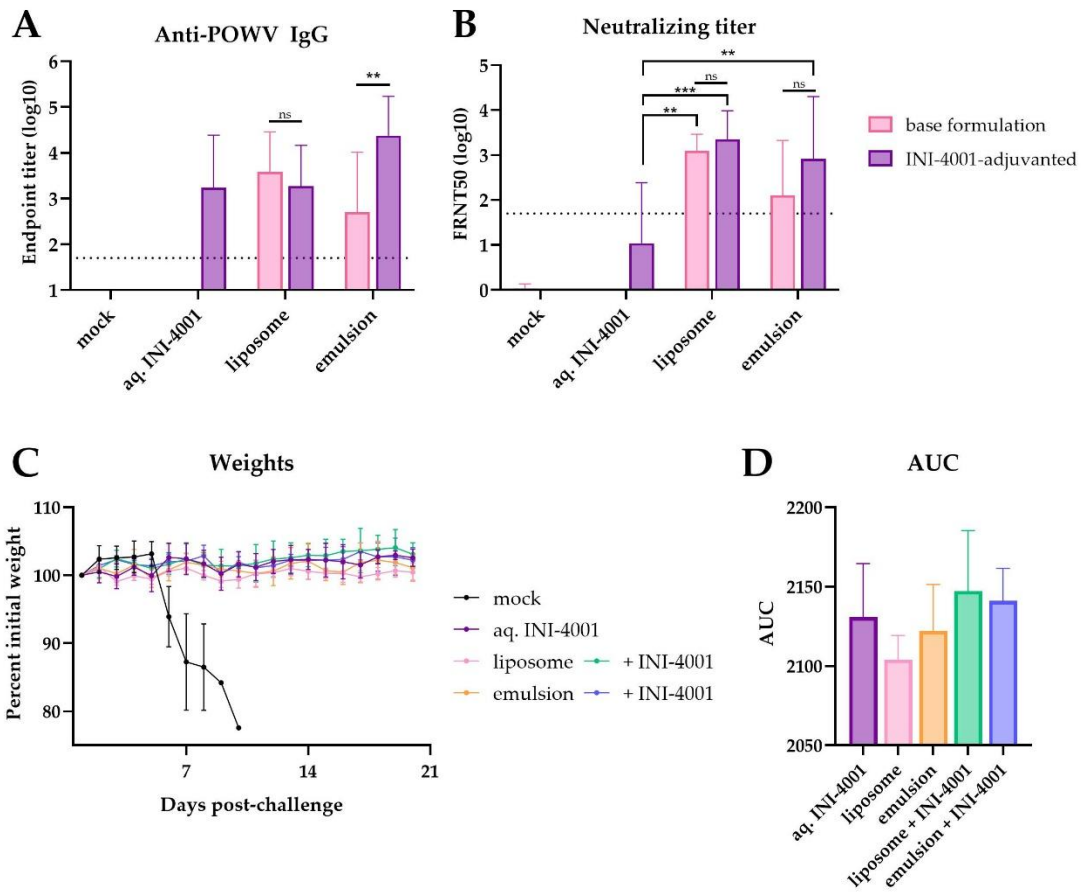

Figure 3.1: Liposome- and emulsion-formulations improve neutralizing antibody response.

A-D: Mice prime-boost vaccinated 3 weeks apart sc with 10^6 FFUe of POW-VLP adjuvanted either with aqueous INI-4001, cationic liposomes formulated with or without INI-4001, or emulsion formulated with or without INI-4001. Sera collected 3 weeks post-boost and analyzed by (**A**) whole-virus ELISA using and (**B**) FRNT. **A-B:** n = 9/group for mock and aqueous INI-4001; n = 10/group for all other groups. Data represent two independent experiments. Vaccinated mice challenged with a lethal 10^3 FFU POWV-LB ip 3.5 weeks post-boost. Weights measured (**C**) to day 21 post-challenge. **C-D:** n = 5/group, data represent one experiment included in A-B. **A.** Data reported as log-transformed IgG endpoint titers + SD. **B.** Data reported as log-transformed reciprocal FRNT50 + SD. **C.** Weights of lethally challenged mice represented as mean percent of initial weights ± SD. **D.** Area under the curve (AUC) of individual mouse weight percentages after lethal challenge infection + SD. **A, B, D:** Statistical significance determined by one-way ANOVA and Šídák's multiple comparisons test to compare aqueous INI-4001 vaccine group to all other vaccine groups and base formulations to their adjuvanted counterparts (after log transformation for those data log-transformed). ns – not significant; **p < 0.01; ***p < 0.001.

Sera were next analyzed by focus reduction neutralization test (FRNT) to quantify the POWV-I neutralizing antibody responses. Interestingly, both

liposome vaccine groups and the INI-4001-adjuvanted emulsion group had significantly higher neutralizing antibody titers than mice that received aqueous INI-4001 despite no significant differences in total IgG titers (Figure 3.1B). The addition of INI-4001 to either liposome or emulsion formulations did not significantly impact the neutralizing antibody responses.

Mice were then challenged at 3.5 weeks post-boost with a lethal 10^3 FFU dose of POWV-I intraperitoneally (ip). Survival and weights were monitored for 3 weeks post-challenge. While all mock vaccinated mice succumbed to infection within 11 days, all vaccinated animals survived and maintained their weights (Figure 3.1C). There were no significant differences in the area under the curve (AUC) for the weights of the five vaccine groups (Figure 3.1D). Together, these data show that while our POW-VLP vaccine adjuvanted with aqueous INI-4001 is fully protective, both cationic liposome formulations as well as INI-4001-adjuvanted AS03-like emulsion improve the vaccine response by enhancing neutralizing antibody titers.

Improving antibody breadth with liposome and emulsion formulations

We next sought to investigate whether reformulating our vaccine affects the breadth of the antibody response. For this, we tested sera for binding to POWV-II,

the closely related tick-borne flavivirus LGTV, or the more distantly related mosquito-borne flavivirus West Nile virus (WNV). Both unadjuvanted liposome and INI-4001-adjuvanted emulsion vaccine groups had significantly higher IgG responses to both POWV-II and LGTV compared to aqueous INI-4001 (Figure 3.2A-B). It is notable that the higher anti-POWV-II IgG titer in the INI-4001-adjuvanted liposome group was very nearly significant ($p = 0.075$). No group had significant responses to WNV compared to mock (Figure 3.2C).

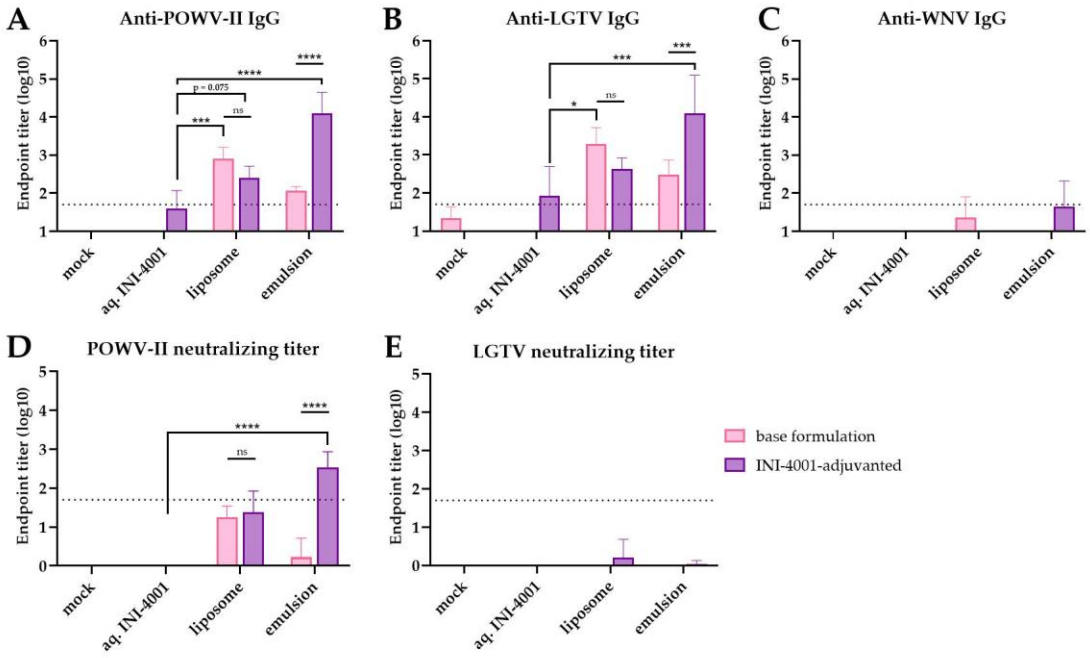

Figure 3.2: Liposome- and emulsion-formulations improve antibody breadth.

A-E: Mice prime-boost vaccinated 3 weeks apart *sc* with 10^6 FFUe of POW-VLP adjuvanted either with aqueous INI-4001, cationic liposomes formulated with or without INI-4001, or emulsion formulated with or without INI-4001. Sera collected 3 weeks post-boost and analyzed by (**A-C**) whole-virus ELISA and (**D-E**) FRNT using (**A+D**) POWV-II, (**B+E**) LGTV, or (**C**) WNV. n = 4/group for mock and aqueous INI-4001; n = 5/group for all other groups. Data represent single experiment. (**A-C**) Data reported as log-transformed IgG endpoint titers + SD. (**D-E**) Data reported as log-transformed reciprocal FRNT50 + SD. (**A-B & D**) Statistical significance determined by one-way ANOVA and Šídák's multiple comparisons test to compare INI-4001 vaccine group to all vaccine groups and base formulations to their adjuvanted counterparts after log transformation. (**C**) Statistical significance determined by one-way ANOVA and Šídák's multiple comparisons test to compare all groups to mock. ns – not significant; *p < 0.05; ***p < 0.001; ****p < 0.0001.

We next looked at cross-neutralizing antibody titers to both POWV-II and LGTV. We found that only emulsion adjuvanted with INI-4001 had significant POWV-II neutralizing antibodies (Figure 3.2D). Though both liposome-formulated vaccines elicited measurable neutralizing activity, most of the reciprocal FRNT50s in these groups were below the threshold of least dilute serum tested (1:50) which was used for determining significance as described in the

methods. No group had significant neutralizing titers for LGTV (Figure 3.2E). These data demonstrate that both unadjuvanted cationic liposomes and INI-4001-adjuvanted emulsion enhance the breadth of the antibody response, while adjuvanted emulsion is alone capable of eliciting a neutralizing antibody response to both lineages of POWV at these low vaccine doses.

INI-4001-adjuvanted lipid formulations further reduce POWV tissue burden and dissemination of cytotoxic effector cells into the brains of infected mice

Lastly, we sought to test whether reformulating our vaccine could reduce viremia and tissue burden of POWV during infection. To determine which timepoints were optimal for evaluating tissue burden, we infected naïve mice with POWV-I and collected various tissues at multiple timepoints post-infection. The burden of POWV RNA in the blood was uniformly high at day 2 post-infection which is in line with previous studies demonstrating that POWV viremia peaks around days 1 and 2 (Supplemental Figure S3.1A) [648, 666]. POWV RNA in the liver and spleen remained consistent through the study whereas RNA in the brain continued to increase until day 7, at which point mice began to succumb to

infection. We therefore chose to collect blood at day 2 and all other tissues at day 7 to evaluate vaccine efficacy.

We infected vaccinated mice with a lethal dose of 10^3 FFU POWV-I ip and collected tissues. We found no viremia in any of the four reformulated vaccine groups and in only one of the four mice that received aqueous INI-4001-adjuvanted vaccine (Figure 3.3A). Statistical testing comparing all groups to the aqueous INI-4001 group revealed no significant difference in viremia between aqueous INI-4001 and reformulated vaccine groups. At day 7, two of the four aqueous INI-4001 mice had extremely high POWV titers in the brain while there were no measurable titers in any of the experimental vaccine mice. This difference was not statistically significant. However, all reformulated vaccine groups had significantly lower POWV RNA in the liver compared to aqueous INI-4001 control. In the spleen, both liposome and emulsion formulated with INI-4001 had significantly less POWV RNA, with no measurable RNA in any of the mice that received INI-4001-adjuvanted liposome. In fact, mice that received INI-4001-adjuvanted liposome were the only group that had no measurable POWV RNA in any tissue at the timepoints tested.

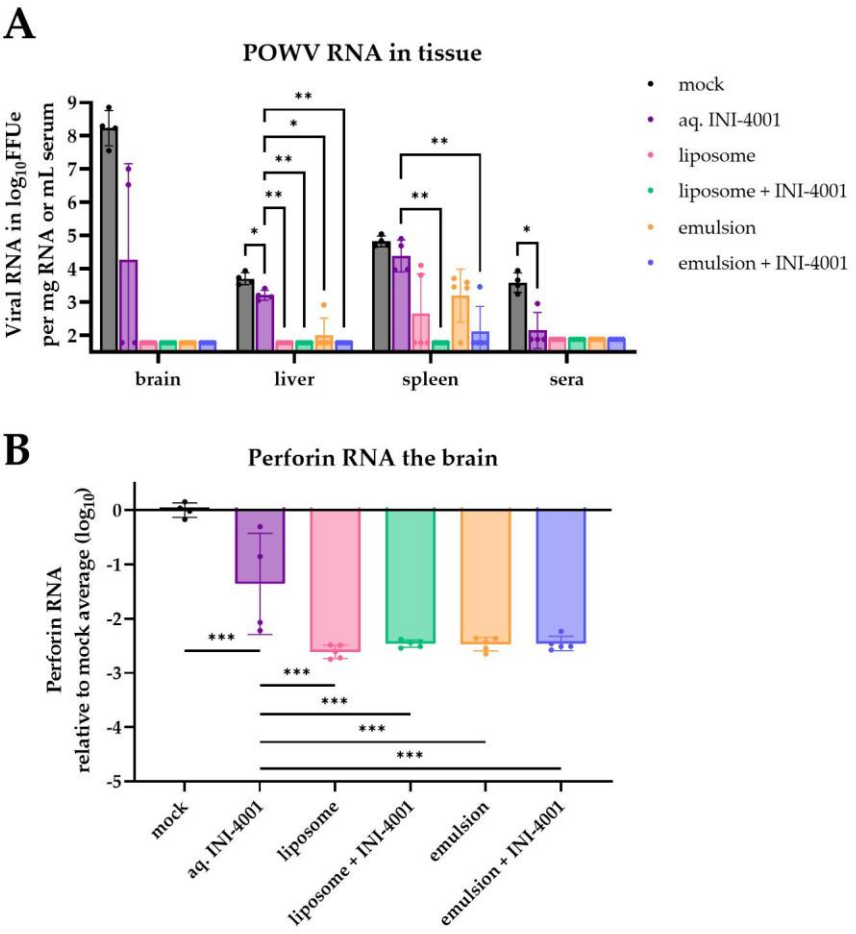
A
POWV RNA in tissue
Viral RNA in log10FFUe per mg RNA or mL serum
brain
liver
spleen
sera
mock
aq. INI-4001
liposome
liposome + INI-4001
emulsion
emulsion + INI-4001
B
Perforin RNA the brain
Perforin RNA relative to mock average (log10)
mock
aq. INI-4001
liposome
liposome + INI-4001
emulsion
emulsion + INI-4001

Figure 3.3: Liposome- and emulsion-formulations reduce viral tissue burden and perforin in the brain.

A-B: Mice prime-boost vaccinated 3 weeks apart *sc* with 10^6 FFUe of POW-VLP either unadjuvanted or adjuvanted with INI-4001 and either unformulated in PBS or formulated with either liposome or emulsion with or without adjuvant. Mice challenged with a lethal 10^3 FFU POWV-LB *ip* 3.5 weeks post-boost. n = 4/group for mock and INI-4001 alone; n = 5/group for other groups, data represent single experiment. POWV RNA was quantified in sera collected 2 days post-challenge and both POWV and perforin RNA in the brain, liver, and spleen collected 7 days post-challenge by RT-qPCR. **A:** POWV genome copy numbers in the tissue represented as FFUe per mg of total RNA in solid tissue or FFUe per mL of serum. Statistical significance determined by repeated measure two-way ANOVA and Šídák's multiple comparisons test to compare all groups to aqueous INI-4001 within tissues after log-transformation. **B**: Perforin RNA abundance in the brain represented as log-transformed abundance relative to mock vaccinated mouse average. Statistical significance determined by one-way ANOVA and Šídák's multiple comparisons test to all groups to aqueous INI-4001 after log-transformation of relative abundance. *$p < 0.05$; **$p < 0.01$; ***$p < 0.001$.

Lastly, we looked for perforin RNA in the brain of infected mice 7 days post-infection as a surrogate marker for neuroinvasive cytotoxic effector cells

which may play a pathological role in POWV infection [609]. We confirmed that both perforin and TCRα RNA increase in the brain of infected mice at 7 days post-infection with perforin increasing by an average of >500-fold (Supplemental Figure S3.1B). We found that aqueous INI-4001-adjuvanted vaccine significantly reduced perforin in the brain compared to mock mice by about 20-fold while all new formulations further reduced perforin levels by an average of 275- to 383-fold compared to mock. (Figure 3.3B). The two mice with measurable POWV in the brain in Figure 3.3A were the same as those with higher abundance of perforin in Figure 3.3B. Together, these data demonstrate that all lipid-based vaccine formulations tested here help further reduce the tissue burden of POWV RNA in infected mice compared to vaccine adjuvanted with aqueous INI-4001 alone. Cationic liposome and emulsion formulated with INI-4001 seem particularly effective in this regard. Furthermore, all experimental vaccine formulations reduce the dissemination of cytotoxic effector cells into the brain which may help prevent POWV-associated immunopathologies.

Discussion

We sought to determine whether re-formulating our low-dose aqueous INI-4001-adjuvanted POW-VLP vaccine with cationic liposomes or an AS03-like

emulsion could enhance vaccine immunogenicity. We found that inclusion of liposomes with or without INI-4001 as well as INI-4001-adjuvanted emulsion improved the neutralizing antibody response and reduction of POWV burden in the liver. Adjuvanted liposome and emulsion were also effective at reducing POWV burden in the spleen, one of the main targets for POWV infection [648, 667]. Adjuvanted emulsion was particularly effective at improving the breadth of the antibody response to both POWV-II and LGTV. Lastly, we demonstrate that all formulations tested significantly reduced dissemination of cytotoxic effector cells into the brains of infected mice which matched the reduced burden of POWV RNA in that tissue and may help prevent immunopathologies thought to be caused by POWV infection [609].

It is interesting that addition of INI-4001 was so particularly potent at enhancing the antibody response to emulsion-based vaccine but not liposome. This is conflict with data from Short *et al.* who previously demonstrated that addition of INI-4001 in an AS03-like emulsion does not improve the total IgG response to homologous SARS-CoV-2 RBD and may in fact reduce neutralizing breadth to other variants [577]. However, there are some key differences to our study that may account for this discrepancy including route of immunization (subcutaneous vs intramuscular), the antigen and dose (70ng VLP vs 1μg RBD recombinant protein), time between prime and boost vaccination (3 weeks vs 2),

and the time of serum collection (3 weeks post-boost vs 2). Evaluating the efficacy of adjuvant and formulation in the context of our low-dose vaccine is specifically interrogating the ability of vaccine components to drive an immune response to minimal antigen. The significant enhancement of antibody response magnitude and breadth to POWV for INI-4001-adjuvanted emulsion over emulsion alone may likely stem from INI-4001's unique ability to enhance responses to very limited antigen as we have previously shown [665]. In another study, Van Hoeven *et al.* demonstrated that addition of the TLR7/8 agonist 3M-052 to a squalene-emulsion-based low-dose (100ng) influenza subunit vaccine delivered intramuscularly improved the breadth of antibody binding and neutralization to heterologous flu strains and reduces viral shedding in the lungs [569]. This would suggest that the increased antibody breadth driven by addition of INI-4001 to our emulsion-based vaccine is indeed specific to the context of low-dose vaccination. AS03 has been shown to activate NF-κB at the site of injection and enhance antigen uptake by monocytes [668]. It has been shown that MF59, a similar oil-in-water vaccine adjuvant, mediates antibody responses in an IFN-independent manner [669]. Evidence reported in Chapter 6 demonstrates the INI-4001 mediates its immunogenicity via IFN-I which is known to stimulate cDCs and B cells. Together, this suggests that INI-4001 and AS03-like emulsion work synergistically through different pathways to promote a stronger immune response.

We demonstrate that while unadjuvanted and adjuvanted formulations elicit comparable neutralizing antibody responses to POWV-I, adjuvanted liposome and emulsion are more capable of reducing the burden of POWV in the spleen. One possible explanation for this is that INI-4001 may be driving more robust cellular immunity. Mehradnia *et al.* found that addition of INI-4001 to an influenza subunit vaccine formulated with cationic liposome did not improve the IgG response over liposome alone but did enhance markers of T_H1 cellular immunity [579]. Auderset *et al.* had similar findings with DOEPC-based cationic liposomes and 3M-052 [662]. Short *et al.* found that addition of INI-4001 also enhanced T_H1 cellular immunity in emulsion-based vaccine, and this was confirmed by Lathrop *et al.* in a later study that found enhanced T cell responses when AS03-like emulsion was adjuvanted with INI-4001 [577, 578]. Importantly, Lathrop *et al.* demonstrated that INI-4001 significantly improved $CD8^+$ T cell responses in the spleen. Enhanced T_H1 cellular immunity and cytotoxic effector cells in the spleen could explain why INI-4001 adjuvanted formulations are more effective at reducing POWV burden there. However, further work is needed to assess T cell responses. It would also be necessary to evaluate Fc-mediated antibody responses before concluding that these differences are not antibody-mediated.

This study demonstrates the utility of lipid-based vaccine formulations for improving the vaccine responses to low-dose INI-4001-adjuvanated POW-VLP. More work is needed to elucidate the mechanisms by which INI-4001 and liposomes or emulsions synergize to enhance immunity, though we speculate that this may stem from the ability of TLR7/8 agonists to boost cellular immune responses.

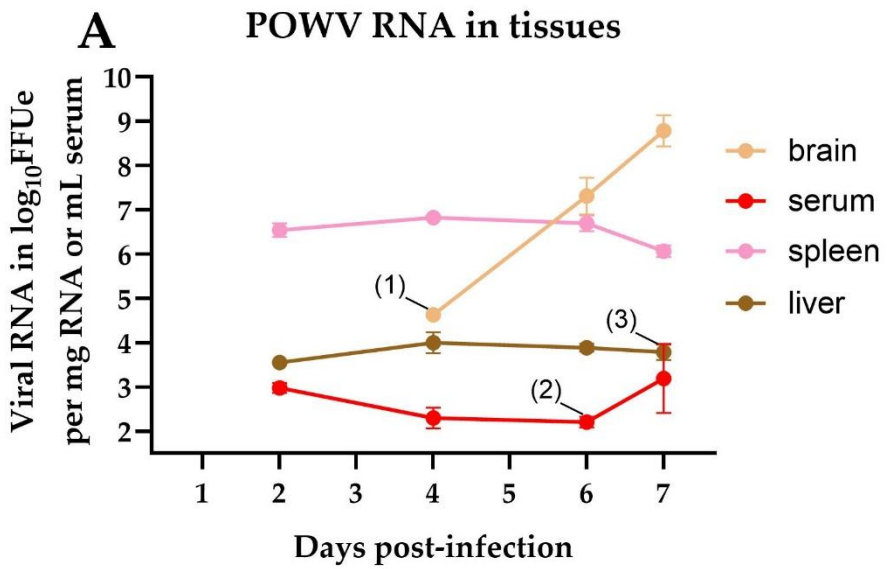
A
POWV RNA in tissues
Viral RNA in log10FFUe per mg RNA or mL serum
10
9
8
7
6
5
4
3
2
1
2
3
4
5
6
7
Days post-infection
(1)
(2)
(3)
brain
serum
spleen
liver

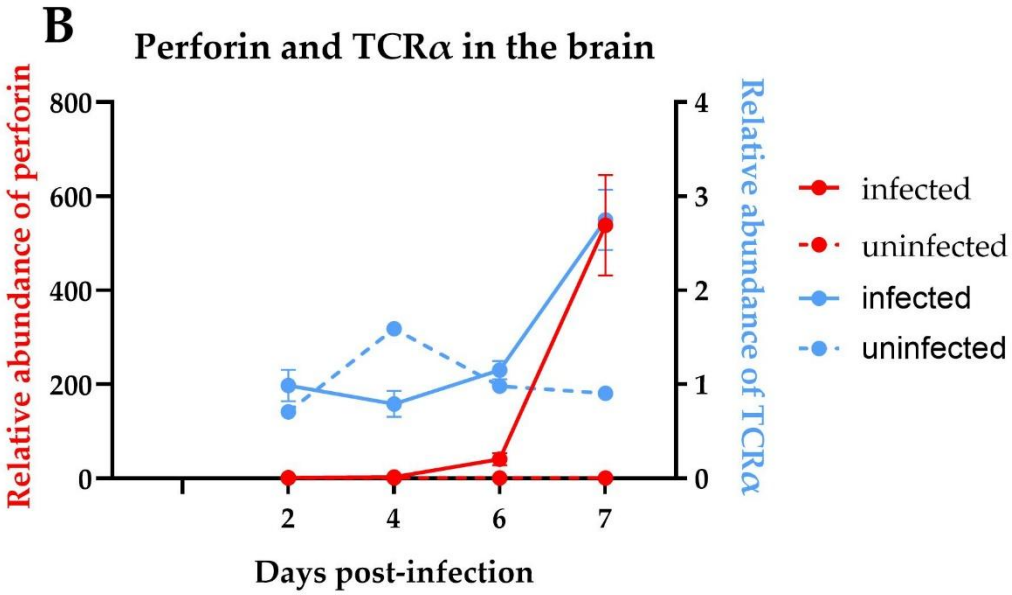
B
Perforin and TCRα in the brain
Relative abundance of perforin
800
600
400
200
0
Relative abundance of TCRα
4
3
2
1
0
2
4
6
7
Days post-infection
infected
uninfected
infected
uninfected

Figure S3.1: Kinetics of POWV RNA burden in various tissues and TCR marker RNA in the brain of infected mice.

A-B: Naïve mice challenged with a lethal dose of 10^3 FFU POWV-LB *sc* or PBS for control uninfected mice. Brains, liver, spleen, and sera collected from n = 4 mice per timepoint at days 2, 4, 6, and 7 post-challenge. Data represent single experiment. POWV/perforin/TCRα RNA quantified in tissue by RT-qPCR. **A**: POWV genome copy numbers in the tissue reported as FFUe per mg of total RNA in solid tissue or FFUe per mL of serum. **B**: Perforin (red) and TCRα (blue) RNA abundance in the brain relative to abundance in uninfected mice averaged over all timepoints.

Materials & Methods

Mouse experiments

5-week old male or female C57BL/6 mice were purchased from Jackson Laboratory and housed in an ABSL-3 facility at Oregon Health & Science University's (OHSU) Vaccine and Gene Therapy Institute accredited by the Association for Accreditation and Assessment of Laboratory Animal Care (AALAC) in compliance with protocols approved by the OHSU's Institutional Animal Care and Use Committee (IACUC) #1432. All experiments were performed with male mice.

Primary vaccinations were administered at 7-weeks of age subcutaneously (*sc*) in the dorsal region using 10^6 FFU equivalents of POW-VLP and either 10nmol of aqueous INI-4001 diluted in PBS; 10nmol INI-4001 encapsulated into cationic liposomes or the equivalent amount of unadjuvanted cationic liposome both diluted in 100 mM NaCl and 50 mM sodium phosphate at pH 7.4; or 10nmol INI-4001 incorporated into AS03-like emulsion or the equivalent amount of unadjuvanted emulsion both diluted in DPBS at pH 6.8. All buffers were sterile. All solutions were brought to a final volume of 100uL for injection. Aqueous INI-4001 was synthesized as described by Miller *et al.* [572]. Aqueous formulation of INI-4001 was prepared as described by Crawford *et al.* [665]. Concentration of INI-4001 was determined by RP-HPLC as described by Siram *et al.* [575]. Cationic liposomes with or without INI-4001 were prepared as described by Mehradnia *et al.* [579]. AS03-like emulsions with or without INI-4001 were prepared as described by Short *et al.* [577]. Mock-vaccinated mice received 100uL of PBS alone. Boost-vaccinations were administered 3-weeks post-primary vaccination in the same manner. For ELISA and FRNT, blood was collected by tail-vein at 3 weeks post-boost and left to clot at room-temperature for 30 minutes before centrifugation twice at 10,600 x *g* to collect the serum. Serum was then stored at -20°C until use. For other viremia blood collection and analysis of other tissues, see the following section (RT-qPCR).

For lethal challenge infections, 10^3 FFU of POWV LB (POWV-I) was diluted into 100uL sterile PBS and injected intraperitoneally (*ip*) or *sc*. Mice were weighed and monitored for up to three weeks for signs of morbidity including piloerection, hunched posture, ataxia, malaise, paralysis, and weight loss. Moribund mice were defined as those that experienced substantial weight loss ≥ 20% original body weight, paralysis, and/or other signs of morbidity. Moribund mice were euthanized by isoflurane followed by cervical dislocation to limit suffering.

Reverse transcription-quantitative polymerase chain reaction (RT-qPCR)

For tissue harvest, mice were euthanized at specified timepoints with CO_2, blood was collected (description follows), tissues were perfused with 10mL DPBS passed through the right ventricle, and tissues were collected in TRIzol. Tissues were homogenized by bead-beating with SiLiBeads using a Precellys 24 bead beater homogenizer (Bertin Technologies). Samples were clarified by centrifugation at ~21,000 x *g* and supernatant RNA was isolated by Quick-RNA Viral Kit (Zymo Research #R1034). RNA was quantified by NanoDrop 2000c (ThermoFisher). To measure viremia, blood was collected by cardiac puncture, processed for serum as described in the previous section (Mouse experiments), combined with DNA/RNA Shield (Zymo Research #R1100), and processed for

RNA using the Quick-RNA Viral Kit. RT-qPCR was performed on 200ng of total RNA from tissue per reaction or 4uL of serum RNA samples using 1) POWV NS5-specific primers (Invitrogen: forward TGTTCTGCTGTTCCCGTGAGT; reverse GATGCGCAGCATGTCTTCTG) and probe (Applied Biosystems: AGCATCCACGCGAGTG); 2) murine perforin (Prf1) specific primers and probe (ThermoFisher Catalog #4331182 Assay ID Mm00812512_m1); or 3) murine TCRα (Tcra) specific primers and probe (ThermoFisher Assay ID Mm01313019_g1); along with TaqMan RNA-to-CT 1-Step Kit (Catalog #4392656) on an AB StepOne Real-Time PCR System (ThermoFisher). Dilutions of known quantities (FFU and total RNA) of POWV RNA prepared using DNA/RNA Shield and Quick-RNA Viral Kit were used to produce a standard curve for absolute FFUe quantitation.

Cells

HEK293T and Vero E6 cells were maintained in Dulbecco's Modified Eagle Medium (DMEM) (Corning) supplemented with 5% fetal bovine serum (FBS; HyClone #3039603), 100U/mL penicillin, 100μg/mL streptomycin, and 292μg/mL L-glutamine (Gibco #10378016). Cells were passaged using trypsin 0.05% EDTA (Gibco #25-300-120).

VLP production

The generation of HEK293 cells expressing POWV prM-E was described previously [609, 665]. To produce POW-VLP, HEK293-POWV-prME cells were cultured with 1μg/mL doxycycline in DMEM supplemented with 2% FBS, 100U/mL penicillin, 100 μg/mL streptomycin, and 292 μg/mL L-glutamine. Supernatant was collected 4 days post-induction, centrifuged at 1,000 x *g* for 10min, and filtered through a 0.45μm to remove cellular debris. VLPs were then concentrated and purified by ultra-centrifugation through a 20% sorbitol 50mM Tris 1mM $MgCl_2$ pH 8.0 buffer at 150,000 x *g* for 2 hours at 4°C. Pellets were then resuspended in 1/100th of the original volume with 10mM Tris 150mM NaCl buffer supplemented with 5% trehalose for protein stability and stored at -80°C until use. For VLP quantification, see Enzyme-linked immunosorbent assay (ELISA) methods section.

Viruses

POWV LB (POWV-I) and Spooner (POWV-II) strains were generously provided by Michael S. Diamond (Washington University School of Medicine, St. Louis, MO). LGTV TP21 (NR-51658) was obtained from the Biodefense and Emerging Infections Research Resources Repository (BEI Resources). All viruses were propagated on Vero E6 cells (5 days for LGTV; 7 days for POWVs and WNV

385-99 [658]). Supernatant was collected, centrifuged at 1,000 x *g* for 10min, and filtered through a 0.45μm to remove cellular debris. Virus was then concentrated and purified by ultra-centrifugation through a 20% sorbitol 50mM Tris 1mM $MgCl_2$ pH 8.0 buffer at 150,000 x *g* for 2 hours at 4°C. Pellets were then resuspended in 1/100th of the original volume in DMEM with 0.1% FBS and stored at -80°C until use. Viruses were titered using limited dilution focus forming assay on Vero cell monolayers. Briefly, cells were infected by rocking for 1 hour at 37°C in 5% CO_2. Cells were then overlaid with a formula consisting of 2 parts DMEM with 5% FBS, 100U/mL penicillin, 100 μg/mL streptomycin, and 292μg/mL L-glutamine and 1 part 1% high / 1% low viscosity carboxymethylcellulose (CMC) diluted in a 60% PBS aqueous solution. Cultures were then aspirated and fixed at 24 hours (WNV) or 48 hours (POWVs and LGTV) post-infection with 4% paraformaldehyde for 30 minutes. Staining protocol to visualize foci was then performed as described in "Focus reduction neutralization test (FRNT)" section of methods. Foci were counted using AID Elispot 7.0 (Autoimmun Diagnostika GMBH) and titers were determined from these numbers.

Focus reduction neutralization test (FRNT)

Serial dilutions of sera were prepared in DMEM with 2% FBS and incubated with POWV-I, POWV-II, LGTV, or WNV for 1 hour at 37°C to allow for antibody

binding. Serum treated virus was then used to infect monolayers of Vero cells and overlaid with CMC as described previously in "Viruses". The least dilute serum used to neutralize virus was 1:50. Cells were then fixed with 4% paraformaldehyde at 48 hours post-infection for 30 minutes, blocked and permeabilized in PBS with 2% goat serum (ThermoFisher) and 0.4% Triton X-100 (ThermoFisher). Cells were then stained with 4G2 (WNV) or T077 (POWVs and LGTV), a monoclonal antibody from a TBEV-infected individual sequenced and characterized by Agudelo *et. al* that binds both POWV-I, POWV-II, and LGTV [218]. We cloned the T077 heavy and light variable chain sequences into pcDNA-3-RhIgG1 and -RhIgK, respectively, for antibody production in Expi293 cells. Viral foci were then visualized by secondary staining with monkey IgG gamma peroxidase-conjugated antibody (Rockland) diluted 1:1,000 in blocking buffer followed by Vector VIP Substrate Peroxidase (HRP) Kit (Vector Laboratories SK-4600) after washing. Foci were counted using AID Elispot 7.0 (Autoimmun Diagnostika GMBH) and reciprocal FRNT50s determined by non-linear regression analysis with a variable slope on GraphPad Prism v10.2.2. Values < 1 were adjusted to FRNT50 = 1 for figures. Values extrapolated by GraphPad below the least dilute serum tested (log(1/50)= 1.7) were set to 1.7 for all statistical analyses.

Enzyme-linked immunosorbent assay (ELISA)

To titer whole virus binding antibodies, Corning Costar Brand 96-Well EIA/RIA plates (Corning #9018) were coated with 10^5 FFU of POWV-I, LGTV, or WNV or $3.2X10^4$ FFU of POWV-II purified through a sorbitol cushion as described in "Viruses" methods above and resuspended in PBS containing 0.1% FBS for stabilizing particles. Viruses were plated in 100μL PBS per well overnight at 4°C. Titers used for plating were chosen to be consistent with our validated 10^5 FFU/well for POWV-I (Figure S2.6, page 157). $3.2X10^4$ FFU of POWV-II was chosen as this was the highest titer without significant background binding. Plates were then washed with PBS 0.05% Tween 20 (ThermoFisher BP337-500) and blocked in wash buffer with 5% milk (Safeway). Serum complement was heat inactivated at 55°C for 30 minutes and serially diluted in blocking buffer with the least dilution of 1:50. Sera dilutions were then incubated on ELISA plates for 1.5 hours at room temperature. These were then washed and stained with anti-mouse IgG (γ-chain specific)−peroxidase antibody (MilliporeSigma #A3673) diluted 1:10,000 in wash buffer for 1 hour at room temperature. Secondary antibody was then washed and replaced with 100μL of 4μg/mL o-Phenylene diamine in a buffer of 50mM citric acid 100mM dibasic sodium phosphate 0.01% hydrogen peroxide pH 5.0 for 10 minutes before color change reaction was stopped with equal amount of 1M HCl. Absorbance at 490nm was measured using BioTek Synergy HTX Multimode

Reader and Gen5 Microplate Reader and Imager Software v3.11 (Agilent). Background absorbance was defined as the lowest absorbance value on a plate and subtracted from each well. Linear regression curves were fit using Microsoft Excel INTERCEPT and SLOPE functions to determine endpoint titer defined as when absorbance was 0.1, a baseline absorbance not exceeded by negative controls (Figure S2.6, page 157). Values < 1 were adjusted to an endpoint titer = 1 for figures. Values below the least dilute serum tested (log(1/50)= 1.7) were set to 1.7 for all statistical analyses.

To titer VLPs, plates were coated similarly to assay described above, but with serially diluted VLP alongside POWV of known titer. Plates were blocked and washed as described and stained for 1 hour at room temperature with T077 anti-E antibody (described in the next section) followed by 1 hour with monkey IgG gamma peroxidase-conjugated antibody (Rockland #617-103-012). Endpoint titers were calculated in the same manner as described previously, and these were used to determine the FFUe of VLP using the known FFU of POWV as standard.

Area under the curve (AUC) analysis

Areas under the curve of individual mouse weights were measured for curves of percent initial weight from day 0 through 21 using GraphPad Prism v10.6.1.

Statistical analyses

All appropriate statistical analyses were performed using GraphPad Prism v10.6.1.

Chapter 4: The effect of virus-like particle maturity on Powassan virus vaccine

Michael W. Crawford[1,2], Christopher J. Parkins[1], Henry F. Harrison[1], Jessica L. Smith[2,3], Alec J. Hirsch[2,3]

Affiliations

[1]Vaccine and Gene Therapy Institute, Oregon Health & Science University, Beaverton, OR, USA

[2]Department of Molecular Microbiology and Immunology, Oregon Health & Science University, Portland, OR, USA

[3]Division of Pathobiology & Immunology, Oregon National Primate Research Center, Oregon Health & Science University, Beaverton, OR, USA

Author contributions

Conceptualization and methodology MWC, JLS, AJH; investigation MWC, CJP, HFH; project administration MWC, CJP; resources MWC, JLS, AJH; data curation, formal analysis, validation, visualization, and writing of original draft MWC; funding acquisition, supervision, and review & editing AJH.

Unpublished

Abstract

Powassan virus (POWV) is a tick-borne flavivirus emerging in North America for which we have no vaccine. We have previously demonstrated the utility of Powassan virus-like particles (POW-VLPs) as vaccine antigen in generating a protective antibody response to POWV. Studies with mosquito-borne flavivirus vaccines have demonstrated that more mature flavivirus-like particles elicit greater neutralizing antibody responses and greater protection from lethal infection. Here, we investigate the effects of POW-VLP antigen maturity on the antibody response and protection elicited by our vaccine. We find that antigen maturity affects neither the antibody response nor protection for POWV. This study highlights a fundamental difference between tick-borne and mosquito-borne flavivirus immunity and the need for independent approaches to vaccine design for these two groups of pathogens.

Introduction

Maturation is an important process during flavivirus replication that affects infection and immunity. During replication, immature flavivirus particles bearing trimeric heterodimers of the structural proteins pre-membrane (prM) and envelope (E) bud into the ER [61, 62]. These particles then transit through the acidic

environment of the Golgi for secretion. This environment causes the prM-E trimers on immature particles to rearrange into prM-E dimers, exposing a site within prM that is cleaved by the host protease furin into a 'pr' fragment and the membrane-bound M [62, 63, 69]. The pr fragment then separates from M-E after secretion into the neutral extracellular environment rendering the particle mature [68, 69].

Maturation is not always an efficient process, however, and infected cells often produce a spectrum of immature, partially mature, and mature particles containing varying levels of uncleaved prM [74-76]. To study flavivirus maturation, immature particles are commonly generated from cells treated with ammonium chloride (NH_4Cl) [63, 69, 670]. NH_4Cl prevents maturation by raising the pH of the Golgi which prevents prM-E rearrangement and exposure of the furin cleavage site. Because such particles are substantially less infectious than their more mature counterparts, the field has long asserted that fully immature particles are not independently infectious [63, 69, 80, 670].

It follows, then, that vaccines targeting mature particles would be more advantageous than those targeting immature particles. Indeed, several studies have demonstrated that antibodies targeting immature epitopes on mosquito-borne flaviviruses (MBFVs) tend to be less neutralizing than those targeting mature epitopes [75, 89, 91, 93, 96-99, 671]. Surprisingly, very few studies have

investigated the effects of antigen maturity on flavivirus vaccine efficacy. The few studies that have been published suggest that more mature vaccine antigens generate stronger neutralizing antibody responses and enhance protection against MBFVs like West Nile virus (WNV) and dengue virus serotype 2 (DENV-2) [87, 105-107]. However, no consensus has been reached, as one study evaluating an insect-specific DENV-2 chimera found that partially mature antigen generated greater neutralizing antibody response than fully mature antigen [108]. The discrepancy between these studies may be due to the maturity of virus used for neutralizing tests, which was not reported.

The effect of vaccine antigen maturity on tick-borne flaviviruses (TBFVs) has not been explored. In this study, we investigated the effects of antigen maturity on TBFV vaccine efficacy using our Powassan virus-like particle (POW-VLP) based vaccine. We generated immature and mature POW-VLPs using NH_4Cl and furin overexpression, respectively. We immunized mice with these VLP preparations adjuvanted with alum to interrogate differences in the antibody responses and protection elicited by immature vs mature antigen. We found that antigen maturity did not affect the antibody binding or neutralizing responses, nor did it affect sensitivity to virus maturity. Protection from lethal POWV infection was also not affected by antigen maturity, though animals immunized with

antigen lacking prM trended towards less protected. We conclude that for the TBFV POWV, more mature antigen does not improve the vaccine response.

Results

Generating mature VLP

We have previously produced a cell line that expresses prM and E from POWV lineage 1 LB strain (POWV-LB) when induced with doxycycline [665]. These proteins self-assemble and secrete into the cell culture supernatant as POW-VLP, which we then collect and purify. We quantify these particles relative to FFU of POWV by ELISA of the E protein using anti-E monoclonal antibody T077 [218]. We then confirm the quantities by western blot by probing a given amount of focus-forming unit equivalents (FFUe) of POW-VLP with T077 alongside an equivalent FFU of POWV. When we stain western blot of POWV and POW-VLP with convalescent mouse serum from an unvaccinated mouse that survived POWV infection, both E and prM can be visualized as two prominent bands near 55 and 17 kDa, respectively (Figure 4.1A). This confirmed the equal abundance of E protein but revealed a stark difference in the abundance of prM between POWV and POW-VLP; the VLPs appear to have substantially greater ratios of prM to E than virus. This can also be seen in the Coomassie stain from our previous publication (Figure 2.1C, page 110). This suggests that prM is not cleaved during

preparation and our POW-VLP is immature. In contrast, it appears our preparation of virus is quite mature with much less uncleaved prM.

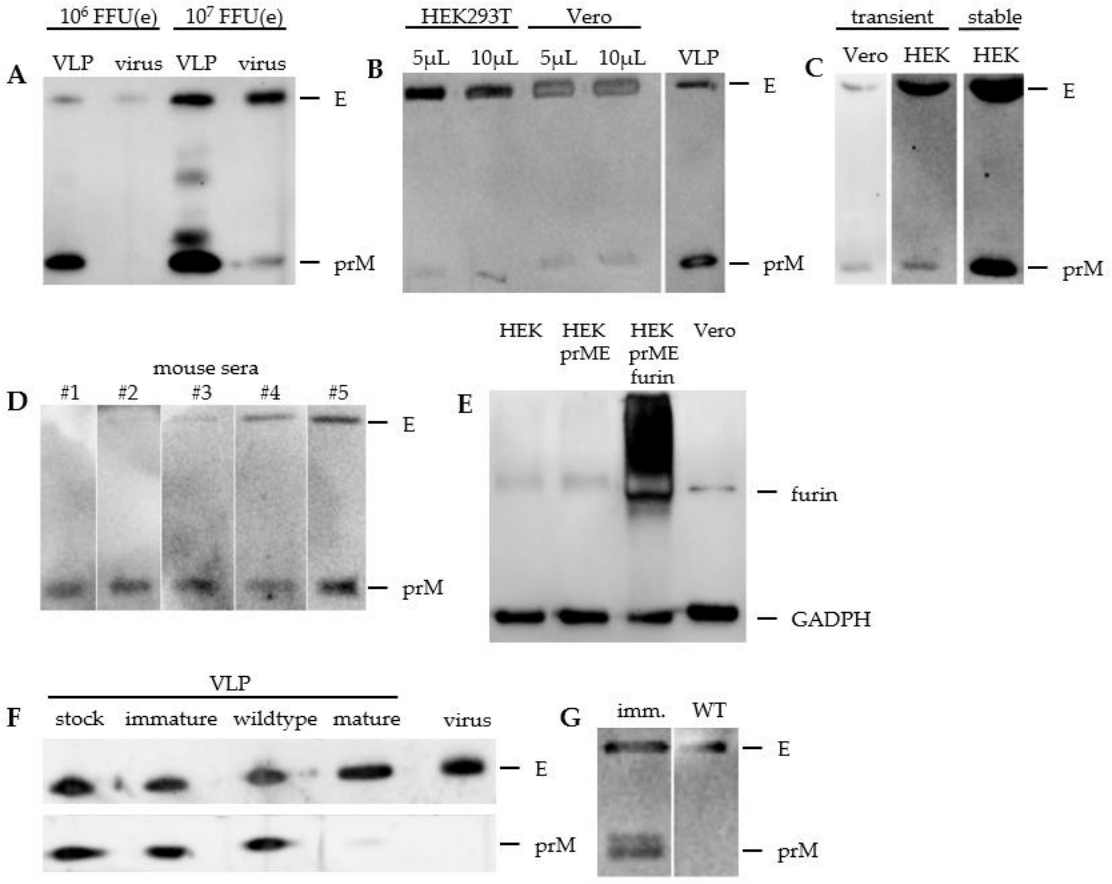

Figure 4.1: Manipulating POWV and POW-VLP maturity with NH_4Cl and furin overexpression.

A-G: Western blots. **A**. 10^6 or 10^7 FFU(e) of POW-VLP or POWV stained with POWV-convalescent mouse serum. **B**. 5 or 10μL of viral supernatant collected but not purified from HEK293T and Vero cells compared to purified 10^6 FFUe POW-VLP stained with convalescent serum. Image depicts a single western blot. **C**. Equivalent amounts of unpurified supernatant from Vero or HEK cells transfected with POWV-prME and induced with doxycycline. Control VLP produced in parallel using stable HEK293T-POWV-prME cell line. Image depicts two western blots: one with Vero-generated VLP the other with both samples produced from HEK cells. Blots treated equivalently, but image of Vero blot produced with longer exposure time. **D**. $3X10^6$ FFUe POW-VLP in each lane with lanes individually stained with serum from one of 5 mice vaccinated with 10^6 FFUe of POW-VLP twice *sc* 4 weeks apart. Sera collected 3 weeks post-boost. **E**. 5μg cell lysate protein from HEK293T-POWV-prME-hFurin or various controls stained with anti-furin and anti-GAPDH for loading control. **F**. $4X10^5$ FFUe of immature, wildtype, or mature VLP. Controls include wildtype stock VLP and $4X10^5$ FFU of virus. Image depicts a single western first developed with anti-E T077 then with serum from a POW-VLP-vaccinated mouse to visualize prM. **G**. 10^6 FFU immature or wildtype virus stained with convalescent serum.

One of our first questions was whether the difference in maturity was due to the different cell lines used to generate VLP and virus (HEK293T human

embryonic kidney cells vs Vero African green monkey epithelial kidney cells), or whether it was a difference in producing particles via ectopic expression of prM-E vs infection. To answer this, we propagated POWV on either HEK or Vero cells. Maturity of these virus preparations was evaluated by western blot using convalescent mouse serum (Figure 4.1B). Bands for E were much more prominent than those for prM for both HEK- and Vero-propagated virus in contrast to POW-VLP control. Next, we tested maturity of VLP generated from HEK293T and Vero cells by transfecting these cell lines with POWV prM-E and inducing expression with doxycycline. Western blots revealed a considerably higher ratio of prM to E in transfected Vero cells compared to what is seen during infection (Figure 4.1C.) Interestingly, transient transfection of prM-E into HEK293T cells appeared to have improved maturity compared to VLP produced from a stable doxycycline-inducible prM-E HEK293T cell line. These data are consistent with the conclusion that ectopic expression of prM-E generates more immature particles than POWV infection.

The high prM-content of our VLP vaccine antigen raised the question of whether the immaturity of VLP was affecting the antibody response to our low-dose POW-VLP vaccine. To answer this, we stained 5 individual lanes of a western blot loaded with $3X10^6$ POW-VLP per lane with serum samples from 5 individual mice vaccinated with our INI-4001-adjuvanted POW-VLP vaccine. This revealed

a substantial anti-prM antibody response with bands for prM more prominent than those for E (Figure 4.1D.) This suggests that the immaturity of our vaccine antigen was affecting the antibody response.

Next, we generated a clonal population of furin-overexpressing HEK293T-POWV-prME-hFurin to improve the maturity of our VLP. Furin overexpression is a well-established method for driving flavivirus particle maturity [81, 88, 672, 673]. Overexpression of furin was validated by western blot using HEK293T, HEK293T-POWV-prME, and Vero cells as controls (Figure 4.1E.) We then produced mature VLP by inducing furin-overexpressing prM-E-stable cells with doxycycline. Wildtype VLP was produced using our progenitor prM-E stable cell line in the same manner. Immature VLP was also produced from this line but using media containing 20mM NH_4Cl as described by Heinz *et al.* [670]. Equivalent FFUe of each preparation was run on a western blot and stained for E and prM. All but mature VLP generated by furin-overexpressing cells and virus control had appreciable prM (Figure 4.1F.) These experiments demonstrate the utility of furin-overexpression for enhancing flavi-VLP maturity.

Treating cell culture with NH_4Cl was also used to generate immature virus on Vero cells (Figure 4.1G). Reduced specific infectivity was confirmed both by 1) RT-qPCR of POWV RNA to quantify genomes per infectious unit and 2) T077

POWV-E ELISA to quantify E per infectious unit. Immature virus was ~8-fold less infectious than wildtype as measured by PCR (890 vs 120 genome/FFU) and ~2.5-fold as measured by ELISA.

Antigen maturity does not affect antibody responses or protection

prM is generally considered a poor antibody target for neutralizing flaviviruses while antibody responses targeting epitopes on mature virus tend to be more neutralizing. To investigate the effects of VLP antigen maturity on the efficacy of our POW-VLP vaccine, we prime-boost vaccinated mice with either immature, wildtype, or mature alum-adjuvanted VLP (n = 10/group). For negative control, mock mice were vaccinated with PBS vehicle. For positive control, stock-vaccinated mice were vaccinated with wildtype VLP from a previous preparation used in prior experiments (n = 5/group for these control groups). Serum samples were collected three weeks post-boost to evaluate antibody responses. Anti-POWV IgG titers were measured by whole-virion ELISA using either immature or more mature wildtype virus to assess antibody sensitivity to maturity (Figure 4.2.A). There was no significant difference in binding between vaccine groups to either immature or more mature POWV. Interestingly, the antibody responses to immature virus were higher than those to more mature wildtype virus in every group. Only immature- and mature-immunized groups had antibody titers

significantly higher than the mock group, and this was only for immature virus, not wildtype.

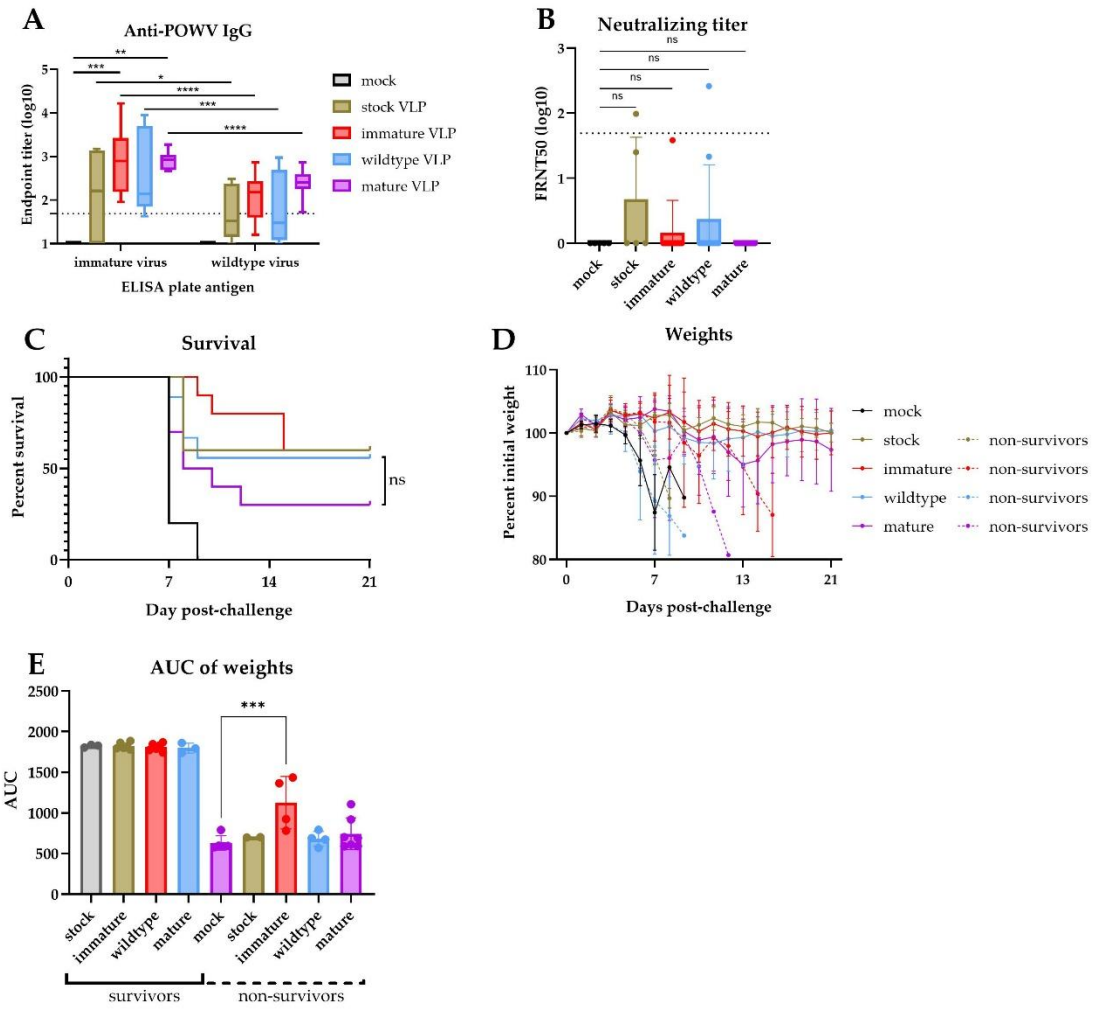

Figure 4.2: VLP maturity does not significantly affect the antibody response or protection elicited by vaccination.

A-E: Mice prime-boost vaccinated 3 weeks apart *sc* with 10^6 FFUe of stock (gold), immature (red), wildtype (blue), or mature (purple) VLP adjuvanted with 300 μg alum or mock vaccinated with PBS vehicle (black). mock, stock: n = 5/group; immature, wildtype, mature: n = 10/group. Serum collected 3 weeks post-boost and analyzed by (**A**) whole-virus ELISA using immature (left) or wildtype virus (right), and (**B**) FRNT. Vaccinated mice challenged with a lethal 10^3 FFU POWV-LB 4 weeks post-boost. Survival assessed (**C**) and weights measured (**D**) to day 21 post-challenge. **A.** Data reported as box & whiskers plots of log-transformed IgG endpoint titers. Statistical significance was determined by two-way ANOVA and Tukey's multiple comparisons test to compare all vaccine groups to one-another within and between plate antigen groups after log transformation. **B.** Data reported as log-transformed reciprocal FRNT50 + SD. Statistical significance determined by one-way ANOVA and Dunnett's multiple comparisons test to compare all groups to mock. **C.** Survival curves of lethally challenged mice. Statistical significance determined by log-rank test with Bonferroni correction comparing all vaccine groups. **D.** Weights of lethally challenged mice represented as mean percent of initial weights ± SD grouped by those that survived (solid lines) and those that succumbed (dashed lines) to infection. **E.** Area under the curve (AUC) of individual mice that did (left) or did not (right) survive lethal challenge infection ± SD. Statistical significance determined by one-way ANOVA with Šídák's

multiple comparisons test to compare AUC survivor groups to one another and non-survivor groups to mock. Data represent single experiment. ns – not significant; **p < 0.01; ***p < 0.001; ****p < 0.0001.

Neutralizing antibody titers to wildtype POWV were measured by focus reduction neutralization test (FRNT; Figure 4.2.B). FRNT50 was undetectable for most mice. There was no significant difference in neutralization for any group compared to mock vaccinated mice.

Mice were subsequently challenged with a lethal dose of POWV subcutaneously (sc) four weeks post-boost. Survival (Figure 4.2.C) and weights (Figure 4.2.D) were monitored for three weeks post-challenge. There was no significant difference in survival of mice that received wildtype or mature vaccine antigen. However, the survival of mature-vaccinated mice trended lower than the other groups while the survival for immature-vaccinated mice trended longer. The survivors in the mature group trended towards more weight-loss, but there was no significant difference in the area under the curve (AUC) between vaccine groups of survivor weights (Figure 4.2.E). Among the groups of mice that succumbed to challenge, only those that received immature vaccine had significantly higher AUC of weights compared to mock-vaccinated animals. Together these data do not support the hypothesis that more mature vaccine

antigen improves the antibody response or protection. To the contrary, the data suggest that mature VLP is less protective and VLP generated under basic conditions is slightly more protective than wildtype.

Discussion

In this study, we find that POW-VLPs generated via ectopic expression of prM-E are more immature than virus. This difference does not appear to be due to differences in the cell types used for preparing VLP (HEK293T) vs virus (Vero) but rather due to a difference underlying ectopic expression of prM-E vs propagation of virus by infection (Figure 4.1B-C.) The concentration of E in our wildtype VLP is ~20-fold higher than in wildtype virus despite similar cell counts per culture suggesting more protein is being produced per cell. Ectopic expression may, therefore, over-burden furin-processing allowing some prM to escape cleavage. Contribution by other viral proteins during infection may also contribute to maturation. Additional experiments are required to evaluate the role other viral proteins play in particle maturation.

The effects of antigen maturity on antibody and protective responses to POW-VLP were tested by generating immature VLP under basic culture conditions and mature VLP by overexpression of furin. Low-dose, alum-

adjuvanted vaccines using these antigens alongside wildtype VLP were tested for their ability to drive an anti-POWV binding and neutralizing response. There was no significant difference in the virus-binding IgG endpoint titers between vaccine groups, and none of the vaccines induced significant neutralizing antibody responses.

Interrogating further, there appeared to be no differences in antibody sensitivity between vaccine groups to either immature virus produced under basic culture-conditions or more mature wildtype virus. This seems to refute the hypothesis that the maturity of vaccine antigen affects the epitopes targeted by the antibody response, though this may be due to several factors. First, our vaccine platform uses a very low ~70ng dose of total protein. Experiments by Ohtaki *et al.* with WNV showed no appreciable differences in virus-binding antibody responses to similar doses of unadjuvanted 30-270ng of WN-VLP and only saw differences in neutralization at the higher dose of 270ng [106]. Meanwhile, other studies investigating the effects of antigen maturity on vaccine efficacy have used much higher vaccine doses. Suphatrakul *et al.* demonstrated differences in epitope binding responses and neutralizing antibody responses to immature v mature DENV-2, but they immunized mice with two doses of 1μg DEN2-VLP (unadjuvanted) [107]. Shen *et al.* showed that more mature DEN2-VLP antigen sensitized the antibody response to maturity, but mice were immunized with two

4μg doses (unadjuvanted) [87]. Sensitivity to antigen maturity may, therefore, depend on dosage, with antigen availability during the vaccine response driving this sensitization. Secondly, there may not be a strong enough contrast in maturity between our immature and wildtype virus to render our assay sensitive enough to detect differences. The 2.5- to 8-fold reduction in specific infectivity we observed in immature virus is much less than previous studies investigating immature TBEV. Heinz *et al.* reported a 20- to 50-fold decrease in specific infectivity and hemagglutination activity of TBEV prepared on chicken embryo cells using a similar NH_4Cl method compared to wildtype virus produced on untreated cells [670]. Stadler *et al.* showed that the specific infectivity of immature virus prepared in this same way was enhanced 100-fold when acidified and treated with recombinant furin in a cell-free system [63]. This suggests that the difference in maturity between our immature and wildtype virus is modest and may therefore be insufficient to detect antibody sensitivity.

Protection from lethal POWV infection was subsequently assessed by monitoring survival and weight of mice after lethal infection. There was no significant difference in survival between the vaccine groups. However, mature-vaccinated mouse survival trended lower than other groups, and immature-vaccinated mice tended to survive longer. In addition, immature-vaccinated mice that succumbed to infection survived longer than mock vaccinated animals as

indicated by AUC of weights for the trial period. Together, these data do not support the hypothesis that more mature VLP antigen improves vaccine protection. Rather, the data suggest the opposite: the presence of uncleaved prM might enhance protection.

This study was designed on the assumption that the infectious potential of TBFVs is dependent on particle maturity. However, a study recently published by Holoubek *et al.* in August 2025 (after our experiments had concluded) challenges this assumption [73]. Holoubek *et al.* demonstrated that immature TBFVs generated in furin-deficient LoVo cells are fully infectious, and that this infectivity is dependent on the presence of furin on target cells. They also demonstrate that the prM furin-cleavage site remains fully exposed on immature TBFVs produced in LoVo cells, in contrast to MBFVs. This is supported by previous studies demonstrating that TBFV prM-E dimerization under acidic conditions is irreversible regardless of prM cleavage, while uncleaved MBFV prM-E dimers revert to spike trimers after exiting into the neutral pH of the extracellular environment [63, 69].

These findings have several implications for our current study. Firstly, this suggests that our immature virus and immature VLP generated under basic culture-conditions generates artificial trimeric-spike prM-E-enveloped particles

which are likely not present during actual infection. It follows that the immature VLP produced in this way is likely an irrelevant antigen, and our ELISA assay design using immature vs more mature virus to measure antibody responses is flawed. It is, therefore, not surprising that immature-vaccinated mice were one of the only groups with significant anti-immature virus IgG binding titers. It is quite surprising, however, that mature-vaccinated mice were the only other group with significant anti-immature virus antibody titers, as mature VLP lacks both prM and trimeric prM-E epitopes.

Secondly, Holoubek *et al.*'s demonstration that the uncleaved prM on immature virus propagated under physiologically relevant pH are subject to cleavage by downstream extracellular proteases suggests that the uncleaved prM on the wildtype VLP presented in our study may also be subject to cleavage post-vaccination. How this affects the host immune response may not be straightforward and raises additional questions. Is prM on our wildtype VLP cleaved by extracellular furin? If so, does the generation of pr fragment post-inoculation lead to a significant anti-pr response that can target prM of immature virus? These questions are testable. Cleavage of prM from immature VLPs could be probed by incubating these particles on furin-competent cells and evaluating prM cleavage by western blot. It would also be pertinent to test whether reducing prM cleavage by mutating the furin cleavage site or fixing particles with

formaldehyde prior to vaccination prevents post-vaccination cleavage of prM and whether this affects the antibody response.

Lastly, the findings of Holoubek *et al.* challenge the core of our current study's hypothesis; that a vaccine designed to elicit an antibody response to more infectious mature virus would be more protective than vaccine targeting immature non-infectious particles. By demonstrating that immature TBFVs generated in furin-deficient cells are equally as infectious as their mature counterparts, Holoubek *et al.* have flipped the paradigm that targeting mature epitopes is more advantageous. If we assume that infectious immature particles are generated during animal infection, then vaccines that target both immature and mature viruses would be more protective. The data presented in our current study seem to align with this new hypothesis. Neutralizing titers were only observed in mice that had received vaccine with appreciable amounts of uncleaved prM. Though neutralization was evaluated using more mature wildtype virus, even they are not completely mature (Figure 4.1A) which may affect the FRNT. Additionally, survival was highest in groups that received appreciable amounts of prM antigen. Retrospectively grouping vaccinated mice by those that received substantial prM (stock, immature, and wildtype VLP) vs those that received minimal prM (mature) revealed that prM-containing vaccine was very nearly significantly more protective than vaccine that lacked this antigen ($p = 0.065$; Figure S4.1A). The AUC

of the weight curves for mice that succumbed to infection revealed that those immunized with prM lost weight more slowly, which was also very nearly significantly higher than those that succumbed after receiving vaccine lacking prM ($p = 0.064$; Figure S4.1B-C). Together, this suggests that immunizing with prM may be uniquely advantageous for TBFV vaccines.

Jarmer *et al.* have previously demonstrated that though anti-prM antibodies are found in both TBEV-convalescent and TBEV-vaccinated individuals, these antibodies do not contribute to neutralization [674]. However, they acknowledge that the maturity of the virus used in their neutralization tests was not reported, so, unfortunately, no conclusion can be drawn about the role of anti-immature TBEV antibodies in neutralization. They also demonstrated that antibodies targeting DI and DII but not DIII contributed to neutralization of TBEV from these individuals, which is in stark contrast with MBFVs whose major neutralizing antibody target is DIII. This suggests there could be a fundamental difference in the neutralization of TBFVs vs MBFVs.

Future experiments investigating the role of antigen maturity in TBFV vaccination should focus on whether inclusion of both mature particles generated by furin-overexpression and immature particles generated with LoVo furin-deficient cells improves the vaccine response over mature or immature antigen

alone. The maturity of virus in the saliva of infectious ticks should also be assessed to determine which antigens should be targeted to generate a protective first line of defense to invading particles during initial tick-bite. Though Holoubek *et al.* have convincingly demonstrated that immature TBFV is infectious, the role of immature particles during initial inoculation of virus from a tick is unknown. Additionally, virus maturity post-replication in the host should be assessed to quantify the proportion of immature to mature virus generated after replication in infected mammals. The data in our current study demonstrate a trend towards more protection in mice that received vaccine with prM which suggests that immature particles play a role in infection after initial inoculation.

In summary, our findings demonstrate that more mature TBFV vaccine antigen does not offer a protective advantage over immature antigen. This contradicts previous studies demonstrating better outcomes with more mature MBFV vaccine antigen. This is likely a result of fundamental differences in the maturation of MBFVs and TBFVs. More work is needed to evaluate whether TBFV vaccine methodology should consider combination of immature and mature vaccine antigens to protect from both forms of infectious particles.

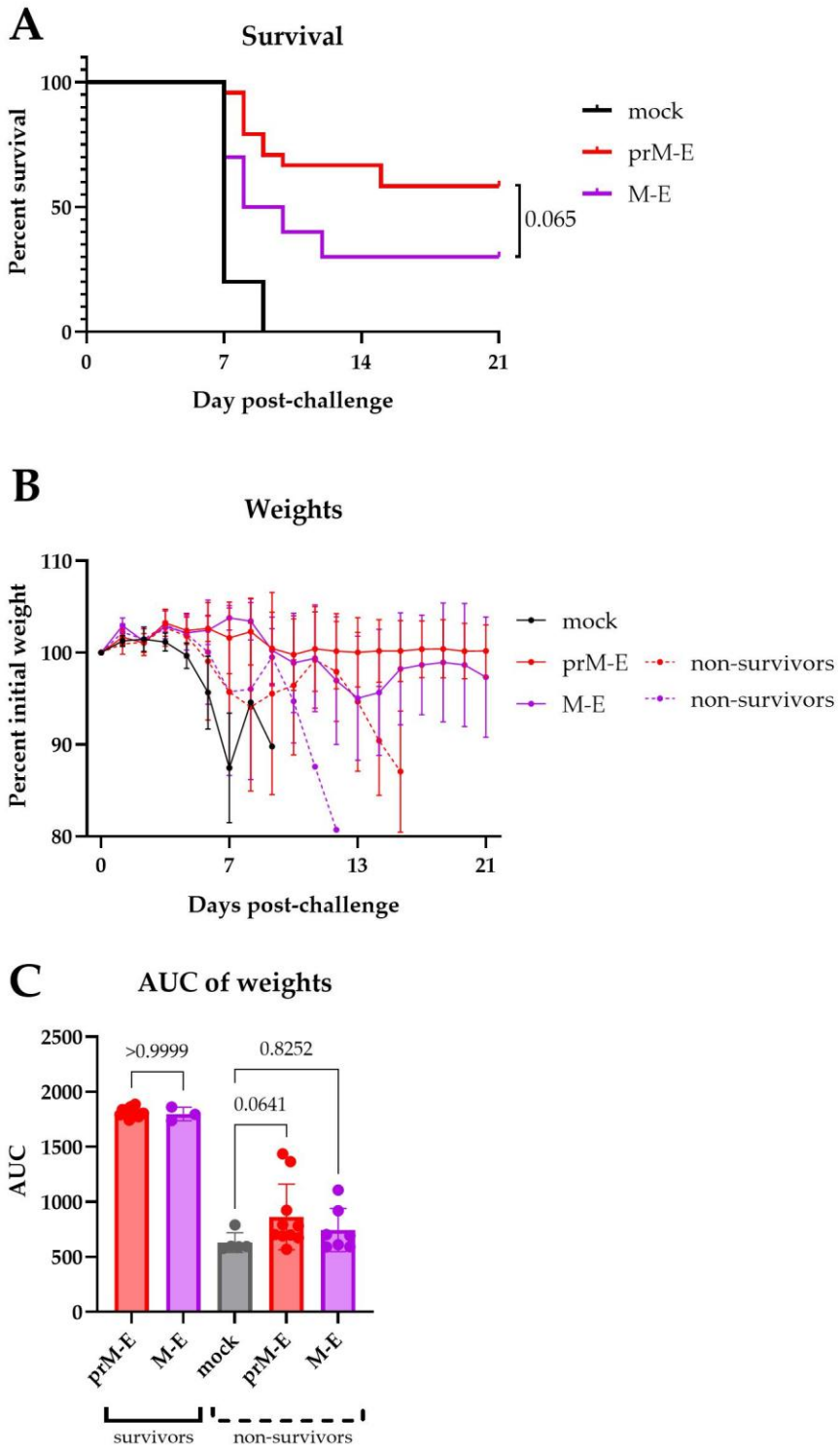
A
Survival
Percent survival
100
50
0
0
7
14
21
Day post-challenge
mock
prM-E
M-E
0.065
B
Weights
Percent initial weight
110
100
90
80
0
7
13
21
Days post-challenge
mock
prM-E
M-E
non-survivors
non-survivors
C
AUC of weights
AUC
2500
2000
1500
1000
500
0
>0.9999
0.8252
0.0641
prM-E
M-E
mock
prM-E
M-E
survivors
non-survivors

Figure S4.1: prM-containing vaccine trends towards greater protection.

(**A-C**) Mice prime-boost vaccinated 3 weeks apart *sc* with 10^6 FFUe of stock/immature/wildtype VLP containing prM-E (red) or mature (purple) VLP containing M-E adjuvanted with 300 μg alum or mock vaccinated with PBS vehicle (black). mock, stock: n = 5/group; prM-E: n = 30/group; M-E: n = 10. Vaccinated mice challenged with a lethal 10^3 FFU POWV-LB 4 weeks post-boost. Survival assessed (**A**) and weights measured (**B**) to day 21 post-challenge. **A.** Survival curves of lethally challenged mice. Statistical significance determined by log-rank test comparing two vaccine groups. **B.** Weights of lethally challenged mice represented as mean percent of initial weights ± SD grouped by those that survived (solid lines) and those that succumbed (dashed lines) to infection. **C.** Area under the curve (AUC) of individual mice that did (left) or did not (right) survive lethal challenge infection ± SD. Statistical significance determined by one-way ANOVA with Bonferroni multiple comparisons test to compare survivor groups to each other and non-survivor groups to mock. Data represent single experiment presented previously in Figure 4.2.

Materials & Methods

Cells

HEK293T and Vero E6 cells were maintained in Dulbecco's Modified Eagle Medium (DMEM) (Corning) supplemented with 5% fetal bovine serum (FBS; HyClone #3039603), 100 U/mL penicillin, 100 μg/mL streptomycin, and 292 μg/mL

L-glutamine (Gibco #10378016). Cells were passaged using trypsin 0.05% EDTA (Gibco #25-300-120).

Virus

POWV-LB and Spooner strains were generously provided by Michael S. Diamond (Washington University School of Medicine, St. Louis, MO). Wildtype virus used for Figure 4.1A was propagated on Vero E6 cells infected at an MOI of ~0.001 for 7 days before collection. For viruses of varying maturity, Vero E6 cells were infected at an MOI of 3. For immature virus in the western blot in Figure 4.1.G and the ELISA in Figure 4.2.A, media was replaced with media containing 20mM NH_4Cl at 22hpi and then again at 24hpi as described by Anastasina *et al* [675]. Wildtype virus was generated in parallel replacing media with regular growth media sans NH_4Cl. Virus was collected at 48hpi. Viral supernatants were centrifuged at 1000 × *g* for 10 min, and filtered through a 0.45 μm filter to remove cellular debris. Virus was then concentrated and purified by ultra-centrifugation through a 20% sorbitol, 50 mM Tris, 1 mM $MgCl_2$, pH 8.0 buffer at 150,000 × *g* for 2 h at 4 °C. Pellets were then resuspended in 1/100th of the original volume in DMEM with 0.1% FBS and stored at −80 °C until use. Viruses were titered using a limited dilution focus-forming assay on Vero cell monolayers. Briefly, cells were infected by rocking for 1 h at 37 °C in 5% CO_2. Cells were then overlaid with a

formula consisting of 2 parts DMEM with 5% FBS, 100 U/mL penicillin, 100 μg/mL streptomycin, 292 μg/mL L-glutamine, and 1 part 1% high/1% low viscosity carboxymethylcellulose (CMC) diluted in a 60% PBS aqueous solution. Cultures were then aspirated and fixed at 48 h post-infection with 4% paraformaldehyde for 30 min. Staining protocol to visualize foci was then performed as described in the "Focus reduction neutralization test (FRNT)" section. Foci were counted using AID Elispot 7.0 (Autoimmun Diagnostika GMBH), and titers were determined from these numbers.

VLP production

The generation of HEK293 cells expressing POWV prME was described previously [609, 665]. To produce stock POW-VLP, HEK293T-POWV-prME cells were cultured with 1 μg/mL doxycycline in DMEM supplemented with 2% FBS, 100 U/mL penicillin, 100 μg/mL streptomycin, and 292 μg/mL L-glutamine. Supernatant was collected 4 days post-induction, centrifuged at 1000 × g for 10 min, and filtered through a 0.45 μm filter to remove cellular debris. VLPs were then concentrated and purified by ultra-centrifugation through a 20% sorbitol, 50 mM Tris, 1 mM MgCl2, pH 8.0 buffer at 150,000 × g for 2 h at 4 °C. Pellets were then resuspended in 1/100th of the original volume with 10 mM Tris, 150 mM NaCl buffer supplemented with 5% trehalose for protein stability and stored at −80 °C

until use. For quantification, ELISA using T077 (described in "ELISA" method section) to detect POWV-E was performed using a known quantity of POWV (FFU). Quantification was validated by western blot (see "Western blot" method section).

For VLPs of varying maturity, stable HEK293T-POWV-prME cells were plated for immature and wildtype VLP and HEK293T-POWV-prME-hFurin cells for mature VLP (see "Furin overexpression" method section for how these cells were generated). All three were induced in parallel with doxycycline as described above. Immature induction media contained 20mM NH_4Cl. Supernatants were then collected at 4 days post-induction and VLPs purified as described above.

Reverse transcription-quantitative polymerase chain reaction (RT-qPCR)

Viral RNA was isolated from 4 μL purified virus by Quick-RNA Viral Kit and eluted into 50 μL water (Zymo Research #R1034). RT-qPCR was performed with 5 μL of serum RNA samples using POWV NS5-specific primers (Invitrogen: forward TGTTCTGCTGTTCCCGTGAGT; reverse GATGCGCAGCATGTCTTCTG), probe (Applied Biosystems: AGCATCCACGCGAGTG), and TaqMan RNA-to-CT 1-Step Kit (Catalog #4392656) on an AB StepOne Real-Time PCR System (ThermoFisher). Dilutions of

known quantities of stock POWV RNA (NanoDrop) were used to produce a standard curve for absolute genome quantitation.

Western blot

For cell lysate, cells were collected in RIPA buffer and aspirated multiple times with a 23G needle to shear debris and DNA. Lysate, virus, or VLP preparations were boiled at 95 °C for 5 min in reducing sample buffer. Samples were then run on a 10% SDS-PAGE gel. Gels were transferred to Immobilon-P PVDF 0.45 μm Membrane (MilliporeSigma #IPVH00010), and immunoblotted with T077 (described in "ELISA" methods) to visualize E, anti-GAPDH (Abcam ab8245), anti-furin (Abcam ab3467), or with convalescent mouse serum to visualize prM and E. Mouse IgG (MilliporeSigma #A3673), rabbit IgG (Jackson ImmunoResearch #111-035-003), or monkey IgG gamma peroxidase-conjugated antibody for T077 (Rockland #617-103-012) were used as secondary stain. Pierce ECL Western Blotting Substrate (ThermoFisher #32106) was used to develop. Pictures were taken using G:Box imager (Syngene) or ChemiDoc Touch Imaging System (Bio-Rad).

Furin overexpression

Plasmid containing human furin was generously provided by William Messer (Oregon Health & Science University, Portland, OR). Furin was then PCR-amplified using primers 5′-AAGCGGCCGCTCATCAGAGGGCGCTCTGGTCT-TTG-3′ and 5′-AATCTAGAACCATGGAGCTGAGGCCCTGG -3′ which include restriction sites NotI and XbaI. PCR product was digested and cloned into pLVX-IRES-Hygro to produce pLVX-IRES-Hyg-hFurin. Plasmid was whole-plasmid sequenced (Eurofins Genomics) to confirm correct furin sequence. HEK293T cells were transfected with pLVX-IRES-Hyg-hFurin using Lipofectamine 3000 (ThermoFisher #L3000015) according to the manufacturer's instructions. Stably transfected cells were selected for using 1 μg/mL hygromycin to generate a HEK293-furin cell line that expresses POWV-prME upon doxycycline-induction. Furin expression validated by western blot (Figure 4.1E) using anti-furin (Abcam ab3467) and anti-GAPDH (Abcam ab8245) for loading control (see "Western blot" methods for more information).

Mouse experiments

5-week old male or female C57BL/6 mice were purchased from Jackson Laboratory and housed in an ABSL-3 facility at Oregon Health & Science University's (OHSU) Vaccine and Gene Therapy Institute accredited by the

Association for Accreditation and Assessment of Laboratory Animal Care (AALAC) in compliance with protocols approved by the OHSU's Institutional Animal Care and Use Committee (IACUC) #1432. All experiments were performed with male mice unless otherwise stated.

Primary vaccinations were administered at 7 weeks of age subcutaneously (*sc*) in the dorsal region using 10^6 FFU equivalents of POW-VLP and 11 μmol of Alhydrogel 2% adjuvant (300 μg) at a final volume of 100 μL in sterile injection-grade PBS. Mock-vaccinated mice received 100 μL of PBS alone. Boost vaccinations were administered 3 weeks post-primary vaccination in the same manner. Blood was collected by tail vein at 3 weeks post-boost and left to clot at room temperature for 30 min before centrifugation twice at 10,600 × *g* to collect the serum. Serum was then stored at −20 °C until use.

For lethal challenge infections, 10^3 FFU of POWV-LB was diluted into 100 μL sterile PBS and injected intraperitoneally (*ip*) at 4 weeks post-boost. Mice were monitored for up to three weeks for signs of morbidity, including piloerection, hunched posture, ataxia, malaise, paralysis, and weight loss. Moribund mice were defined as those that experienced substantial weight loss ≥20% original body weight, paralysis, and/or other signs of morbidity. Moribund mice were euthanized by isoflurane followed by cervical dislocation to limit suffering.

Convalescent mouse serum

Naïve mice were infected twice with varying titers of POWV-LB either subcutaneously or intraperitoneally and allowed to convalesce. Mice were euthanized by CO_2. Blood was collected by cardiac puncture and allowed to clot at room temperature for 30 min before centrifugation twice at 10,600 x *g* to collect serum. Serum was heat treated at 55 °C for 30 min to eliminate the possibility of retaining infectious virus and then stored at 4°C until use.

Enzyme-linked immunosorbent assay (ELISA)

To titer whole-virus binding antibodies, Corning Costar Brand 96-Well EIA/RIA plates (Corning #9018) were coated with 10^5 FFU of POWV-I purified through a sorbitol cushion as described in "Viruses" methods above and resuspended in PBS containing 0.1% FBS for stabilizing particles. Viruses were plated in 100μL PBS per well overnight at 4 °C. Plates were then washed with PBS 0.05% Tween 20 (ThermoFisher BP337-500) and blocked in wash buffer with 5% milk (Safeway). Serum complement was heat inactivated at 55 °C for 30 min and serially diluted in blocking buffer with the least dilution of 1:50. Sera dilutions were then incubated on ELISA plates for 1.5 h at room temperature. These were then washed and stained with anti-mouse IgG (γ-chain specific)–peroxidase

antibody (MilliporeSigma #A3673) diluted 1:10,000 in wash buffer for 1 h at room temperature. Secondary antibody was then washed and replaced with 100 μL of 4 μg/mL o-Phenylene diamine in a buffer of 50 mM citric acid, 100 mM dibasic sodium phosphate, 0.01% hydrogen peroxide, pH 5.0, for 10 min before the color change reaction was stopped with an equal amount of 1 M HCl. Absorbance at 490 nm was measured using BioTek Synergy HTX Multimode Reader and Gen5 Microplate Reader, and Imager Software v3.11 (Agilent). Background absorbance was defined as the lowest absorbance value on a plate and subtracted from each well. Linear regression curves were fit using Microsoft Excel INTERCEPT and SLOPE functions to determine endpoint titer, defined as when absorbance was 0.1, a baseline absorbance not exceeded by negative controls (Figure S2.6). Values < 1 were adjusted to an endpoint titer = 1 for figures. Values below the least dilute serum tested (log(1/50) = 1.7) were set to 1.7 for all statistical analyses.

To titer VLPs, plates were coated similarly to the assay described above, but with serially diluted VLP alongside POWV of known titer. Plates were blocked and washed as described and stained for 1 h at room temperature with T077 anti-E antibody (described in the next "FRNT" method section), followed by 1 h with monkey IgG gamma peroxidase-conjugated antibody (Rockland #617-103-012). Endpoint titers were calculated in the same manner as described previously, and

these were used to determine the FFUe of VLP using the known FFU of POWV as a standard.

Focus reduction neutralization test (FRNT)

Serial dilutions of sera were prepared in DMEM with 2% FBS and incubated with POWV-I propagated with the 7 day methodology described in "Viruses" method section for 1 h at 37 °C to allow for antibody binding. Serum-treated virus was then used to infect monolayers of Vero cells and overlaid with CMC as described previously in "Viruses". The least dilute serum used to neutralize the virus was 1:50. Cells were then fixed with 4% paraformaldehyde at 48 h post-infection for 30 min, blocked and permeabilized in PBS with 2% goat serum (ThermoFisher) and 0.4% Triton X-100 (ThermoFisher). Cells were then stained with T077, a monoclonal antibody from a TBEV-infected individual sequenced and characterized by Agudelo et al. that binds POWV-I [218]. We cloned the T077 heavy and light variable chain sequences into pcDNA-3-RhIgG1 and -RhIgK, respectively, for antibody production in Expi293 cells. POWV foci were then visualized by secondary staining with monkey IgG gamma peroxidase-conjugated antibody (Rockland #617-103-012) diluted 1:1000 in blocking buffer, followed by Vector VIP Substrate Peroxidase (HRP) Kit (Vector Laboratories SK-4600) after washing. Foci were counted using AID Elispot 7.0 (Autoimmun Diagnostika

GMBH) and reciprocal FRNT50s determined by non-linear regression analysis with a variable slope on GraphPad Prism v10.2.2. Values < 1 were adjusted to FRNT50 = 1 for figures. Values extrapolated by GraphPad below the least dilute serum tested (log(1/50) = 1.7) were set to 1.7 for all statistical analyses.

Area under the curve (AUC) analysis

Areas under the curve of individual mouse weights were measured for curves of percent initial weight from day 0 through 21 using GraphPad Prism v10.6.1.

Statistical analyses

All appropriate statistical analyses were performed using GraphPad Prism v10.6.1.

Chapter 5: Correlates of protection in a mouse vaccination-challenge model for Powassan virus

Michael W. Crawford[1,2], Walid M. Abdelwahab[3,4], Karthik Siram[3,4], Christopher J. Parkins[1], Henry F. Harrison[1], Dillon Schweitzer[3,4], David J. Burkhart[5], Jessica L. Smith[1,7], Alec J. Hirsch[1,7]

Affiliations

[1]Vaccine and Gene Therapy Institute, Oregon Health & Science University, Beaverton, OR, USA.

[2]Department of Molecular Microbiology and Immunology, Oregon Health & Science University, Portland, OR, USA.

[3]Department of Biomedical and Pharmaceutical Sciences, University of Montana, Missoula, MT, USA.

[4]Center for Translational Medicine – Adjuvant Research Team, University of Montana, Missoula, MT, USA.

[5]Inimmune Corporation, Missoula, MT, USA.

[7]Division of Pathobiology & Immunology, Oregon National Primate Research Center, Oregon Health & Science University, Beaverton, OR, USA

Author contributions

M.W.C., J.L.S., W.M.A., D.J.B., and A.J.H.: designed experiments. M.W.C., C.J.P., H.F.H., and J.L.S.: performed experiments. W.M.A., K.S., D.S., and D.J.B.: adjuvant synthesis and QCETS. M.W.C.: prepared figures, wrote the paper.

Unpublished

Abstract

Correlates of protection (CoP) are valuable tools for vaccine development that help facilitate the evaluation of vaccine efficacy. CoP have not been identified for Powassan virus (POWV), a rare tick-borne flavivirus emerging in North America. Here, I present evidence that both binding and neutralizing antibodies correlate with protection from lethal POWV challenge in vaccinated mice. Furthermore, I demonstrate that passively transferred antibodies protect naïve mice from infection. These findings establish binding and neutralizing antibody responses as functional CoP for POWV.

Introduction

CoP for vaccines are biomarkers in vaccinated individuals that correlate with protection from disease. They are often readily measurable responses such as neutralizing antibodies that act as surrogates for evaluating vaccine efficacy on the path to licensure [676]. However, correlation is not causation. Though a CoP may suggest a possible mechanism of protection, a statistical correlation is not sufficient to conclude mechanism. A correlation between neutralizing antibody titers and protection may suggest that neutralizing antibodies confer protection, but it does not confirm this, nor does it rule out protection mediated by non-neutralizing antibodies, cellular immunity, or a combination of multiple factors [677, 678]. However, correlation is often conflated with causation, and some scientists include causality in their definition of CoP for vaccines [679]. There is good reason in defining both correlation and mechanisms of protection, so I will explore both here.

It is also important to note that CoP and the mechanisms behind immunity depend on the way in which immunity is established. The mechanism by which natural infection may confer immunity may be different from vaccination, which may itself depend on vaccine composition. A great example of this comes from an Ebola virus (EBOV) vaccine study published by Stronsky *et al.* in which the authors evaluate various adjuvants for use in an EBO-VLP vaccine [680]. They found that

three adjuvants elicited very similar antibody responses to their vaccine and conferred full protection to EBOV challenge. However, only two conferred full protection to naïve mice via passive serum transfer indicating that the protection conferred by the third adjuvant likely involves cellular immunity. Therefore, while antibodies may be the ideal metric for evaluating the efficacy of the first two vaccine formulations, a metric of cellular immunity would likely be more appropriate for the third.

Neutralizing antibodies are considered the primary CoP for many pathogenic viruses including flaviviruses [206, 208-211, 655, 678, 681]. For some flaviviruses like yellow fever virus (YFV) and dengue virus (DENV), the correlation between neutralizing antibody titers and protection is well established [208, 682]. For others like tick-borne encephalitis virus (TBEV), the use of neutralizing antibody titer as a CoP for TBEV vaccines originates from the observation that neutralizing antibodies can protect lab animals from disease and not from experiments establishing a correlation in vaccinated animals or individuals [655]. In fact, evidence suggests that neutralizing antibody titers for TBEV underestimate protection in human vaccinees, underscoring the need to define more reliable CoP for tick-borne flaviviruses [683-687].

The prevalence of neutralizing antibody titers as CoP is likely at least somewhat attributable to the emphasis placed on humoral immune responses to

vaccines and the ease with which neutralizing antibody responses can be measured. This is certainly the case here given the neutralizing-antibody bias to the data presented in this dissertation. However, there is growing appreciation for the role of non-neutralizing antibodies and cellular immunity in protection, which are historically overlooked and should be kept in mind [677, 688, 689].

There are currently no defined CoP for POWV. In this chapter, I use the data generated elsewhere in this dissertation to probe whether binding or neutralizing antibody titers correlate with protection in our POWV vaccine-challenge mouse model and whether CoP depends on the adjuvant used. I also interrogate whether immunity is conferred via humoral or cellular immunity to help establish the mechanism of protection. I find that both binding and neutralizing antibody titers act as functional CoP for our POWV vaccine-challenge mouse model in an adjuvant-dependent manner.

Results

Anti-POWV IgG endpoint titers and FRNT50 values correlate with protection from lethal POWV challenge.

To identify whether binding or neutralizing antibody titers correlate with protection in the studies presented in this dissertation, I compiled IgG endpoint titers and FRNT50 values for 91 individual mice which 1) were prime-boost

vaccinated 2-3 weeks apart with 10^6 FFUe of wildtype POW-VLP either alone or adjuvanted with 11 μmol (300 μg) alum, 1nmol INI-2002, or 10nmol aqueous INI-4001; 2) had serum samples collected 2-3 weeks post-boost; 3) were challenged at 2-4 weeks post-boost with 10^3 FFU POWV; and 4) had paired survival data with time of demise. These data correspond to Figures 2.2A-C, S2.1, 3.1, and 4.2 and include both male (n = 61) and female (n = 30) mice.

Mice that survived POWV challenge had a significantly higher mean IgG endpoint titer (3.675 vs 2.239, $\log_{10}$) as well as median FRNT50 value (1.778 vs 0.000, $\log_{10}$) than non-survivors (Figure 5.1A-B). I generated receiver operating characteristic (ROC) curves for survival outcomes and either IgG endpoint titers or FRNT50 values to determine the utility of these metrics as predictors of survival. The AUC for these were ~0.80 for IgG endpoint titers and ~0.82 for FRNT50s, demonstrating that these metrics discriminate survivors from non-survivors quite well (Figure 5.1C-D). Using these curves, I calculate a Youden's J Index of 0.53 (sensitivity of 80%, specificity of 73%) for IgG titer and 0.63 (sensitivity 95%, specificity 68%) for FRNT50 values corresponding to cutoff titers of 3.08 and 1.35, respectively. This suggests that a cutoff of ≥ 1.35 for FRNT50 values will correctly identify 95% of survivors but misclassify 32% of non-survivors. In practical terms, most survivors have a neutralizing titer of ≥ 1.35, but about 1/3 non-survivors do as well, indicating that a modest neutralizing antibody titer is a good indicator for

survival but does not guarantee it. IgG endpoint titer is a less fit predictive metric, with a titer of ≥ 3.08 correctly identifying 80% of survivors but misclassifying 27% of non-survivors. I have represented these cutoffs as dashed lines in Figures 5.1A-B.

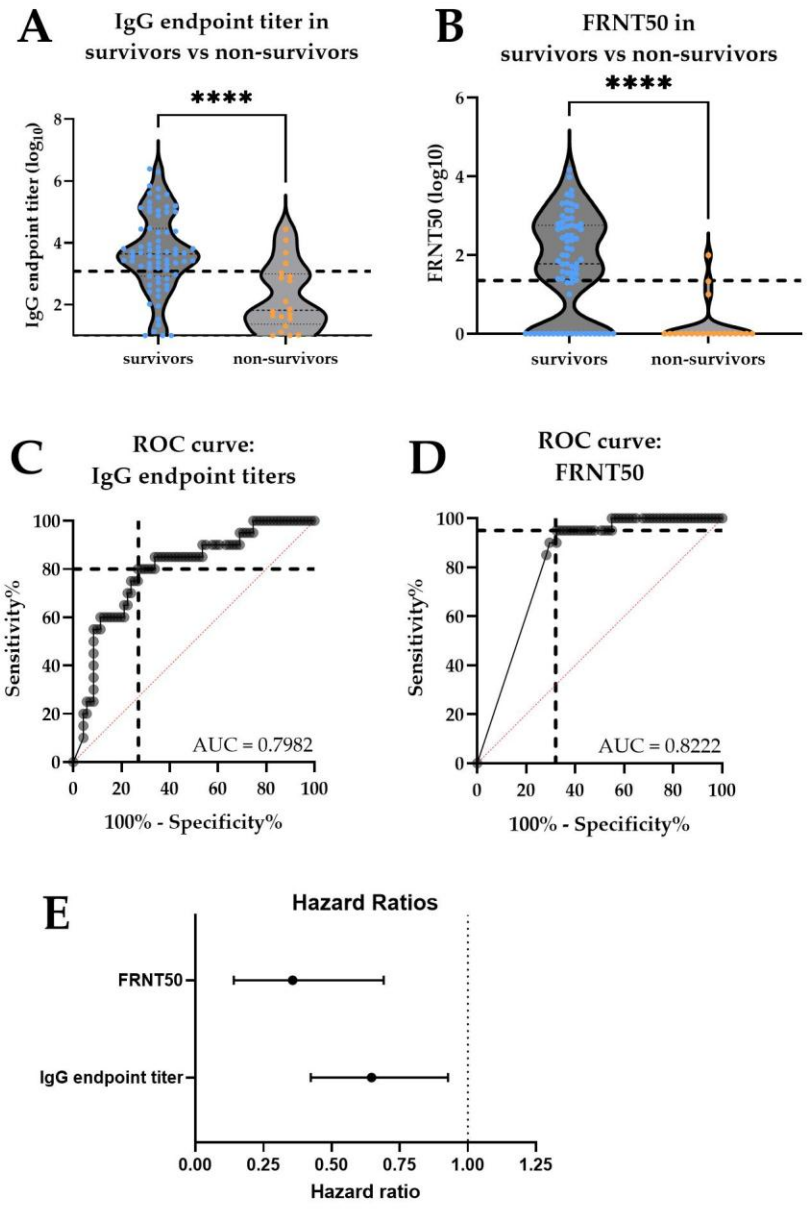

Figure 5.1: ELISA IgG endpoint titer and FRNT50 correlate with protection from lethal POWV challenge.

Male and female mice prime-boost vaccinated 2-3 weeks apart with 10^6 FFUe of wildtype POW-VLP either alone or adjuvanted with 11 μmol (300 μg) alum, 1nmol INI-2002, or 10nmol aqueous INI-4001. Serum samples collected 2-3 weeks post-boost. Mice challenged 2-4 weeks post-boost with 10^3 FFU POWV intraperitoneally. Survival monitored for 21 days post-challenge. Data represent multiple independent experiments also represented in Figures 2.2A-C, S2.1, 3.1, and 4.2. n = 91 mice total. **A-B:** Violin plots of IgG endpoint titers (A) and FRNT50 values (B) in survivors vs non-survivors. The black dashed lines represent the cutoffs corresponding to the Youden's J indices. Statistical significance determined by one-tailed Welch's t-test for A and a one-tailed Mann-Whitney test for B. **** = $p < 0.0001$. **C-D:** ROC curves generating from survival outcomes and IgG endpoint titers (C) or FRNT50 values (D). The red dashed line represents where the curve would fall if it were to have no discriminatory ability. The black dashed lines indicate the sensitivity and specificity corresponding to Youden's J indices. The AUCs are displayed in the bottom right of each graph. **E:** Forest plot of hazard ratios for death after POWV challenge shown with 95% confidence intervals.

To quantify the extent that binding and neutralizing antibodies are associated with reduced risk of death from POWV infection, I used multivariable Cox proportional hazards model. The hazard ratio for death is 0.65 per $\log_{10}$ increase in IgG endpoint titer (0.4240 to 0.9271 95% confidence interval) and 0.36 per $\log_{10}$ FRNT50 (0.1415 to 0.6910 95% confidence interval) (Figure 5.1E). Both

were significant, indicating that increases in binding and neutralizing titers are associated with a lower hazard of death. Together, these results demonstrate that binding and neutralizing antibody titers across vaccine groups correlate with protection but do not fully predict survival.

To determine if these correlations are adjuvant-dependent, I stratified data by those mice that received vaccine adjuvanted with alum, INI-2002, INI-4001, or unadjuvanted vaccine (VLP-alone). This stratification greatly reduces the sample sizes which affects the power of these statistical analyses. However, some conclusions can still be drawn. Only survivors from the INI-2002 group had both significantly higher mean binding and neutralizing antibody titers than non-survivors (Figure 5.2C&G). For alum-adjuvanted vaccine recipients, the differences in the mean binding and neutralizing titer between survivors and non-survivors were not significant, though they came very close at $p = 0.0611$ and $p = 0.0836$, respectively (Figure 5.2B&F). For unadjuvanted vaccine recipients, only the mean neutralizing antibody response was significantly different between survivors and non-survivors (Figure 5.2A&E). There were not enough non-survivors in the INI-4001 group to compare antibody responses with survivors (Figure 5.2D&H). Furthermore, while the FRNT50 value cutoff calculated from the ROC curves in Figure 5.1 seems to be fairly appropriate for predicting survival in for each group, the IgG endpoint titer cutoff does not and may be too influenced

by INI-4001-adjuvanted vaccine recipients to apply to the other groups (dashed lines). Together, these analyses confirm that both binding and neutralizing antibody responses are CoP for INI-2002-adjuvanted vaccine recipients, but that this may not extend to unadjuvanted or alum-adjuvanted vaccinees.

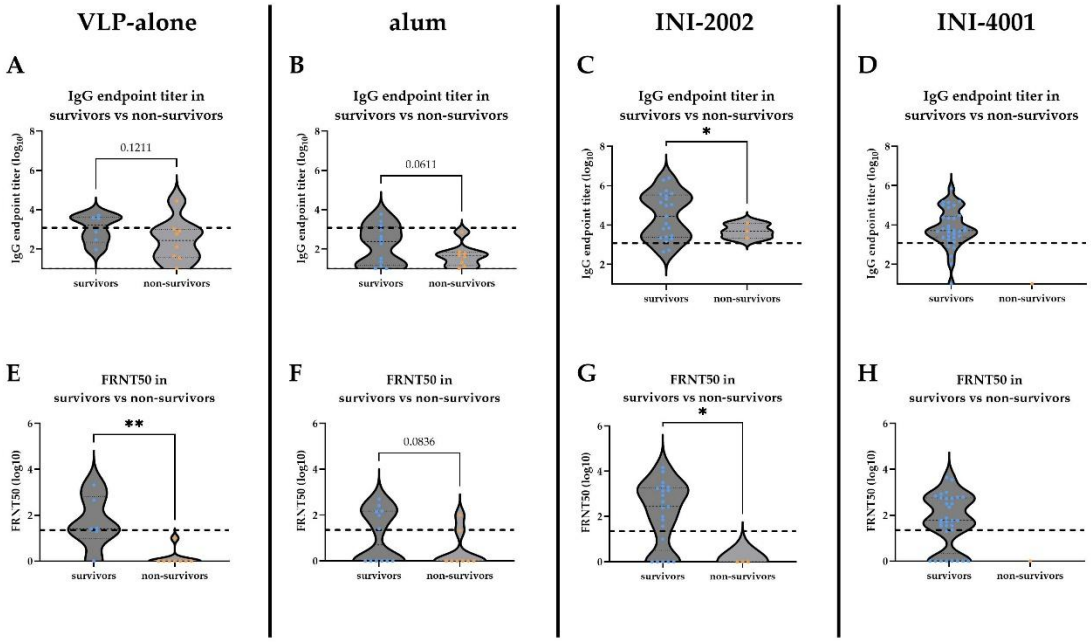

Figure 5.2: Correlation between antibody responses and survival varies by adjuvant.

Data from Figure 5.1 stratified by adjuvant. **A-H:** Violin plots of IgG endpoint titers (A-D) and FRNT50 values (E-H) in survivors vs non-survivors. The black dashed lines represent the cutoffs corresponding to the Youden's J Indices established in Figure 5.1. Statistical significance determined by one-tailed Welch's t-test for A-D and a one-tailed Mann-Whitney test for E-H. VLP-alone n = 14; alum n = 20; INI-2002 n = 24; INI-4001 n = 33. * = $p < 0.05$; ** = $p < 0.01$.

Protection is mediated by humoral immune responses.

Here, I will discuss the evidence that antibodies mediate protection in POW-VLP vaccinated mice. Data presented earlier in this dissertation (Chapter 2, Figures 2.3 p. 121, 2.4 p. 124, and S2.2 p. 153) demonstrate that the protection elicited by our INI-4001-adjuvanted vaccine is mediated by the humoral immune response as 1) it can be passively transferred via serum; 2) it is not affected by the absence of $CD4^+$ or $CD8^+$ T cells; and 3) there are no measurable T cell responses in vaccinated mice. Additional data from these experiments not presented in Chapter 2 extends this conclusion to alum- and INI-2002-adjuvanted vaccines as well (Figure 5.3A-C). In these experiments, there were no significant differences in survival for $CD4^+$ or $CD8^+$ T cell-depleted mice that received either alum-adjuvanted or INI-2002-adjuvanted vaccines (Figure 5.3A-B). This supports the conclusion that T cells do not play a critical role in protection for any vaccine group. It is notable, however, that only 1/5 mice in the CD4-depleted alum group survived infection compared to 3/5 in the isotype control. Repeating this experiment with more mice is warranted to improve the statistical power and confirm that $CD4^+$ T cells do not play a role in the protection elicited by alum-adjuvanted vaccine.

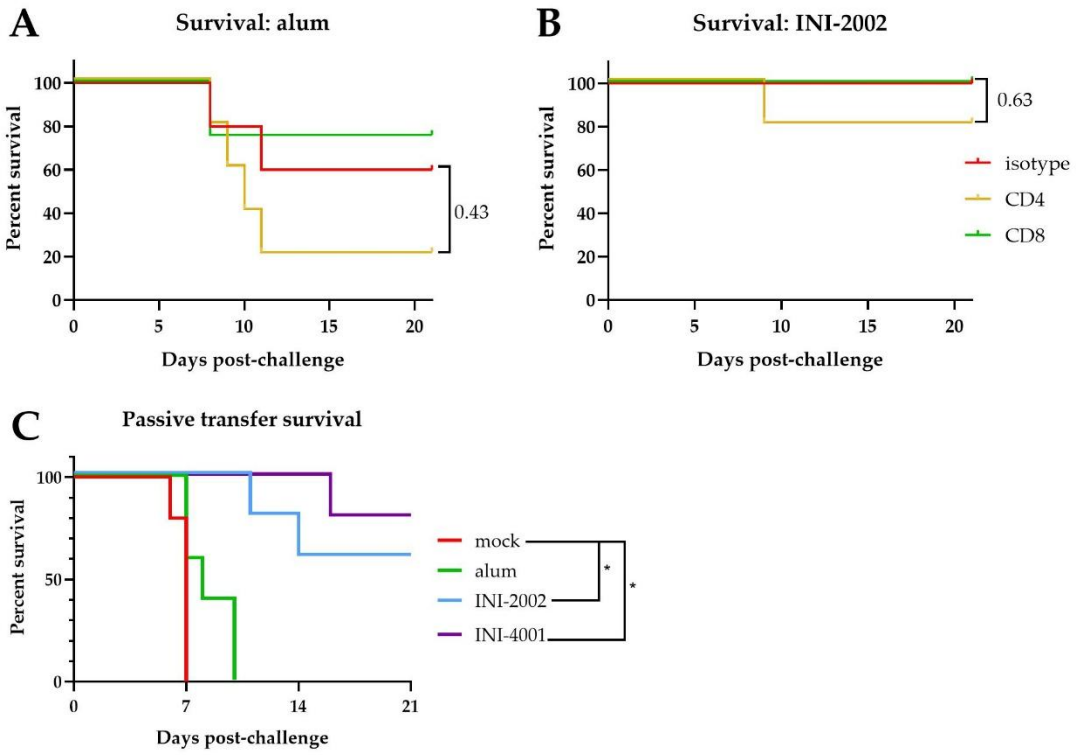
A
Survival: alum
Percent survival
Days post-challenge
0.43
B
Survival: INI-2002
Percent survival
Days post-challenge
0.63
isotype
CD4
CD8
C
Passive transfer survival
Percent survival
Days post-challenge
mock
alum
INI-2002
INI-4001
*
*

Figure 5.3: T cell depletion does not affect survival in alum- or INI-2002-adjuvanted vaccine recipients, and passive transfer of mouse sera from mice immunized with INI-2002-adjuvanted vaccine protects naïve mice from lethal challenge.

Mice were prime-boost vaccinated 3 weeks apart *sc* with 10^6 FFUe of POW-VLP adjuvanted either 11 μmol (300 μg) alum, 1nmol INI-2002, or 10nmol INI-4001. **A-B:** Mice for depletion were then treated *ip* with either 100 μg of either CD4-depleting, CD8-depleting, or non-depleting isotype control (n=5/group) 3 weeks post-boost and again three days later. Mice were challenged with a lethal 10^4 FFU dose of POWV-LB *ip* at time of second depletion. Blood was collected by tail vein 3 days after second administration of depleting antibodies to confirm T cell depletion (representative flow plots of T cells shown in Figure 2.4 on page 124). Survival and weights of mice monitored to day 21 endpoint post-challenge. Survival of vaccinated mice after depletion of either $CD4^+$ (yellow) or $CD8^+$ (green) T cells compared to isotype control (red). Statistical significance determined by log rank test with Bonferroni correction to compare depleted groups to isotype control. No significant differences were found; p-values shown on graph. Data here and in Figure 2.4 represent one experiment. **C:** Unvaccinated mice received 200uL of pooled sera from vaccinated mice *ip* one day before *ip* infection with 10^4 FFU POWV-LB. Survival monitored for 21 days post-challenge. Statistical significance determined by log rank Mantel-Cox test to compare vaccinated animals to mock. * = $p < 0.05$. Data here and in Figure 2.3 (page 121) represent single experiment.

Naïve mice that received pooled sera from INI-2002-vaccine recipients were significantly more likely to survive challenge than those that received pooled sera from naïve mice, further supporting the conclusion that protection is mediated via

humoral immunity (Figure 5.3C). However, this was not the case with alum. This may be because 200μL of serum is too little to confer protection in a group with the lowest antibody responses. Alternatively, this may allude to a difference in the protection elicited by the alum-adjuvanted vaccine. The lack of protection via passive transfer and the trend towards less protection in the $CD4^+$ T cell-depleted alum group suggests that a memory response such as a memory B cells response may be important for this adjuvant. Such a response does not appear to be critical to protection for either INI-2002 or INI-4001 as demonstrated by passive transfer. More experiments are needed to fully assess the role of memory responses in the protection elicited by alum.

Discussion

These analyses demonstrate correlation between protection and both whole-virus binding IgG ELISA endpoint titers and FRNT50 values in our POWV vaccine-challenge model. Together with mechanistic evidence that humoral-mediated responses are sufficient for protection from lethal POWV challenge, these findings support the use of binding and especially neutralizing antibody responses as CoP for POWV. The associations are not perfect, however, and additional work is needed to determine whether memory B cell or non-

neutralizing antibody responses may help better predict survival in vaccinated mice with weak or undetectable binding or neutralizing antibody responses.

Importantly, the protection elicited by vaccination appears to be influenced by adjuvant. The analyses I present here suggest that binding and neutralizing antibody responses are best applied as CoP for INI-2002-adjuvanted vaccine recipients and may not be as applicable to those that receive alum-adjuvanted vaccine. Alum may confer protection through a distinct mechanism. More work is needed to explore this possibility and how this may influence CoP for alum-adjuvanted vaccine recipients.

Materials & Methods

Mouse experiments

5-week old male or female C57BL/6 mice were purchased from Jackson Laboratory and housed in an ABSL-3 facility at Oregon Health & Science University's (OHSU) Vaccine and Gene Therapy Institute accredited by the Association for Accreditation and Assessment of Laboratory Animal Care (AALAC) in compliance with protocols approved by the OHSU's Institutional Animal Care and Use Committee (IACUC) #1432. All experiments were performed with male mice unless otherwise stated.

Primary vaccinations were administered at 7-weeks of age subcutaneously (*sc*) in the dorsal region using 10^6 FFU equivalents of POW-VLP and either 11μmol of Alhydrogel 2% adjuvant, 1nmol of INI-2002, or 10nmol of INI-4001 diluted to a final volume of 100uL in sterile injection-grade PBS. INI-2002 and INI-4001 were synthesized as described by Miller *et al.* [572]. The concentrations of INI-4001 and INI-2002 were determined by RP-HPLC according to a previously published method [575]. Aqueous formulations of both were prepared as described by Crawford *et al.* [665]. Mock-vaccinated mice received 100uL of PBS alone. Boost-vaccinations were administered 2- to 3-weeks post-primary vaccination in the same manner. Blood was collected by tail-vein 2- to 3-weeks post-vaccination and left to clot at room-temperature for 30 minutes before centrifugation twice at 10,600 x *g* to collect the serum. Serum was then stored at -20°C until use.

For lethal challenge infections, 10^3 or 10^4 FFU of POWV LB was diluted into 100uL sterile PBS and injected subcutaneously (*sc*) or intraperitoneally (*ip*) 2- to 4-weeks post-boost. Mice were monitored for up to three weeks for signs of morbidity including piloerection, hunched posture, ataxia, malaise, paralysis, and weight loss. Moribund mice were defined as those that experienced substantial weight loss ≥ 20% original body weight, paralysis, and/or other signs of morbidity. Moribund mice were euthanized by isoflurane followed by cervical dislocation to limit suffering.

Passive transfer

Mice were vaccinated as described in "Mouse experiments" with either alum-, INI-2002-, or INI-4001-adjuvanted vaccine or PBS alone. Sera were collected 3 weeks post-boost, pooled within each group, and heat-treated at 55°C for 30 minutes to inactivate complement. 200μL of pooled serum was passively transferred *ip* to unvaccinated mice. Mice were then challenged with 10^4 FFU of POWV LB *ip* the day after passive transfer and monitored for three weeks for signs of morbidity and survival.

T cell depletion and flow cytometry

Mice were vaccinated as described in "Mouse experiments". At both days 19- and 21-post boost-vaccination, 100 μg of either CD4-depleting antibody (Clone GK1.5 IgG2b Fisher), CD8-depleting antibody (Clone 2.43 IgG2b Fisher), or non-depleting isotype control (Clone LTF-2 Fisher) was administered *ip*. Mice were then challenged with 10^4 FFU of POWV LB as described in "Mouse experiments". To confirm depletion, 100μL of blood was collected by tail vein 3 days post-infection into 500uL of 100mmol EDTA (Invitrogen), washed with FACS buffer (PBS with 5% FBS and 1mM EDTA), and stained with CD45 AlexaFluor 700 (BioLegend rat anti-mouse clone 30-F11 Cat#103218), CD3 BUV395 (BD Horizon

rat anti-mouse Clone 17A2 (RUO) Cat#: 569614), CD19 PE (BioLegend rat anti-mouse clone 1D3/CD19 Cat#: 152408), CD4 V450 (BD Horizon rat anti-mouse clone: RM-4-5 Cat#: 560468), and CD8b PerCP/Cy5.5 (BioLegend rat anti-mouse clone YTS156.7.7 Cat#: 126609) for 30 minutes at room temperature. Cells were then washed and fixed using RBC lysis/fixation solution (BioLegend #422401) for 10 minutes, washed, and resuspend in FACS buffer. Cells were then analyzed by flow cytometry using a BD FACSymphony Spectral Cell Analyzer. T cells were gated as CD45+ CD3+ CD19-.

Cells

HEK293T and Vero E6 cells were maintained in Dulbecco's Modified Eagle Medium (DMEM) (Corning) supplemented with 5% fetal bovine serum (FBS; HyClone #3039603), 100U/mL penicillin, 100 μg/mL streptomycin, and 292 μg/mL L-glutamine (Gibco #10378016). Cells were passaged using trypsin 0.05% EDTA (Gibco #25-300-120).

VLP production

The generation of HEK293 cells expressing POWV prM-E was described previously [609]. To produce POW-VLP, HEK293-POWV-prME cells were cultured with 1μg/mL doxycycline in DMEM supplemented with 2% FBS,

100U/mL penicillin, 100 μg/mL streptomycin, and 292 μg/mL L-glutamine. Supernatant was collected 4 days post-induction, centrifuged at 1,000 x *g* for 10min, and filtered through a 0.45μm to remove cellular debris. VLPs were then concentrated and purified by ultra-centrifugation through a 20% sorbitol 50mM Tris 1mM $MgCl_2$ pH 8.0 buffer at 150,000 x *g* for 2 hours at 4°C. Pellets were then resuspended in 1/100th of the original volume with 10mM Tris 150mM NaCl buffer supplemented with 5% trehalose for protein stability and stored at -80°C until use. For quantification, see "ELISA" methods below.

Virus

POWV LB was generously provided by Michael S. Diamond (Washington University School of Medicine, St. Louis, MO). POWV was propagated on Vero E6 cells for 7 days [658]). Supernatant was collected, centrifuged at 1,000 x *g* for 10min, and filtered through a 0.45μm to remove cellular debris. Virus was then concentrated and purified by ultra-centrifugation through a 20% sorbitol 50mM Tris 1mM $MgCl_2$ pH 8.0 buffer at 150,000 x *g* for 2 hours at 4°C. Pellets were then resuspended in 1/100th of the original volume in DMEM with 0.1% FBS and stored at -80°C until use. Viruses were titered using limited dilution focus forming assay on Vero cell monolayers. Briefly, cells were infected by rocking for 1 hour at 37°C in 5% CO_2. Cells were then overlaid with a formula consisting of 2 parts DMEM

with 5% FBS, 100U/mL penicillin, 100 μg/mL streptomycin, and 292μg/mL L-glutamine and 1 part 1% high / 1% low viscosity carboxymethylcellulose (CMC) diluted in a 60% PBS aqueous solution. Cultures were then aspirated and fixed at 48 hours post-infection with 4% paraformaldehyde for 30 minutes. Staining protocol to visualize foci was then performed as described in "Focus reduction neutralization test (FRNT)" section of methods. Foci were counted using AID Elispot 7.0 (Autoimmun Diagnostika GMBH) and titers were determined from these numbers.

Enzyme-linked immunosorbent assay (ELISA)

To titer whole virus binding antibodies, Corning Costar Brand 96-Well EIA/RIA plates (ThermoFisher) were coated with 10^5 FFU of POWV purified through a sorbitol cushion as described in "Viruses" methods above and resuspended in PBS containing 0.1% FBS for stabilizing particles. Virus was plated in 100μL PBS per well overnight at 4°C. Plates were then washed with PBS 0.05% Tween 20 (ThermoFisher) and blocked in wash buffer with 5% milk (Safeway). Serum complement was heat inactivated at 55°C for 30 minutes and serially diluted in blocking buffer with the least dilution of 1:50. Sera dilutions were then incubated on ELISA plates for 1.5 hours at room temperature. These were then washed and stained with anti-mouse IgG (γ-chain specific)−peroxidase antibody

(MilliporeSigma #A3673) diluted 1:10,000 in wash buffer for 1 hour at room temperature. Secondary antibody was then washed and replaced with 100μL of 4μg/mL o-Phenylene diamine in a buffer of 50mM citric acid 100mM dibasic sodium phosphate 0.01% hydrogen peroxide pH 5.0 for 10 minutes before color change reaction was stopped with equal amount of 1M HCl. Absorbance at 490nm was measured using BioTek Synergy HTX Multimode Reader and Gen5 Microplate Reader and Imager Software v3.11 (Agilent). Background absorbance was defined as the lowest absorbance value on a plate and subtracted from each well. Linear regression curves were fit using Microsoft Excel INTERCEPT and SLOPE functions to determine endpoint titer defined as when absorbance was 0.1, a baseline absorbance not exceeded by negative controls (Figure S2.6, page 157). Values < 1 were adjusted to an endpoint titer = 1 for analyses.

To titer VLPs, plates were coated similarly to assay described above, but with serially diluted VLP alongside POWV of known titer. Plates were blocked and washed as described and stained for 1 hour at room temperature with T077 anti-E antibody (described in the next section) followed by 1 hour with monkey IgG gamma peroxidase-conjugated antibody (Rockland #617-103-012). Endpoint titers were calculated in the same manner as described previously, and these were used to determine the FFUe of VLP using the known FFU of POWV as standard.

Focus reduction neutralization test (FRNT)

Serial dilutions of sera were prepared in DMEM with 2% FBS and incubated with POWV for 1 hour at 37°C to allow for antibody binding. Serum treated virus was then used to infect monolayers of Vero cells and overlaid with CMC as described previously in "Viruses". The least dilute serum used to neutralize virus was 1:50. Cells were then fixed with 4% paraformaldehyde at 48 hours post-infection for 30 minutes, blocked and permeabilized in PBS with 2% goat serum (ThermoFisher) and 0.4% Triton X-100 (ThermoFisher). Cells were then stained with T077, a monoclonal antibody from a TBEV-infected individual sequenced and characterized by Agudelo *et. al* that binds both POWV [218]. We cloned the T077 heavy and light variable chain sequences into pcDNA-3-RhIgG1 and -RhIgK, respectively, for antibody production in Expi293 cells. POWV foci were then visualized by secondary staining with monkey IgG gamma peroxidase-conjugated antibody (Rockland) diluted 1:1,000 in blocking buffer followed by Vector VIP Substrate Peroxidase (HRP) Kit (Vector Laboratories SK-4600) after washing. Foci were counted using AID Elispot 7.0 (Autoimmun Diagnostika GMBH) and reciprocal FRNT50s determined by non-linear regression analysis with a variable slope on GraphPad Prism v10.2.2. Samples with no measurable neutralizing activity were assigned 0.

Data processing and statistical analyses

All appropriate analyses were performed using GraphPad Prism v10.6.1.

Chapter 6: Summary, conclusions, and future directions

Section 6.1: Summary and conclusions

Evaluation of adjuvant

In Chapter 2, we demonstrate the effectiveness of the novel synthetic TLR7/8 agonist INI-4001 as an adjuvant for a low-dose POW-VLP vaccine. INI-4001 improves the magnitude, breadth, and durability of the vaccine response and fully protects mice from both lineages of POWV. We further show that this protection is mediated by humoral immunity. The superiority of INI-4001 over both the TLR4 agonist INI-2002 and traditional alum appears to be specific to this low-dose (10^6 FFUe of VLP) vaccine platform, as single high dose (1.5×10^7 FFUe) is fully protective 3 weeks post-boost for every adjuvant group. This highlights the ability of INI-4001 to elicit a protective immune response to small amounts of antigen which is a desirable trait in vaccine manufacturing. More work is needed to evaluate the comparative utility of these adjuvants in the context of a single high dose POW-VLP vaccine. It would be interesting to see whether the superiority of INI-4001 in eliciting durable, broad antibody responses is also restricted to the context of low-dose, prime-boost vaccination. Additionally, it will be necessary to evaluate the utility of adjuvant combinations such as INI-4001 + alum which have

proven effective for other vaccine platforms (see section 1.3.8, page 86). Work is underway to address the mechanisms by which INI-4001 elicits such a robust immune response by comparing the cellular responses to alum, INI-2002, and INI-4001 in the draining lymph nodes of vaccinated mice using single-cell RNA sequencing.

Evaluation of formulation

In Chapter 3, we demonstrated that formulating our INI-4001-adjuvanted POW-VLP vaccine with cationic liposomes or AS03-like emulsion improves the neutralizing antibody response. Additionally, all lipid formulations, regardless of INI-4001 adjuvantation, further reduced the presence of POWV in various tissues and cytotoxic effector cells in the brains of POWV-challenged mice relative to aqueous INI-4001 alone. This suggests that the immunostimulatory properties of both cationic liposomes and AS03-like emulsion are effective on their own at improving our POW-VLP vaccine. However, the addition of INI-4001 improved several features of the vaccine response. AS03-like emulsion formulated with INI-4001 proved particularly effective at improving the breadth of the antibody response over aqueous INI-4001 alone by eliciting cross-binding antibodies to POWV-II and LGTV and neutralizing antibodies to POWV-II. This alludes to a synergy between INI-4001 and the immunostimulatory components of AS03 that

likely improves germinal center B cell responses. INI-4001-formulated cationic liposomes also demonstrated great potential as a new formulation for our vaccine by improving POWV-I neutralizing antibody titers and rendering POWV RNA undetectable in all tissues tested post-challenge. Liposome alone was unable to achieve this level of protection in the spleen despite there being no measurable differences in the anti-POWV-I antibody responses these formulations elicit. This is likely due to the INI-4001 enhancing T_H1 immunity and cytotoxic T cell responses, but this remains to be tested. Evaluating the Fc-mediated functions of the antibody responses to these new formulations would be important to determine whether non-neutralizing antibody activity is playing a critical role in the phenotypes observed in this study.

Evaluation of antigen

In Chapter 4, we demonstrate that POW-VLP produced by ectopic expression of prM-E in HEK293T cells produces immature particles while POWV propagated on Vero cells is more mature. We find that the difference in maturity is due to ectopic expression vs infection and not cell type. More work is needed to investigate whether the co-expression of other flaviviral proteins such as C or the non-structural proteins can enhance maturity in our POW-VLP system.

We further demonstrate that more mature POW-VLP does not improve the protective efficacy of our vaccine, but that the omission of prM may in fact reduce protection. This likely reflects a key difference in the infectivity of immature TBFVs compared to MBFVs. Recent research has shown that furin activity after particle egress can influence TBFV particle maturity. It remains to be seen whether immature TBF-VLPs such as POW-VLPs may be rendered mature after vaccination and how this might influence the immune response to prM. Parallel experiments evaluating the effect of VLP maturity on vaccine responses to MBFVs vs TBFVs are necessary to draw any conclusions. These experiments would ideally evaluate the effects of generating immature particles on furin-deficient vs NH_4Cl-treated cells as well as the effects of generating mature particles using furin overexpression vs furin cleavage site mutagenesis.

Correlates of protection

In Chapter 5, we demonstrate correlation between antibody titers (both binding and neutralizing) and protection from lethal POWV challenge in our mouse model. These analyses alongside the mechanistic evidence that humoral immune responses mediate the protection elicited by our various vaccine formulations support the use of binding and neutralizing antibody titers as correlates of protection for POWV. However, antibody titers are not perfectly

predictive of survival, and correlation with protection varies by adjuvant. More work is needed to evaluate other metrics as possible correlates of protection including memory B cell and non-neutralizing antibody responses.

Section 6.2: Future directions

Adjuvant mechanism of action

We are currently interrogating the mechanisms by which INI-4001 elicits such a robust immune response by comparing the cellular responses to alum, INI-2002, and INI-4001 in the draining lymph nodes of vaccinated mice using single-cell RNA sequencing. Though this data is not ready for presentation here in this dissertation, preliminary results suggest that INI-4001 uniquely elicits a robust IFN-I response. This finding is not unexpected, as TLR7 is most active in pDCs which are known to produce large amounts of IFN-I. This result led us to evaluate the role of IFN-I in the vaccine response to INI-2002 and INI-4001. For this, 500μg of either anti-IFNAR MAR1-5A3 or isotype control antibody were administered intraperitoneally (ip) the day before prime and boost vaccination with either INI-2002- or INI-4001-adjuvanted POW-VLP. Prime and boost vaccinations were administered 3 weeks apart. Serum samples collected 3 weeks post-prime and 3 weeks post-boost were used to quantify anti-POWV IgG and neutralizing antibody titers by whole-virus binding ELISA and FRNT, respectively. While anti-

IFNAR treatment significantly reduced the neutralizing antibody response to vaccine adjuvanted with INI-2002 pre-boost and nearly significantly reduced the IgG response at this timepoint as well, there was no significant difference to the post-boost titers (Figure 6.1A-D). In contrast, anti-IFNAR treatment abolished the binding and neutralizing antibody response to the vaccine adjuvanted with INI-4001. Interestingly, there were no measurable antibody responses to the INI-4001-adjuvanted vaccine at the pre-boost timepoint in control mice, revealing a difference in the kinetics of the immune responses to INI-2002 and INI-4001. INI-2002 appears to elicit a very rapid immune response after a single vaccine dose, while INI-4001 requires boosting.

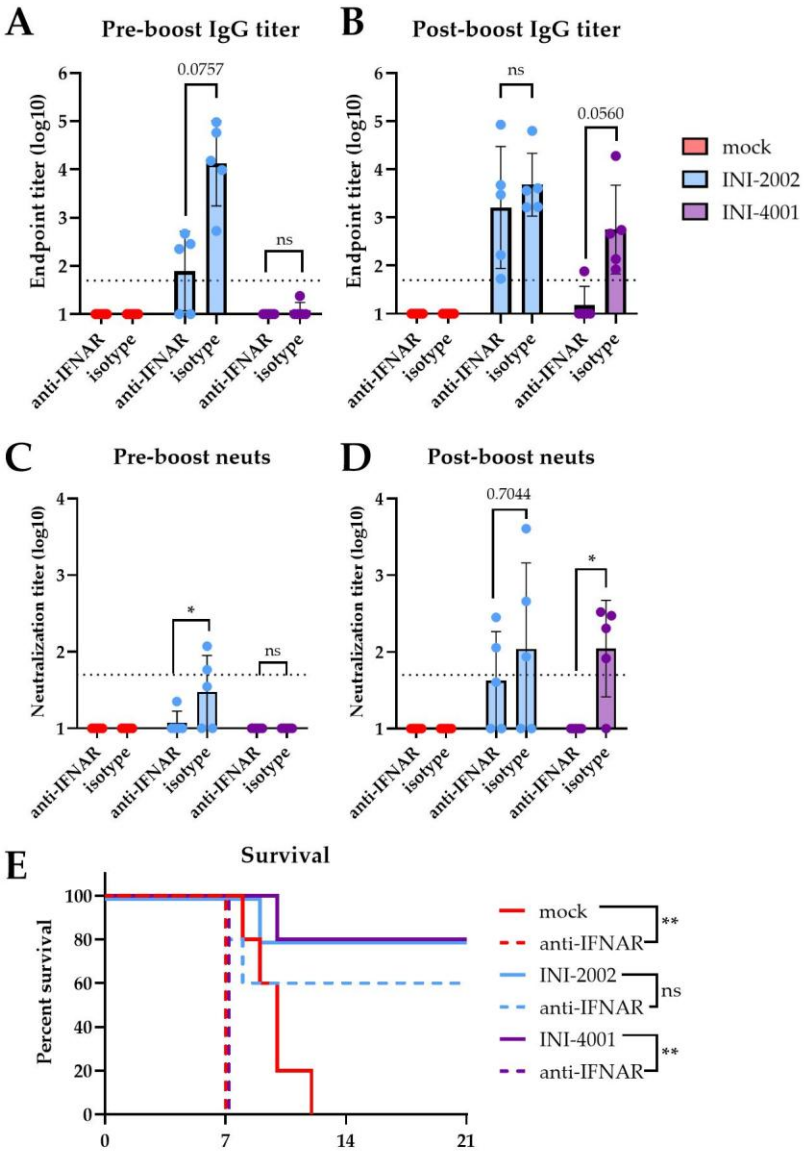
A
Pre-boost IgG titer
Endpoint titer (log10)
0.0757
ns
anti-IFNAR
isotype
B
Post-boost IgG titer
ns
0.0560
mock
INI-2002
INI-4001
C
Pre-boost neuts
Neutralization titer (log10)
*
ns
D
Post-boost neuts
0.7044
*
E
Survival
Percent survival
mock
anti-IFNAR
INI-2002
INI-4001
**
ns

Figure 6.1: IFNAR blockade significantly abolishes INI-4001 vaccine response.

Mice prime-boost vaccinated 3 weeks apart sc with 10^6 FFUe of POW-VLP adjuvanted with either INI-2002 or INI-4001. Mock group injected with PBS vehicle alone. Anti-IFNAR MAR1-5A3 antibody or isotype control administered ip 1 day prior to each vaccination. n = 5 per vaccine/treatment group. Sera collected 3 weeks post-prime (A&C) just prior to booster dose, and 3 weeks post-boost. Sera analyzed by whole-virus ELISA (A-B) and FRNT (C-D). **A-B:** Data reported as log-transformed IgG endpoint titers ± SD. **C-D:** Data reported as log-transformed reciprocal FRNT50 ± SD. **A-D**: Statistical significance determined by Kruskal-Wallis test with Dunn's multiple comparisons test to compare anti-IFNAR treatment to isotype within the INI-2002 and INI-4001 vaccine groups. **E:** Mice challenged with a lethal 10^3 FFU POWV-LB ip 4 weeks post-boost. Survival assessed to day 21 post-challenge. Statistical significance determined by log rank test with Bonferroni correction to compare anti-IFNAR to isotype treatment within each vaccine group. ns – not significant ($p > 0.9999$); *$p < 0.05$; **$p < 0.01$. All data represent single experiment. See Chapter 2 Materials & Methods (page 138) for more information.

Mice were challenged with a lethal dose of POWV (10^3 FFU) sc 1 week post-boost and monitored for disease and survival for 3 weeks. Anti-IFNAR treatment did not significantly affect the survival of mice in the INI-2002 vaccine group (Figure 6.1E). In contrast, anti-IFNAR treatment of mice in the INI-4001 vaccine

group eliminated the protective efficacy of the vaccine, with all mice succumbing to infection compared to only 1/5 mice succumbing in the control group. It appears that anti-IFNAR treatment significantly affected the survival of mock mice, decreasing the median survival time from 10 days to 7. This is apparent in the INI-4001 vaccine experimental group as well. This phenomenon may be due to lingering anti-IFNAR antibody 4 weeks post-treatment or secondary effects of the treatment that left mice more vulnerable to challenge.

Together, these data demonstrate kinetic and mechanistic differences to the vaccine responses elicited by INI-2002 and INI-4001. The INI-4001-adjuvanted vaccine depends entirely on the IFN-I response and boosting. In contrast, the post-boost vaccine response to INI-2002 appears to depend on neither, though the pre-boost response is reduced by IFNAR blockade indicating partial dependence. Further analysis of the single-cell RNA sequencing data is forthcoming and will determine the future directions for this project.

Evaluation of antigen uptake

One crucial function of vaccine adjuvants and formulations is to influence antigen retention at the site of injection as well as antigen uptake. To study the effects of INI-2002, INI-4001, and lipid-based formulations on antigen uptake, we

generated FITC-labeled POW-VLPs to assess antigen trafficking post-vaccination (Figure 6.2A-B). We have confirmed that FITC-VLP can be used to evaluate antigen uptake *in vitro* using the mouse dendritic cell line DC2.4 (Figure 6.3). The next step is to use FITC-VLP to evaluate how vaccine adjuvant and formulation affect retention and uptake of POW-VLP *in vivo*.

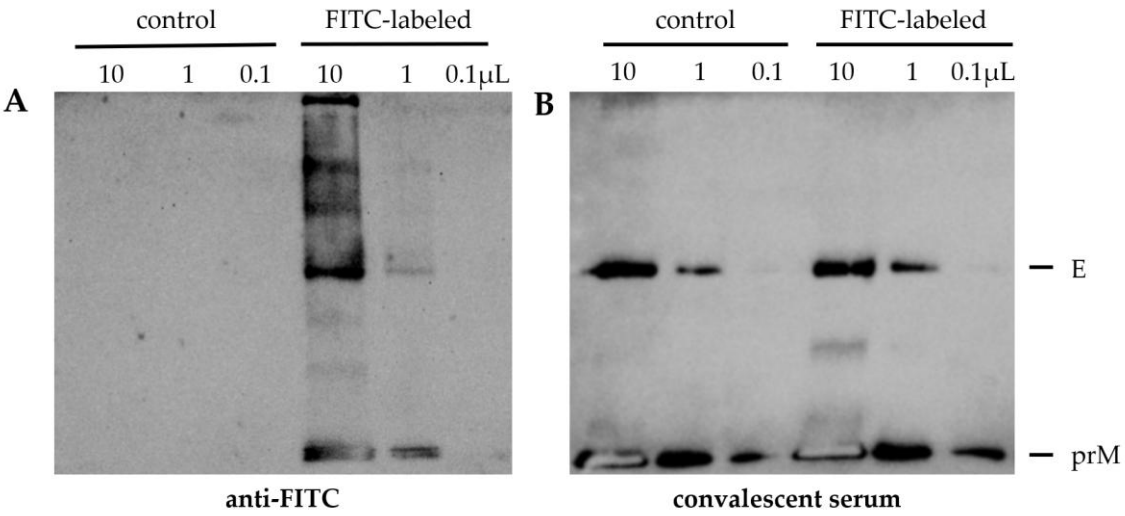

Figure 6.2: The generation of FITC-labeled POW-VLP.

FITC-labeled POW-VLPs were generated in parallel to unlabeled control VLPs as described elsewhere in this dissertation (page 144) with slight modification. Briefly, pelleted VLP was resuspended in 0.1M carbonate-bicarbonate pH 9.0 buffer with or without 0.1mM FITC for 2 hours at room temperature before dialyzing into standard 10mM Tris 150mM NaCl buffer. **A-B:** Western blots of 10, 1, or 0.1μL of FITC-labeled or control un-labeled POW-VLP stained with (A) anti-FITC antibody (ThermoFisher MA5-14709) or (B) convalescent mouse serum to stain prM and E (serum produced described page 217).

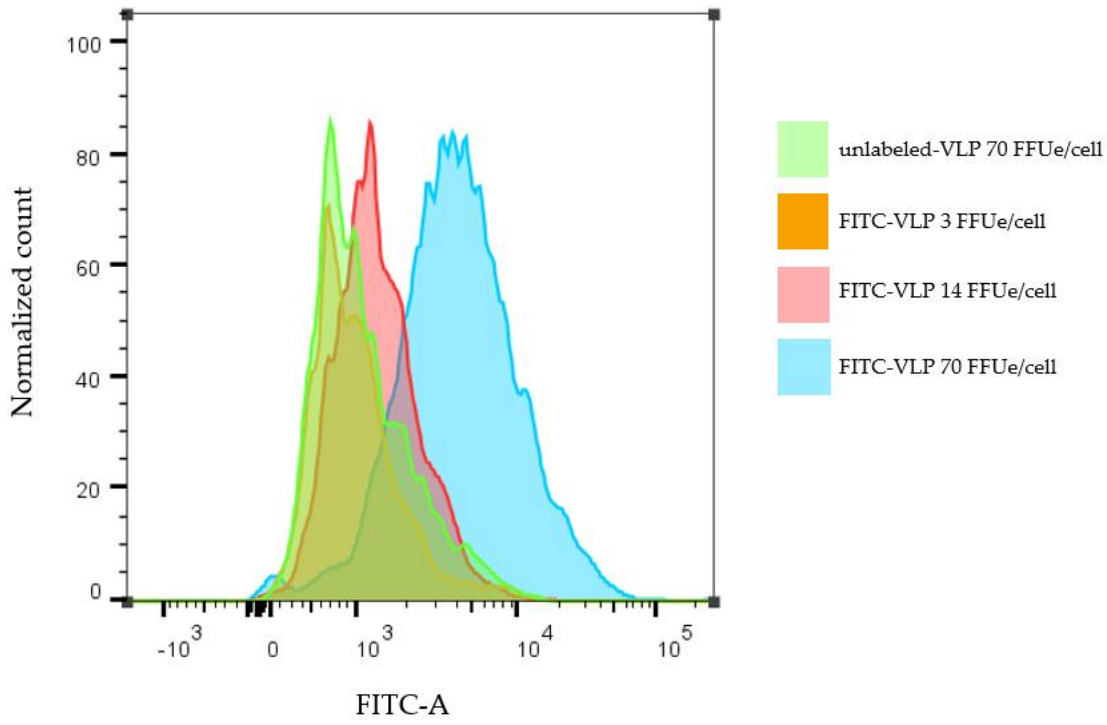

Figure 6.3: Dose-dependent antigen uptake in DC2.4.

DC2.4 cells were incubated with FITC-labeled POW-VLP or unlabeled control VLP for 4 hours. Cells were then trypsinized, washed with FACS buffer, fixed in 4% PFA for 15min, and washed once more before resuspension in FACS buffer. Cells were then analyzed by flow cytometry as described on page 237. Figure is a normalized histogram showing FITC fluorescence intensity of cells incubated with approximately 70 FFUe/cell (in blue), 14 FFUe/cell (in pink), or 3 FFUe/cell (in orange) FITC-labeled VLP or 70 FFUe/cell of control unlabeled VLP (in green).

Evaluation of B cell responses

We hypothesize that many of the differences we observe between the vaccine responses to INI-2002, INI-4001, and lipid-based formulations are caused by differences in vaccine induced germinal center B cell responses. Future

experiments to evaluate the size and frequency of germinal centers in draining lymph nodes of vaccinated mice are needed to test this. These POWV-specific B cell responses can be monitored using the FITC-labeled POWV-VLPs discussed above. Isolation of POWV-specific B cells would allow for the evaluation of clonal responses and affinity maturation using BCR sequencing. We have already confirmed that these particles stain lymphocytes from POW-VLP-vaccinated mice (Figure 6.4). Interestingly, these particles stain both B cells and T cells in the blood of vaccinated animals at extremely high proportions, but not B or T cells from control animals. As T cells would not be expected to bind POW-VLP outside the context of peptide presentation on MHC, this suggests these particles are not just staining POWV-specific lymphocytes. The high proportion of lymphocytes stained post-vaccination after the immune system has been stimulated by INI-4001 suggests that FITC-VLPs are binding a factor on lymphocytes that is upregulated by vaccination. The expression of TAM, a known flavivirus receptor, is mediated by IFN-I responses and can be found on activated B and T cells [14, 17, 690, 691]. Using anti-TAM monoclonal antibody to block possible VLP-TAM interactions may be used to both 1) evaluate TAM as a candidate receptor involved in POWV attachment/entry and also 2) render this B cell staining assay functional for the isolation of anti-POWV B cells.

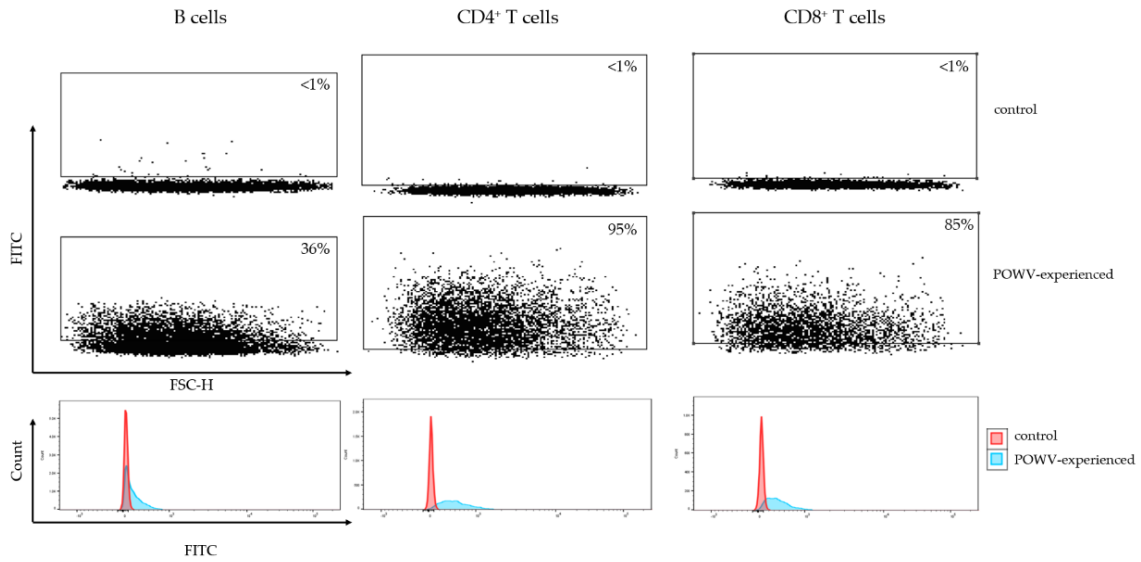

Figure 6.4: B and T cell staining using FITC-labeled POW-VLP.

Whole mouse peripheral blood mononuclear cells (PBMCs) from a naïve mouse (red) or an INI-4001-adjuvanted POW-VLP vaccinated mouse (blue; vaccination method described on page 138) stained with FITC-labeled POW-VLP and fluorescent antibodies against CD45, CD3, CD19, CD4, and CD8b (methods described on page 237). Cells gated as lymphocytes by SSC and FSC, singlets (using both SSC and FSC), and CD45+. B cells gated as CD3- and CD19+. $CD4^+$ T cells gated as CD3+ CD4+ CD8-. $CD8^+$ T cells gated as CD3+ CD4- CD8+. Percentage of $FITC^+$ cells represented in dot plots with threshold determined by control naïve mouse. Y-axis represents FITC-A intensity and is aligned across all graphs. Lower row of histograms represent FITC-A intensity by cell count.

References

1. Acheson, N.H., *Fundamentals of molecular virology*. 2nd ed. 2011, Hoboken, NJ: John Wiley & Sons. xxv, 500 p.
2. Postler, T.S., et al., *Renaming of the genus Flavivirus to Orthoflavivirus and extension of binomial species names within the family Flaviviridae.* Arch Virol, 2023. **168**(9): p. 224.
3. Blitvich, B.J. and A.E. Firth, *A Review of Flaviviruses that Have No Known Arthropod Vector.* Viruses, 2017. **9**(6).
4. Halabi, K. and I. Mayrose, *Mechanisms Underlying Host Range Variation in Flavivirus: From Empirical Knowledge to Predictive Models.* J Mol Evol, 2021. **89**(6): p. 329-340.
5. Rathore, A.P.S. and A.L. St John, *Cross-Reactive Immunity Among Flaviviruses.* Front Immunol, 2020. **11**: p. 334.
6. Calisher, C.H., et al., *Antigenic relationships between flaviviruses as determined by cross-neutralization tests with polyclonal antisera.* J Gen Virol, 1989. **70 (Pt 1)**: p. 37-43.
7. Haddow, A.D., et al., *Genetic characterization of Zika virus strains: geographic expansion of the Asian lineage.* PLoS Negl Trop Dis, 2012. **6**(2): p. e1477.
8. Barrows, N.J., et al., *Biochemistry and Molecular Biology of Flaviviruses.* Chem Rev, 2018. **118**(8): p. 4448-4482.
9. Filomatori, C.V., et al., *A 5′ RNA element promotes dengue virus RNA synthesis on a circular genome.* Genes Dev, 2006. **20**(16): p. 2238-49.
10. Clyde, K. and E. Harris, *RNA secondary structure in the coding region of dengue virus type 2 directs translation start codon selection and is required for viral replication.* J Virol, 2006. **80**(5): p. 2170-82.
11. Bidet, K. and M.A. Garcia-Blanco, *Flaviviral RNAs: weapons and targets in the war between virus and host.* Biochem J, 2014. **462**(2): p. 215-30.
12. Khromykh, A.A., et al., *Essential role of cyclization sequences in flavivirus RNA replication.* J Virol, 2001. **75**(14): p. 6719-28.
13. Hilgard, P. and R. Stockert, *Heparan sulfate proteoglycans initiate dengue virus infection of hepatocytes.* Hepatology, 2000. **32**(5): p. 1069-77.
14. Laureti, M., et al., *Flavivirus Receptors: Diversity, Identity, and Cell Entry.* Front Immunol, 2018. **9**: p. 2180.
15. Perera-Lecoin, M., et al., *Flavivirus entry receptors: an update.* Viruses, 2013. **6**(1): p. 69-88.
16. Cruz-Oliveira, C., et al., *Receptors and routes of dengue virus entry into the host cells.* FEMS Microbiol Rev, 2015. **39**(2): p. 155-70.
17. Anwar, M.N., et al., *The interactions of flaviviruses with cellular receptors: Implications for virus entry.* Virology, 2022. **568**: p. 77-85.
18. Miller, J.L., et al., *The mannose receptor mediates dengue virus infection of macrophages.* PLoS Pathog, 2008. **4**(2): p. e17.

19. van den Elsen, K., J.P. Quek, and D. Luo, *Molecular Insights into the Flavivirus Replication Complex.* Viruses, 2021. **13**(6).
20. Kroschewski, H., et al., *Role of heparan sulfate for attachment and entry of tick-borne encephalitis virus.* Virology, 2003. **308**(1): p. 92-100.
21. Zhang, X., et al., *T-Cell Immunoglobulin and Mucin Domain 1 (TIM-1) Is a Functional Entry Factor for Tick-Borne Encephalitis Virus.* mBio, 2022. **13**(1): p. e0286021.
22. Mittler, E., et al., *LRP8 is a receptor for tick-borne encephalitis virus.* Nature, 2025.
23. Li, P., et al., *LRP8 is an entry receptor for tick-borne encephalitis viruses.* Proc Natl Acad Sci U S A, 2025. **122**(44): p. e2525771122.
24. Phillpotts, R.J., J.R. Stephenson, and J.S. Porterfield, *Antibody-dependent enhancement of tick-borne encephalitis virus infectivity.* J Gen Virol, 1985. **66 (Pt 8)**: p. 1831-7.
25. Xu, Q., et al., *Caveolin-1-mediated Japanese encephalitis virus entry requires a two-step regulation of actin reorganization.* Future Microbiol, 2016. **11**: p. 1227-1248.
26. Carro, S.D. and S. Cherry, *Beyond the Surface: Endocytosis of Mosquito-Borne Flaviviruses.* Viruses, 2020. **13**(1).
27. Krishnan, M.N., et al., *Rab 5 is required for the cellular entry of dengue and West Nile viruses.* J Virol, 2007. **81**(9): p. 4881-5.
28. Fritz, R., K. Stiasny, and F.X. Heinz, *Identification of specific histidines as pH sensors in flavivirus membrane fusion.* J Cell Biol, 2008. **183**(2): p. 353-61.
29. Allison, S.L., et al., *Oligomeric rearrangement of tick-borne encephalitis virus envelope proteins induced by an acidic pH.* J Virol, 1995. **69**(2): p. 695-700.
30. Heinz, F.X. and S.L. Allison, *Structures and mechanisms in flavivirus fusion.* Adv Virus Res, 2000. **55**: p. 231-69.
31. Ferlenghi, I., et al., *Molecular organization of a recombinant subviral particle from tick-borne encephalitis virus.* Mol Cell, 2001. **7**(3): p. 593-602.
32. Stiasny, K., et al., *Impact of structural dynamics on biological functions of flaviviruses.* FEBS J, 2023. **290**(8): p. 1973-1985.
33. Stocks, C.E. and M. Lobigs, *Signal peptidase cleavage at the flavivirus C-prM junction: dependence on the viral NS2B-3 protease for efficient processing requires determinants in C, the signal peptide, and prM.* J Virol, 1998. **72**(3): p. 2141-9.
34. Chambers, T.J., et al., *Evidence that the N-terminal domain of nonstructural protein NS3 from yellow fever virus is a serine protease responsible for site-specific cleavages in the viral polyprotein.* Proc Natl Acad Sci U S A, 1990. **87**(22): p. 8898-902.
35. Ci, Y., et al., *Zika NS1-induced ER remodeling is essential for viral replication.* J Cell Biol, 2020. **219**(2).
36. Ci, Y. and L. Shi, *Compartmentalized replication organelle of flavivirus at the ER and the factors involved.* Cell Mol Life Sci, 2021. **78**(11): p. 4939-4954.
37. Miller, S., et al., *The non-structural protein 4A of dengue virus is an integral membrane protein inducing membrane alterations in a 2K-regulated manner.* J Biol Chem, 2007. **282**(12): p. 8873-82.

38. Roosendaal, J., et al., *Regulated cleavages at the West Nile virus NS4A-2K-NS4B junctions play a major role in rearranging cytoplasmic membranes and Golgi trafficking of the NS4A protein.* J Virol, 2006. **80**(9): p. 4623-32.
39. Kaufusi, P.H., et al., *Induction of endoplasmic reticulum-derived replication-competent membrane structures by West Nile virus non-structural protein 4B.* PLoS One, 2014. **9**(1): p. e84040.
40. Yasuzumi, G., et al., *Analysis of the Development of Japanese B Encephalitis (Jbe) Visus. I. Electron Microscope Studies of Microglia Infected with Jbe Virus.* J Ultrastruct Res, 1964. **11**: p. 213-29.
41. Bell, T.M., E.J. Field, and H.K. Narang, *Zika virus infection of the central nervous system of mice.* Arch Gesamte Virusforsch, 1971. **35**(2): p. 183-93.
42. Stohlman, S.A., et al., *Dengue virus-induced modifications of host cell membranes.* J Virol, 1975. **16**(4): p. 1017-26.
43. Murphy, K. and C. Weaver, *Janeway's immunobiology*. 9th edition. ed. 2016, New York, NY: Garland Science/Taylor & Francis Group, LLC. xx, 904 pages.
44. Overby, A.K., et al., *Tick-borne encephalitis virus delays interferon induction and hides its double-stranded RNA in intracellular membrane vesicles.* J Virol, 2010. **84**(17): p. 8470-83.
45. Miorin, L., et al., *Formation of membrane-defined compartments by tick-borne encephalitis virus contributes to the early delay in interferon signaling.* Virus Res, 2012. **163**(2): p. 660-6.
46. Uchida, L., et al., *The dengue virus conceals double-stranded RNA in the intracellular membrane to escape from an interferon response.* Sci Rep, 2014. **4**: p. 7395.
47. Romero-Brey, I. and R. Bartenschlager, *Membranous replication factories induced by plus-strand RNA viruses.* Viruses, 2014. **6**(7): p. 2826-57.
48. Gillespie, L.K., et al., *The endoplasmic reticulum provides the membrane platform for biogenesis of the flavivirus replication complex.* J Virol, 2010. **84**(20): p. 10438-47.
49. Welsch, S., et al., *Composition and three-dimensional architecture of the dengue virus replication and assembly sites.* Cell Host Microbe, 2009. **5**(4): p. 365-75.
50. Cortese, M., et al., *Ultrastructural Characterization of Zika Virus Replication Factories.* Cell Rep, 2017. **18**(9): p. 2113-2123.
51. Xie, X., et al., *Dengue NS2A Protein Orchestrates Virus Assembly.* Cell Host Microbe, 2019. **26**(5): p. 606-622 e8.
52. Zhang, X., et al., *Zika Virus NS2A-Mediated Virion Assembly.* mBio, 2019. **10**(5).
53. Kummerer, B.M. and C.M. Rice, *Mutations in the yellow fever virus nonstructural protein NS2A selectively block production of infectious particles.* J Virol, 2002. **76**(10): p. 4773-84.
54. Scaturro, P., et al., *Dengue Virus Non-structural Protein 1 Modulates Infectious Particle Production via Interaction with the Structural Proteins.* PLoS Pathog, 2015. **11**(11): p. e1005277.
55. Leung, J.Y., et al., *Role of nonstructural protein NS2A in flavivirus assembly.* J Virol, 2008. **82**(10): p. 4731-41.

56. Patkar, C.G. and R.J. Kuhn, *Yellow Fever virus NS3 plays an essential role in virus assembly independent of its known enzymatic functions.* J Virol, 2008. **82**(7): p. 3342-52.
57. Pijlman, G.P., N. Kondratieva, and A.A. Khromykh, *Translation of the flavivirus kunjin NS3 gene in cis but not its RNA sequence or secondary structure is essential for efficient RNA packaging.* J Virol, 2006. **80**(22): p. 11255-64.
58. Xie, X., et al., *Two distinct sets of NS2A molecules are responsible for dengue virus RNA synthesis and virion assembly.* J Virol, 2015. **89**(2): p. 1298-313.
59. Khromykh, A.A., et al., *Coupling between replication and packaging of flavivirus RNA: evidence derived from the use of DNA-based full-length cDNA clones of Kunjin virus.* J Virol, 2001. **75**(10): p. 4633-40.
60. Wengler, G. and G. Wengler, *Cell-associated West Nile flavivirus is covered with E+pre-M protein heterodimers which are destroyed and reorganized by proteolytic cleavage during virus release.* J Virol, 1989. **63**(6): p. 2521-6.
61. Zhang, Y., et al., *Structures of immature flavivirus particles.* EMBO J, 2003. **22**(11): p. 2604-13.
62. Zhang, Y., et al., *Structure of immature West Nile virus.* J Virol, 2007. **81**(11): p. 6141-5.
63. Stadler, K., et al., *Proteolytic activation of tick-borne encephalitis virus by furin.* J Virol, 1997. **71**(11): p. 8475-81.
64. Seksek, O., J. Biwersi, and A.S. Verkman, *Direct measurement of trans-Golgi pH in living cells and regulation by second messengers.* J Biol Chem, 1995. **270**(10): p. 4967-70.
65. Kuhn, R.J., et al., *Structure of dengue virus: implications for flavivirus organization, maturation, and fusion.* Cell, 2002. **108**(5): p. 717-25.
66. Zhang, W., et al., *Visualization of membrane protein domains by cryo-electron microscopy of dengue virus.* Nat Struct Biol, 2003. **10**(11): p. 907-12.
67. Zhang, Y., et al., *Conformational changes of the flavivirus E glycoprotein.* Structure, 2004. **12**(9): p. 1607-18.
68. Li, L., et al., *The flavivirus precursor membrane-envelope protein complex: structure and maturation.* Science, 2008. **319**(5871): p. 1830-4.
69. Yu, I.M., et al., *Structure of the immature dengue virus at low pH primes proteolytic maturation.* Science, 2008. **319**(5871): p. 1834-7.
70. Molloy, S.S., et al., *Intracellular trafficking and activation of the furin proprotein convertase: localization to the TGN and recycling from the cell surface.* EMBO J, 1994. **13**(1): p. 18-33.
71. Zheng, A., M. Umashankar, and M. Kielian, *In vitro and in vivo studies identify important features of dengue virus pr-E protein interactions.* PLoS Pathog, 2010. **6**(10): p. e1001157.
72. Yu, I.M., et al., *Association of the pr peptides with dengue virus at acidic pH blocks membrane fusion.* J Virol, 2009. **83**(23): p. 12101-7.
73. Holoubek, J., et al., *Irreversible furin cleavage site exposure renders immature tick-borne flaviviruses fully infectious.* Nat Commun, 2025. **16**(1): p. 7491.

74. Junjhon, J., et al., *Influence of pr-M cleavage on the heterogeneity of extracellular dengue virus particles.* J Virol, 2010. **84**(16): p. 8353-8.
75. Pierson, T.C. and M.S. Diamond, *Degrees of maturity: the complex structure and biology of flaviviruses.* Curr Opin Virol, 2012. **2**(2): p. 168-75.
76. Cherrier, M.V., et al., *Structural basis for the preferential recognition of immature flaviviruses by a fusion-loop antibody.* EMBO J, 2009. **28**(20): p. 3269-76.
77. van der Schaar, H.M., et al., *Characterization of the early events in dengue virus cell entry by biochemical assays and single-virus tracking.* J Virol, 2007. **81**(21): p. 12019-28.
78. Plevka, P., et al., *Maturation of flaviviruses starts from one or more icosahedrally independent nucleation centres.* EMBO Rep, 2011. **12**(6): p. 602-6.
79. Zerfu, B., T. Kassa, and M. Legesse, *Epidemiology, biology, pathogenesis, clinical manifestations, and diagnosis of dengue virus infection, and its trend in Ethiopia: a comprehensive literature review.* Trop Med Health, 2023. **51**(1): p. 11.
80. Zybert, I.A., et al., *Functional importance of dengue virus maturation: infectious properties of immature virions.* J Gen Virol, 2008. **89**(Pt 12): p. 3047-3051.
81. Mukherjee, S., et al., *The infectivity of prM-containing partially mature West Nile virus does not require the activity of cellular furin-like proteases.* J Virol, 2011. **85**(22): p. 12067-72.
82. Richter, M.K., et al., *Immature dengue virus is infectious in human immature dendritic cells via interaction with the receptor molecule DC-SIGN.* PLoS One, 2014. **9**(6): p. e98785.
83. Davis, C.W., et al., *West Nile virus discriminates between DC-SIGN and DC-SIGNR for cellular attachment and infection.* J Virol, 2006. **80**(3): p. 1290-301.
84. Rodenhuis-Zybert, I.A., et al., *Immature dengue virus: a veiled pathogen?* PLoS Pathog, 2010. **6**(1): p. e1000718.
85. Dowd, K.A. and T.C. Pierson, *Antibody-mediated neutralization of flaviviruses: a reductionist view.* Virology, 2011. **411**(2): p. 306-15.
86. Galula, J.U., et al., *Does structurally-mature dengue virion matter in vaccine preparation in post-Dengvaxia era?* Hum Vaccin Immunother, 2019. **15**(10): p. 2328-2336.
87. Shen, W.F., et al., *Epitope resurfacing on dengue virus-like particle vaccine preparation to induce broad neutralizing antibody.* Elife, 2018. **7**.
88. Nelson, S., et al., *Maturation of West Nile virus modulates sensitivity to antibody-mediated neutralization.* PLoS Pathog, 2008. **4**(5): p. e1000060.
89. Dejnirattisai, W., et al., *Cross-reacting antibodies enhance dengue virus infection in humans.* Science, 2010. **328**(5979): p. 745-8.
90. Oliphant, T., et al., *Antibody recognition and neutralization determinants on domains I and II of West Nile Virus envelope protein.* J Virol, 2006. **80**(24): p. 12149-59.
91. Beltramello, M., et al., *The human immune response to Dengue virus is dominated by highly cross-reactive antibodies endowed with neutralizing and enhancing activity.* Cell Host Microbe, 2010. **8**(3): p. 271-83.

92. Dowd, K.A., et al., *prM-reactive antibodies reveal a role for partially mature virions in dengue virus pathogenesis.* Proc Natl Acad Sci U S A, 2023. **120**(3): p. e2218899120.
93. Smith, S.A., et al., *Dengue Virus prM-Specific Human Monoclonal Antibodies with Virus Replication-Enhancing Properties Recognize a Single Immunodominant Antigenic Site.* J Virol, 2016. **90**(2): p. 780-9.
94. Lai, C.Y., et al., *Antibodies to envelope glycoprotein of dengue virus during the natural course of infection are predominantly cross-reactive and recognize epitopes containing highly conserved residues at the fusion loop of domain II.* J Virol, 2008. **82**(13): p. 6631-43.
95. Oliphant, T., et al., *Development of a humanized monoclonal antibody with therapeutic potential against West Nile virus.* Nat Med, 2005. **11**(5): p. 522-30.
96. Oliphant, T., et al., *Induction of epitope-specific neutralizing antibodies against West Nile virus.* J Virol, 2007. **81**(21): p. 11828-39.
97. Sukupolvi-Petty, S., et al., *Type- and subcomplex-specific neutralizing antibodies against domain III of dengue virus type 2 envelope protein recognize adjacent epitopes.* J Virol, 2007. **81**(23): p. 12816-26.
98. Rouvinski, A., et al., *Recognition determinants of broadly neutralizing human antibodies against dengue viruses.* Nature, 2015. **520**(7545): p. 109-13.
99. Dejnirattisai, W., et al., *A new class of highly potent, broadly neutralizing antibodies isolated from viremic patients infected with dengue virus.* Nat Immunol, 2015. **16**(2): p. 170-177.
100. Sevvana, M. and R.J. Kuhn, *Mapping the diverse structural landscape of the flavivirus antibody repertoire.* Curr Opin Virol, 2020. **45**: p. 51-64.
101. Dowd, K.A., et al., *Combined effects of the structural heterogeneity and dynamics of flaviviruses on antibody recognition.* J Virol, 2014. **88**(20): p. 11726-37.
102. Stiasny, K., et al., *Cryptic properties of a cluster of dominant flavivirus cross-reactive antigenic sites.* J Virol, 2006. **80**(19): p. 9557-68.
103. Holzmann, H., et al., *Tick-borne encephalitis virus envelope protein E-specific monoclonal antibodies for the study of low pH-induced conformational changes and immature virions.* Arch Virol, 1995. **140**(2): p. 213-21.
104. Guirakhoo, F., R.A. Bolin, and J.T. Roehrig, *The Murray Valley encephalitis virus prM protein confers acid resistance to virus particles and alters the expression of epitopes within the R2 domain of E glycoprotein.* Virology, 1992. **191**(2): p. 921-31.
105. Keelapang, P., et al., *Generation and preclinical evaluation of a DENV-1/2 prM+E chimeric live attenuated vaccine candidate with enhanced prM cleavage.* Vaccine, 2013. **31**(44): p. 5134-40.
106. Ohtaki, N., et al., *Immunogenicity and efficacy of two types of West Nile virus-like particles different in size and maturation as a second-generation vaccine candidate.* Vaccine, 2010. **28**(40): p. 6588-96.
107. Suphatrakul, A., et al., *Generation and preclinical immunogenicity study of dengue type 2 virus-like particles derived from stably transfected mosquito cells.* Vaccine, 2015. **33**(42): p. 5613-5622.

108. Scott, C.A.P., et al., *Implications of Dengue Virus Maturation on Vaccine Induced Humoral Immunity in Mice.* Viruses, 2021. **13**(9).
109. Reed, W. and J. Carroll, *The Etiology of Yellow Fever: A Supplemental Note.* Military Medicine, 2001. **166**(suppl_1): p. 62-66.
110. Ashburn, P.M., C.F. Craig, and U.S.A.B.f.t.S.o.T. Diseases, *Experimental investigations regarding the etiology of dengue fever. 1907.* J Infect Dis, 2004. **189**(9): p. 1747-83; discussion 1744-6.
111. Finlay, C., *[The mosquito hypothetically considered as an agent of yellow fever transmission. 1881].* Salud Publica Mex, 1992. **34**(4): p. 474-83.
112. Sabin, A.B., *Research on dengue during World War II.* Am J Trop Med Hyg, 1952. **1**(1): p. 30-50.
113. Snow, G.E., et al., *Review article: Research on dengue during World War II revisited.* Am J Trop Med Hyg, 2014. **91**(6): p. 1203-17.
114. Graham, H., *The dengue : a study of its pathology and mode of propagation.* J. Trop. Med., 1903. **6**: p. 209-214.
115. Young, P.R., *Arboviruses: A Family on the Move.* Adv Exp Med Biol, 2018. **1062**: p. 1-10.
116. Reed, W., et al., *The Etiology of Yellow Fever-A Preliminary Note.* Public Health Pap Rep, 1900. **26**: p. 37-53.
117. Gubler, D.J. and L. Rosen, *A simple technique for demonstrating transmission of dengue virus by mosquitoes without the use of vertebrate hosts.* Am J Trop Med Hyg, 1976. **25**(1): p. 146-50.
118. Hurlbut, H.S., *Mosquito salivation and virus transmission.* Am J Trop Med Hyg, 1966. **15**(6): p. 989-93.
119. Nuttall, P.A., et al., *Adaptations of arboviruses to ticks.* J Med Entomol, 1994. **31**(1): p. 1-9.
120. Lim, P.Y., et al., *Keratinocytes are cell targets of West Nile virus in vivo.* J Virol, 2011. **85**(10): p. 5197-201.
121. Wu, S.J., et al., *Human skin Langerhans cells are targets of dengue virus infection.* Nat Med, 2000. **6**(7): p. 816-20.
122. Briant, L., et al., *Role of skin immune cells on the host susceptibility to mosquito-borne viruses.* Virology, 2014. **464-465**: p. 26-32.
123. Zhou, W., et al., *Exosomes serve as novel modes of tick-borne flavivirus transmission from arthropod to human cells and facilitates dissemination of viral RNA and proteins to the vertebrate neuronal cells.* PLoS Pathog, 2018. **14**(1): p. e1006764.
124. Labuda, M., et al., *Importance of localized skin infection in tick-borne encephalitis virus transmission.* Virology, 1996. **219**(2): p. 357-66.
125. Johnston, L.J., G.M. Halliday, and N.J. King, *Langerhans cells migrate to local lymph nodes following cutaneous infection with an arbovirus.* J Invest Dermatol, 2000. **114**(3): p. 560-8.
126. Diamond, M.S., et al., *B cells and antibody play critical roles in the immediate defense of disseminated infection by West Nile encephalitis virus.* J Virol, 2003. **77**(4): p. 2578-86.

127. McMinn, P.C., L. Dalgarno, and R.C. Weir, *A comparison of the spread of Murray Valley encephalitis viruses of high or low neuroinvasiveness in the tissues of Swiss mice after peripheral inoculation.* Virology, 1996. **220**(2): p. 414-23.
128. Miller, B.R., C.J. Mitchell, and M.E. Ballinger, *Replication, tissue tropisms and transmission of yellow fever virus in Aedes albopictus.* Trans R Soc Trop Med Hyg, 1989. **83**(2): p. 252-5.
129. Nuttall, P.A. and M. Labuda, *Dynamics of infection in tick vectors and at the tick-host interface.* Adv Virus Res, 2003. **60**: p. 233-72.
130. Nosek, J., et al., *Localization of tick-borne encephalitis virus in alveolar cells of salivary glands of Dermacentor marginatus and Haemaphysalis inermis ticks.* Acta Virol, 1972. **16**(6): p. 493-7.
131. Rajcani, J., et al., *Reaction of the host to the tick-bite. II. Distribution of tick borne encephalitis virus in sucking ticks.* Zentralbl Bakteriol Orig A, 1976. **236**(1): p. 1-9.
132. Huang, Y.S., S. Higgs, and D.L. Vanlandingham, *Arbovirus-Mosquito Vector-Host Interactions and the Impact on Transmission and Disease Pathogenesis of Arboviruses.* Front Microbiol, 2019. **10**: p. 22.
133. Gunther, J., et al., *Evidence of vertical transmission of dengue virus in two endemic localities in the state of Oaxaca, Mexico.* Intervirology, 2007. **50**(5): p. 347-52.
134. Angel, B. and V. Joshi, *Distribution and seasonality of vertically transmitted dengue viruses in Aedes mosquitoes in arid and semi-arid areas of Rajasthan, India.* J Vector Borne Dis, 2008. **45**(1): p. 56-9.
135. Comeau, G., et al., *Vertical Transmission of Zika Virus in Aedes aegypti Produces Potentially Infectious Progeny.* Am J Trop Med Hyg, 2020. **103**(2): p. 876-883.
136. Chernesky, M.A. and D.M. McLean, *Localization of Powassan virus in Dermacentor andersoni ticks by immunofluorescence.* Can J Microbiol, 1969. **15**(12): p. 1399-408.
137. Labuda, M. and P.A. Nuttall, *Tick-borne viruses.* Parasitology, 2004. **129 Suppl**: p. S221-45.
138. Rehacek, J., *Experimental hibernation of the tick-borne encephalitis virus in engorged larvae of the tick Ixodes ricinus L.* Acta Virol, 1960. **4**: p. 106-9.
139. Labuda, M., et al., *Amplification of tick-borne encephalitis virus infection during co-feeding of ticks.* Med Vet Entomol, 1993. **7**(4): p. 339-42.
140. Alekseev, A.N. and S.P. Chunikhin, *[The exchange of the tick-borne encephalitis virus between ixodid ticks feeding jointly on animals with a subthreshold level of viremia].* Med Parazitol (Mosk), 1990(2): p. 48-50.
141. Nguyen-Tien, T., A. Lundkvist, and J. Lindahl, *Urban transmission of mosquito-borne flaviviruses - a review of the risk for humans in Vietnam.* Infect Ecol Epidemiol, 2019. **9**(1): p. 1660129.
142. D, V. *TBE in Lithuania*. in *Proceedings of the Fourth International Potsdam Symposium on Tick-Borne Diseases*. 1997. Potsdam, Germany: Pabst Science Publishers.
143. Kerlik, J., et al., *Breast Milk as Route of Tick-Borne Encephalitis Virus Transmission from Mother to Infant.* Emerg Infect Dis, 2022. **28**(5): p. 1060-1061.

144. Suss, J., *Tick-borne encephalitis 2010: epidemiology, risk areas, and virus strains in Europe and Asia-an overview.* Ticks Tick Borne Dis, 2011. **2**(1): p. 2-15.
145. Blohm, G.M., et al., *Complete Genome Sequences of Identical Zika virus Isolates in a Nursing Mother and Her Infant.* Genome Announc, 2017. **5**(17).
146. Blohm, G.M., et al., *Evidence for Mother-to-Child Transmission of Zika Virus Through Breast Milk.* Clin Infect Dis, 2018. **66**(7): p. 1120-1121.
147. Russell, K., et al., *Male-to-Female Sexual Transmission of Zika Virus-United States, January-April 2016.* Clin Infect Dis, 2017. **64**(2): p. 211-213.
148. Ades, A.E., et al., *Vertical transmission of Zika virus and its outcomes: a Bayesian synthesis of prospective studies.* Lancet Infect Dis, 2021. **21**(4): p. 537-545.
149. Arragain, L., et al., *Vertical Transmission of Dengue Virus in the Peripartum Period and Viral Kinetics in Newborns and Breast Milk: New Data.* J Pediatric Infect Dis Soc, 2017. **6**(4): p. 324-331.
150. Lewis, J., et al., *Intrinsic factors driving mosquito vector competence and viral evolution: a review.* Front Cell Infect Microbiol, 2023. **13**: p. 1330600.
151. Junglen, S., et al., *Host Range Restriction of Insect-Specific Flaviviruses Occurs at Several Levels of the Viral Life Cycle.* mSphere, 2017. **2**(1).
152. Eisen, R.J. and L. Eisen, *The Blacklegged Tick, Ixodes scapularis: An Increasing Public Health Concern.* Trends Parasitol, 2018. **34**(4): p. 295-309.
153. Alkishe, A. and A.T. Peterson, *Potential geographic distribution of Ixodes cookei, the vector of Powassan virus.* J Vector Ecol, 2021. **46**(2): p. 155-162.
154. Vasilakis, N., et al., *Fever from the forest: prospects for the continued emergence of sylvatic dengue virus and its impact on public health.* Nat Rev Microbiol, 2011. **9**(7): p. 532-41.
155. Bhatt, S., et al., *The global distribution and burden of dengue.* Nature, 2013. **496**(7446): p. 504-7.
156. Ilic, I. and M. Ilic, *Global Patterns of Trends in Incidence and Mortality of Dengue, 1990-2019: An Analysis Based on the Global Burden of Disease Study.* Medicina (Kaunas), 2024. **60**(3).
157. Pierson, T.C. and M.S. Diamond, *The continued threat of emerging flaviviruses.* Nat Microbiol, 2020. **5**(6): p. 796-812.
158. Campbell, O. and P.J. Krause, *The emergence of human Powassan virus infection in North America.* Ticks Tick Borne Dis, 2020. **11**(6): p. 101540.
159. Khan, M., et al., *An Overview of Powassan Virus Disease.* Neurohospitalist, 2019. **9**(4): p. 181-182.
160. Mladinich, M.C., et al., *Age-dependent Powassan virus lethality is linked to glial cell activation and divergent neuroinflammatory cytokine responses in a murine model.* J Virol, 2024. **98**(8): p. e0056024.
161. Mlera, L., W. Melik, and M.E. Bloom, *The role of viral persistence in flavivirus biology.* Pathog Dis, 2014. **71**(2): p. 137-63.
162. Puerta-Guardo, H., et al., *Flavivirus NS1 Triggers Tissue-Specific Vascular Endothelial Dysfunction Reflecting Disease Tropism.* Cell Rep, 2019. **26**(6): p. 1598-1613 e8.

163. Stone, E.T. and A.K. Pinto, *T Cells in Tick-Borne Flavivirus Encephalitis: A Review of Current Paradigms in Protection and Disease Pathology.* Viruses, 2023. **15**(4).
164. Hirano, M., et al., *Dendritic transport of tick-borne flavivirus RNA by neuronal granules affects development of neurological disease.* Proc Natl Acad Sci U S A, 2017. **114**(37): p. 9960-9965.
165. Hirano, M., et al., *Tick-borne flaviviruses alter membrane structure and replicate in dendrites of primary mouse neuronal cultures.* J Gen Virol, 2014. **95**(Pt 4): p. 849-861.
166. Marshall, E.M., M.P.G. Koopmans, and B. Rockx, *A Journey to the Central Nervous System: Routes of Flaviviral Neuroinvasion in Human Disease.* Viruses, 2022. **14**(10).
167. Verma, S., et al., *West Nile virus infection modulates human brain microvascular endothelial cells tight junction proteins and cell adhesion molecules: Transmigration across the in vitro blood-brain barrier.* Virology, 2009. **385**(2): p. 425-33.
168. Lai, C.Y., et al., *Endothelial Japanese encephalitis virus infection enhances migration and adhesion of leukocytes to brain microvascular endothelia via MEK-dependent expression of ICAM1 and the CINC and RANTES chemokines.* J Neurochem, 2012. **123**(2): p. 250-61.
169. Patabendige, A., et al., *Brain microvascular endothelial-astrocyte cell responses following Japanese encephalitis virus infection in an in vitro human blood-brain barrier model.* Mol Cell Neurosci, 2018. **89**: p. 60-70.
170. Palus, M., et al., *Tick-borne encephalitis virus infects human brain microvascular endothelial cells without compromising blood-brain barrier integrity.* Virology, 2017. **507**: p. 110-122.
171. Wang, H., et al., *West Nile virus preferentially transports along motor neuron axons after sciatic nerve injection of hamsters.* J Neurovirol, 2009. **15**(4): p. 293-9.
172. Brown, A.N., et al., *Tissue tropism and neuroinvasion of West Nile virus do not differ for two mouse strains with different survival rates.* Virology, 2007. **368**(2): p. 422-30.
173. Shrestha, B., D. Gottlieb, and M.S. Diamond, *Infection and injury of neurons by West Nile encephalitis virus.* J Virol, 2003. **77**(24): p. 13203-13.
174. Puerta-Guardo, H., D.R. Glasner, and E. Harris, *Dengue Virus NS1 Disrupts the Endothelial Glycocalyx, Leading to Hyperpermeability.* PLoS Pathog, 2016. **12**(7): p. e1005738.
175. Beatty, P.R., et al., *Dengue virus NS1 triggers endothelial permeability and vascular leak that is prevented by NS1 vaccination.* Sci Transl Med, 2015. **7**(304): p. 304ra141.
176. Ruzek, D., et al., *CD8+ T-cells mediate immunopathology in tick-borne encephalitis.* Virology, 2009. **384**(1): p. 1-6.
177. Atrasheuskaya, A.V., T.M. Fredeking, and G.M. Ignatyev, *Changes in immune parameters and their correction in human cases of tick-borne encephalitis.* Clin Exp Immunol, 2003. **131**(1): p. 148-54.

178. Wang, Y., et al., *CD8+ T cells mediate recovery and immunopathology in West Nile virus encephalitis.* J Virol, 2003. **77**(24): p. 13323-34.
179. Gelpi, E., et al., *Inflammatory response in human tick-borne encephalitis: analysis of postmortem brain tissue.* J Neurovirol, 2006. **12**(4): p. 322-7.
180. Semenov, B.F., V.V. Khozinsky, and V.V. Vargin, *The damaging action of cellular immunity in flavivirus infections of mice.* Med Biol, 1975. **53**(5): p. 331-6.
181. Kumar, M., S. Verma, and V.R. Nerurkar, *Pro-inflammatory cytokines derived from West Nile virus (WNV)-infected SK-N-SH cells mediate neuroinflammatory markers and neuronal death.* J Neuroinflammation, 2010. **7**: p. 73.
182. Miorin, L., et al., *Antagonism of type I interferon by flaviviruses.* Biochem Biophys Res Commun, 2017. **492**(4): p. 587-596.
183. Kato, H., et al., *Differential roles of MDA5 and RIG-I helicases in the recognition of RNA viruses.* Nature, 2006. **441**(7089): p. 101-5.
184. Fredericksen, B.L., et al., *Establishment and maintenance of the innate antiviral response to West Nile Virus involves both RIG-I and MDA5 signaling through IPS-1.* J Virol, 2008. **82**(2): p. 609-16.
185. Loo, Y.M., et al., *Distinct RIG-I and MDA5 signaling by RNA viruses in innate immunity.* J Virol, 2008. **82**(1): p. 335-45.
186. Fredericksen, B.L. and M. Gale, Jr., *West Nile virus evades activation of interferon regulatory factor 3 through RIG-I-dependent and -independent pathways without antagonizing host defense signaling.* J Virol, 2006. **80**(6): p. 2913-23.
187. Goubau, D., et al., *Antiviral immunity via RIG-I-mediated recognition of RNA bearing 5'-diphosphates.* Nature, 2014. **514**(7522): p. 372-375.
188. Kato, H., et al., *Length-dependent recognition of double-stranded ribonucleic acids by retinoic acid-inducible gene-I and melanoma differentiation-associated gene 5.* J Exp Med, 2008. **205**(7): p. 1601-10.
189. Hornung, V., et al., *5'-Triphosphate RNA is the ligand for RIG-I.* Science, 2006. **314**(5801): p. 994-7.
190. Berghall, H., et al., *The interferon-inducible RNA helicase, mda-5, is involved in measles virus-induced expression of antiviral cytokines.* Microbes Infect, 2006. **8**(8): p. 2138-44.
191. Yoneyama, M., et al., *The RNA helicase RIG-I has an essential function in double-stranded RNA-induced innate antiviral responses.* Nat Immunol, 2004. **5**(7): p. 730-7.
192. Barral, P.M., et al., *Functions of the cytoplasmic RNA sensors RIG-I and MDA-5: key regulators of innate immunity.* Pharmacol Ther, 2009. **124**(2): p. 219-34.
193. Jiang, D., et al., *Identification of five interferon-induced cellular proteins that inhibit west nile virus and dengue virus infections.* J Virol, 2010. **84**(16): p. 8332-41.
194. Lim, J.K., et al., *Genetic variation in OAS1 is a risk factor for initial infection with West Nile virus in man.* PLoS Pathog, 2009. **5**(2): p. e1000321.
195. Brass, A.L., et al., *The IFITM proteins mediate cellular resistance to influenza A H1N1 virus, West Nile virus, and dengue virus.* Cell, 2009. **139**(7): p. 1243-54.

196. Daffis, S., et al., *2'-O methylation of the viral mRNA cap evades host restriction by IFIT family members.* Nature, 2010. **468**(7322): p. 452-6.
197. Schoggins, J.W., et al., *Corrigendum: A diverse range of gene products are effectors of the type I interferon antiviral response.* Nature, 2015. **525**(7567): p. 144.
198. Aguirre, S., et al., *Dengue virus NS2B protein targets cGAS for degradation and prevents mitochondrial DNA sensing during infection.* Nat Microbiol, 2017. **2**: p. 17037.
199. Daffis, S., et al., *Toll-like receptor 3 has a protective role against West Nile virus infection.* J Virol, 2008. **82**(21): p. 10349-58.
200. Town, T., et al., *Toll-like receptor 7 mitigates lethal West Nile encephalitis via interleukin 23-dependent immune cell infiltration and homing.* Immunity, 2009. **30**(2): p. 242-53.
201. Pan, Y., et al., *Flaviviruses: Innate Immunity, Inflammasome Activation, Inflammatory Cell Death, and Cytokines.* Front Immunol, 2022. **13**: p. 829433.
202. Chung, K.M., et al., *Antibody recognition of cell surface-associated NS1 triggers Fc-gamma receptor-mediated phagocytosis and clearance of West Nile Virus-infected cells.* J Virol, 2007. **81**(17): p. 9551-5.
203. Mehlhop, E., et al., *Complement activation is required for induction of a protective antibody response against West Nile virus infection.* J Virol, 2005. **79**(12): p. 7466-77.
204. Conde, J.N., et al., *The Complement System in Flavivirus Infections.* Front Microbiol, 2017. **8**: p. 213.
205. Bos, S., et al., *Protection against symptomatic dengue infection by neutralizing antibodies varies by infection history and infecting serotype.* Nat Commun, 2024. **15**(1): p. 382.
206. Kubinski, M., et al., *Tick-Borne Encephalitis Virus: A Quest for Better Vaccines against a Virus on the Rise.* Vaccines (Basel), 2020. **8**(3).
207. Pierson, T.C. and M.S. Diamond, *Molecular mechanisms of antibody-mediated neutralisation of flavivirus infection.* Expert Rev Mol Med, 2008. **10**: p. e12.
208. Katzelnick, L.C., et al., *Neutralizing antibody titers against dengue virus correlate with protection from symptomatic infection in a longitudinal cohort.* Proc Natl Acad Sci U S A, 2016. **113**(3): p. 728-33.
209. Kreil, T.R., et al., *Neutralizing antibodies protect against lethal flavivirus challenge but allow for the development of active humoral immunity to a nonstructural virus protein.* J Virol, 1998. **72**(4): p. 3076-81.
210. Van Gessel, Y., et al., *Correlation of protection against Japanese encephalitis virus and JE vaccine (IXIARO((R))) induced neutralizing antibody titers.* Vaccine, 2011. **29**(35): p. 5925-31.
211. Flores, H.E., et al., *From Antibodies to Immunity: Assessing Correlates of Flavivirus Protection and Cross-Reactivity.* Vaccines (Basel), 2025. **13**(5).
212. Crill, W.D. and J.T. Roehrig, *Monoclonal antibodies that bind to domain III of dengue virus E glycoprotein are the most efficient blockers of virus adsorption to Vero cells.* J Virol, 2001. **75**(16): p. 7769-73.

213. Gollins, S.W. and J.S. Porterfield, *A new mechanism for the neutralization of enveloped viruses by antiviral antibody.* Nature, 1986. **321**(6067): p. 244-6.
214. Stiasny, K., et al., *Probing the flavivirus membrane fusion mechanism by using monoclonal antibodies.* J Virol, 2007. **81**(20): p. 11526-31.
215. Montoya, M., et al., *Symptomatic versus inapparent outcome in repeat dengue virus infections is influenced by the time interval between infections and study year.* PLoS Negl Trop Dis, 2013. **7**(8): p. e2357.
216. Anderson, K.B., et al., *A shorter time interval between first and second dengue infections is associated with protection from clinical illness in a school-based cohort in Thailand.* J Infect Dis, 2014. **209**(3): p. 360-8.
217. Collins, M.H., et al., *Lack of Durable Cross-Neutralizing Antibodies Against Zika Virus from Dengue Virus Infection.* Emerg Infect Dis, 2017. **23**(5): p. 773-781.
218. Agudelo, M., et al., *Broad and potent neutralizing human antibodies to tick-borne flaviviruses protect mice from disease.* J Exp Med, 2021. **218**(5).
219. Wieten, R.W., et al., *A Single 17D Yellow Fever Vaccination Provides Lifelong Immunity; Characterization of Yellow-Fever-Specific Neutralizing Antibody and T-Cell Responses after Vaccination.* PLoS One, 2016. **11**(3): p. e0149871.
220. Grifoni, A., et al., *Prior Dengue Virus Exposure Shapes T Cell Immunity to Zika Virus in Humans.* J Virol, 2017. **91**(24).
221. Kalimuddin, S., et al., *Vaccine-induced T cell responses control Orthoflavivirus challenge infection without neutralizing antibodies in humans.* Nat Microbiol, 2025. **10**(2): p. 374-387.
222. Weiskopf, D., et al., *Comprehensive analysis of dengue virus-specific responses supports an HLA-linked protective role for CD8+ T cells.* Proc Natl Acad Sci U S A, 2013. **110**(22): p. E2046-53.
223. Mishra, N., et al., *A Chimeric Japanese Encephalitis Vaccine Protects against Lethal Yellow Fever Virus Infection without Inducing Neutralizing Antibodies.* mBio, 2020. **11**(2).
224. Wullimann, D. and H.G. Ljunggren, *Human T Cell Responses to Flavivirus Vaccines.* Eur J Immunol, 2025. **55**(8): p. e70027.
225. Hawkes, R.A., *Enhancement of the Infectivity of Arboviruses by Specific Antisera Produced in Domestic Fowls.* Aust J Exp Biol Med Sci, 1964. **42**: p. 465-82.
226. Hawkes, R.A. and K.J. Lafferty, *The enchancement of virus infectivity by antibody.* Virology, 1967. **33**(2): p. 250-61.
227. Halstead, S.B., et al., *Hemorrhagic fever in Thailand; recent knowledge regarding etiology.* Jpn J Med Sci Biol, 1967. **20 Suppl**: p. 96-103.
228. Halstead, S.B., H. Shotwell, and J. Casals, *Studies on the pathogenesis of dengue infection in monkeys. II. Clinical laboratory responses to heterologous infection.* J Infect Dis, 1973. **128**(1): p. 15-22.
229. Halstead, S.B., *In vivo enhancement of dengue virus infection in rhesus monkeys by passively transferred antibody.* J Infect Dis, 1979. **140**(4): p. 527-33.
230. Morens, D.M., *Antibody-dependent enhancement of infection and the pathogenesis of viral disease.* Clin Infect Dis, 1994. **19**(3): p. 500-12.

231. Kouri, G.P., et al., *Dengue haemorrhagic fever/dengue shock syndrome: lessons from the Cuban epidemic, 1981.* Bull World Health Organ, 1989. **67**(4): p. 375-80.
232. Tay, M.Z., K. Wiehe, and J. Pollara, *Antibody-Dependent Cellular Phagocytosis in Antiviral Immune Responses.* Front Immunol, 2019. **10**: p. 332.
233. Halstead, S.B., E.J. O'Rourke, and A.C. Allison, *Dengue viruses and mononuclear phagocytes. II. Identity of blood and tissue leukocytes supporting in vitro infection.* J Exp Med, 1977. **146**(1): p. 218-29.
234. Halstead, S.B. and E.J. O'Rourke, *Dengue viruses and mononuclear phagocytes. I. Infection enhancement by non-neutralizing antibody.* J Exp Med, 1977. **146**(1): p. 201-17.
235. Kulkarni, R.H., *Antibody-Dependent Enhancement of Viral Infections.* Dynamics of Immune Activation in Viral Diseases, 2019: p. 9 - 41.
236. Gollins, S.W. and J.S. Porterfield, *Flavivirus infection enhancement in macrophages: an electron microscopic study of viral cellular entry.* J Gen Virol, 1985. **66 (Pt 9)**: p. 1969-82.
237. Gollins, S.W. and J.S. Porterfield, *Flavivirus infection enhancement in macrophages: radioactive and biological studies on the effect of antibody on viral fate.* J Gen Virol, 1984. **65 (Pt 8)**: p. 1261-72.
238. Ochiai, H., et al., *Infection enhancement of influenza A NWS virus in primary murine macrophages by anti-hemagglutinin monoclonal antibody.* J Med Virol, 1992. **36**(3): p. 217-21.
239. Robinson, W.E., Jr., D.C. Montefiori, and W.M. Mitchell, *Antibody-dependent enhancement of human immunodeficiency virus type 1 infection.* Lancet, 1988. **1**(8589): p. 790-4.
240. Linn, M.L., J.G. Aaskov, and A. Suhrbier, *Antibody-dependent enhancement and persistence in macrophages of an arbovirus associated with arthritis.* J Gen Virol, 1996. **77 (Pt 3)**: p. 407-11.
241. Osiowy, C., D. Horne, and R. Anderson, *Antibody-dependent enhancement of respiratory syncytial virus infection by sera from young infants.* Clin Diagn Lab Immunol, 1994. **1**(6): p. 670-7.
242. Lidbury, B.A. and S. Mahalingam, *Specific ablation of antiviral gene expression in macrophages by antibody-dependent enhancement of Ross River virus infection.* J Virol, 2000. **74**(18): p. 8376-81.
243. Halstead, S.B., et al., *Intrinsic antibody-dependent enhancement of microbial infection in macrophages: disease regulation by immune complexes.* Lancet Infect Dis, 2010. **10**(10): p. 712-22.
244. Ubol, S., et al., *Mechanisms of immune evasion induced by a complex of dengue virus and preexisting enhancing antibodies.* J Infect Dis, 2010. **201**(6): p. 923-35.
245. Chareonsirisuthigul, T., S. Kalayanarooj, and S. Ubol, *Dengue virus (DENV) antibody-dependent enhancement of infection upregulates the production of anti-inflammatory cytokines, but suppresses anti-DENV free radical and pro-inflammatory cytokine production, in THP-1 cells.* J Gen Virol, 2007. **88**(Pt 2): p. 365-375.

246. Chen, L.C., et al., *Correlation of serum levels of macrophage migration inhibitory factor with disease severity and clinical outcome in dengue patients.* Am J Trop Med Hyg, 2006. **74**(1): p. 142-7.
247. Katzelnick, L.C., et al., *Antibody-dependent enhancement of severe dengue disease in humans.* Science, 2017. **358**(6365): p. 929-932.
248. Thomas, S.J., *Is new dengue vaccine efficacy data a relief or cause for concern?* NPJ Vaccines, 2023. **8**(1): p. 55.
249. Hadinegoro, S.R., et al., *Efficacy and Long-Term Safety of a Dengue Vaccine in Regions of Endemic Disease.* N Engl J Med, 2015. **373**(13): p. 1195-206.
250. Simmons, C.P., *A Candidate Dengue Vaccine Walks a Tightrope.* N Engl J Med, 2015. **373**(13): p. 1263-4.
251. Sridhar, S., et al., *Effect of Dengue Serostatus on Dengue Vaccine Safety and Efficacy.* N Engl J Med, 2018. **379**(4): p. 327-340.
252. Halstead, S.B., *Licensed Dengue Vaccine: Public Health Conundrum and Scientific Challenge.* Am J Trop Med Hyg, 2016. **95**(4): p. 741-745.
253. Halstead, S.B., *Dengvaxia sensitizes seronegatives to vaccine enhanced disease regardless of age.* Vaccine, 2017. **35**(47): p. 6355-6358.
254. Shukla, R., et al., *Antibody-Dependent Enhancement: A Challenge for Developing a Safe Dengue Vaccine.* Front Cell Infect Microbiol, 2020. **10**: p. 572681.
255. Dans, A.L., et al., *Controversy and debate on dengue vaccine series-paper 1: review of a licensed dengue vaccine: inappropriate subgroup analyses and selective reporting may cause harm in mass vaccination programs.* J Clin Epidemiol, 2018. **95**: p. 137-139.
256. Sabchareon, A., et al., *Protective efficacy of the recombinant, live-attenuated, CYD tetravalent dengue vaccine in Thai schoolchildren: a randomised, controlled phase 2b trial.* Lancet, 2012. **380**(9853): p. 1559-67.
257. Villar, L., et al., *Efficacy of a tetravalent dengue vaccine in children in Latin America.* N Engl J Med, 2015. **372**(2): p. 113-23.
258. Capeding, M.R., et al., *Clinical efficacy and safety of a novel tetravalent dengue vaccine in healthy children in Asia: a phase 3, randomised, observer-masked, placebo-controlled trial.* Lancet, 2014. **384**(9951): p. 1358-65.
259. Wilder-Smith, A., et al., *Deliberations of the Strategic Advisory Group of Experts on Immunization on the use of CYD-TDV dengue vaccine.* Lancet Infect Dis, 2019. **19**(1): p. e31-e38.
260. Prevention, C.f.D.C.a. *About a Dengue Vaccine*. 2025 May 15, 2025 [cited 2025 October 10]; Available from: https://www.cdc.gov/dengue/vaccine/index.html.
261. Edelman, R. and J. Hombach, *"Guidelines for the clinical evaluation of dengue vaccines in endemic areas": summary of a World Health Organization Technical Consultation.* Vaccine, 2008. **26**(33): p. 4113-9.
262. Bardina, S.V., et al., *Enhancement of Zika virus pathogenesis by preexisting antiflavivirus immunity.* Science, 2017. **356**(6334): p. 175-180.
263. Dejnirattisai, W., et al., *Dengue virus sero-cross-reactivity drives antibody-dependent enhancement of infection with zika virus.* Nat Immunol, 2016. **17**(9): p. 1102-8.

264. Elsterova, J., et al., *Tick-borne encephalitis virus neutralization by high dose intravenous immunoglobulin.* Ticks Tick Borne Dis, 2017. **8**(2): p. 253-258.
265. Waldvogel, K., et al., *Severe tick-borne encephalitis following passive immunization.* Eur J Pediatr, 1996. **155**(9): p. 775-9.
266. Kluger, G., et al., *Tickborne encephalitis despite specific immunoglobulin prophylaxis.* Lancet, 1995. **346**(8988): p. 1502.
267. Anderson, K.B., et al., *Preexisting Japanese encephalitis virus neutralizing antibodies and increased symptomatic dengue illness in a school-based cohort in Thailand.* PLoS Negl Trop Dis, 2011. **5**(10): p. e1311.
268. Roehrig, J.T., R.A. Bolin, and R.G. Kelly, *Monoclonal antibody mapping of the envelope glycoprotein of the dengue 2 virus, Jamaica.* Virology, 1998. **246**(2): p. 317-28.
269. Haslwanter, D., et al., *A novel mechanism of antibody-mediated enhancement of flavivirus infection.* PLoS Pathog, 2017. **13**(9): p. e1006643.
270. Beasley, D.W. and A.D. Barrett, *Identification of neutralizing epitopes within structural domain III of the West Nile virus envelope protein.* J Virol, 2002. **76**(24): p. 13097-100.
271. Gromowski, G.D. and A.D. Barrett, *Characterization of an antigenic site that contains a dominant, type-specific neutralization determinant on the envelope protein domain III (ED3) of dengue 2 virus.* Virology, 2007. **366**(2): p. 349-60.
272. Sanchez, M.D., et al., *Characterization of neutralizing antibodies to West Nile virus.* Virology, 2005. **336**(1): p. 70-82.
273. Shrestha, B., et al., *The development of therapeutic antibodies that neutralize homologous and heterologous genotypes of dengue virus type 1.* PLoS Pathog, 2010. **6**(4): p. e1000823.
274. Swanstrom, J.A., et al., *Dengue Virus Envelope Dimer Epitope Monoclonal Antibodies Isolated from Dengue Patients Are Protective against Zika Virus.* mBio, 2016. **7**(4).
275. Khare, B. and R.J. Kuhn, *The Japanese Encephalitis Antigenic Complex Viruses: From Structure to Immunity.* Viruses, 2022. **14**(10).
276. Ebel, G.D., *Update on Powassan virus: emergence of a North American tick-borne flavivirus.* Annu Rev Entomol, 2010. **55**: p. 95-110.
277. Leonova, G.N., et al., *Characterization of Powassan viruses from Far Eastern Russia.* Arch Virol, 2009. **154**(5): p. 811-20.
278. Hermance, M.E. and S. Thangamani, *Powassan Virus: An Emerging Arbovirus of Public Health Concern in North America.* Vector Borne Zoonotic Dis, 2017. **17**(7): p. 453-462.
279. McLean, D.M. and R.P. Larke, *Powassan and Silverwater viruses: ecology of two Ontario arboviruses.* Can Med Assoc J, 1963. **88**(4): p. 182-5.
280. McLean, D.M., et al., *Powassan Virus: Summer Infection Cycle, 1964.* Can Med Assoc J, 1964. **91**(26): p. 1360-2.
281. Smith, R.P., Jr., et al., *Diversity of tick species biting humans in an emerging area for Lyme disease.* Am J Public Health, 1992. **82**(1): p. 66-9.

282. Deardorff, E.R., et al., *Powassan virus in mammals, Alaska and New Mexico, U.S.A., and Russia, 2004-2007.* Emerg Infect Dis, 2013. **19**(12): p. 2012-6.
283. Ebel, G.D., et al., *Enzootic transmission of deer tick virus in New England and Wisconsin sites.* Am J Trop Med Hyg, 2000. **63**(1-2): p. 36-42.
284. Dupuis, A.P., 2nd, et al., *Isolation of deer tick virus (Powassan virus, lineage II) from Ixodes scapularis and detection of antibody in vertebrate hosts sampled in the Hudson Valley, New York State.* Parasit Vectors, 2013. **6**: p. 185.
285. Johnson, H.N., *Isolation of Powassan virus from a spotted skunk in California.* J Wildl Dis, 1987. **23**(1): p. 152-3.
286. McLean, D.M., A. Devos, and E.J. Quantz, *Powassan Virus: Field Investigations during the Summer of 1963.* Am J Trop Med Hyg, 1964. **13**: p. 747-53.
287. Main, A.J., A.B. Carey, and W.G. Downs, *Powassan virus in Ixodes cookei and Mustelidae in New England.* J Wildl Dis, 1979. **15**(4): p. 585-91.
288. Hinten, S.R., et al., *Increased recognition of Powassan encephalitis in the United States, 1999-2005.* Vector Borne Zoonotic Dis, 2008. **8**(6): p. 733-40.
289. Costero, A. and M.A. Grayson, *Experimental transmission of Powassan virus (Flaviviridae) by Ixodes scapularis ticks (Acari:Ixodidae).* Am J Trop Med Hyg, 1996. **55**(5): p. 536-46.
290. Woodall, J.P. and A. Roz, *Experimental milk-borne transmission of Powassan virus in the goat.* Am J Trop Med Hyg, 1977. **26**(1): p. 190-2.
291. Mathews-Martin, L., et al., *Persistence of Tick-Borne Encephalitis Virus in Goat and Cow Milks Under Different Storage Conditions and Following Thermal Inactivation.* Food Environ Virol, 2025. **17**(2): p. 26.
292. Mc, L.D. and W.L. Donohue, *Powassan virus: isolation of virus from a fatal case of encephalitis.* Can Med Assoc J, 1959. **80**(9): p. 708-11.
293. *Powassan Virus: Historic Data (2004-2022)*. 2023; Available from: https://www.cdc.gov/powassan/statistics-data/historic-data.html.
294. Mead, P., *Epidemiology of Lyme Disease.* Infect Dis Clin North Am, 2022. **36**(3): p. 495-521.
295. (CDC), C.f.D.C.a.P. *Lyme Disease, Lyme Disease Surveillance Data*. 2025 February 11, 2025 [cited 2025 October 20]; Available from: https://www.cdc.gov/lyme/data-research/facts-stats/surveillance-data-1.html.
296. Vogels, C.B.F., et al., *Phylogeographic reconstruction of the emergence and spread of Powassan virus in the northeastern United States.* Proc Natl Acad Sci U S A, 2023. **120**(16): p. e2218012120.
297. Alkishe, A., R.K. Raghavan, and A.T. Peterson, *Likely Geographic Distributional Shifts among Medically Important Tick Species and Tick-Associated Diseases under Climate Change in North America: A Review.* Insects, 2021. **12**(3).
298. Hassett, E.M. and S. Thangamani, *Ecology of Powassan Virus in the United States.* Microorganisms, 2021. **9**(11).
299. (CDC), C.f.D.C.a.P. *Powassan Virus, Historic Data (2004-2024)*. 2026 February 24, 2026 [cited 2025 March 19]; Available from: https://www.cdc.gov/powassan/data-maps/historic-data.html.

300. Telford, S.R., 3rd, et al., *A new tick-borne encephalitis-like virus infecting New England deer ticks, Ixodes dammini.* Emerg Infect Dis, 1997. **3**(2): p. 165-70.
301. Ebel, G.D., A. Spielman, and S.R. Telford, *Phylogeny of North American Powassan virus.* J Gen Virol, 2001. **82**(Pt 7): p. 1657-1665.
302. Kuno, G., et al., *Genomic sequencing of deer tick virus and phylogeny of powassan-related viruses of North America.* Am J Trop Med Hyg, 2001. **65**(5): p. 671-6.
303. Dai, X., et al., *A new subtype of eastern tick-borne encephalitis virus discovered in Qinghai-Tibet Plateau, China.* Emerg Microbes Infect, 2018. **7**(1): p. 74.
304. Bondaryuk, A.N., et al., *Phylogeography and Re-Evaluation of Evolutionary Rate of Powassan Virus Using Complete Genome Data.* Biology (Basel), 2021. **10**(12).
305. Pesko, K.N., et al., *Molecular epidemiology of Powassan virus in North America.* J Gen Virol, 2010. **91**(Pt 11): p. 2698-705.
306. Reynolds, E.S., et al., *Comparative Pathogenesis of Two Lineages of Powassan Virus Reveals Distinct Clinical Outcome, Neuropathology, and Inflammation.* Viruses, 2024. **16**(6).
307. Beasley, D.W., et al., *Nucleotide sequencing and serological evidence that the recently recognized deer tick virus is a genotype of Powassan virus.* Virus Res, 2001. **79**(1-2): p. 81-9.
308. Feder, H.M., et al., *Powassan Virus Encephalitis Following Brief Attachment of Connecticut Deer Ticks.* Clin Infect Dis, 2021. **73**(7): p. e2350-e2354.
309. Kapoor, T., et al., *Prevalence of Powassan Virus Seropositivity Among People with History of Lyme Disease and Non-Lyme Community Controls in the Northeastern United States.* Vector Borne Zoonotic Dis, 2024. **24**(4): p. 226-236.
310. Thomm, A.M., et al., *Development and Validation of a Serologic Test Panel for Detection of Powassan Virus Infection in U.S. Patients Residing in Regions Where Lyme Disease Is Endemic.* mSphere, 2018. **3**(1).
311. Vahey, G.M., et al., *Seroprevalence of Powassan Virus Infection in an Area Experiencing a Cluster of Disease Cases: Sussex County, New Jersey, 2019.* Open Forum Infect Dis, 2022. **9**(3): p. ofac023.
312. Smith, R.P., Jr., et al., *Seroprevalence of Borrelia burgdorferi, B. miyamotoi, and Powassan Virus in Residents Bitten by Ixodes Ticks, Maine, USA.* Emerg Infect Dis, 2019. **25**(4): p. 804-807.
313. Frost, H.M., et al., *Serologic Evidence of Powassan Virus Infection in Patients with Suspected Lyme Disease(1).* Emerg Infect Dis, 2017. **23**(8): p. 1384-1388.
314. Sack, A., et al., *Passive Surveillance of Human-Biting Ixodes scapularis Ticks in Massachusetts from 2015-2019.* Int J Environ Res Public Health, 2023. **20**(5).
315. Pak, D., S.B. Jacobs, and J.M. Sakamoto, *A 117-year retrospective analysis of Pennsylvania tick community dynamics.* Parasit Vectors, 2019. **12**(1): p. 189.
316. Kakoullis, L., et al., *Powassan Virus Infections: A Systematic Review of Published Cases.* Trop Med Infect Dis, 2023. **8**(12).
317. Prevention, C.f.D.C.a. *National Notifiable Diseases Surveillance System (NNDSS): Arboviral Diseases, Neuroinvasive and Non-neuroinvasive 2015 Case Definition*. 2015 April 16, 2021; Available from: https://ndc.services.cdc.gov/case-

definitions/arboviral-diseases-neuroinvasive-and-non-neuroinvasive-2015/#print.
318. Gross, C.P. and K.A. Sepkowitz, *The myth of the medical breakthrough: smallpox, vaccination, and Jenner reconsidered.* Int J Infect Dis, 1998. **3**(1): p. 54-60.
319. Gould, G.M., *Medical Discoveries by the Non-Medical.* JAMA, 1903.
320. Bonanni, P. and J.I. Santos, *Vaccine evolution.* Perspectives in Vaccinology, 2011. **1**(1): p. 1-24.
321. Salmon, D.E. and T. Smith. *On a new method of producing immunity from contagious diseases*.
322. Smith, T. and F.L. Kilborne. *Investigations Into the Nature, Causation, and Prevention of Texas or Southern Cattle Fever*. 2012.
323. Schultz, M.G., *Theobald Smith.* Emerging Infectious Diseases, 2008. **14**: p. 1940 - 1942.
324. Smith, K.A., *Louis pasteur, the father of immunology?* Front Immunol, 2012. **3**: p. 68.
325. D'Amelio, E., S. Salemi, and R. D'Amelio, *Anti-Infectious Human Vaccination in Historical Perspective.* Int Rev Immunol, 2016. **35**(3): p. 260-90.
326. Wright, J.G., et al., *Use of anthrax vaccine in the United States: recommendations of the Advisory Committee on Immunization Practices (ACIP), 2009.* MMWR. Recommendations and reports : Morbidity and mortality weekly report. Recommendations and reports, 2010. **59 RR-6**: p. 1-30.
327. Greenfield, W.S., *Anthrax. William Smith Greenfield, M.D., F.R.C.P., Professor Superintendent, The Brown Animal Sanatory Institution (1878–81) Concerning the priority due to him for the production of the first vaccine against anthrax.* Journal of Hygiene, 1980. **85**: p. 415 - 420.
328. Weller, T.H., F.C. Robbins, and J.F. Enders, *Cultivation of poliomyelitis virus in cultures of human foreskin and embryonic tissues.* Proc Soc Exp Biol Med, 1949. **72**(1): p. 153-5.
329. Enders, J.F., T.H. Weller, and F.C. Robbins, *Cultivation of the Lansing Strain of Poliomyelitis Virus in Cultures of Various Human Embryonic Tissues.* Science, 1949. **109**(2822): p. 85-7.
330. Brown, F., *Review of accidents caused by incomplete inactivation of viruses.* Dev Biol Stand, 1993. **81**: p. 103-7.
331. Offit, P.A., *The Cutter incident, 50 years later.* N Engl J Med, 2005. **352**(14): p. 1411-2.
332. Ramon, G. and R. Richou, *[Serum Anatoxytherapy Du Tetanus Declared].* Presse Med (1893), 1945. **53**: p. 277.
333. Glenny, A.T. and B.E. Hopkins, *Diphtheria Toxoid as an Immunising Agent.* Br J Exp Pathol, 1923. **4**(5): p. 283-8.
334. Peck, F.B., Jr., *Purified influenza virus vaccine. A study of viral reactivity and antigenicity.* JAMA, 1968. **206**(10): p. 2277-82.
335. Gross, P.A., et al., *A controlled double-blind comparison of reactogenicity, immunogenicity, and protective efficacy of whole-virus and split-product influenza vaccines in children.* J Infect Dis, 1977. **136**(5): p. 623-32.

336. Macleod, C.M., et al., *Prevention of Pneumococcal Pneumonia by Immunization with Specific Capsular Polysaccharides.* J Exp Med, 1945. **82**(6): p. 445-65.
337. Sato, Y., M. Kimura, and H. Fukumi, *Development of a pertussis component vaccine in Japan.* Lancet, 1984. **1**(8369): p. 122-6.
338. Nascimento, I.P. and L.C. Leite, *Recombinant vaccines and the development of new vaccine strategies.* Braz J Med Biol Res, 2012. **45**(12): p. 1102-11.
339. Valenzuela, P., et al., *Synthesis and assembly of hepatitis B virus surface antigen particles in yeast.* Nature, 1982. **298**(5872): p. 347-50.
340. Helgeson, J.S. *FDA Approves a Genetically Engineered Vaccine for Hepatitis B*. 2023 [cited 2025 October 21]; Available from: https://www.ebsco.com/research-starters/politics-and-government/fda-approves-genetically-engineered-vaccine-hepatitis-b?utm_source=chatgpt.com.
341. Berg, P. and J.E. Mertz, *Personal reflections on the origins and emergence of recombinant DNA technology.* Genetics, 2010. **184**(1): p. 9-17.
342. Burnet, F.M., *Specific Agglutination of Bacteriophage Particles.* Br J Exp Pathol, 1933. **14**(5): p. 302-8.
343. Hyman, P., G. Trubl, and S.T. Abedon, *Virus-Like Particle: Evolving Meanings in Different Disciplines.* Phage (New Rochelle), 2021. **2**(1): p. 11-15.
344. Mohsen, M.O. and M.F. Bachmann, *Virus-like particle vaccinology, from bench to bedside.* Cell Mol Immunol, 2022. **19**(9): p. 993-1011.
345. Chackerian, B., *Virus-like particles: flexible platforms for vaccine development.* Expert Rev Vaccines, 2007. **6**(3): p. 381-90.
346. Zabel, F., T.M. Kundig, and M.F. Bachmann, *Virus-induced humoral immunity: on how B cell responses are initiated.* Curr Opin Virol, 2013. **3**(3): p. 357-62.
347. Link, A., et al., *Innate immunity mediates follicular transport of particulate but not soluble protein antigen.* J Immunol, 2012. **188**(8): p. 3724-33.
348. Bachmann, M.F. and R.M. Zinkernagel, *Neutralizing antiviral B cell responses.* Annu Rev Immunol, 1997. **15**: p. 235-70.
349. Bessa, J., et al., *Low-affinity B cells transport viral particles from the lung to the spleen to initiate antibody responses.* Proc Natl Acad Sci U S A, 2012. **109**(50): p. 20566-71.
350. Roozendaal, R., et al., *Conduits mediate transport of low-molecular-weight antigen to lymph node follicles.* Immunity, 2009. **30**(2): p. 264-76.
351. Zepeda-Cervantes, J., J.O. Ramirez-Jarquin, and L. Vaca, *Interaction Between Virus-Like Particles (VLPs) and Pattern Recognition Receptors (PRRs) From Dendritic Cells (DCs): Toward Better Engineering of VLPs.* Front Immunol, 2020. **11**: p. 1100.
352. Buonaguro, L., et al., *Baculovirus-derived human immunodeficiency virus type 1 virus-like particles activate dendritic cells and induce ex vivo T-cell responses.* J Virol, 2006. **80**(18): p. 9134-43.
353. Nooraei, S., et al., *Virus-like particles: preparation, immunogenicity and their roles as nanovaccines and drug nanocarriers.* J Nanobiotechnology, 2021. **19**(1): p. 59.
354. Boigard, H., et al., *Zika virus-like particle (VLP) based vaccine.* PLoS Negl Trop Dis, 2017. **11**(5): p. e0005608.

355. Fan, Y.C., et al., *Formalin Inactivation of Japanese Encephalitis Virus Vaccine Alters the Antigenicity and Immunogenicity of a Neutralization Epitope in Envelope Protein Domain III.* PLoS Negl Trop Dis, 2015. **9**(10): p. e0004167.
356. Zhou, J., et al., *Expression of vaccinia recombinant HPV 16 L1 and L2 ORF proteins in epithelial cells is sufficient for assembly of HPV virion-like particles.* Virology, 1991. **185**(1): p. 251-7.
357. Siddiqui, M.A. and C.M. Perry, *Human papillomavirus quadrivalent (types 6, 11, 16, 18) recombinant vaccine (Gardasil).* Drugs, 2006. **66**(9): p. 1263-71; discussion 1272-3.
358. Stanley, M., *Tumour virus vaccines: hepatitis B virus and human papillomavirus.* Philos Trans R Soc Lond B Biol Sci, 2017. **372**(1732).
359. Office of Technology Transfer, O.o.I.R., National Institutes of Health. *HHS License-Based Vaccines & Therapeutics*. 2025 [cited 2025 October 22]; Available from: https://www.techtransfer.nih.gov/reports/hhs-license-based-vaccines-therapeutics?utm_source=chatgpt.com.
360. Qian, C., et al., *Recent Progress on the Versatility of Virus-Like Particles.* Vaccines (Basel), 2020. **8**(1).
361. Ioannidis, J.P.A., et al., *Global Estimates of Lives and Life-Years Saved by COVID-19 Vaccination During 2020-2024.* JAMA Health Forum, 2025. **6**(7): p. e252223.
362. Tang, J., M.A. Amin, and J.L. Campian, *Past, Present, and Future of Viral Vector Vaccine Platforms: A Comprehensive Review.* Vaccines (Basel), 2025. **13**(5).
363. Robinson, H.L. and C.A. Torres, *DNA vaccines.* Semin Immunol, 1997. **9**(5): p. 271-83.
364. Yang, K., *Accelerating vaccine development: Plug-and-play platforms for emerging infectious diseases.* Virus Res, 2025. **358**: p. 199601.
365. Vang, L., et al., *Zika virus-like particle vaccine protects AG129 mice and rhesus macaques against Zika virus.* PLoS Negl Trop Dis, 2021. **15**(3): p. e0009195.
366. Thoresen, D., et al., *A tetravalent dengue virus-like particle vaccine induces high levels of neutralizing antibodies and reduces dengue replication in non-human primates.* J Virol, 2024. **98**(5): p. e0023924.
367. Yang, L., et al., *A VLP-Based Vaccine Candidate Protects Mice against Japanese Encephalitis Virus Infection.* Vaccines (Basel), 2022. **10**(2).
368. Tang, J., et al., *Development of a novel virus-like particle-based vaccine for preventing tick-borne encephalitis virus infection.* Virol Sin, 2023. **38**(5): p. 767-777.
369. Shattock, A.J., et al., *Contribution of vaccination to improved survival and health: modelling 50 years of the Expanded Programme on Immunization.* Lancet, 2024. **403**(10441): p. 2307-2316.
370. Thucydides and R. Crawley, *The history of the Peloponnesian war*. 1876, London,: Longmans, Green, and co. xxxiii, 630 p.
371. von Behring, E. and S. Kitasato, *[The mechanism of diphtheria immunity and tetanus immunity in animals. 1890].* Mol Immunol, 1991. **28**(12): p. 1317, 1319-20.

372. Lindenmann, J., *Origin of the terms 'antibody' and 'antigen'.* Scand J Immunol, 1984. **19**(4): p. 281-5.
373. Araki, K. and R. Maeda, *A Brief Chronicle of Antibody Research and Technological Advances.* Antibodies (Basel), 2024. **13**(4).
374. Burnet, F.M., *A modification of Jerne's theory of antibody production using the concept of clonal selection.* CA Cancer J Clin, 1976. **26**(2): p. 119-21.
375. Janeway, C.A., Jr., *Approaching the asymptote? Evolution and revolution in immunology.* Cold Spring Harb Symp Quant Biol, 1989. **54 Pt 1**: p. 1-13.
376. Medzhitov, R., *Pattern recognition theory and the launch of modern innate immunity.* J Immunol, 2013. **191**(9): p. 4473-4.
377. Bretscher, P. and M. Cohn, *A theory of self-nonself discrimination.* Science, 1970. **169**(3950): p. 1042-9.
378. Medzhitov, R., P. Preston-Hurlburt, and C.A. Janeway, Jr., *A human homologue of the Drosophila Toll protein signals activation of adaptive immunity.* Nature, 1997. **388**(6640): p. 394-7.
379. Poltorak, A., et al., *Defective LPS signaling in C3H/HeJ and C57BL/10ScCr mice: mutations in Tlr4 gene.* Science, 1998. **282**(5396): p. 2085-8.
380. Wicherska-Pawlowska, K., T. Wrobel, and J. Rybka, *Toll-Like Receptors (TLRs), NOD-Like Receptors (NLRs), and RIG-I-Like Receptors (RLRs) in Innate Immunity. TLRs, NLRs, and RLRs Ligands as Immunotherapeutic Agents for Hematopoietic Diseases.* Int J Mol Sci, 2021. **22**(24).
381. Duan, T., et al., *Toll-Like Receptor Signaling and Its Role in Cell-Mediated Immunity.* Front Immunol, 2022. **13**: p. 812774.
382. Kadowaki, N., et al., *Subsets of human dendritic cell precursors express different toll-like receptors and respond to different microbial antigens.* J Exp Med, 2001. **194**(6): p. 863-9.
383. Simon-Fuentes, M., et al., *TLR7 Activation in M-CSF-Dependent Monocyte-Derived Human Macrophages Potentiates Inflammatory Responses and Prompts Neutrophil Recruitment.* J Innate Immun, 2023. **15**(1): p. 517-530.
384. Nagase, H., et al., *Expression and function of Toll-like receptors in eosinophils: activation by Toll-like receptor 7 ligand.* J Immunol, 2003. **171**(8): p. 3977-82.
385. Mansson, A., et al., *A distinct Toll-like receptor repertoire in human tonsillar B cells, directly activated by PamCSK, R-837 and CpG-2006 stimulation.* Immunology, 2006. **118**(4): p. 539-48.
386. Li, D. and M. Wu, *Pattern recognition receptors in health and diseases.* Signal Transduct Target Ther, 2021. **6**(1): p. 291.
387. Shi, Z., et al., *A novel Toll-like receptor that recognizes vesicular stomatitis virus.* J Biol Chem, 2011. **286**(6): p. 4517-24.
388. Andrade, W.A., et al., *Combined action of nucleic acid-sensing Toll-like receptors and TLR11/TLR12 heterodimers imparts resistance to Toxoplasma gondii in mice.* Cell Host Microbe, 2013. **13**(1): p. 42-53.
389. Kawai, T. and S. Akira, *The role of pattern-recognition receptors in innate immunity: update on Toll-like receptors.* Nat Immunol, 2010. **11**(5): p. 373-84.

390. Iwasaki, A., *A virological view of innate immune recognition.* Annu Rev Microbiol, 2012. **66**: p. 177-96.
391. Akashi-Takamura, S. and K. Miyake, *TLR accessory molecules.* Curr Opin Immunol, 2008. **20**(4): p. 420-5.
392. Murphy, K., et al., *Janeway's immunobiology*. 8th ed. 2012, New York: Garland Science. xix, 868 p.
393. Bonham, K.S., et al., *A promiscuous lipid-binding protein diversifies the subcellular sites of toll-like receptor signal transduction.* Cell, 2014. **156**(4): p. 705-16.
394. Nilsen, K.E., et al., *TIRAP/Mal Positively Regulates TLR8-Mediated Signaling via IRF5 in Human Cells.* Biomedicines, 2022. **10**(7).
395. Cao, W., et al., *Regulation of TLR7/9 responses in plasmacytoid dendritic cells by BST2 and ILT7 receptor interaction.* J Exp Med, 2009. **206**(7): p. 1603-14.
396. Takaoka, A., et al., *Integral role of IRF-5 in the gene induction programme activated by Toll-like receptors.* Nature, 2005. **434**(7030): p. 243-9.
397. Bender, A.T., et al., *TLR7 and TLR8 Differentially Activate the IRF and NF-kappaB Pathways in Specific Cell Types to Promote Inflammation.* Immunohorizons, 2020. **4**(2): p. 93-107.
398. Gorden, K.B., et al., *Synthetic TLR agonists reveal functional differences between human TLR7 and TLR8.* J Immunol, 2005. **174**(3): p. 1259-68.
399. Schoenemeyer, A., et al., *The interferon regulatory factor, IRF5, is a central mediator of toll-like receptor 7 signaling.* J Biol Chem, 2005. **280**(17): p. 17005-12.
400. Izaguirre, A., et al., *Comparative analysis of IRF and IFN-alpha expression in human plasmacytoid and monocyte-derived dendritic cells.* J Leukoc Biol, 2003. **74**(6): p. 1125-38.
401. Oshiumi, H., et al., *TICAM-1, an adaptor molecule that participates in Toll-like receptor 3-mediated interferon-beta induction.* Nat Immunol, 2003. **4**(2): p. 161-7.
402. Iwasaki, A. and R. Medzhitov, *Toll-like receptor control of the adaptive immune responses.* Nat Immunol, 2004. **5**(10): p. 987-95.
403. Berouti, M., et al., *Lysosomal endonuclease RNase T2 and PLD exonucleases cooperatively generate RNA ligands for TLR7 activation.* Immunity, 2024. **57**(7): p. 1482-1496 e8.
404. Greulich, W., et al., *TLR8 Is a Sensor of RNase T2 Degradation Products.* Cell, 2019. **179**(6): p. 1264-1275 e13.
405. Zhang, Z., et al., *Structural Analysis Reveals that Toll-like Receptor 7 Is a Dual Receptor for Guanosine and Single-Stranded RNA.* Immunity, 2016. **45**(4): p. 737-748.
406. Zhang, Z., et al., *Structural Analyses of Toll-like Receptor 7 Reveal Detailed RNA Sequence Specificity and Recognition Mechanism of Agonistic Ligands.* Cell Rep, 2018. **25**(12): p. 3371-3381 e5.
407. Tanji, H., et al., *Toll-like receptor 8 senses degradation products of single-stranded RNA.* Nat Struct Mol Biol, 2015. **22**(2): p. 109-15.
408. Hornung, V., et al., *Quantitative expression of toll-like receptor 1-10 mRNA in cellular subsets of human peripheral blood mononuclear cells and sensitivity to CpG oligodeoxynucleotides.* J Immunol, 2002. **168**(9): p. 4531-7.

409. Ketloy, C., et al., *Expression and function of Toll-like receptors on dendritic cells and other antigen presenting cells from non-human primates.* Vet Immunol Immunopathol, 2008. **125**(1-2): p. 18-30.
410. Jarrossay, D., et al., *Specialization and complementarity in microbial molecule recognition by human myeloid and plasmacytoid dendritic cells.* Eur J Immunol, 2001. **31**(11): p. 3388-93.
411. Krug, A., et al., *Toll-like receptor expression reveals CpG DNA as a unique microbial stimulus for plasmacytoid dendritic cells which synergizes with CD40 ligand to induce high amounts of IL-12.* Eur J Immunol, 2001. **31**(10): p. 3026-37.
412. Edwards, A.D., et al., *Toll-like receptor expression in murine DC subsets: lack of TLR7 expression by CD8 alpha+ DC correlates with unresponsiveness to imidazoquinolines.* Eur J Immunol, 2003. **33**(4): p. 827-33.
413. Cosgrove, H.A., et al., *B cell-intrinsic TLR7 expression drives severe lupus in TLR9-deficient mice.* JCI Insight, 2023. **8**(16).
414. Hinkelmann, L., et al., *Murine Toll-like receptor 8 is a nucleic acid multi-sensor detecting 2',3'-cyclic monophosphate guanosine as well as combinations of ribo-, deoxy-, cyclic nucleotides, and nucleosides.* bioRxiv, 2025.
415. Zhang, Z.J., et al., *TLR8 and its endogenous ligand miR-21 contribute to neuropathic pain in murine DRG.* J Exp Med, 2018. **215**(12): p. 3019-3037.
416. Frost, R.A., G.J. Nystrom, and C.H. Lang, *Lipopolysaccharide stimulates nitric oxide synthase-2 expression in murine skeletal muscle and C(2)C(12) myoblasts via Toll-like receptor-4 and c-Jun NH(2)-terminal kinase pathways.* Am J Physiol Cell Physiol, 2004. **287**(6): p. C1605-15.
417. Vaure, C. and Y. Liu, *A comparative review of toll-like receptor 4 expression and functionality in different animal species.* Front Immunol, 2014. **5**: p. 316.
418. Kawai, T., et al., *Decoding Toll-like receptors: Recent insights and perspectives in innate immunity.* Immunity, 2024. **57**(4): p. 649-673.
419. Modhiran, N., et al., *Dengue virus NS1 protein activates cells via Toll-like receptor 4 and disrupts endothelial cell monolayer integrity.* Sci Transl Med, 2015. **7**(304): p. 304ra142.
420. Chao, C.H., et al., *Dengue virus nonstructural protein 1 activates platelets via Toll-like receptor 4, leading to thrombocytopenia and hemorrhage.* PLoS Pathog, 2019. **15**(4): p. e1007625.
421. Crouse, J., U. Kalinke, and A. Oxenius, *Regulation of antiviral T cell responses by type I interferons.* Nat Rev Immunol, 2015. **15**(4): p. 231-42.
422. Barchet, W., et al., *Virus-induced interferon alpha production by a dendritic cell subset in the absence of feedback signaling in vivo.* J Exp Med, 2002. **195**(4): p. 507-16.
423. Boehm, U., et al., *Cellular responses to interferon-gamma.* Annu Rev Immunol, 1997. **15**: p. 749-95.
424. Perussia, B., *Lymphokine-activated killer cells, natural killer cells and cytokines.* Curr Opin Immunol, 1991. **3**(1): p. 49-55.
425. Temizoz, B. and K.J. Ishii, *Type I and II interferons toward ideal vaccine and immunotherapy.* Expert Rev Vaccines, 2021. **20**(5): p. 527-544.

426. Liu, Y.G., et al., *Interferon lambda in respiratory viral infection: immunomodulatory functions and antiviral effects in epithelium.* Front Immunol, 2024. **15**: p. 1338096.
427. Nguyen, K.B., et al., *Critical role for STAT4 activation by type 1 interferons in the interferon-gamma response to viral infection.* Science, 2002. **297**(5589): p. 2063-6.
428. Wang, L., et al., *The multiple roles of interferon regulatory factor family in health and disease.* Signal Transduct Target Ther, 2024. **9**(1): p. 282.
429. Platanias, L.C., *Mechanisms of type-I- and type-II-interferon-mediated signalling.* Nat Rev Immunol, 2005. **5**(5): p. 375-86.
430. Ronnblom, L. and D. Leonard, *Interferon pathway in SLE: one key to unlocking the mystery of the disease.* Lupus Sci Med, 2019. **6**(1): p. e000270.
431. Braun, D., I. Caramalho, and J. Demengeot, *IFN-alpha/beta enhances BCR-dependent B cell responses.* Int Immunol, 2002. **14**(4): p. 411-9.
432. Gallucci, S., M. Lolkema, and P. Matzinger, *Natural adjuvants: endogenous activators of dendritic cells.* Nat Med, 1999. **5**(11): p. 1249-55.
433. Cho, H.J., et al., *IFN-alpha beta promote priming of antigen-specific CD8+ and CD4+ T lymphocytes by immunostimulatory DNA-based vaccines.* J Immunol, 2002. **168**(10): p. 4907-13.
434. Le Bon, A., et al., *Direct stimulation of T cells by type I IFN enhances the CD8+ T cell response during cross-priming.* J Immunol, 2006. **176**(8): p. 4682-9.
435. Le Bon, A., et al., *Cross-priming of CD8+ T cells stimulated by virus-induced type I interferon.* Nat Immunol, 2003. **4**(10): p. 1009-15.
436. Sikora, A.G., et al., *IFN-alpha enhances peptide vaccine-induced CD8+ T cell numbers, effector function, and antitumor activity.* J Immunol, 2009. **182**(12): p. 7398-407.
437. Dahlgren, M.W., et al., *Type I Interferons Promote Germinal Centers Through B Cell Intrinsic Signaling and Dendritic Cell Dependent Th1 and Tfh Cell Lineages.* Front Immunol, 2022. **13**: p. 932388.
438. De Giovanni, M., et al., *Spatiotemporal regulation of type I interferon expression determines the antiviral polarization of CD4(+) T cells.* Nat Immunol, 2020. **21**(3): p. 321-330.
439. Santini, S.M., et al., *Type I interferon as a powerful adjuvant for monocyte-derived dendritic cell development and activity in vitro and in Hu-PBL-SCID mice.* J Exp Med, 2000. **191**(10): p. 1777-88.
440. Parlato, S., et al., *Expression of CCR-7, MIP-3beta, and Th-1 chemokines in type I IFN-induced monocyte-derived dendritic cells: importance for the rapid acquisition of potent migratory and functional activities.* Blood, 2001. **98**(10): p. 3022-9.
441. Le Bon, A., et al., *Cutting edge: enhancement of antibody responses through direct stimulation of B and T cells by type I IFN.* J Immunol, 2006. **176**(4): p. 2074-8.
442. Zhu, J., X. Huang, and Y. Yang, *Type I IFN signaling on both B and CD4 T cells is required for protective antibody response to adenovirus.* J Immunol, 2007. **178**(6): p. 3505-10.

443. Le Bon, A., et al., *Type i interferons potently enhance humoral immunity and can promote isotype switching by stimulating dendritic cells in vivo.* Immunity, 2001. **14**(4): p. 461-70.
444. Villadangos, J.A. and L. Young, *Antigen-presentation properties of plasmacytoid dendritic cells.* Immunity, 2008. **29**(3): p. 352-61.
445. Kim, T.H., et al., *Plasmacytoid Dendritic Cells Contribute to the Production of IFN-beta via TLR7-MyD88-Dependent Pathway and CTL Priming during Respiratory Syncytial Virus Infection.* Viruses, 2019. **11**(8).
446. Swiecki, M., et al., *Plasmacytoid dendritic cell ablation impacts early interferon responses and antiviral NK and CD8(+) T cell accrual.* Immunity, 2010. **33**(6): p. 955-66.
447. Bekeredjian-Ding, I.B., et al., *Plasmacytoid dendritic cells control TLR7 sensitivity of naive B cells via type I IFN.* J Immunol, 2005. **174**(7): p. 4043-50.
448. Audsley, K.M., et al., *IFNbeta Is a Potent Adjuvant for Cancer Vaccination Strategies.* Front Immunol, 2021. **12**: p. 735133.
449. Bracci, L., et al., *Type I IFN as a vaccine adjuvant for both systemic and mucosal vaccination against influenza virus.* Vaccine, 2006. **24 Suppl 2**: p. S2-56-7.
450. Tovey, M.G. and C. Lallemand, *Safety, Tolerability, and Immunogenicity of Interferons.* Pharmaceuticals (Basel), 2010. **3**(4): p. 1162-1186.
451. Kayesh, M.E.H., M. Kohara, and K. Tsukiyama-Kohara, *TLR agonists as vaccine adjuvants in the prevention of viral infections: an overview.* Front Microbiol, 2023. **14**: p. 1249718.
452. Hilligan, K.L. and F. Ronchese, *Antigen presentation by dendritic cells and their instruction of CD4+ T helper cell responses.* Cell Mol Immunol, 2020. **17**(6): p. 587-599.
453. Schuler, G. and R.M. Steinman, *Murine epidermal Langerhans cells mature into potent immunostimulatory dendritic cells in vitro.* J Exp Med, 1985. **161**(3): p. 526-46.
454. Kambayashi, T. and T.M. Laufer, *Atypical MHC class II-expressing antigen-presenting cells: can anything replace a dendritic cell?* Nat Rev Immunol, 2014. **14**(11): p. 719-30.
455. Blum, J.S., P.A. Wearsch, and P. Cresswell, *Pathways of antigen processing.* Annu Rev Immunol, 2013. **31**: p. 443-73.
456. Carroll, S.L., C. Pasare, and G.M. Barton, *Control of adaptive immunity by pattern recognition receptors.* Immunity, 2024. **57**(4): p. 632-648.
457. Cheng, Z., et al., *Nanomaterial-Based Drug Delivery System Targeting Lymph Nodes.* Pharmaceutics, 2022. **14**(7).
458. Lee, H.G., M.J. Cho, and J.M. Choi, *Author Correction: Bystander CD4(+) T cells: crossroads between innate and adaptive immunity.* Exp Mol Med, 2023. **55**(6): p. 1275.
459. O'Shea, J.J. and W.E. Paul, *Mechanisms underlying lineage commitment and plasticity of helper CD4+ T cells.* Science, 2010. **327**(5969): p. 1098-102.
460. Groux, H., et al., *A CD4+ T-cell subset inhibits antigen-specific T-cell responses and prevents colitis.* Nature, 1997. **389**(6652): p. 737-42.

461. Veldhoen, M., et al., *Transforming growth factor-beta 'reprograms' the differentiation of T helper 2 cells and promotes an interleukin 9-producing subset.* Nat Immunol, 2008. **9**(12): p. 1341-6.
462. Eyerich, S., et al., *Th22 cells represent a distinct human T cell subset involved in epidermal immunity and remodeling.* J Clin Invest, 2009. **119**(12): p. 3573-85.
463. Trifari, S., et al., *Identification of a human helper T cell population that has abundant production of interleukin 22 and is distinct from T(H)-17, T(H)1 and T(H)2 cells.* Nat Immunol, 2009. **10**(8): p. 864-71.
464. Araujo-Pires, A.C., et al., *Simultaneous analysis of T helper subsets (Th1, Th2, Th9, Th17, Th22, Tfh, Tr1 and Tregs) markers expression in periapical lesions reveals multiple cytokine clusters accountable for lesions activity and inactivity status.* J Appl Oral Sci, 2014. **22**(4): p. 336-46.
465. Gilmour, B.C., A. Corthay, and I. Oynebraten, *High production of IL-12 by human dendritic cells stimulated with combinations of pattern-recognition receptor agonists.* NPJ Vaccines, 2024. **9**(1): p. 83.
466. Schoenborn, J.R. and C.B. Wilson, *Regulation of interferon-gamma during innate and adaptive immune responses.* Adv Immunol, 2007. **96**: p. 41-101.
467. Martin-Fontecha, A., et al., *Induced recruitment of NK cells to lymph nodes provides IFN-gamma for T(H)1 priming.* Nat Immunol, 2004. **5**(12): p. 1260-5.
468. Zundler, S. and M.F. Neurath, *Interleukin-12: Functional activities and implications for disease.* Cytokine Growth Factor Rev, 2015. **26**(5): p. 559-68.
469. Allen, J.E. and T.E. Sutherland, *Host protective roles of type 2 immunity: parasite killing and tissue repair, flip sides of the same coin.* Semin Immunol, 2014. **26**(4): p. 329-40.
470. Yoshimoto, T., *The Hunt for the Source of Primary Interleukin-4: How We Discovered That Natural Killer T Cells and Basophils Determine T Helper Type 2 Cell Differentiation In Vivo.* Front Immunol, 2018. **9**: p. 716.
471. Perrigoue, J.G., et al., *MHC class II-dependent basophil-CD4+ T cell interactions promote T(H)2 cytokine-dependent immunity.* Nat Immunol, 2009. **10**(7): p. 697-705.
472. Sokol, C.L., et al., *Basophils function as antigen-presenting cells for an allergen-induced T helper type 2 response.* Nat Immunol, 2009. **10**(7): p. 713-20.
473. Korn, T., et al., *IL-17 and Th17 Cells.* Annu Rev Immunol, 2009. **27**: p. 485-517.
474. contributors, W. *Antibody*. 2025 [cited 2025 October 27]; Available from: https://en.wikipedia.org/wiki/Antibody.
475. Cousin, V.N., et al., *Lymphoid stromal cells - potential implications for the pathogenesis of CVID.* Front Immunol, 2023. **14**: p. 1122905.
476. Krimpenfort, L.T., S.E. Degn, and B.A. Heesters, *The follicular dendritic cell: At the germinal center of autoimmunity?* Cell Rep, 2024. **43**(3): p. 113869.
477. Phan, T.G., et al., *Immune complex relay by subcapsular sinus macrophages and noncognate B cells drives antibody affinity maturation.* Nat Immunol, 2009. **10**(7): p. 786-93.
478. Heath, W.R., et al., *Antigen presentation by dendritic cells for B cell activation.* Curr Opin Immunol, 2019. **58**: p. 44-52.

479. Cyster, J.G., et al., *Follicular stromal cells and lymphocyte homing to follicles.* Immunol Rev, 2000. **176**: p. 181-93.
480. Rodda, L.B., et al., *Single-Cell RNA Sequencing of Lymph Node Stromal Cells Reveals Niche-Associated Heterogeneity.* Immunity, 2018. **48**(5): p. 1014-1028 e6.
481. Song, W. and J. Craft, *T follicular helper cell heterogeneity: Time, space, and function.* Immunol Rev, 2019. **288**(1): p. 85-96.
482. Wishnie, A.J., et al., *BCR Affinity Influences T-B Interactions and B Cell Development in Secondary Lymphoid Organs.* Front Immunol, 2021. **12**: p. 703918.
483. Liu, X., R.I. Nurieva, and C. Dong, *Transcriptional regulation of follicular T-helper (Tfh) cells.* Immunol Rev, 2013. **252**(1): p. 139-45.
484. Kroenke, M.A., et al., *Bcl6 and Maf cooperate to instruct human follicular helper CD4 T cell differentiation.* J Immunol, 2012. **188**(8): p. 3734-44.
485. Parrish-Novak, J., et al., *Interleukin 21 and its receptor are involved in NK cell expansion and regulation of lymphocyte function.* Nature, 2000. **408**(6808): p. 57-63.
486. Elsner, R.A. and M.J. Shlomchik, *Germinal Center and Extrafollicular B Cell Responses in Vaccination, Immunity, and Autoimmunity.* Immunity, 2020. **53**(6): p. 1136-1150.
487. Fink, K., *Origin and Function of Circulating Plasmablasts during Acute Viral Infections.* Front Immunol, 2012. **3**: p. 78.
488. MacLennan, I.C., et al., *Extrafollicular antibody responses.* Immunol Rev, 2003. **194**: p. 8-18.
489. Henry, B. and B.J. Laidlaw, *Functional heterogeneity in the memory B-cell response.* Curr Opin Immunol, 2023. **80**: p. 102281.
490. Ma, X. and S. Nakayamada, *Multi-Source Pathways of T Follicular Helper Cell Differentiation.* Front Immunol, 2021. **12**: p. 621105.
491. Collins, A.M., *IgG subclass co-expression brings harmony to the quartet model of murine IgG function.* Immunol Cell Biol, 2016. **94**(10): p. 949-954.
492. Snapper, C.M. and W.E. Paul, *Interferon-gamma and B cell stimulatory factor-1 reciprocally regulate Ig isotype production.* Science, 1987. **236**(4804): p. 944-7.
493. Reinhardt, R.L., H.E. Liang, and R.M. Locksley, *Cytokine-secreting follicular T cells shape the antibody repertoire.* Nat Immunol, 2009. **10**(4): p. 385-93.
494. Hirota, K., et al., *Plasticity of Th17 cells in Peyer's patches is responsible for the induction of T cell-dependent IgA responses.* Nat Immunol, 2013. **14**(4): p. 372-9.
495. Lan, J., et al., *Basic Properties and Development Status of Aluminum Adjuvants Used for Vaccines.* Vaccines (Basel), 2024. **12**(10).
496. Facciola, A., et al., *An Overview of Vaccine Adjuvants: Current Evidence and Future Perspectives.* Vaccines (Basel), 2022. **10**(5).
497. Chippaux, J.P., *Gaston Ramon's Big Four.* Toxins (Basel), 2024. **16**(1).
498. Ramon, G., *Sur le traitement sérique spécifique des plaies infectées.* Bulletin de la Société centrale de médecine vétérinaire, 1913. **67**: p. 166-167.
499. Ramon, G., *Sur l'augmentation anormale de l'antitoxine chez les chevaux producteurs de sérum antidiphtérique.* Bulletin de la Société centrale de médecine vétérinaire, 1925. **101**: p. 227-234.

500. Ramon, G., *Sur un procédé d'immunisation antitoxique et de production des antitoxines.* Bulletin de la Société centrale de médecine vétérinaire, 1925. **101**: p. 348-351.
501. Glenny, A.T., et al., *Immunological Notes: XVII–XXIV.* Journal of Pathology and Bacteriology, 1926. **29**: p. 38-39.
502. Park, W.H. and M.C. Schroder, *Diphtheria Toxin-Antitoxin and Toxoid : A Comparison.* Am J Public Health Nations Health, 1932. **22**(1): p. 7-16.
503. White, J.L. and E.A. Schlageter, *DIPHTHERIA TOXOID*
COMPARATIVE IMMUNIZING VALUE WITH AND WITH-OUT ALUM, AS INDICATED BY THE SCHICK TEST. JAMA, 1934. **102**: p. 12.
504. Kendrick, P.L., *Use of Alum-Treated Pertussis Vaccine, and of Alum-Precipitated Combined Pertussis Vaccine and Diphtheria Toxoid, for Active Immunization.* Am J Public Health Nations Health, 1942. **32**(6): p. 615-26.
505. Bergey, D.H., *Active Immunization against Tetanus Infection with Tetanus Toxoid.* The Journal of Infectious Diseases, 1934. **55**: p. 72-78.
506. Alving, C.R., et al., *Adjuvants for vaccines to drugs of abuse and addiction.* Vaccine, 2014. **32**(42): p. 5382-9.
507. Martinon, S., et al., *Chemical and Immunological Characteristics of Aluminum-Based, Oil-Water Emulsion, and Bacterial-Origin Adjuvants.* J Immunol Res, 2019. **2019**: p. 3974127.
508. Masson, J.D., et al., *Calcium phosphate: a substitute for aluminum adjuvants?* Expert Rev Vaccines, 2017. **16**(3): p. 289-299.
509. Glenny, A.T., G.A.H. Buttle, and M.F. Stevens, *Rate of disappearance of diphtheria toxoid injected into rabbits and guinea - pigs: Toxoid precipitated with alum.* The Journal of Pathology and Bacteriology, 1931. **34**: p. 267-275.
510. Harrison, W.T., *Some Observations on the Use of Alum Precipitated Diphtheria Toxoid.* Am J Public Health Nations Health, 1935. **25**(3): p. 298-300.
511. Hutchison, S., et al., *Antigen depot is not required for alum adjuvanticity.* FASEB J, 2012. **26**(3): p. 1272-9.
512. Heimlich, J.M., et al., *The in vitro displacement of adsorbed model antigens from aluminium-containing adjuvants by interstitial proteins.* Vaccine, 1999. **17**(22): p. 2873-81.
513. Gupta, R.K., et al., *In vivo distribution of radioactivity in mice after injection of biodegradable polymer microspheres containing 14C-labeled tetanus toxoid.* Vaccine, 1996. **14**(15): p. 1412-6.
514. Eisenbarth, S.C., et al., *Crucial role for the Nalp3 inflammasome in the immunostimulatory properties of aluminium adjuvants.* Nature, 2008. **453**(7198): p. 1122-6.
515. Li, H., S. Nookala, and F. Re, *Aluminum hydroxide adjuvants activate caspase-1 and induce IL-1beta and IL-18 release.* J Immunol, 2007. **178**(8): p. 5271-6.
516. Kool, M., et al., *Alum adjuvant boosts adaptive immunity by inducing uric acid and activating inflammatory dendritic cells.* J Exp Med, 2008. **205**(4): p. 869-82.

517. Franchi, L. and G. Nunez, *The Nlrp3 inflammasome is critical for aluminium hydroxide-mediated IL-1beta secretion but dispensable for adjuvant activity.* Eur J Immunol, 2008. **38**(8): p. 2085-9.
518. McKee, A.S., et al., *Alum induces innate immune responses through macrophage and mast cell sensors, but these sensors are not required for alum to act as an adjuvant for specific immunity.* J Immunol, 2009. **183**(7): p. 4403-14.
519. Marichal, T., et al., *DNA released from dying host cells mediates aluminum adjuvant activity.* Nat Med, 2011. **17**(8): p. 996-1002.
520. McKee, A.S., et al., *Host DNA released in response to aluminum adjuvant enhances MHC class II-mediated antigen presentation and prolongs CD4 T-cell interactions with dendritic cells.* Proc Natl Acad Sci U S A, 2013. **110**(12): p. E1122-31.
521. Stephen, J., et al., *Neutrophil swarming and extracellular trap formation play a significant role in Alum adjuvant activity.* NPJ Vaccines, 2017. **2**: p. 1.
522. Jordan, M.B., et al., *Promotion of B cell immune responses via an alum-induced myeloid cell population.* Science, 2004. **304**(5678): p. 1808-10.
523. Mannhalter, J.W., et al., *Modulation of the human immune response by the non-toxic and non-pyrogenic adjuvant aluminium hydroxide: effect on antigen uptake and antigen presentation.* Clin Exp Immunol, 1985. **61**(1): p. 143-51.
524. He, P., Y. Zou, and Z. Hu, *Advances in aluminum hydroxide-based adjuvant research and its mechanism.* Hum Vaccin Immunother, 2015. **11**(2): p. 477-88.
525. Marrack, P., A.S. McKee, and M.W. Munks, *Towards an understanding of the adjuvant action of aluminium.* Nat Rev Immunol, 2009. **9**(4): p. 287-93.
526. Pellegrina, D., et al., *Transcriptional Systems Vaccinology Approaches for Vaccine Adjuvant Profiling.* Vaccines (Basel), 2025. **13**(1).
527. Xing, J., et al., *The recent advances in vaccine adjuvants.* Front Immunol, 2025. **16**: p. 1557415.
528. Azarpanah, H., et al., *Vaccine hesitancy: evidence from an adverse events following immunization database, and the role of cognitive biases.* BMC Public Health, 2021. **21**(1): p. 1686.
529. Grun, J.L. and P.H. Maurer, *Different T helper cell subsets elicited in mice utilizing two different adjuvant vehicles: the role of endogenous interleukin 1 in proliferative responses.* Cell Immunol, 1989. **121**(1): p. 134-45.
530. Imran, M., et al., *Relative Effectiveness of the MF59-Adjuvanted Influenza Vaccine Versus High-Dose Influenza Vaccine in Older Adults With Influenza Risk Factors During the 2019-2020 US Influenza Season.* Open Forum Infect Dis, 2024. **11**(8): p. ofae459.
531. Cruz-Valdez, A., et al., *MF59-adjuvanted influenza vaccine (FLUAD(R)) elicits higher immune responses than a non-adjuvanted influenza vaccine (Fluzone(R)): A randomized, multicenter, Phase III pediatric trial in Mexico.* Hum Vaccin Immunother, 2018. **14**(2): p. 386-395.
532. *Vaccinology and Methods in Vaccine Research*. First ed. Developments in Immunology. 2022: Academic Press (Elsevier).
533. Roman, F., et al., *Adjuvant system AS01: from mode of action to effective vaccines.* Expert Rev Vaccines, 2024. **23**(1): p. 715-729.

534. Zhao, T., et al., *Vaccine adjuvants: mechanisms and platforms.* Signal Transduct Target Ther, 2023. **8**(1): p. 283.
535. O'Hagan, D.T., et al., *"World in motion" - emulsion adjuvants rising to meet the pandemic challenges.* NPJ Vaccines, 2021. **6**(1): p. 158.
536. Vono, M., et al., *The adjuvant MF59 induces ATP release from muscle that potentiates response to vaccination.* Proc Natl Acad Sci U S A, 2013. **110**(52): p. 21095-100.
537. Cioncada, R., et al., *Vaccine adjuvant MF59 promotes the intranodal differentiation of antigen-loaded and activated monocyte-derived dendritic cells.* PLoS One, 2017. **12**(10): p. e0185843.
538. Lofano, G., et al., *Oil-in-Water Emulsion MF59 Increases Germinal Center B Cell Differentiation and Persistence in Response to Vaccination.* J Immunol, 2015. **195**(4): p. 1617-27.
539. Cantisani, R., et al., *Vaccine adjuvant MF59 promotes retention of unprocessed antigen in lymph node macrophage compartments and follicular dendritic cells.* J Immunol, 2015. **194**(4): p. 1717-25.
540. Foged, C., et al., *Interaction of dendritic cells with antigen-containing liposomes: effect of bilayer composition.* Vaccine, 2004. **22**(15-16): p. 1903-13.
541. Henriksen-Lacey, M., et al., *Liposomal cationic charge and antigen adsorption are important properties for the efficient deposition of antigen at the injection site and ability of the vaccine to induce a CMI response.* J Control Release, 2010. **145**(2): p. 102-8.
542. Coccia, M., et al., *Cellular and molecular synergy in AS01-adjuvanted vaccines results in an early IFNgamma response promoting vaccine immunogenicity.* NPJ Vaccines, 2017. **2**: p. 25.
543. Centers for Disease, C. and Prevention, *FDA licensure of bivalent human papillomavirus vaccine (HPV2, Cervarix) for use in females and updated HPV vaccination recommendations from the Advisory Committee on Immunization Practices (ACIP).* MMWR Morb Mortal Wkly Rep, 2010. **59**(20): p. 626-9.
544. Didierlaurent, A.M., et al., *AS04, an aluminum salt- and TLR4 agonist-based adjuvant system, induces a transient localized innate immune response leading to enhanced adaptive immunity.* J Immunol, 2009. **183**(10): p. 6186-97.
545. Giannini, S.L., et al., *Enhanced humoral and memory B cellular immunity using HPV16/18 L1 VLP vaccine formulated with the MPL/aluminium salt combination (AS04) compared to aluminium salt only.* Vaccine, 2006. **24**(33-34): p. 5937-49.
546. Lee, G.H. and S.G. Lim, *CpG-Adjuvanted Hepatitis B Vaccine (HEPLISAV-B(R)) Update.* Expert Rev Vaccines, 2021. **20**(5): p. 487-495.
547. Kundi, M., *New hepatitis B vaccine formulated with an improved adjuvant system.* Expert Rev Vaccines, 2007. **6**(2): p. 133-40.
548. Einstein, M.H., et al., *Comparison of the immunogenicity and safety of Cervarix and Gardasil human papillomavirus (HPV) cervical cancer vaccines in healthy women aged 18-45 years.* Hum Vaccin, 2009. **5**(10): p. 705-19.
549. Kuzmich, N.N., et al., *TLR4 Signaling Pathway Modulators as Potential Therapeutics in Inflammation and Sepsis.* Vaccines (Basel), 2017. **5**(4).

550. Qureshi, N., K. Takayama, and E. Ribi, *Purification and structural determination of nontoxic lipid A obtained from the lipopolysaccharide of Salmonella typhimurium.* J Biol Chem, 1982. **257**(19): p. 11808-15.
551. Ribi, E., et al., *Peptides as requirement for immunotherapy of the guinea-pig line-10 tumor with endotoxins.* Cancer Immunology, Immunotherapy, 1979. **7**: p. 43-58.
552. Casella, C.R. and T.C. Mitchell, *Putting endotoxin to work for us: monophosphoryl lipid A as a safe and effective vaccine adjuvant.* Cell Mol Life Sci, 2008. **65**(20): p. 3231-40.
553. Sasaki, S., et al., *Monophosphoryl lipid A enhances both humoral and cell-mediated immune responses to DNA vaccination against human immunodeficiency virus type 1.* Infect Immun, 1997. **65**(9): p. 3520-8.
554. Johansen, K., U. Schroder, and L. Svensson, *Immunogenicity and protective efficacy of a formalin-inactivated rotavirus vaccine combined with lipid adjuvants.* Vaccine, 2003. **21**(5-6): p. 368-75.
555. Samuel, J., et al., *Immunogenicity and antitumor activity of a liposomal MUC1 peptide-based vaccine.* Int J Cancer, 1998. **75**(2): p. 295-302.
556. Richards, R.L., et al., *Liposomes containing lipid A serve as an adjuvant for induction of antibody and cytotoxic T-cell responses against RTS,S malaria antigen.* Infect Immun, 1998. **66**(6): p. 2859-65.
557. Coler, R.N., et al., *Immunization with a polyprotein vaccine consisting of the T-Cell antigens thiol-specific antioxidant, Leishmania major stress-inducible protein 1, and Leishmania elongation initiation factor protects against leishmaniasis.* Infect Immun, 2002. **70**(8): p. 4215-25.
558. Qiao, M., et al., *Hepatitis C virus-like particles combined with novel adjuvant systems enhance virus-specific immune responses.* Hepatology, 2003. **37**(1): p. 52-9.
559. Carter, D., et al., *The success of toll-like receptor 4 based vaccine adjuvants.* Vaccine, 2025. **61**: p. 127413.
560. Garçon, N., G. Leroux-Roels, and W.-F. Cheng, *Vaccine adjuvants.* Perspectives in Vaccinology, 2011. **1**(1): p. 89-113.
561. Bhagchandani, S., J.A. Johnson, and D.J. Irvine, *Evolution of Toll-like receptor 7/8 agonist therapeutics and their delivery approaches: From antiviral formulations to vaccine adjuvants.* Adv Drug Deliv Rev, 2021. **175**: p. 113803.
562. Hemmi, H., et al., *Small anti-viral compounds activate immune cells via the TLR7 MyD88-dependent signaling pathway.* Nat Immunol, 2002. **3**(2): p. 196-200.
563. Patinote, C., et al., *Agonist and antagonist ligands of toll-like receptors 7 and 8: Ingenious tools for therapeutic purposes.* Eur J Med Chem, 2020. **193**: p. 112238.
564. Gibson, S.J., et al., *Plasmacytoid dendritic cells produce cytokines and mature in response to the TLR7 agonists, imiquimod and resiquimod.* Cell Immunol, 2002. **218**(1-2): p. 74-86.
565. Jurk, M., et al., *Human TLR7 or TLR8 independently confer responsiveness to the antiviral compound R-848.* Nat Immunol, 2002. **3**(6): p. 499.

566. Burns, R.P., Jr., et al., *The imidazoquinolines, imiquimod and R-848, induce functional, but not phenotypic, maturation of human epidermal Langerhans' cells.* Clin Immunol, 2000. **94**(1): p. 13-23.
567. Miller, S.M., et al., *Novel Lipidated Imidazoquinoline TLR7/8 Adjuvants Elicit Influenza-Specific Th1 Immune Responses and Protect Against Heterologous H3N2 Influenza Challenge in Mice.* Front Immunol, 2020. **11**: p. 406.
568. Smirnov, D., et al., *Vaccine adjuvant activity of 3M-052: an imidazoquinoline designed for local activity without systemic cytokine induction.* Vaccine, 2011. **29**(33): p. 5434-42.
569. Van Hoeven, N., et al., *A Formulated TLR7/8 Agonist is a Flexible, Highly Potent and Effective Adjuvant for Pandemic Influenza Vaccines.* Sci Rep, 2017. **7**: p. 46426.
570. Dowling, D.J., et al., *TLR7/8 adjuvant overcomes newborn hyporesponsiveness to pneumococcal conjugate vaccine at birth.* JCI Insight, 2017. **2**(6): p. e91020.
571. Mehravaran, A., et al., *Immunogenicity and protection effects of cationic liposome containing imiquimod adjuvant on leishmaniasis in BALB/c mice.* Iran J Basic Med Sci, 2019. **22**(8): p. 922-931.
572. Miller, S.M., et al., *A lipidated TLR7/8 adjuvant enhances the efficacy of a vaccine against fentanyl in mice.* NPJ Vaccines, 2023. **8**(1): p. 97.
573. Schon, M.P. and M. Schon, *TLR7 and TLR8 as targets in cancer therapy.* Oncogene, 2008. **27**(2): p. 190-9.
574. Dotiwala, F. and A.K. Upadhyay, *A comprehensive review of BBV152 vaccine development, effectiveness, safety, challenges, and prospects.* Front Immunol, 2022. **13**: p. 940715.
575. Siram, K., et al., *Co-Delivery of Novel Synthetic TLR4 and TLR7/8 Ligands Adsorbed to Aluminum Salts Promotes Th1-Mediated Immunity against Poorly Immunogenic SARS-CoV-2 RBD.* Vaccines (Basel), 2023. **12**(1).
576. Miller, S.M., et al., *A first-in-human phase 1 clinical trial of INI-4001, a novel TLR7/8 agonist, in patients with advanced solid tumors.* Journal of Clinical Oncology, 2025.
577. Short, K.K., et al., *Using Dual Toll-like Receptor Agonism to Drive Th1-Biased Response in a Squalene- and alpha-Tocopherol-Containing Emulsion for a More Effective SARS-CoV-2 Vaccine.* Pharmaceutics, 2022. **14**(7).
578. Lathrop, S.K., et al., *Vaccination with ancestral SARS-CoV-2 spike adjuvanted with TLR agonists provides cross-protection against XBB.1.* Npj Viruses, 2024. **2**(1): p. 28.
579. Mehradnia, F., et al., *Encapsulation of the lipidated TLR7/8 agonist INI-4001 into ionic liposomes impacts H7 influenza antigen-specific immune responses.* Drug Deliv Transl Res, 2025.
580. Abdelwahab, W.M., et al., *Co-Delivery of a Novel Lipidated TLR7/8 Agonist and Hemagglutinin-Based Influenza Antigen Using Silica Nanoparticles Promotes Enhanced Immune Responses.* Pharmaceutics, 2024. **16**(1).
581. Zhang, X., H. Shi, and T.M. Ross, *Elicitation of protective immune responses against influenza a viruses in elderly ferrets by adjuvanted recombinant universal influenza hemagglutinin vaccines.* Immun Ageing, 2025. **22**(1): p. 41.

582. Crouse, B., et al., *A TLR7/8 agonist increases efficacy of anti-fentanyl vaccines in rodent and porcine models.* NPJ Vaccines, 2023. **8**(1): p. 107.
583. Hamid, F.A., et al., *A novel cationic liposome-formulated toll like receptor (TLR) 7/8 agonist enhances the efficacy of a vaccine against fentanyl toxicity.* J Control Release, 2025. **384**: p. 113901.
584. Roman-Cruz, V.C., et al., *Adjuvanted Vaccine Induces Functional Antibodies against Pseudomonas aeruginosa Filamentous Bacteriophages.* Vaccines (Basel), 2024. **12**(2).
585. Frierson, J.G., *The yellow fever vaccine: a history.* Yale J Biol Med, 2010. **83**(2): p. 77-85.
586. Unali, G. and F. Douam, *Orthoflavivirus Vaccine Platforms: Current Strategies and Challenges.* Vaccines (Basel), 2025. **13**(10).
587. Gotuzzo, E., S. Yactayo, and E. Cordova, *Efficacy and duration of immunity after yellow fever vaccination: systematic review on the need for a booster every 10 years.* Am J Trop Med Hyg, 2013. **89**(3): p. 434-44.
588. Lindsey, N.P., et al., *Adverse event reports following yellow fever vaccination, 2007-13.* J Travel Med, 2016. **23**(5).
589. Porudominsky, R. and E.H. Gotuzzo, *Yellow fever vaccine and risk of developing serious adverse events: a systematic review.* Rev Panam Salud Publica, 2018. **42**: p. e75.
590. Dutta, S.K. and T. Langenburg, *A Perspective on Current Flavivirus Vaccine Development: A Brief Review.* Viruses, 2023. **15**(4).
591. Davis, E.H., et al., *Japanese encephalitis virus live attenuated vaccine strains display altered immunogenicity, virulence and genetic diversity.* NPJ Vaccines, 2021. **6**(1): p. 112.
592. Das, M., *Brazil develops and rolls out single-dose dengue vaccine.* Lancet Microbe, 2026: p. 101387.
593. Gritsun, T.S., V.A. Lashkevich, and E.A. Gould, *Tick-borne encephalitis.* Antiviral Res, 2003. **57**(1-2): p. 129-46.
594. McArthur, M.A. and M.R. Holbrook, *Japanese Encephalitis Vaccines.* J Bioterror Biodef, 2011. **S1**: p. 2.
595. Marinaik, C.B., et al., *Adjuvantation of Kyasanur Forest Disease vaccine with TLR9 agonist CpG adjuvant enhances immunological efficacy and potency of the vaccine.* PLoS One, 2025. **20**(7): p. e0329348.
596. Vadrevu, K.M., et al., *Persistence of Immune Responses With an Inactivated Japanese Encephalitis Single-Dose Vaccine, JENVAC and Interchangeability With a Live-Attenuated Vaccine.* J Infect Dis, 2020. **222**(9): p. 1478-1487.
597. *JENVAC*. 2025 [cited 2026 March 19]; Available from: https://www.bharatbiotech.com/jenvac.html?
598. Wang, X., et al., *Effects of Adjuvants on the Immunogenicity and Efficacy of a Zika Virus Envelope Domain III Subunit Vaccine.* Vaccines (Basel), 2019. **7**(4).
599. Valdes, I., et al., *Addition of nucleotide adjuvants enhances the immunogenicity of a recombinant subunit vaccine against the Zika virus in BALB/c mice.* Vaccine, 2024. **42**(25): p. 126213.

600. Zimna, M., et al., *Influence of adjuvant type and route of administration on the immunogenicity of Leishmania-derived tick-borne encephalitis virus-like particles - A recombinant vaccine candidate.* Antiviral Res, 2024. **228**: p. 105941.
601. Rajaiah, P., *Kyasanur Forest Disease in India: innovative options for intervention.* Hum Vaccin Immunother, 2019. **15**(10): p. 2243-2248.
602. Kasabi, G.S., et al., *Coverage and effectiveness of Kyasanur forest disease (KFD) vaccine in Karnataka, South India, 2005-10.* PLoS Negl Trop Dis, 2013. **7**(1): p. e2025.
603. Dandawate, C.N., et al., *Field evaluation of formalin inactivated Kyasanur forest disease virus tissue culture vaccine in three districts of Karnataka state.* Indian J Med Res, 1994. **99**: p. 152-8.
604. Srikanth, U.G.K., et al., *Evaluation of Safety and Potency of Kyasanur Forest Disease (KFD) Vaccine Inactivated with Different Concentrations of Formalin and Comparative Evaluation of In Vitro and In Vivo Methods of Virus Titration in KFD Vaccine.* Biomedicines, 2023. **11**(7).
605. Kasabi, G.S., et al., *Kyasanur Forest disease, India, 2011-2012.* Emerg Infect Dis, 2013. **19**(2): p. 278-81.
606. Holbrook, M.R., et al., *An animal model for the tickborne flavivirus--Omsk hemorrhagic fever virus.* J Infect Dis, 2005. **191**(1): p. 100-8.
607. Sawatsky, B., et al., *Comparative pathogenesis of Alkhumra hemorrhagic fever and Kyasanur forest disease viruses in a mouse model.* PLoS Negl Trop Dis, 2014. **8**(6): p. e2934.
608. Palus, M., et al., *Mice with different susceptibility to tick-borne encephalitis virus infection show selective neutralizing antibody response and inflammatory reaction in the central nervous system.* J Neuroinflammation, 2013. **10**: p. 77.
609. Stone, E.T., et al., *Balanced T and B cell responses are required for immune protection against Powassan virus in virus-like particle vaccination.* Cell Rep, 2022. **38**(7): p. 110388.
610. Weiner, L.P., G.A. Cole, and N. Nathanson, *Experimental encephalitis following peripheral inoculation of West Nile virus in mice of different ages.* J Hyg (Lond), 1970. **68**(3): p. 435-46.
611. Mlera, L., et al., *Modeling Powassan virus infection in Peromyscus leucopus, a natural host.* PLoS Negl Trop Dis, 2017. **11**(1): p. e0005346.
612. Santos, R.I., et al., *Salivary gland extract from the deer tick, Ixodes scapularis, facilitates neuroinvasion by Powassan virus in BALB/c mice.* Sci Rep, 2021. **11**(1): p. 20873.
613. VanBlargan, L.A., et al., *An mRNA Vaccine Protects Mice against Multiple Tick-Transmitted Flavivirus Infections.* Cell Rep, 2018. **25**(12): p. 3382-3392 e3.
614. Chen, R.E. and M.S. Diamond, *Dengue mouse models for evaluating pathogenesis and countermeasures.* Curr Opin Virol, 2020. **43**: p. 50-58.
615. Frolova, M.P., et al., *Experimental encephalitis in monkeys caused by the Powassan virus.* Neurosci Behav Physiol, 1985. **15**(1): p. 62-9.

616. Illarionova, V., et al., *Inapparent Tick-Borne Orthoflavivirus Infection in Macaca fascicularis: A Model for Antiviral Drug and Vaccine Research.* Vaccines (Basel), 2023. **11**(12).
617. Choi, H., et al., *A novel synthetic DNA vaccine elicits protective immune responses against Powassan virus.* PLoS Negl Trop Dis, 2020. **14**(10): p. e0008788.
618. Malonis, R.J., et al., *A Powassan virus domain III nanoparticle immunogen elicits neutralizing and protective antibodies in mice.* PLoS Pathog, 2022. **18**(6): p. e1010573.
619. Cheung, A.M., et al., *Characterization of Live-Attenuated Powassan Virus Vaccine Candidates Identifies an Efficacious Prime-Boost Strategy for Mitigating Powassan Virus Disease in a Murine Model.* Vaccines (Basel), 2023. **11**(3).
620. Cimica, V., et al., *A Virus-Like Particle-Based Vaccine Candidate against the Tick-Borne Powassan Virus Induces Neutralizing Antibodies in a Mouse Model.* Pathogens, 2021. **10**(6).
621. Himmler, G.E., et al., *Passage-attenuated Powassan virus LI9P protects mice from lethal LI9 challenge and links envelope residue D308 to neurovirulence.* mBio, 2025. **16**(4): p. e0006525.
622. Nguyen, T.L. and H. Kim, *Immunoinformatics and computational approaches driven designing a novel vaccine candidate against Powassan virus.* Sci Rep, 2024. **14**(1): p. 5999.
623. Administration, U.S.F.D. *Vaccines Licensed for Use in the United States*. 2025 05/31/2025 [cited 2025 October 30]; Available from: https://www.fda.gov/vaccines-blood-biologics/vaccines/vaccines-licensed-use-united-states.
624. McLean, D.M., et al., *Powassan virus: persistence of virus activity during 1966.* Can Med Assoc J, 1967. **96**(11): p. 660-4.
625. H., A., *Powassan encephalitis*, in *The Arboviruses: Epidemiology and Ecology*, T. Monath, Editor. 1989, CRC Press: Boca Raton, FL. p. 29-49.
626. Leonova, G.N., et al., *[Role of Powassan virus in the etiological structure of tick-borne encephalitis in the Primorsky Kray].* Vopr Virusol, 1980(2): p. 173-6.
627. Nofchissey, R.A., et al., *Seroprevalence of Powassan virus in New England deer, 1979-2010.* Am J Trop Med Hyg, 2013. **88**(6): p. 1159-62.
628. Eisen, R.J., L. Eisen, and C.B. Beard, *County-Scale Distribution of Ixodes scapularis and Ixodes pacificus (Acari: Ixodidae) in the Continental United States.* J Med Entomol, 2016. **53**(2): p. 349-86.
629. Dennis, D.T., et al., *Reported distribution of Ixodes scapularis and Ixodes pacificus (Acari: Ixodidae) in the United States.* J Med Entomol, 1998. **35**(5): p. 629-38.
630. Ogden, N.H., et al., *Estimated effects of projected climate change on the basic reproductive number of the Lyme disease vector Ixodes scapularis.* Environ Health Perspect, 2014. **122**(6): p. 631-8.
631. Wang, Y., et al., *Generation of Multiple Arbovirus-like Particles Using a Rapid Recombinant Vaccinia Virus Expression Platform.* Pathogens, 2022. **11**(12).

632. Dussupt, V., et al., *Potent Zika and dengue cross-neutralizing antibodies induced by Zika vaccination in a dengue-experienced donor.* Nat Med, 2020. **26**(2): p. 228-235.
633. Gallichotte, E.N., et al., *A new quaternary structure epitope on dengue virus serotype 2 is the target of durable type-specific neutralizing antibodies.* mBio, 2015. **6**(5): p. e01461-15.
634. Wong, S.H., et al., *Virus-Like Particle Systems for Vaccine Development against Viruses in the Flaviviridae Family.* Vaccines (Basel), 2019. **7**(4).
635. Grgacic, E.V. and D.A. Anderson, *Virus-like particles: passport to immune recognition.* Methods, 2006. **40**(1): p. 60-5.
636. Krol, E., G. Brzuska, and B. Szewczyk, *Production and Biomedical Application of Flavivirus-like Particles.* Trends Biotechnol, 2019. **37**(11): p. 1202-1216.
637. Lo-Man, R., et al., *A recombinant virus-like particle system derived from parvovirus as an efficient antigen carrier to elicit a polarized Th1 immune response without adjuvant.* Eur J Immunol, 1998. **28**(4): p. 1401-7.
638. Bachmann, M.F., et al., *Dendritic cells process exogenous viral proteins and virus-like particles for class I presentation to CD8+ cytotoxic T lymphocytes.* Eur J Immunol, 1996. **26**(11): p. 2595-600.
639. Moron, G., et al., *CD8alpha- CD11b+ dendritic cells present exogenous virus-like particles to CD8+ T cells and subsequently express CD8alpha and CD205 molecules.* J Exp Med, 2002. **195**(10): p. 1233-45.
640. Zimna, M., et al., *Functional characterization and immunogenicity of a novel vaccine candidate against tick-borne encephalitis virus based on Leishmania-derived virus-like particles.* Antiviral Res, 2023. **209**: p. 105511.
641. Kushnir, N., S.J. Streatfield, and V. Yusibov, *Virus-like particles as a highly efficient vaccine platform: diversity of targets and production systems and advances in clinical development.* Vaccine, 2012. **31**(1): p. 58-83.
642. Jain, N.K., et al., *Formulation and stabilization of recombinant protein based virus-like particle vaccines.* Adv Drug Deliv Rev, 2015. **93**: p. 42-55.
643. Gatt, Z., et al., *Review: Unravelling the Role of DNA Sensing in Alum Adjuvant Activity.* Discov Immunol, 2023. **2**(1): p. kyac012.
644. Gorden, K.K., et al., *Cutting edge: activation of murine TLR8 by a combination of imidazoquinoline immune response modifiers and polyT oligodeoxynucleotides.* J Immunol, 2006. **177**(10): p. 6584-7.
645. Fathi, A., M.M. Addo, and C. Dahlke, *Sex Differences in Immunity: Implications for the Development of Novel Vaccines Against Emerging Pathogens.* Front Immunol, 2020. **11**: p. 601170.
646. Fink, A.L., et al., *Biological sex affects vaccine efficacy and protection against influenza in mice.* Proc Natl Acad Sci U S A, 2018. **115**(49): p. 12477-12482.
647. Marriott, I., K.L. Bost, and Y.M. Huet-Hudson, *Sexual dimorphism in expression of receptors for bacterial lipopolysaccharides in murine macrophages: a possible mechanism for gender-based differences in endotoxic shock susceptibility.* J Reprod Immunol, 2006. **71**(1): p. 12-27.

648. Santos, R.I., et al., *Spinal Cord Ventral Horns and Lymphoid Organ Involvement in Powassan Virus Infection in a Mouse Model.* Viruses, 2016. **8**(8).
649. Tavakoli, N.P., et al., *Fatal case of deer tick virus encephalitis.* N Engl J Med, 2009. **360**(20): p. 2099-107.
650. Ebel, G.D. and L.D. Kramer, *Short report: duration of tick attachment required for transmission of powassan virus by deer ticks.* Am J Trop Med Hyg, 2004. **71**(3): p. 268-71.
651. Vieira, P. and K. Rajewsky, *The half-lives of serum immunoglobulins in adult mice.* Eur J Immunol, 1988. **18**(2): p. 313-6.
652. Siegel, E., et al., *Passive surveillance of Powassan virus in human-biting ticks and health outcomes of associated bite victims.* Clin Microbiol Infect, 2024.
653. Ishikawa, T., A. Yamanaka, and E. Konishi, *A review of successful flavivirus vaccines and the problems with those flaviviruses for which vaccines are not yet available.* Vaccine, 2014. **32**(12): p. 1326-37.
654. Goff, P.H., et al., *Synthetic Toll-like receptor 4 (TLR4) and TLR7 ligands as influenza virus vaccine adjuvants induce rapid, sustained, and broadly protective responses.* J Virol, 2015. **89**(6): p. 3221-35.
655. Hills, S.L., et al., *Tick-Borne Encephalitis Vaccine: Recommendations of the Advisory Committee on Immunization Practices, United States, 2023.* MMWR Recomm Rep, 2023. **72**(5): p. 1-29.
656. *Vaccines against tick-borne encephalitis: WHO position paper.* Wkly Epidemiol Rec, 2011. **86**(24): p. 241-56.
657. Uhrlaub, J.L., et al., *Repeated in vivo stimulation of T and B cell responses in old mice generates protective immunity against lethal West Nile virus encephalitis.* J Immunol, 2011. **186**(7): p. 3882-91.
658. Xiao, S.Y., et al., *West Nile virus infection in the golden hamster (Mesocricetus auratus): a model for West Nile encephalitis.* Emerg Infect Dis, 2001. **7**(4): p. 714-21.
659. Henriksen-Lacey, M., et al., *Comparison of the depot effect and immunogenicity of liposomes based on dimethyldioctadecylammonium (DDA), 3beta-[N-(N',N'-Dimethylaminoethane)carbomyl] cholesterol (DC-Chol), and 1,2-Dioleoyl-3-trimethylammonium propane (DOTAP): prolonged liposome retention mediates stronger Th1 responses.* Mol Pharm, 2011. **8**(1): p. 153-61.
660. Tada, R., et al., *Intranasal Immunization with DOTAP Cationic Liposomes Combined with DC-Cholesterol Induces Potent Antigen-Specific Mucosal and Systemic Immune Responses in Mice.* PLoS One, 2015. **10**(10): p. e0139785.
661. Benne, N., et al., *Direct immunomodulatory effects of DSPC:DSPG:CHOL liposomes on murine dendritic cells.* Eur J Pharm Sci, 2025. **212**: p. 107201.
662. Auderset, F., et al., *A TLR7/8 Agonist-Including DOEPC-Based Cationic Liposome Formulation Mediates Its Adjuvanticity Through the Sustained Recruitment of Highly Activated Monocytes in a Type I IFN-Independent but NF-kappaB-Dependent Manner.* Front Immunol, 2020. **11**: p. 580974.

663. Grigoryan, L., et al., *AS03 adjuvant enhances the magnitude, persistence, and clonal breadth of memory B cell responses to a plant-based COVID-19 vaccine in humans.* Sci Immunol, 2024. **9**(94): p. eadi8039.
664. Khurana, S., et al., *AS03-adjuvanted H5N1 vaccine promotes antibody diversity and affinity maturation, NAI titers, cross-clade H5N1 neutralization, but not H1N1 cross-subtype neutralization.* NPJ Vaccines, 2018. **3**: p. 40.
665. Crawford, M.W., et al., *The TLR7/8 agonist INI-4001 enhances the immunogenicity of a Powassan virus-like-particle vaccine.* NPJ Vaccines, 2025. **10**(1): p. 156.
666. Hermance, M.E. and S. Thangamani, *Tick Saliva Enhances Powassan Virus Transmission to the Host, Influencing Its Dissemination and the Course of Disease.* J Virol, 2015. **89**(15): p. 7852-60.
667. Nemeth, N.M., et al., *Powassan Virus Experimental Infections in Three Wild Mammal Species.* Am J Trop Med Hyg, 2021. **104**(3): p. 1048-1054.
668. Olafsdottir, T., M. Lindqvist, and A.M. Harandi, *Molecular signatures of vaccine adjuvants.* Vaccine, 2015. **33**(40): p. 5302-7.
669. Caproni, E., et al., *MF59 and Pam3CSK4 boost adaptive responses to influenza subunit vaccine through an IFN type I-independent mechanism of action.* J Immunol, 2012. **188**(7): p. 3088-98.
670. Heinz, F.X., et al., *Structural changes and functional control of the tick-borne encephalitis virus glycoprotein E by the heterodimeric association with protein prM.* Virology, 1994. **198**(1): p. 109-17.
671. Luo, Y.Y., et al., *Identification of a novel infection-enhancing epitope on dengue prM using a dengue cross-reacting monoclonal antibody.* BMC Microbiol, 2013. **13**: p. 194.
672. Inou, N., et al., *[A case report of primary pulmonary neurogenic sarcoma (author's transl)].* Kyobu Geka, 1980. **33**(9): p. 706-11.
673. VanBlargan, L.A., et al., *Broadly neutralizing monoclonal antibodies protect against multiple tick-borne flaviviruses.* J Exp Med, 2021. **218**(5).
674. Jarmer, J., et al., *Variation of the specificity of the human antibody responses after tick-borne encephalitis virus infection and vaccination.* J Virol, 2014. **88**(23): p. 13845-57.
675. Anastasina, M., et al., *The structure of immature tick-borne encephalitis virus supports the collapse model of flavivirus maturation.* Sci Adv, 2024. **10**(27): p. eadl1888.
676. Sadarangani, M., A. Marchant, and T.R. Kollmann, *Immunological mechanisms of vaccine-induced protection against COVID-19 in humans.* Nat Rev Immunol, 2021. **21**(8): p. 475-484.
677. Boudreau, C.M. and G. Alter, *Extra-Neutralizing FcR-Mediated Antibody Functions for a Universal Influenza Vaccine.* Front Immunol, 2019. **10**: p. 440.
678. Plotkin, S.A., *Recent updates on correlates of vaccine-induced protection.* Front Immunol, 2022. **13**: p. 1081107.
679. Plotkin, S.A., *Correlates of protection induced by vaccination.* Clin Vaccine Immunol, 2010. **17**(7): p. 1055-65.

680. Stronsky, S.M., et al., *Adjuvant selection impacts the correlates of vaccine protection against Ebola infection.* Vaccine, 2020. **38**(29): p. 4601-4608.
681. Who, P., *Vaccines against tick-borne encephalitis: WHO position paper--recommendations.* Vaccine, 2011. **29**(48): p. 8769-70.
682. Mason, R.A., et al., *Yellow fever vaccine: direct challenge of monkeys given graded doses of 17D vaccine.* Appl Microbiol, 1973. **25**(4): p. 539-44.
683. Konior, R., et al., *Seropersistence of TBE virus antibodies 10 years after first booster vaccination and response to a second booster vaccination with FSME-IMMUN 0.5mL in adults.* Vaccine, 2017. **35**(28): p. 3607-3613.
684. Paulke-Korinek, M., et al., *Factors associated with seroimmunity against tick borne encephalitis virus 10 years after booster vaccination.* Vaccine, 2013. **31**(9): p. 1293-7.
685. Nygren, T.M., et al., *Author Correction: Tick-borne encephalitis vaccine effectiveness and barriers to vaccination in Germany.* Sci Rep, 2024. **14**(1): p. 2504.
686. Zens, K.D., et al., *Retrospective, matched case-control analysis of tickborne encephalitis vaccine effectiveness by booster interval, Switzerland 2006-2020.* BMJ Open, 2022. **12**(4): p. e061228.
687. Ackermann-Gaumann, R., P. Lang, and K.D. Zens, *Defining the "Correlate(s) of Protection" to tick-borne encephalitis vaccination and infection - key points and outstanding questions.* Front Immunol, 2024. **15**: p. 1352720.
688. Bowman, K.A., P. Kaplonek, and R.P. McNamara, *Understanding Fc function for rational vaccine design against pathogens.* mBio, 2024. **15**(1): p. e0303623.
689. Dias, A.G., Jr., et al., *Antibody Fc characteristics and effector functions correlate with protection from symptomatic dengue virus type 3 infection.* Sci Transl Med, 2022. **14**(651): p. eabm3151.
690. Giroud, P., et al., *Expression of TAM-R in Human Immune Cells and Unique Regulatory Function of MerTK in IL-10 Production by Tolerogenic DC.* Front Immunol, 2020. **11**: p. 564133.
691. Fujimori, T., et al., *The Axl receptor tyrosine kinase is a discriminator of macrophage function in the inflamed lung.* Mucosal Immunol, 2015. **8**(5): p. 1021-1030.